TECHNICAL UNIVERSITY OF CIVIL ENGINEERING BUCHAREST

PROCEEDINGS OF THE 16TH WORKSHOP ON MATHEMATICS, COMPUTER SCIENCE AND TECHNICAL EDUCATION

DEPARTMENT OF MATHEMATICS AND COMPUTER SCIENCE

VOLUME 2 / 2019

Bucharest, May 25, 2019

ISSN 2601-9299
ISSN-L 2601-9299

CONTENT

A THEOREM OF TYPE " PARTITION OF UNITY " WITH APPLICATIONS IN THE LOCALIZABILITY OF A LINEAR SUBSPACE OF A WEIGHTED SPACES

Ileana Bucur
Department of Mathematics and Computer Science
Technical University of Civil Engineering Bucharest, Romania
E-mail: bucurileana@yahoo.com
Gavriil Păltineanu
Department of Mathematics and Computer Science
Technical University of Civil Engineering Bucharest, Romania
E-mail: gavriil.paltineanu@gmail.com

Abstract: In the first part of the paper we present Theorem 1 (a theorem of type "partition of unity"), which generalizes Lemma 1 of [1] and some of its consequences. In the second part, some theorems of localizability (or density) of a linear subspaces of a weighted space are presented.
Mathematical Subject Classification (2010): Primary 41A10; Secondary 46J10

Key words: Stone- Čech compactification, partition of unity, Nachbin family, weighted space, localizability of a linear subspace, set with (VN) property, convex cone

Let X be a Hausdorff locally compact space and let $\mathcal{F}$ be a subset of continuous functions on X with values in the interval $[0,1]$. The set $\mathcal{F}$ induces on X the following equivalence relation:

$$x \sim_{\mathcal{F}} y \quad \Leftrightarrow \quad f(x) = f(y),\ \forall f \in \mathcal{F}.$$

For any $x \in X$ we denote by $[x]_{\mathcal{F}}$ the set:

$$[x]_{\mathcal{F}} = \left\{ y \in X;\ f(y) = f(x),\ \forall f \in \mathcal{F} \right\}.$$

Obviously, $[x]_{\mathcal{F}}$ is a closed subset of X and any element $f \in \mathcal{F}$ is constant on this set. In fact $[x]_{\mathcal{F}}$ is the maximal set containing x with this property, and for any $x, y \in X$ we have $[x]_{\mathcal{F}} = [y]_{\mathcal{F}}$ or $[x]_{\mathcal{F}} \cap [y]_{\mathcal{F}} = \phi$. We denote by $X / \sim_{\mathcal{F}}$ the space of all equivalence classes, i.e.:

$$X / \sim_{\mathcal{F}} = \left\{ [x]_{\mathcal{F}};\ x \in X \right\}.$$

Further we denote by βX the Stone- Čech compactification of the locally compact space X i.e. the compact space (uniquely determined up to a topological isomorphism) such that X is a dense subset of βX.

The topology of X coincides with the trace topology of βX on X and any bounded continuous function on X may be extended to a unique continuous function on βX.

If for any $f \in C_b(X)$ (i.e. f is a continuous bounded function on X) we shall denote by βf the continuous extension of f to βX, then the map $\beta : C_b(X) \to C(\beta X)$ is an isomorphism between two Banach algebras.

The family $\beta\mathcal{F} = \{\beta f;\ f \in \mathcal{F}\}$ induces on βX the following equivalence relation:

$$u \sim_{\beta\mathcal{F}} v \quad \Leftrightarrow \quad (\beta f)(u) = (\beta f)(v),\ \forall f \in \mathcal{F}.$$

We denote by Z the quotient space $\beta X / \sim_{\beta\mathcal{F}}$ and by $\pi : \beta X \to Z$ the canonical mapping.

For any $f \in \mathcal{F}$ the function $\tilde{f} : Z \to \mathbb{K}$ is given by $\tilde{f}(z) = (\beta f)(y)$ if $z = \pi(y)$. Clearly the function $\tilde{f}$ is well definite. If denote by $\tilde{\mathcal{F}} = \left\{\tilde{f}\right\}_{f \in \mathcal{F}}$ then $\tilde{\mathcal{F}} \subset C(Z)$.

Theorem 1. *Let $\mathcal{F} \subset C(X, [0,1])$ with the property that $\tilde{\mathcal{F}} = C(Z, [0,1])$. Suppose in addition that for any $x \in X$ there exists a compact subset $K_x \subset X$ such that $[x]_{\mathcal{F}} \cap K_x = \phi$.*

Then there exists a finite set $\left\{[x_1]_{\mathcal{F}}, [x_2]_{\mathcal{F}}, ..., [x_n]_{\mathcal{F}}\right\}$ of equivalence classes and there exists a finite number of functions $f_1, f_2, ..., f_n \in \mathcal{F}$ with the properties:

$$f_i \big| K_{x_i} = 0,\ i = \overline{1,n},\ \sum_{i=1}^{n} f_i = 1.$$

Proof. We remark that for any $x \in X$ we have $[x]_{\mathcal{F}} = \pi(x) \cap X$ and if $y \in \beta X$ is such that $\pi(y) \cap X \neq \phi$ then we have $\pi(y) \cap X = [x]_{\mathcal{F}}$ for any $x \in \pi(y) \cap X$. Hence π may be seen as an injection from $\left\{ [x]_{\mathcal{F}};\ x \in X \right\}$ into Z, namely:

$$\pi\left([x]_{\mathcal{F}}\right) = \pi(y),\ \forall y \in [x]_{\mathcal{F}}.$$

In fact we have a bijection between the set $\left\{ [x]_{\mathcal{F}};\ x \in X \right\}$ and the subspace $\pi(X)$ of Z.

Since the set $[x]_{\mathcal{F}} = \pi(y) \cap X$ and the compact subset K_x are disjoint it follows that $\pi(x)$ does not belongs to the compact subset $\pi(K_x)$ of $\pi(X)$. This implies that $\bigcap_{x \in X} \pi(K_x) = \phi$.

Since $\pi(K_x)$ is compact we deduce that there exists a finite subset $\{x_1, ..., x_n\} \subset X$ such that $\bigcap_{i=1}^{n} \pi(K_{x_i}) = \phi$ and therefore the compact space Z is covered by a finite family of open subsets of Z:

$$Z = \bigcup_{i=1}^{n} \left(Z \setminus \pi(K_{x_i})\right).$$

We consider now a partition $\sum_{i=1}^{n} g_i$ of the constant function $\mathbf{1}$, $g_i : Z \to [0,1]$, g_i vanishing outside $Z \setminus \pi(K_{x_i})$, g_i continuous for any $i = \overline{1,n}$.

Since $\tilde{\mathcal{F}} = C(Z,\ [0,1])$ it follows that there exists $f_i \in \mathcal{F}$ such that $g_i = \tilde{f}_i,\ \forall i = \overline{1,n}.$.

Clearly $\tilde{f}_i \circ \pi = \beta f_i$ and that for any $x \in X$ we have:

$$f_i(x) = (\beta f_i)(x) = (\tilde{f}_i \circ \pi)(x) = g_i[\pi(x)] \geq 0\ ;$$

$$f_i \left| K_{x_i} = g_i \right| \left(\pi[K_{x_i}]\right) = 0 \text{ and } \sum_{i=1}^{n} f_i(x) = \sum_{i=1}^{n} g_i[\pi(x)] = 1\,.$$

Corollary 1. (L. Nachbin [1], Lemma 1) *Let X be a Hausdorff locally compact space and let $\mathcal{A} \subset \mathrm{C}_b(X)$ be a closed subalgebra which contains the constant functions (selfadjoint in the complex case). We suppose in addition that for any $x \in X$ there exists a compact subset $K_x \subset X$ such that $[x]_{\mathcal{F}} \cap K_x = \phi$. Then there exists a finite set $\left\{[x_1]_{\mathcal{A}}\ ,[x_2]_{\mathcal{A}}\ ,...,[x_n]_{\mathcal{A}}\right\}$ of equivalence classes and also there exists a finite set of functions $\{a_1, a_2, ..., a_n\} \subset \mathcal{A}$ with the properties:*

$$a_i \geq 0,\ \ a_i \left| K_{x_i} = 0,\ \ i = \overline{1,n}\ ,\ \ \sum_{i=1}^{n} a_i = 1\,.\right.$$

Proof. First we remark that if we denote by $\mathcal{A}_1 = \{a \in \mathcal{A};\ \ 0 \leq a \leq 1\}$ then $x \sim_{\mathcal{A}} y$ iff $x \sim_{\mathcal{A}_1} y$, i.e.: $a(x) = a(y),\ \forall a \in \mathcal{A}$ iff $b(x) = b(y),\ \ \forall b \in \mathcal{A}_1$.

It is sufficient we show that $b(x) = b(y),\ \ \forall b \in \mathcal{A}_1$ involves $a(x) = a(y),\ \forall a \in \mathcal{A}$. Indeed, if $a \in \mathcal{A}_+$ then $b = \frac{a}{\|a\|} \in \mathcal{A}_1$ and so $a(x) = a(y)$. On the other hand we remark that $\mathcal{A}$ is lattice since is a closed subalgebra containing the constant functions.

Therefore for any $a \in \mathcal{A}$, we have $a_+ = \frac{|a| + a}{2} \in \mathcal{A}_+,\ \ a_- = \frac{|a| - a}{2} \in \mathcal{A}_+$ and hence :

$$a(x) = a_+(x) - a_-(x) = a_+(y) - a_-(y) = a(y)\,.$$

Now the proof of the Corollary 1 follows from Theorem 1 for $\mathcal{F} = \mathcal{A}_1 = \{a \in \mathcal{A};\ 0 \leq a \leq 1\}$.

Indeed, $\tilde{\mathcal{A}}$ is a closed subalgebra which contains the constant functions and separates the points of the compact set Z. Therefore, by Stone –Weierstrass theorem we have $\tilde{\mathcal{A}} = C(Z)$.

Obviously, $\tilde{\mathcal{A}}_1 = C(Z,\ [0,1])$.

Definition 1. *We shall say that a subset* $\mathcal{M} \subset C(X,\ [0,1])$ *has the property* (VN) *if:*

$$f \cdot g + (1-f)\cdot h \in \mathcal{M},\ \forall f, g, h \in \mathcal{M}.$$

Corollary 2. *Let* X *be a Hausdorff locally compact space and let* $\mathcal{M} \subset C(X,\ [0,1])$ *be a closed subset with the property* (VN) *which contains the constant functions* 0, 1 *and least a constant function* $0 < c < 1$.

We suppose in addition that for any $x \in X$ *there exists a compact subset* $K_x \subset X$ *such that* $[x]_{\mathcal{M}} \cap K_x = \phi$. *Then there exists a finite set* $\left\{[x_1]_{\mathcal{M}}, [x_2]_{\mathcal{M}}, ..., [x_n]_{\mathcal{M}}\right\}$ *of equivalence classes and there exists a finite set of functions* $m_1, m_2, ..., m_n \in \mathcal{M}$ *with the properties:*

$$m_i \big| K_{x_i} = 0,\ i = \overline{1,n},\ \sum_{i=1}^{n} m_i = 1.$$

Proof. The proof results from Theorem 1 for $\mathcal{F} = \mathcal{M}$. Indeed, the set $\tilde{\mathcal{M}}$ is a closed subset of $C(Z,\ [0,1])$ which separates the points of the compact set $Z = \beta X / \sim_{\beta,\mathcal{M}}$ and contains the constant functions 0, 1 and least a constant function $0 < c < 1$. From Theorem 4.18 of [2] it follows that $\tilde{\mathcal{M}} = C(Z,\ [0,1])$.

Corollary 3. *Let* X *be a Hausdorff locally compact space and let* $\mathcal{C} \subset C_b^{+}(X)$ *be a closed convex cone containing the constant functions* 0, 1 *and has the property: for any* $u, v \in \beta X$ *such that* $\pi(u) \neq \pi(v)$ *there is some* $\varphi \in C(X,\ [0,1])$ *such that*

$$\varphi \cdot f + (1-\varphi)\cdot h \in \mathcal{C},\ \forall f, h \in \mathcal{C} \text{ and } (\beta\varphi)(u) \neq (\beta\varphi)(v).$$

Suppose also that for any $x \in X$ *there exists a compact subset* $K_x \subset X$ *such that* $[x]_{\mathcal{C}} \cap K_x = \phi$.

Then there exists a finite number of equivalence classes $[x_1]_{\mathcal{C}}, [x_2]_{\mathcal{C}}, ..., [x_n]_{\mathcal{C}}$ *and an equal number of functions* $h_1, h_2, ..., h_n \in \mathcal{C}$ *with the properties:*

$$h_i \big| K_{x_i} = 0,\ i = \overline{1,n},\ \sum_{i=1}^{n} h_i = 1.$$

Proof. The proof results from Theorem 1 for $\mathcal{F} = \mathcal{C}_1 = \{h \in \mathcal{C};\ h \leq 1\}$. Indeed, $\tilde{\mathcal{C}}$ is a closed convex cone of $C^{+}(Z)$ which contains the constant functions 0, 1, separates the points of the compact set Z and has the property that for any $z_1, z_2 \in Z,\ z_1 \neq z_2$, there is a multiplier $\tilde{\varphi} \in C(Z,\ [0,1])$, i.e. $\tilde{\varphi}\cdot\tilde{f} + (1-\tilde{\varphi})\cdot\tilde{h} \in \tilde{\mathcal{C}},\ \forall \tilde{f}, \tilde{h} \in \tilde{\mathcal{C}}$ with the property

$$\tilde{\varphi}(z_1) = (\beta\varphi)(u) \neq (\beta\varphi)(v) = \tilde{\varphi}(z_2)$$

where $z_1 = \pi(u),\ z_2 = \pi(v)$.

From Theorem 2, Corollary 1 of [3], it follows that $\tilde{\mathcal{C}} = C^{+}(Z)$ and hence that:

$$\tilde{\mathcal{C}}_1 = C(Z,\ [0,1]).$$

Definition 2. *A family V of upper semicontinuous, non-negative functions on the Hausdorff locally compact space X such that for any $v_1, v_2 \in V$ and any $\lambda \in \mathbb{R},\ \lambda > 0$ there exists $w \in V$ such that :*

$$v_i(x) \le \lambda \cdot w(x),\ \ \forall x \in X,\ \ i = 1, 2$$

is called a Nachbin family. Any element of V will be called a weight.

We shall denote by $CV_0(X, \mathbb{R})$ or by $CV_0(X)$ the set of all continuous functions f on X such that the function $f \cdot v$ vanishes at infinity for all $v \in V$.

Any weight $v \in V$ generates a seminorm $p_v : CV_0(X) \to \mathbb{R}_+$ defined by:

$$p_v(f) = \sup\left\{v(x) \cdot \left|f(x)\right|;\ \ x \in X\right\},\ \ \forall f \in CV_0(X).$$

The locally convex topology defined by this family of seminorms is denoted by ω_V and it will be called the weighted topology on $CV_0(X)$. The space $CV_0(X)$ endowed with the topology ω_V is called weighted space.

If for any $x \in X$ there exists $v_x \in V$, such that $v_x(x) > 0$, then $(CV_0(X),\ \omega_V)$ is a Hausdorff locally convex space. Further we suppose that $CV_0(X)$ is Hausdorff.

Definition 3. *A linear subspace $\mathcal{W}$ of $CV_0(X)$ is called localizable with respect to the family $\mathcal{F}$ of $C_b(X)$ if:*

$$\overline{\mathcal{W}} = \left\{f \in CV_0(X);\ \ f \,\middle|\, [x]_{\mathcal{F}} \in \overline{\mathcal{W}\,|\ [x]_{\mathcal{F}}},\ \ \forall x \in X\right\}.$$

Remark 1. *The linear subspace $\mathcal{W} \subset CV_0(X)$ is dense in $CV_0(X)$ if the following conditions are satisfied:*

a) *$\mathcal{W}$ is localizable with respect to $\mathcal{F}$.*

b) *$\mathcal{F}$ separates the points of X.*

c) *for any $x \in X$ there exists a $w \in \mathcal{W}$ such that $w(x) \neq 0$.*

Theorem 2. *Let* $\mathcal{F} \subset C(X;\ [0,1])$ *be a subset with the property* $\tilde{\mathcal{B}} = C(Z,[0,1])$, *where* $\mathcal{B} = \overline{\mathcal{F}}$ *is the closure of* $\mathcal{F}$ *in* $C(X;\ [0,1])$. *If* $\mathcal{W} \subset CV_0(X)$ *is a linear subspaces with the property* $\mathcal{F} \cdot \mathcal{W} \subset \mathcal{W}$ *then* $\mathcal{W}$ *is localizable with respect to, i.e.:*

$$\overline{\mathcal{W}} = \left\{ f \in CV_0(X);\ \ f \,\middle|\, [x]_{\mathcal{F}} \in \overline{\mathcal{W}\,|\,[x]_{\mathcal{F}}}\ ,\ \forall x \in X \right\}.$$

Proof. Since it is obviously that the set of the left side of the previous equality belongs to the set of the right side of this, it is sufficient to proof the inverse inclusion.

Let $g \in CV_0(X)$ such that $g \,|\, [x]_{\mathcal{F}} \in \overline{\mathcal{W}\,|\,[x]_{\mathcal{F}}},\ \forall x \in X$. We shall prove that $g \in \overline{\mathcal{W}}$.

Let $v \in V$ and $\varepsilon > 0$ arbitrary fixed. Then for any $x \in X$ there exists $w_x \in \mathcal{W}$ such that:

$$v(y)\left|g(y) - w_x(y)\right| < \varepsilon,\ \forall y \in [x]_{\mathcal{F}}.$$

If we denote by $K_x = \left\{ y \in X;\ v(y)\left|g(y) - w_x(y)\right| \geq \varepsilon \right\}$, then K_x is a compact set and:

$$[x]_{\mathcal{F}} \cap K_x = \phi,\ [x]_{\mathcal{F}} \cup K_x = X\ .$$

Since by hypothesis $\tilde{\mathcal{B}} = C(Z,[0,1])$ where $\mathcal{B} = \overline{\mathcal{F}}$, from Theorem 1 it follows that there exists a finite number $[x_1]_{\mathcal{F}}, [x_2]_{\mathcal{F}}, ..., [x_n]_{\mathcal{F}}$ of equivalence classes and there exists also a finite number of functions $b_1, b_2, ..., b_n \in \mathcal{B}$ with the properties:

$$b_i \left| K_{x_i} = 0,\ i = \overline{1,n}\ ,\ \sum_{i=1}^{n} b_i = 1. \right.$$

Further, for any $i \in \{1,2,...,n\}$ we have:

$$b_i(y) \cdot v(y) \cdot \left|g(y) - w_{x_i}(y)\right| \leq \varepsilon \cdot b_i(y),\ \forall y \in X. \qquad (1)$$

Indeed, if $y \in [x_i]_{\mathcal{F}}$ then we have $v(y) \cdot \left|g(y) - w_{x_i}(y)\right| < \varepsilon$ and if $x \notin [x_i]_{\mathcal{F}}$, then $b_i(y) = 0$.

From (1) it follows:

$$v(y) \cdot \sum_{i=1}^{n} b_i(y) \cdot \left|g(y) - w_{x_i}(y)\right| < \varepsilon \cdot \sum_{i=1}^{n} b_i(y) = \varepsilon,\ \forall y \in X.$$

Further we have:

$$v(y) \cdot \left| g(y) - \sum_{i=1}^{n} b_i(y) \cdot w_{x_i}(y) \right| = v(y) \cdot \left| \sum_{i=1}^{n} b_i(y) \cdot [g(y) - w_{x_i}(y)] \right| \leq v(y) \cdot \sum_{i=1}^{n} b_i(y) \cdot \left|g(y) - w_{x_i}(y)\right| \leq \varepsilon,\ \forall x \in X.$$

Since $b_1, b_2, ..., b_n \in \overline{\mathcal{F}}$, it results that for any $i \in \{1,...,n\}$ and any $\delta > 0$ there is a $f_i \in \mathcal{F}$, such that:

$$\left|b_i(y) - f_i(y)\right| < \delta,\ \forall y \in X\ .$$

Since the functions $v\cdot w_{x_i}$ vanishe at infinity it follows that these are bounded on X and therefore there exists:

$$\alpha_i=\sup\left\{v(y)\cdot\left|w_{x_i}\right|;\ y\in X\right\},\ i\in\overline{1,n}.$$

Further we have:

$$v(y)\cdot\left|\sum_{i=1}^{n}f_i(y)\cdot w_{x_i}(y)-g(y)\right|\le v(y)\cdot\left|\sum_{i=1}^{n}f_i(y)\cdot w_{x_i}(y)-\sum_{i=1}^{n}b_i(y)\cdot w_{x_i}(y)\right|+v(y)\cdot\left|\sum_{i=1}^{n}b_i(y)\cdot w_{x_i}(y)-g(y)\right|\le$$

$$\le\sum_{i=1}^{n}\left|f_i(y)-b_i(y)\right|\cdot v(y)\cdot\left|w_{x_i}(y)\right|+\varepsilon\le\delta\cdot\sum_{i=1}^{n}\alpha_i+\varepsilon.$$

If we suppose that:

$$\delta<\frac{\varepsilon}{\sum_{i=1}^{n}\alpha_i},$$

then:

$$v(y)\cdot\left|\sum_{i=1}^{n}f_i(y)\cdot w_{x_i}(y)-g(y)\right|\le 2\cdot\varepsilon,\ \forall y\in X.$$

Finally, if we denote by $w=\sum_{i=1}^{n}f_i\cdot w_{x_i}$, then $w\in\mathcal{F}\cdot\mathcal{W}\subset\mathcal{W}$ and so the proof is finished.

Corollary 4. *If we suppose in addition that $\mathcal{F}$ separates the points of X and that for any $x\in X$ there exists a $w\in\mathcal{W}$, such that $w(x)\neq 0$, then $\mathcal{W}$ is dense in $CV_0(X)$, i.e.:*

$$\overline{\mathcal{W}}=CV_0(X).$$

The proof follows from Theorem 2 and Remark 1.

Theorem 3. (Nachbin**)** *Let $\mathcal{A}$ be a subalgebra of $C_b(X)$ containing the constant function* 1*, selfadjoint in the complex case, and let $\mathcal{W}\subset CV_0(X)$ be a linear subspace such that $\mathcal{A}\cdot\mathcal{W}\subset\mathcal{W}$.*

Then $\mathcal{W}$ is localizable with respect to $\mathcal{A}$, i.e.:

$$\overline{\mathcal{W}}=\left\{f\in CV_0(X);\ f\,\middle|\,[x]_{\mathcal{A}}\in\overline{\mathcal{W}|\ [x]}_{\mathcal{A}}\ ,\ \forall x\in X\right\}.$$

The proof follows from Theorem 2 and Corollary 1 for $\mathcal{F}=\mathcal{A}_1=\left\{a\in\mathcal{A};\ 0\le a\le 1\right\}$.

Corollary 5. *If we suppose in addition that $\mathcal{A}$ separates the points of X and that for any $x \in X$ there exists a $w \in \mathcal{W}$ such that $w(x) \neq 0$, then $\mathcal{W}$ is dense in $CV_0(X)$, i.e.:*

$$\overline{\mathcal{W}} = CV_0(X).$$

Theorem 4. *Let $\mathcal{M} \subset C(X; [0,1])$ be a subset with $(VN)-$property which contains the constant functions $0, 1$ and least a constant function $0 < c < 1$. If $\mathcal{W} \subset CV_0(X)$ is a linear subspace with the property $\mathcal{M} \cdot \mathcal{W} \subset \mathcal{W}$, then $\mathcal{W}$ is localizable with respect to $\mathcal{M}$, i.e.:*

$$\overline{\mathcal{W}} = \left\{ f \in CV_0(X);\ f \,\middle|\, [x]_{\mathcal{M}} \in \overline{\mathcal{W}|\ [x]}_{\mathcal{M}}\ ,\ \forall x \in X \right\}.$$

The proof follows from Theorem 2 and Corollary 2 for $\mathcal{F} = \mathcal{M}$.

Corollary 6. *If we suppose in addition that $\mathcal{M}$ separates the points of X and that for any $x \in X$ there exists $w \in \mathcal{W}$ such that $w(x) \neq 0$, then $\mathcal{W}$ is dense in $CV_0(X)$, i.e.:*

$$\overline{\mathcal{W}} = CV_0(X).$$

Theorem 5. *Let X be a Hausdorff locally compact space and let $\mathcal{C} \subset C_b{}^+(X)$ be a convex cone containing the constant functions 0, 1 and has the property that for any $u, v \in \beta X$ such that $\pi(u) \neq \pi(v)$ there is a multiplier $\varphi \in C(X, [0,1])$ (i.e. $\varphi \cdot f + (1-\varphi) \cdot h \in \mathcal{C},\ \forall f, h \in \mathcal{C}$) such that $(\beta\varphi)(u) \neq (\beta\varphi)(v)$, and let $\mathcal{W} \subset CV_0(X)$ be a linear subspace such that $\mathcal{C} \cdot \mathcal{W} \subset \mathcal{W}$. Then $\mathcal{W}$ is localizable with respect to $\mathcal{C}$, i.e.:*

$$\overline{\mathcal{W}} = \left\{ f \in CV_0(X);\ f \,\middle|\, [x]_{\mathcal{C}} \in \overline{\mathcal{W}|\ [x]}_{\mathcal{C}}\ ,\ \forall x \in X \right\}.$$

The proof follows from Theorem 2 and Corollary 3 for $\mathcal{F} = \mathcal{C}$.

Corollary 7. *Let $\mathcal{C} \subset C_b{}^+(X)$ and $\mathcal{W} \subset CV_0(X)$ as in Theorem 4. If we suppose in addition that $\mathcal{C}$ separates the points of X and that for any $x \in X$ there exists a $w \in \mathcal{W}$ such that $w(x) \neq 0$, then $\mathcal{W}$ is dense in $CV_0(X)$, i.e.:*

$$\overline{\mathcal{W}} = CV_0(X).$$

The assertion follows from Theorem 5 and Remark 1.

References

[1] Nachbin, L.: *Weighted approximation for algebras and modules of continuous functions: real and selfadjoint complex cases,* Ann. of Math., 81, 289-302, 1965.

[2] Păltineanu, G., Bucur, I.: *Some Density Theorem in the Set of Continuous Functions with Values in the Unit Interval,* Mediterr, J. (2017) 14:44, *published online* March 2, 2017.

[3] Prolla, J.B.: *A generalized Bernstein approximation theorem,* Math.Camb.Phil.Soc., 104, 317-330, 1988.

PROBABILISTIC AND MONTE-CARLO METHODS COMPARED ON A PRACTICAL EXAMPLE

DAN CARAGHEORGHEOPOL

Abstract. In this note, we aim to illustrate how the probabilistic approach and the Monte-Carlo simulations based approach can be used together and how they complement one another in solving practical, real-life problems. To this end, we consider a classical XVIII-th century problem, known as "Buffon's needle" and discuss two ways to find its solution based on probability theory. Then, we present a Monte Carlo simulations approach to this classical problem and compare the results to the theoretical ones.

Mathematics Subject Classification (2010): 65C50, 65C05, 11K45
Key words: Buffon's needle, geometric probability, Monte-Carlo simulation, Monte-Carlo integration.

1. Introduction

In the following, we propose a discussion on how one can complement the use of probability theory in modelling and solving engineering and real world problems by using Monte Carlo simulation techniques. As an example, we consider the classical, centuries old, problem of Buffon's needle [1, 2], considered the oldest problem to be solved in geometric probability. Let us state the problem in full details:

Problem (*Buffon's needle*) Suppose we are in a room whose floor is made of parallel planks of the same width L. What is the probability that, by randomly throwing a needle of length a on the floor, it intersects a line separating two planks? We will only consider here the so-called "short needle" case, i.e. the case when $a < L$.

It is perhaps worth noting that this old 2-dimensional problem has a 3-dimensional sibling which presents considerable interest in engineering. It's solution through probabilistic and Monte Carlo simulations methods raises interesting questions that will be addresed in a future paper.

The next section is devoted to presenting two probability theoretic solutions to Buffon's needle problem: a geometric probability solution and another probabilistic solution, of a more formal type. In the third section we briefly present the main ideas behind the Monte Carlo simulations techniques and then use them to numerically check the results found by the probabilistic approaches. Finally, the last section is devoted to conclusions.

2. Buffon's needle problem. Two probabilistic solutions

Geometric probability approach.

Let x note the distance from the needle center to the closest line on the floor and let θ note the acute angle of the needle with the direction perpendicular to the parallel lines on the floor. In figure 1, the vertical solid blue lines represent the parallel lines on the floor and the horizontal dashed blue line is the direction perpendicular to them. Recall that a is the length of the needle and L is the distance between the parallel lines on the floor and we assumed $a < L$.

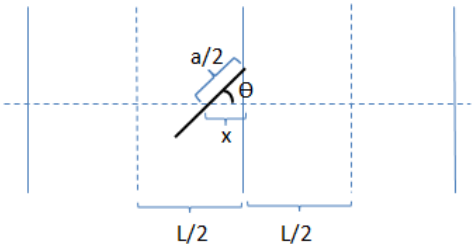

Figure 1. Position of the needle across a line on the floor

The needle can intersect a line on the floor only if $0 \leq x \leq \frac{a}{2}$, i.e., if the needle center lies between the black dashed lines in figure 2. The probability of this to occur is given by $P_1 = \frac{a}{L}$, since the distance between the vertical black dashed lines is a and the distance between the vertical blue dashed lines is L.

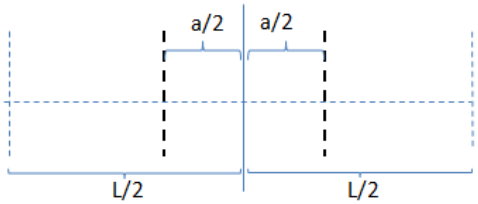

Figure 2. If the middle of the needle lies between the black dashed lines, the needle may cross the line on the floor.

In order for the needle to cross the (closest) floor line, when $0 \leq x \leq \frac{a}{2}$, the angle θ must be below θ_0, where $cos\theta_0 = \frac{x}{\frac{a}{2}} = \frac{2x}{a}$, and therefore $\theta_0 = arccos\frac{2x}{a}$. This means that the needle has to fall inside the circular sector of angle $2\theta_0$ of the circle of radius $\frac{a}{2}$, as shown in figure 3.

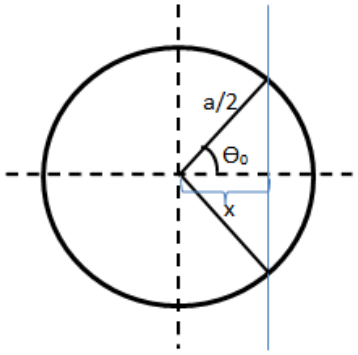

Figure 3. If the needle lies within the circular sector shown, it will cross the line on the floor

It follows that the probability of the needle crossing the line, as a function of x, when $0 \leq x \leq \frac{a}{2}$ is given by:

$$P(x) = \frac{Area_{circularsector}}{Area_{semicircle}} = \frac{\pi(\frac{a}{2})^2 \frac{2\pi}{2\theta_0}}{\frac{1}{2}\pi(\frac{a}{2})^2} = \frac{2\theta_0}{\pi} = \frac{2}{\pi} arccos(\frac{2x}{a})$$

By integrating $P(x)$ as a function of x and dividing to the length of the integration interval, we get the probability that for $0 \leq x \leq \frac{a}{2}$, the needle will intersect the nearest line on the floor:

$$P_2 = \frac{2}{a}\int_0^{\frac{a}{2}} \frac{2}{\pi} arccos(\frac{2x}{a})dx = \frac{2}{\pi}\int_0^{\frac{a}{2}} \frac{2}{a} arccos(\frac{2x}{a})dx.$$

After changing the variable to $y = \frac{2x}{a}$, we find that:

$$P_2 = \frac{2}{\pi}\int_0^1 arccos(y)dy = \frac{2}{\pi}$$

.

Finally, it follows that the probability of a randomly thrown needle on the floor to intersect a line is given by $P = P_1P_2 = \frac{2a}{L\pi}$.

A more formal probabilistic approach.

Let us use the same notations as above. The probability density function of the uniformly distributed random variable x between 0 and $\frac{L}{2}$ is given by:

$$\begin{cases} \frac{2}{L}, \text{ for } 0 \leq x \leq \frac{L}{2} \\ 0, \text{ otherwise} \end{cases}$$

In a similar way, the probability density function of the uniformly distributed random variable θ between 0 and $\frac{\pi}{2}$ is given by:

$$\begin{cases} \frac{2}{\pi}, \text{ for } 0 \leq \theta \leq \frac{\pi}{2} \\ 0, \text{ otherwise} \end{cases}$$

It follows that, since the two random variables are independent, their joint probability density function is given by:

$$\begin{cases} \frac{4}{L\pi}, \text{ for } 0 \leq x \leq \frac{L}{2}, 0 \leq \theta \leq \frac{\pi}{2} \\ 0, \text{ otherwise} \end{cases}$$

The condition that the needle crosses a line on the floor translates, as one can easily see in figure 1, to : $x \leq \frac{a}{2}cos\theta$. Therefore, the required probability of a needle intersecting a line on the floor is :

$$P = \int_0^{\frac{\pi}{2}}\int_0^{\frac{a}{2}cos\theta} \frac{4}{L\pi}dxd\theta = \frac{4}{L\pi}\int_0^{\frac{\pi}{2}} \frac{a}{2}cos\theta d\theta = \frac{2a}{L\pi}\int_0^{\frac{\pi}{2}} cos\theta d\theta = \frac{2a}{L\pi}.$$

As we can see, the two probabilistic solutions yield the same result, as we would have hoped.

3. The Monte Carlo simulations approach

The idea of the Monte Carlo method, briefly put, is the following: instead of a theoretical calculation of the probability for the needle to intersect a line on the floor, we can do an experiment in which we repeatedly throw a needle on the floor and count how many times the needle intersects a line on the floor. With a large enough number of throws, we will get a good approximation of the probability required by dividing the number of "successes" to the total number of attempts.

Indeed, when using Monte Carlo simulations to estimate the probability of the event A: "needle crosses the line" occuring, it can be shown [3] that $\hat{p}(A) = \frac{n_A}{n}$, where n_A is the number of occurences of A and n is the total number of trials, is un unbiased estimate of $P\{A\}$ (probability of A). Using

BuffonNeedle(n , a , L) :=
H ← 0
for i ∈ 1 .. n
  θ ← rnd(π/2)
  x ← rnd(L/2)
  H ← H + 1 if x < (a/2)·cos(θ)
H/n

Figure 4. Function that implements the algorithm for the Monte Carlo simulation in Mathcad

the central limit theorem [4, 5], it can also be shown that for large values of n, $\hat{p}(A)$ is normally distributed with mean $P\{A\}$ and standard deviation $\sigma_{\hat{p}} = \sqrt{\frac{P\{A\}(1-P\{A\})}{n}}$. In general, the standard error approaches zero with the speed of $\frac{1}{\sqrt{n}}$ (see, e.g. [3, 4]) and therefore, to increase precision by a factor of 10, a multiplication of n by a factor of 100 is required.

The error in Monte Carlo simulation method is probabilistic and therefore we cannot impose strict limits to it, like in the case of some numerical methods. However, with the increase of n, the probability of the error to be larger than a given ϵ approaches zero.

Of course, using a computer and a random (or pseudo-random) number generator, we can conveniently replace the physical experiment with a simulation. Thus, the Mathcad code in figure 4 uses the predefined $rnd(z)$ function, which generates uniformly distributed pseudo-random numbers in the range $(0; z)$ to assign to the angle θ a uniformly distributed random value between 0 and $\frac{\pi}{2}$ and to the distance x a uniformly distributed random value between 0 and $\frac{L}{2}$. Then it checks if the "needle" intersects the "line", i.e., if $x < \frac{a}{2}cos\theta$. We count the "successes" and divide their number H to the total number n of attempts, thus estimating the required probability.

Simulation run no.	$n = 10^2$	$n = 10^4$	$n = 10^6$
1	0.09	0.0528	0.050968
2	0.03	0.0531	0.051326
3	0.05	0.0532	0.051316
4	0.07	0.0498	0.050416
5	0.09	0.0544	0.050772
6	0.03	0.0484	0.051149
7	0.04	0.0509	0.051033
8	0.06	0.0494	0.050861
9	0.04	0.0489	0.051187
10	0.03	0.0501	0.05055
Mean	0.053	0.0511	0.0509578
Standard deviation	0.02359378	0.0021066	0.00030956

Table 1. Results of Monte Carlo simulation performed using function in figure 4 with $L = 50cm$, $a = 4cm$ and $n = 10^2, 10^4, 10^6$

Clearly, the Monte Carlo simulations method cannot be used to find a formula for the desired probability. However, for any specific values of L and a we can compute the estimated probability (and perhaps compare it to the result of a probabilistic theoretical formula, if such a formula was obtained).

For example, we ran the Mathcad function presented in figure 4, using a value of $L = 50cm$ and $a = 4cm$. The theoretically predicted value of the probability of the needle crossing the line is in this case $P = \frac{2a}{L\pi} = 0.05092958$. Table 1 shows the results we obtained when running the simulation program for ten times, first for a number n of "needle throws" of 10^2 (column 2), then 10^4 and 10^6 (column 3 and 4, respectively). On the last two lines we computed the mean and standard deviation for the ten simulations ran for each of the three values of n. As we can see, the data in table 1 is in perfect agreement with the general considerations regarding the error in Monte-Carlo simulations and, e.g., for $n = 10^2, 10^4, 10^6$ we have an error of less than $10^{-1}, 10^{-2}, 10^{-3}$, respectively.

4. Conclusion

We have discussed here two different ways of computing the theoretical probability that represents the answer to Buffon's needle problem and we have compared these theoretical results with the estimation

found by means of Monte Carlo simulations. Since the results of all three methods agree, we can now trust our solution to be accurate and moreover, we can trust that those methods were applied in an adequate manner. As we can see, Monte Carlo simulation methods are a handy alternative to theoretical probabilistic approach. The integrals we had to compute in order to obtain the theoretical probability were in this case very simple, but in many, e.g., engineering problems, we can encounter multidimensional integrals on complicated domains, where the integral can be impossible (or *very* impractical) to compute, even by (traditional) numerical methods. In these cases, the Monte Carlo method may be easily applied. Moreover, the number of Monte Carlo trials that must be considered in order to obtain the desired precision does not depend of the number of dimensions - a huge advantage over traditional numerical methods.

References

[1] L.Schroeder, *Buffon's needle problem: An exciting application of many mathematical concepts.*, Mathematics Teacher **67**(2) (1974), 183-186.

[2] W.Cheney, D. Kincaid *Numerical Mathematics and Computing. 2nd Ed.*, Ed. Pace Grove, California: Brooks/Cole Publishing Company (1985).

[3] Karen Willcox, and Qiqi Wang. 16.90 Computational Methods in Aerospace Engineering. Spring 2014. Massachusetts Institute of Technology: MIT OpenCourseWare, https://ocw.mit.edu.

[4] M.H.Kalos. and P. Whitlock, *Monte Carlo Methods, Second Ed.*,Wiley-VCH Verlag GmbH&Co. KGaA (2008).

[5] R. Durrett *Probability: Theory and Examples. Fourth Ed.*, Cambridge University Press (2010)

Department of Mathematics and Computer Science, Technical University of Civil Engineering Bucharest, Bucharest, Romania

and

"Ilie Murgulescu" Institute of Physical Chemistry, Romanian Academy, Bucharest, Romania

Email address: dancaraghe@gmail.com

COPULA AND CO-COPULA FOR DISCHARGES AND VOLUMES

DANIEL CIUIU, ROMICĂ TRANDAFIR AND RADU DROBOT

ABSTRACT. In this paper we will study the discharges and the volumes of Prut River at Rădăuţi using copula and co-copula.

We will estimate the parameters of the marginals and the parameter θ of the copula separately, using the moments' method, respectively the Kendall's τ.

Mathematics Subject Classification (2010): 62H12, 62P30, 62H10
Key words: copula, co-copula co-copula, discharges, volumes

1. INTRODUCTION

Definition 1.1 (Sungur and Tuncer, 1987; Nelsen, 1991; Flores, 2009). *A copula is a function* $C : [0,1]^n \to [0,1]$ *such that*

(1) If there exists i *such that* $x_i = 0$ *then* $C(x_1, ..., x_n) = 0$.
(2) If $x_j = 1$ *for all* $j \neq i$ *then* $C(x_1, ..., x_n) = x_i$.
(3) C *is increasing in each argument.*

We have the following theorem (Sungur and Tuncer, 1987; Nelsen, 1991; Schweizer, 1991).

Theorem 1.2 (Sklar). *Let* X_1, X_2,..., X_n *be random variables with the cummulative distribution functions* F_1, F_2,..., F_n, *and the common cdf* $H(x_1, ..., x_n) = P(X_1 \leq x_1, ..., X_n \leq x_n)$. *In this case there exists a copula* $C(u_1, ..., u_n)$ *such that* $H(x_1, ..., x_n) = C(F_1(x_1), ..., F_n(x_n))$. *The copula* C *is well defined on the chartesian product of the images of the marginals* F_1, F_2,..., F_n.

For any $n-$copula C we have (Dall' Aglio, 1991)

$$W(x_1, ..., x_n) \leq C(x_1, ..., x_n) \leq \min(x_1, ..., x_n), \text{ where} \tag{1.1}$$

$$W(x_1, ..., x_n) = \sum_{i=1}^{n} x_i - n + 1 \tag{1.1'}$$

is the lower Fréchet bound, and min is the upper Fréchet bound.

Definition 1.3 (Sungur and Tuncer, 1987; Văduva, 1994; Văduva, 2003). *For* $n = 2$ *the copula* C *is Archimedean if* $C(u,u) < u$ *for any* $u \in (0,1)$ *and* $C(C(u,v), w) = C(u, C(v,w))$ *for any* $u, v, w \in [0,1]$. *For* $n > 2$ *the copula* C *is Archimedean if there exists a* $n-1$ *Archimedean copula* C_1 *and a* 2 *Archimedean copula* C_2 *such that* $C(u_1, ..., u_n) =$
$C_2(C_1(u_1, ..., u_{n-1}), u_n)$.

Consider a function $\varphi : [0,1] \to \mathbb{R}$ decreasing and convex with $\varphi(1) = 0$ and its pseudoinverse g ($g(y)$ has the value x if there exists x such that $\varphi(x) = y$ and 0 in the contrary case). We know (Genest, 1993; Sungur and Tuncer, 1987) that a copula C is Archimedean if and only if there exists a function φ as above such that for any $x, y \in [0,1]$ we have

$$C(x,y) = g(\varphi(x) + \varphi(y)). \tag{1.2}$$

In literature (Dall' Aglio, 1991; Genest, 1993; Flores, 2009; Nelsen, 1991; Kotz and Seeger, 1991) there are presented the values of ϕ and g for several families of archimedean copulas, as Clayton, Frank, Gumbel—Hougaard, Gumbel—Barnett and Ali—Mikhail—Haq families.

To compute the above generating function φ we use the ratio of some partial derivatives as in Mereuţă, Albu and Ciuiu (2011); Trandafir, Ciuiu and Drobot (2011); Ciuiu (2010):

$$\frac{\frac{\partial C}{\partial u}}{\frac{\partial C}{\partial v}} = \frac{\varphi'(u;\theta)}{\varphi'(v;\theta)} \tag{1.3}$$

Together with copula, which represents the common non-exceedance probability, for exceedance probability it is used the notion of co-copula. The bivariate co-copula is (Văduva, 1994)

$$\widetilde{C}(u,v) = C(u,v) + 1 - u - v. \tag{1.4}$$

For an $n-$variate co-copula, the value is the sum of the values of C defined on subsets of u_1,..., u_n, multiplied by the sign -1 rised to the power of the number of missing variables u_j. Of course, $C(u) = u$.

2. Methodology

For estimating the parameters of copula, we use the Kendall τ (Nelsen, 1991):

$$\begin{array}{c} \tau = P((X_1 - X_2)(Y_1 - Y_2) > 0) - P((X_1 - X_2)(Y_1 - Y_2) < 0) = \\ 4\int_0^1\int_0^1 C(u,v)\frac{\partial^2 C}{\partial u \partial v}dudv - 1 = 1 - 4\int_0^1\int_0^1 \frac{\partial C}{\partial u}\cdot\frac{\partial C}{\partial v}dudv. \end{array} \tag{2.1}$$

In Trandafir, Ciuiu and Drobot (2010) there are presented analytical formulae for θ in terms of τ:

$$\theta(\tau) = \begin{cases} \frac{2\tau}{1-\tau} \ for\ Clayton \\ \frac{1}{1-\tau} \ for\ Gumbel - Hougaard \\ \frac{9\tau}{2} \ for\ Farlie - Gumbel - Morgestern \end{cases}. \tag{2.2}$$

For the Frank family we have to solve (Mereuţă, Albu and Ciuiu, 2011; Trandafir, Ciuiu and Drobot, 2011) the Cauchy problem

$$\begin{cases} \theta'(\tau) = \frac{\theta^2}{2(1-\tau)+4-\frac{4\cdot\theta}{e^\theta-1}} \ for\ \tau \neq 0 \\ \theta'(0) = 9 \\ \theta(0) = 0 \end{cases}. \tag{2.3}$$

For the Gumbel—Barnett we have (Trandafir, Ciuiu and Drobot, 2011; Mereuţă, Albu and Ciuiu, 2011)

$$\tau(\beta) = -e^\beta \cdot \int_\beta^\infty \frac{e^{-x}}{x}dx < 0, \tag{2.4}$$

where $\beta = \frac{2}{\theta}$.

We perform the change of variable $y = e^{-x}$, and we obtain

$$\tau(\beta) = e^{\beta} \cdot \int_0^{e^{-\beta}} \frac{dy}{\ln y}. \tag{2.4'}$$

By differentiation we obtain first

$$\tau'(\beta) = \frac{\beta \cdot \tau + 1}{\beta}, \text{ and} \tag{2.5}$$

$$\beta'(\tau) = \frac{\beta}{\beta \cdot \tau + 1}. \tag{2.5'}$$

Therefore, denoting by $\alpha = \tau(2) = e^2 \cdot \int_0^{e^{-2}} \frac{dy}{\ln y}$, we have to solve the Cauchy problem

$$\begin{cases} \beta'(\tau) = \frac{\beta}{\beta \cdot \tau + 1} \\ \beta(\alpha) = 2 \end{cases}. \tag{2.6}$$

We solve this Cauchy problem by the Runge—Kutta method as in the Frank case, and the involved integral for computing α is computed by the Simpson method.

For the Ali—Mikhail—Haq copula we have

$$\begin{cases} \tau(\theta) = 1 - \frac{2(1-\theta)^2 \ln(1-\theta)}{3\theta^2} - \frac{2}{3\theta} \\ \tau(-1) = \frac{5 - 8\ln 2}{3} \\ \tau(0) = 0 \\ \tau(1) = \frac{1}{3} \end{cases}, \tag{2.7}$$

and we estimate θ from τ using the bisection method.

After we compute the empirical value of τ as the difference of shares of same increase/ oposite increase, we take into account that not all the families of copula can have any $\tau \in [-1, 1]$. In the followinf table we present the limits of θ.

TABLE 1. The limits of τ for different types of copula

Type	Lower limit	Upper limit
Clayton	0	1
Frank	-1	1
Gumbel—Hougaard	0	1
Gumbel—Barnett	-0.35949 for $\theta = 1$	0 for $\theta = 0$
Ali—Mikhail—Haq	$\frac{5-8\ln 2}{3}$ for $\theta = -1$	$\frac{1}{3}$ for $\theta = 1$
Farlie—Gumbel—Morgestern	$-\frac{2}{9}$ for $\theta = -1$	$\frac{2}{9}$ for $\theta = 1$

We notice that only for the Frank family we can have any $\tau \in [-1, 1]$. For the Ali—Mikhail—Haq family, we mention that $\frac{5-8\ln 2}{3} = -0.18173$.

3. Case study

Consider the yearly data on discharges and volumes of Prut River at Rădăuţi gauge station in the period $1987 - 2016$ (30 years). During this period two extreme events occured: the flood in 2008, characterized by a maximum discharge of $4240 m^3/s$ (probability of the exceedance in the range $0.8 - 1\%$) and the flood in 2010, whose volume was $2.4 \cdot 10^9 m^3$ (probability of the exceedance between $0.5 - 0.8\%$), meaning return periods between $100 - 200$ years. These two values are outliers.

The operation rules of the reservoires during flood period are obtained using so–called synthetic floods. They are derived on the registred floods, which usually cover a period of $30 - 50$ years. By extracting the statistical information from this limited sample maximum discharges and flood volumes with much higher return periods, like 100 years or 1000 years, are obtained. The inverse ratio of the return period T is in fact the probability of exceedance: $P = \frac{1}{T}$.

The most common probabilities of exceedance required in the design and operation of the hydraulic structures (like dams, which creates water reservoirs) are 0.1%, 1% and 10%. The synthetic floods are defined by the maximum discharge, the flood volume, the time to peak and the total duration. It is usually accepted that a flood cannot have in the same time the maximum discharge $Q^{max}_{P\%}$ and the flood volume $V_{P\%}$, corresponding to the same probability of exceedance $P\%$.

Consequently, the pair $(Q^{max}, V)_{P\%}$ representing the couple of variables Q and V characterized by the probability of exceedance $P\%$ is required. The isolines $P\%$ (the co-copula) for 0.1%, 1% and 10% are derived based on registered pairs of values Q^{max} and V.

The Stânca—Costeşti reservoir, which is located downstream the mentioned gauging station has a flood storage of $550 \cdot 10^6 m^3$, being very sensitive to flood volume. For this reason, two scenarios were analised: in the first scenario (S_1) the 2010 flood was excluded from the data series (obtaining 29 data points), while in the second scenario (S_2) it was considered in the data series with an empirical probability of exceedance according to Hazen formula.

Consider the marginal probabilities Pearson III (Gamma with drift). In the case of S_1 scenario we obtain the following parameters using the moments' method.

Table 2. The marginal parameters for discharges and volumes in the case S_1

Discharges or volumes	a	b	c
Discharge	0.522927356	825.4039909	533.4735615
Volume	0.289175769	813.549611	108.0945082

Because $\tau = 0.56322$, we can have only three types of copula, namely Clayton, Frank and Gumbel—Hougaard. The values of θ, according (2.2) and the Cauchy problem in the case of Frank family, are presented in Table 3 that follows.

Table 3. The values of θ if $\tau = 0.56322$ for the three types of copula

Type	θ
Clayton	2.57895
Frank	0.00897
Gumbel—Hougaard	2.28947

Th most appropiate type is the Gumbel—Hougaard case.

In Fig. 1, the isolines correponding to co-copula 0.1%, 1% and 10% for scenarios S_1 and S_2 (with and without the discharge and volume in 2010).

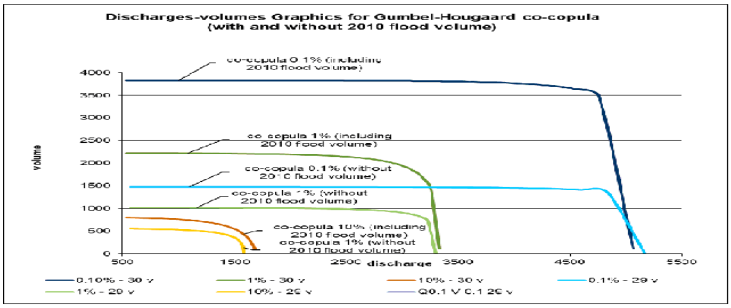

FIGURE 1. Co-copula for the scenarios S_1 and S_2

In the next picture we present the above three level copula and co-copula in the Gumbel—Hougaard case, without the outlier from 2010.

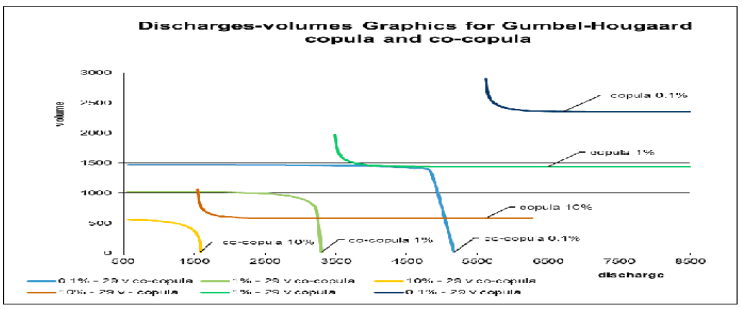

FIGURE 2. Copula and co-copula for 0.1%, 1% and 10%

4. Conclusions

In (Văduva, 1994; Văduva, 2003) there are presented methods to simulate Archimedean copulas.

For the two outliers in the data of Rădăuţi-Prut gauging station special precautions have to be taken in order to capitalize this valuable information about future events, which could occur during the dam life.

In fact, the presence of an outlier (the flood volume in 2010) raised serious problems related to the hydrological soundness of the statistical analysis both for univariate and bivariate analysis. Two alternatives were considered: including the data for 2010 in the series data and neglecting these data respectively. A critical analysis of the obtained results in both alternatives were presented.

References

[1] G. Dall' Aglio, *Fréchet classes: the beginning*, in "Advances in Probability Distributions with Given Marginals. Beyond the Copulas", G. Dall' Aglio, S. Kotz and G. Salinetti (Eds.), Kluwer Academic Publishers (1991), 1-12.

[2] P.A. Bares, G, Rajna and S. Gyger, *Style Consistency and Survival Probability in the Hedge Funds Industry*, EFA 2001, Barcelona Meetings and EFMA (2001), Lugano Meetings.

[3] D. Ciuiu, Simulation of Queing Systems with Many Stations and of Queueing Networks Using Copulas, Scientific Journal Mathematical Modeling in Civil Engineering

[4] A.Q. Flores, *Testing Copula Functions as a Method to Derive Bivariate Weibull Distributions*, Report New York University, Nov. 4, 2009.

[5] C. Genest, *Statistical Inference Procedures for Bivariate Archimedean Copulas*, Journal of American Statistical Association, **88(423)** (1993), 1034-1043.
[6] Ioanis A. Koutrouvelis, *Esimation in the Pearson 3 distribution*, Water Resources research **35 (9)** (1999), 2693-2704.
[7] S. Kotz and J.P. Seeger, *A new approach to dependence in multivariate distributions*, in "Advances in Probability Distributions with Given Marginals. Beyond the Copulas", G. Dall' Aglio, S. Kotz and G. Salinetti (Eds.), Kluwer Academic Publishers (1991), 113-127.
[8] C. Mereuţă, L.L. Albu and D. Ciuiu, *Classification of Competitiveness Types Using Copula*, in "Non-Linear Models Applied in Economics. Beyond Standard Economics", Lucian Liviu Albu (Ed.), Editura Expert (2011), 147-165.
[9] R.B. Nelsen, *Copulas and association*, in *Advances in Probability Distributions with Given Marginals. Beyond the Copulas*, in "Advances in Probability Distributions with Given Marginals. Beyond the Copulas", G. Dall' Aglio, S. Kotz and G. Salinetti (Eds.), Kluwer Academic Publishers (1991), 51-74.
[10] R.B. Nelsen, *An Introduction to Copulas*, Springer-Verlag, New York, 1999.
[11] R. Regnate et al., *Clinical Characteristic and Four-Year Outcomes of Patients in the Rhode Island Takotsubo Cardiomypaty Registry*, American Journal of Cardiology, **103(7)** (2009), 1015-1019.
[12] G. Salvadori and C. De Michele, *On the Use of Copulas in Hydrology: Theory and Practice*, J. Hydrologic Engrg. **12(4)** (2007), 369-380.
[13] V.P. Singh and H. Guo, *Parameter estimation for 3-parameter generalized Pareto distribution by the principle of maximum entropy (POME)*, Hydrological Science **40 (2)** (1995), 165-181.
[14] Schweizer, B. and Sklar, A. (1983), *Probabilistic Metric Spaces*, North-Holland, New York.
[15] Schweizer, B (1991), "Thirty years of copulas", in "Advances in Probability Distributions with Given Marginals. Beyond the Copulas", G. Dall' Aglio, S. Kotz and G. Salinetti (Eds.), Kluwer Academic Publishers (1991), 13-50.
[16] Shih, J.H. and Thomas, L.A. (1995), "Inference of the Association Parameter in Copula Models for Bivariate Survival Data", *Biometrics*, **51(4)**, pp. 1384-1399.
[17] Sklar, A. (1959), "Fonctions de répartition a n dimensions et leur marges", *Publications de l'Institut de Statistique de l'Université de Paris*, **8**, pp. 229-231.
[18] Sungur, E. and Tuncer, Y. (1987), "The Use of Copulas to Generate New Multivariate Distributions", in *The Frontiers of Statistical Computation, Simulation & Modeling. Volume I of the Proceedings of the ICOSCO-I Conference (The First International Conference on Statistical Computing, Çeşme, Izmir, Turcia, 1987*, pp. 197-222.
[19] Trandafir, R., Ciuiu, D. and Drobot, R. (2011), "The Utilization of Copula in Hydrology", *Scientific Journal Mathematical Modeling in Civil Engineering*, **7 (2 BIS)**, pp. 12-19.
[20] Văduva, I. (1994), *Fast Algorithms for Computer Generation of Random Vectors used in Reliability and Applications*, Preprint nr. 1603, ian. 1994, TH—Darmstadt.
[21] Văduva, I. (2003), "Simulation of some Multivariate Distributions", *Analele Universităţii Bucureşti*, **1**, pp. 127-140.

Department of Mathematics and Computer Science, Technical University of Civil Engineering Bucharest, Bucharest, Romania, Center for Macroeconomic Modeling, National Institute for Economic Research Costin C. Kiriţescu
E-mail address: dciuiu@yahoo.com

Department of Mathematics and Computer Science, Technical University of Civil Engineering Bucharest, Bucharest, Romania
E-mail address: romica@utcb.ro

Department of Hydraulic Constructions, Technical University of Civil Engineering Bucharest, Bucharest, Romania
E-mail address: drobot@utcb.ro

ALGORITHMS FOR DETERMINING THE LARGEST EIGENVALUE OF A SQUARE MATRIX

Ştefania Constantinescu
Department of Mathematics and Computer Science
Technical University of Civil Engineering Bucharest, Romania
E-mail: c_aurora32@yahoo.com
Ion Mierluş-Mazilu
Department of Mathematics and Computer Science
Technical University of Civil Engineering Bucharest, Romania
E-mail: mmi@utcb.ro

Abstract: It is well known that in many practical applications in different technical, economic and scientific fields it is very important to know the largest eigenvalue and corresponding eigenvector of a square matrix. The paper presents the power method and its variants and also the corresponding algorithms programmed in R and MathCAD software to determining the largest eigenvalue and associated eigenvector of a square matrix. The results obtained with these algorithms are compared for some examples with the results given by the implemented algorithms in R and MathCAD.
Mathematics Subject Classification (2010): 30B10, 30B50
Key words: square matrix, eigenvalue, eigenvector, Rayleigh quotient, power method

1. Introduction

1.1. Preliminaries: definitions, properties

Definition 1. Let $A \in \mathcal{M}_{n\times n}(R,C)$ be a square matrix of real or complex number. The polynomial $P(\lambda) = \det(A - \lambda I)$ is called characteristic polynomial, and its roots are called its eigenvalues, and the vectors $x^{(i)} \in R^n(C^n) \setminus \{\mathbf{0}\}$, $i = 1,2,..,n$ that are solutions of the system are called eigenvectors corresponding to their eigenvalues.
We consider the eigenvalues order as follows: $|\lambda_1| > |\lambda_2| \geq |\lambda_3| \geq ... \geq |\lambda_n|$.

Definition 2. λ_1 is its dominant value, and the set $\{\lambda_1, \lambda_2, ..., \lambda_n\}$ is the spectrum of the matrix *A*.

Definition 3. The matrix *A* is Hermitian if $A = A^* = \overline{A^T}$ (transposed and conjugated $a_{ij}^* = \overline{a}_{ij}$, $1 \leq i, j \leq n$).

Proposition 1. If *A* is Hermitian, its eigenvalues are real, and if they are distinct, the eigenvectors are orthogonal two by two.

Definition 4. The matrix *A* is positively defined if $(\forall) x \in R^n\left(C^n\right)$, $x \neq \mathbf{0} \Rightarrow x^* Ax > 0$.

Proposition 2. If the matrix *A* is Hermitian and positive defined then the own values of *A* are real and positive.

Proposition 3. If λ is the eigenvalue of the non-singular matrix *A*, then $\frac{1}{\lambda}$ is the eigenvalue of matrix A^{-1}, and the both matrices have the same system of eigen vectors.

1.2. Short history

Euler (18th century) studying the rotation motion of a rigid body and highlighting the importance of the main axis of rotation.

Lagrange has discovered that the main axes are eigenvectors of the inertial matrix.

Cauchy (19th century) introduced the term " racine caracteristique " (the equivalent of eigenvalue); based on the ideas of Fourier and Sturm, Cauchy establishes the fundamental result that any real symmetric matrix has real eigenvalues (Hermite extended this result in 1855 to Hermitian matrices).

Hilbert (20th century) studies the values of the integral operators by considering infinite matrix operators. He is the first scientist to use the German term "eigen", meaning " proper ", to denote eigenvalues / eigenvectors (in 1904). The corresponding English term: "proper value," but "eigenvalue" is standard.

In 1929, Von Mises published the power method, thus defining the first numerical algorithm for calculating the eigenvalues / eigenvectors.

In 1961, John G.F. Francis and Vera Kublanovskaya proposed independently one of the most popular methods, the QR algorithm, to obtain eigenvalues and eigen vectors.

1.3. Some possible areas of application

Principal components analysis (PCA) is a statistic procedure that makes, by orthogonal transformation, the conversion of a sample data set into a set of linearly uncorrelated values, called principal components. The transformation is done so that the first principal component is the largest possible variation (explain the greatest variation of data). The main components are orthogonal because they represent the eigenvectors of the symmetrical matrix of covariance Σ. PCA is defined by a linear orthogonal transformation that bring the initial data into a new coordinate system such that the maximum version obtained by projections of data is on the first coordinate (called the first principal component), the second highest variation on the second coordinated and so on.

In the areas of **artificial vision and portrait recognition**, the main component of the covariance matrix Σ is used, corresponding to the largest eigenvalue of this matrix: $\Sigma = TT^T$ where T is the matrix of training examples.

Determination of the largest λ_1 (low λ_n) eigenvalues of a matrix is a problem of great interest in many real-life applications (**geoseism vibrations, machines and structures, electrical network analysis, quantum mechanics**, etc.) where the calculation of eigenvalue λ_n / λ_1 (and of the corresponding eigenvector x_n / x_1) occurs in the determination of the frequency (and the fundamentally corresponding mode) of a given physical system.

We consider that the presented examples fully justify the interest in more accurately determining the most significant absolute value of eigenvalue and the corresponding vector.

In the following we present the power method and its variants and the corresponding algorithms of these methods. The algorithms are programmed into MathCAD and R and are applied to a square matrix of real numbers. Finally, some comments are made on the results presented.

2. Power method

2.1. Presentation of the method

It's supposed to be inequality

$$|\lambda_1| > |\lambda_2| \geq |\lambda_3| \geq \ldots \geq |\lambda_n| \qquad (1)$$

Consider that the initial vector $x^{(0)}$ has a component in the direction of its own vector $x^{(1)}$ corresponding to its eigenvalue λ_1 (the non-restrictive hypothesis, because in the algorithm we will consider a random vector $y^{(0)}$, $\|y^{(0)}\| = 1$).

We consider the decomposition of vector $y^{(0)}$ based on the basis of its own vectors

$$y^{(0)} = \alpha_1 x^{(1)} + \ldots + \alpha_n x^{(n)}, \ \alpha_1 \neq 0 \qquad (2)$$

and construct the vectors string

$$y^{(k+1)} = Ay^{(k)} = A^2 y^{(k-1)} = \ldots = A^{k+1} y^{(0)} \quad , \; k \geq 0 \tag{3}$$

For $k = 1$ we obtain

$$y^{(1)} = Ay^{(0)} = \lambda_1 \alpha_1 x^{(1)} + \lambda_2 \alpha_2 x^{(2)} + \ldots + \lambda_n \alpha_n x^{(n)} =$$
$$= \lambda_1 \left[\alpha_1 x^{(1)} + \frac{\lambda_2}{\lambda_1} \alpha_2 x^{(2)} + \ldots + \frac{\lambda_n}{\lambda_1} \alpha_n x^{(n)} \right] \tag{4}$$

and so, on

$$y^{(k)} = A^k y^{(0)} == \left(\lambda_1\right)^k \left[\alpha_1 x^{(1)} + \left(\frac{\lambda_2}{\lambda_1} \right)^k \alpha_2 x^{(2)} + \ldots + \left(\frac{\lambda_n}{\lambda_1} \right)^k \alpha_n x^{(n)} \right] \tag{5}$$

Because $|\lambda_1| > |\lambda_2|$ then $\left(\frac{\lambda_2}{\lambda_1} \right)^k \xrightarrow{k \to \infty} 0$ and thus

$$y^{(k)} \approx \left(\lambda_1\right)^k \alpha_1 x^{(1)} = \lambda_1 \left(\lambda_1\right)^{k-1} \alpha_1 x^{(1)} = \lambda_1 y^{(k-1)} \tag{6}$$

So, considering any component $x_i^{(k)}$, $1 \leq i \leq n$

$$\lambda_1 \approx \frac{y_i^{(k)}}{y_i^{(k-1)}} \; , \; 1 \leq i \leq n \tag{7}$$

To avoid the extreme situations that lead to its very small non-component components, it will always be considered that the vector is normalized!

The stop condition will be when two consecutive iterations do not get λ_1 a better value than the previous modulo $\varepsilon > 0$ a fixed value (the accepted error).

2.2. Algorithms

a. Coded in MathCAD

```
Power method
Determining the largest eigenvalue and corresponding eigenvector
A - Hermitian matrix
ε - accepted error
λ - the largest eigenvalue
x - corresponding eigenvector
m - the iteration number

MP(A, ε) :=
    n ← length(A^⟨1⟩)
    m ← 0
    for i ∈ 1..n
        y_i ← rnd(1)
    y ← y / sqrt(y^T · y)
    x ← A · y
    x ← x / sqrt(x^T · x)
    while sqrt((y − x)^T · (y − x)) > ε
        m ← m + 1
        y ← x
        x ← A · y
        x ← x / sqrt(x^T · x)
    λ ← x^T · A · x
    return (x, λ, m)
```

b. Coded in R

```
MP=function(A,eps)
 {
 eps = 10e-8
 n<-length(A[,1]);
 #n
 m<-0;
 #m
 x0<-matrix(c(runif(n)),ncol=1);x0
 #x0
 x0<-x0/as.numeric(sqrt(t(x0)%*%x0));x0
 #x0
 x<-A%*%x0;x
 #x
 x<-x/as.numeric(sqrt(t(x)%*%x));x
 #x
 while(as.numeric(sqrt(t(x-x0)%*%(x-x0)))>eps)
   {m<-m+1;
   #m
   x0<-x;
   #x0
   x<-A%*%x0;
   #x
   x<-x/as.numeric(sqrt(t(x)%*%x));
   #x
   }
 # Determining the largest eigenvalue
 l<-as.numeric(t(x)%*%A%*%x);
 l
 x
 m
 #Return
  #the largest eigenvalue lambda
  #the corresponding eigenvector
  #number of iterations
  return(list(lambda = l,
              eigenvector = x,
              number_iter = m))
}
```

Figure 1

Algorithms for Power Method coded in MathCAD and R

Consider the following numerical example with the hermitic matrix A and the approximate error ε,

$$A = \begin{pmatrix} 5 & 1 & 0 & 1 \\ 1 & 4 & -1 & 1 \\ 0 & -1 & 6 & 2 \\ 1 & 1 & 2 & 7 \end{pmatrix}, \; \varepsilon = 10^{-8}. \tag{8}$$

The Table 1 contains the numerical results obtained with the two programs for the matrix A and the error of approximation ε and those obtained with the algorithms implemented in MathCAD and R.

Table 1
Results obtained with the algorithm

MathCAD						
own	λ_1	$x^{(1)}$	No_ iter	intrinsec	λ_1	$x^{(1)}$
	8.77673288	0.23980451 0.10500736 0.53888261 0.80067021	50		8.77673288	0.23980451 0.10500736 0.53888261 0.80067021

R						
own	λ_1	$x^{(1)}$	No iter	intrinsec	λ_1	$x^{(1)}$
	8.776733	0.2398046 0.1050075 0.5388825 0.8006702	32		8.776733	0.2398045 0.1050074 0.5388826 0.8006702

Since the vector with which the algorithms are initialized are random, the number of iterations varies, but very little, around the displayed values (No_iter ± 2).

3. Rayleigh quotient

3.1. Presentation of the method

Let x be an n-dimensional vector and A the Hermitian square matrix. Then our own values are real, and if two by are different and the eigenvectors are orthogonal two by two.

The ratio $R(x)=\dfrac{x^* Ax}{x^* x}$ is called the *Rayleigh quotient.* It is known that if x is the eigenvector of A corresponding to eigenvalue λ, then $R(x)=\lambda$ it is possible to determine an approximation of its eigenvalue by Rayleigh quotient.

We still assume that $|\lambda_1|>|\lambda_2|\geq|\lambda_3|\geq\ldots\geq|\lambda_n|$ it is known that for every x there is a relationship $|\lambda_1|\geq R(x)\geq|\lambda_n|$.

$$R_k(y)=\frac{\left(y^{(k-1)}\right)^* Ay^{(k-1)}}{\left(y^{(k-1)}\right)^* y^{(k-1)}}=\frac{\alpha_1^*\left(\lambda_1^*\right)^{k-1}\left\{\left(x^{(1)}\right)^*+\alpha_2^*\left(\dfrac{\lambda_2^*}{\lambda_1^*}\right)^{k-1}\left(x^{(2)}\right)^*+O\left[\left(\dfrac{\lambda_2^*}{\lambda_1^*}\right)^{k-1}\right]\right\}}{\alpha_1^*\left(\lambda_1^*\right)^{k-1}\left\{\left(x^{(1)}\right)^*+\alpha_2^*\left(\dfrac{\lambda_2^*}{\lambda_1^*}\right)^{k-1}\left(x^{(2)}\right)^*+O\left[\left(\dfrac{\lambda_2^*}{\lambda_1^*}\right)^{k-1}\right]\right\}} \tag{9}$$

$$\frac{\alpha_1\left(\lambda_1\right)^k\left\{\left(x^{(1)}\right)+\alpha_2\left(\dfrac{\lambda_2}{\lambda_1^*}\right)^{k-1}\left(x^{(2)}\right)+O\left[\left(\dfrac{\lambda_2}{\lambda_1}\right)^{k-1}\right]\right\}}{\alpha_1\left(\lambda_1\right)^{k-1}\left\{\left(x^{(1)}\right)+\alpha_2\left(\dfrac{\lambda_2}{\lambda_1}\right)^{k-1}\left(x^{(2)}\right)+O\left[\left(\dfrac{\lambda_2}{\lambda_1}\right)^{k-1}\right]\right\}}= \tag{10}$$

$$=\lambda_1\frac{1+O(\beta^{2k-1})}{1+O(\beta^{2k-2})}=\lambda_1\left[1+O(\beta^{2k})\right],\ \beta=\frac{\lambda_2}{\lambda_1}. \tag{11}$$

Thus $R=\lim_{k\to\infty}R_k(y)=\lambda_1$.

3.2. Algorithms

a. Coded in MathCAD

Rayleigh quotient

A - Hermitian matrix
ε - accepted eroarea
Determining
λ the largest eigenvalue
x the corresponding eigenvector
m the number of iterations

$$\text{Ray}(A,\varepsilon) := \left| \begin{array}{l} n \leftarrow \text{length}\left(A^{\langle 1 \rangle}\right) \\ m \leftarrow 0 \\ \text{for } i \in 1..n \\ \quad y_i \leftarrow \text{rnd}(1) \\ y \leftarrow \dfrac{y}{\sqrt{y^T \cdot y}} \\ r \leftarrow y^T \cdot A \cdot y \\ x \leftarrow A \cdot y \\ x \leftarrow \dfrac{x}{\sqrt{x^T \cdot x}} \\ R \leftarrow x^T \cdot A \cdot x \\ \text{while } (|R - r| > \varepsilon) \\ \quad \left| \begin{array}{l} m \leftarrow m + 1 \\ r \leftarrow R \\ y \leftarrow x \\ x \leftarrow A \cdot y \\ x \leftarrow \dfrac{x}{\sqrt{x^T \cdot x}} \\ R \leftarrow x^T \cdot A \cdot x \end{array} \right. \\ \text{return} \begin{pmatrix} x \\ R \\ m \end{pmatrix} \end{array} \right.$$

b. Coded in R

```
Ray=function(A,eps)
 {
 # Determining the largest eigenvalue
 #the corresponding eigenvector
 #number of iterations

eps = 10e-8
 n<-length(A[,1]);
 #n
 m<-0;
 #m
 y<-matrix(c(runif(n)),ncol=1);
 #y

 r<-(t(y)%*%A%*%y)/(t(y)%*%y);
 #r
 x<-A%*%y;
 #x
 R<-(t(x)%*%A%*%x)/(t(x)%*%x);
 #R

 while(abs(R-r)>eps)
  {m<-m+1;
  #m
  r<-R;
  y<-x;
  #y
  x<-A%*%y;
  x<-x/as.numeric(sqrt(t(x)%*%x));
  #x
  R<-(t(x)%*%A%*%x);
  #R
  }
  R
 x
 m
#Return the largest eigenvalue,
#the corresponding eigenvector
#number of iterations
 return(list(Rayleigh = R,
        eigenvector = x,
        number_iter = m))
}
```

Figure 2.
Algorithms Rayleigh quotient coded in MathCAD and R

Table 2
Results obtained with the algorithm

MathCAD				R			
	λ_1	$x^{(1)}$	No_ iter		λ_1	$x^{(1)}$	No_ iter
own	8.77673288	0.23983244 0.10503629 0.53885131 0.80067911	21	own	8.776733	0.2398938 0.1050999 0.5387825 0.8006987	20

4. Inverse power method

4.1. Presentation of the method

Applying the A^{-1} matrix power method gives the inverse power method.

We consider the matrix $C = A - \mu I_n$, and then we have

$$Cx = \left(A - \mu I_n\right)x = Ax - \mu I_n x = \lambda x - \mu x = (\lambda - \mu)x \tag{12}$$

If x is the eigenvector for matrix A corresponding to λ, its eigenvalue, then it means that $(\lambda - \mu)$ is the value for matrix C.

If A is inversible then there is $B = \left(A - \mu I_n\right)^{-1}$ and we have

$$Bx = \left(A - \mu I_n\right)^{-1} x = (\lambda - \mu)^{-1} x \tag{13}$$

So, x is eigenvector for matrix B, corresponding to its eigenvalue $(\lambda - \mu)^{-1}$.

Applied to matrix B, the power method is known as the inverse power method. If $|\lambda|$ it is the smallest eigenvalue of matrix A, then $\left|\dfrac{1}{\lambda}\right|$ it is the dominant eigenvalue of matrix A^{-1} (P3).

Considering $(\forall) y \in R^n$ then in the basis given by eigenvectors of matrix B, one may also be written

$$By = \alpha_1 \left(\lambda_1 - \mu\right)x^{(1)} + \ldots + \alpha_n \left(\lambda_n - \mu\right)x^{(n)} \tag{14}$$

and

$$By = \alpha_1 \left(\lambda_1 - \mu\right)^{-1} x^{(1)} + \ldots + \alpha_n \left(\lambda_n - \mu\right)^{-1} x^{(n)} \tag{15}$$

So, the smallest eigenvalue of matrix *B* will have the largest eigenvalue of matrix *C*. Following the same way as in the power method, it determines its eigenvalue.

4.2. Algorithms

Coded in MathCAD

Inverse Power Method
A - Hermitian matrix
ε - accepted error
Determining
λ the largest eigenvalue
x the corresponding eigenvector
m the number of iterations

MP_Inv(A, ε) :=
n ← length(A^⟨1⟩)
m ← 0
for i ∈ 1..n
  y_i ← rnd(1)
y ← y / √(y^T·y)
λ ← y^T·A·y
x ← (A − λ·identity(n))^−1 · y
x ← x / √(x^T·x)
while ⌈√((x − y)^T·(x − y)) > ε⌉
  m ← m + 1
  y ← x
  x ← (A − λ·identity(n))^−1 · y
  x ← x / √(x^T·x)
  λ ← x^T·A·x
return (x, λ, m)

Coded in R

```
MP_Inv=function(A,eps)
 {
 # Determining the largest eigenvalue
 #the corresponding eigenvector
 #number of iterations
eps = 10e-8
 n<-length(A[,1]);
  m<-0;
 y<-y/as.numeric(sqrt(t(y)%*%y));
 #lambda
  lambda<-as.numeric(t(y)%*%A%*%y);
 #x
 x<-solve(A-lambda*diag(1,n,n))%*%y
 x<-x/as.numeric(sqrt(t(x)%*%x));
   while(sqrt(t(x-y)%*%(x-y))>eps)
   {m<-m+1;
   #m
   y<-x;
   x<-solve(A-lambda*diag(1,n,n))%*%y
   x<-x/as.numeric(sqrt(t(x)%*%x));
   #x
   lambda<-as.numeric(t(x)%*%A%*%x);
   #lambda
   }

 lambda
 x
 m
#Return largest eigenvalue,
#corresponding eigenvector
 #and number of iterations
 return(list(lambda_max = lambda,
        eigenvector = x,
        no_iter = m))
}
```

Figure 3.
Inverse power method algorithm coded in MathCAD and R

Table 2 contains the numerical results obtained with the two programs for the matrix *A* and the approximate error *ε*.

Table 3
Results obtained with the algorithm

MathCAD				R			
	λ_1	$x^{(1)}$	No_ iter		λ_1	$x^{(1)}$	No_ iter
own	8.77673288	0.23980451 0.10500736 0.53888261 0.80067021	5	own	8.776733	0.2398045 0.1050074 0.5388826 0.8006702	3

It is noted that after a very small number of iterators, both algorithms converge to the quoted values, making the method preferable to the other two above.

But there is a problem: at each iteration the inverse matrix of $A-\mu I_n$ is calculated, which could lead, if *n* is largest, to increasing the computation time!

Remark: In all 3 presented methods, the convergence is geometric (2nd order)!

5. Conclusions and comments

There are many methods to determine the eigenvalues and the corresponding eigenvectors, either all values, or the largest (small) or one particular. There are also methods of separating their eigenvalues (the Gerschgorin-Based Method), which produce the ranges of a particular value. In the above-mentioned, given the practical and theoretical importance of the largest eigenvalue and corresponding eigenvector, we presented fast and fairly accurate methods for obtaining them and coded these algorithms in MathCAD and R.

References

[1] Halton, H.J.: *A Very Fast Algorithm for Finding Eigenvalues and Eigenvectors*, Department of Computer Science, University of North Carolina at Chapel Hill, 1996.

[2] Chisalita, G.A.: *Calcul numeric al valorilor proprii si al vectorilor proprii*, (2008) https://ftp.utcluj.ro/pub/users/chisalita/Scoala%20Doctorala/2008-2009/CURS%204%20-%20partea%20I.pdf

[3] Păltineanu, G., Matei, P., Trandafir, R.: *Bazele analizei numerice*, Ed. Printech, 2001.
[4] Necoara, I.: *Metode numerice*, 2014.
[5] http://www.islavici.ro/cursuriold/Analiza%20matematica/Slides_MAC_4_and_5.pdf
[6] http://math.ntnu.edu.tw/~min/matrix_computation/power_method.pdf
[7] https://math.unice.fr/~frapetti/CorsoF/cours4part2.pdf

COMMON EXTENSIONS OF A FAMILY OF LATTICE OPERATORS AND EXTREME POINTS OF THE SET OF ALL POSITIVE EXTENSIONS

Rodica-Mihaela Dăneţ
Technical University of Civil Engineering Bucharest, Romania
E-mail: rodica.danet@gmail.com
Marian-Valentin Popescu
Technical University of Civil Engineering Bucharest, Romania
E-mail: popescu.marianvalentin@gmail.com
Nicoleta Popescu
Technical University of Civil Engineering Bucharest, Romania
E-mail: popescu.snicoleta@gmail.com

Abstract: In this work we continue the study started in our previous paper of 2018, titled "Common Extensions for a Family of Lattice Operators". In 1982, Z. Lipecki proved that if the family of lattice operators is reduced to a single (lattice) operator *T*, then all extensions of *T* which are lattice operators are precisely the extreme points of the set of all positive extensions of *T*. In this paper we will extend this result to a family of lattice operators.
Mathematics Subject Classification (2010): 46A22, 47B60, 47B65
Key words: lattice operator, extension of a lattice operator, sublinear operator

1. Introduction

In [4], we studied sufficient conditions for the existence of a lattice operator which extends an arbitrary family of lattice operators. The obtained results generalize our previous results [3] (devoted to the simultaneous extension of two lattice operators) and also the results of Z. Lipecki [6] and [8].

In [7], Z. Lipecki proved that all extensions of a lattice operator T which are lattice operators are precisely the extreme points of the set of all positive extensions of T.

In this paper we generalize this result by Z. Lipecki to a family of lattice operators. A first step in solving this problem was done in our previous work [4], by giving a characterization of the extreme points of the set of all common extensions of a family $\left(T_\delta\right)_{\delta\in\Delta}$ of lattice operators. We mention that we found the idea of this criterion in a result by Z. Lipecki, D. Plachky and W. Thomsen – see [9] – concerning the case $\Delta=\{1\}$.

2. Preliminaries

We begin by recalling the definition of a lattice operator. For other classical notions such as *linear* or *sublinear operator,* and *positive linear operator* or *monotone sublinear operator,* see, for example [4].

Suppose that E and F are two ***vector lattices*** and $T:E\to F$ is a linear operator. Obviously T preserves the algebraic operations. A lattice operator is a linear operator that preserves the lattice operations, too. More precisely we say that T is a *lattice operator* (or, equivalently, *lattice homomorphism*) if for all x,y in E,

$$T(x \vee y) = T(x) \vee T(y) \tag{1}$$

or, equivalently,

$$T(x \wedge y) = T(x) \wedge T(y). \tag{2}$$

We will denote by $H(E,F)$ the set of all lattice operators $T: E \to F$. In [2] are given other properties equivalent with (1). Also are given other definitions and few examples of lattice operators, some of them known from the literature.

Now we will recall other definitions.

1) A *convex set* in a (real) vector space X is a nonempty set $C \subset X$ such that for all $x, y \in C$ and $\alpha \in [0,1]$, it follows that $\alpha x + (1-\alpha) y \in C$.

An *extreme point* for the convex set C is a point $z \in C$ such that if $z = \alpha x + (1-\alpha) y$ with $\alpha \in (0,1)$ and $x, y \in X$, $x \neq y$ then either $x \notin C$ or $y \notin C$. (Intuitively, an extreme point of C is a "corner" or a "vertex" of C.)

We will denote by $extr(C)$ the set of all extreme points of C. For example, if $X = \mathbb{R}$, then $C = [2,5]$ is a convex set and $extr(C) = \{2,5\}$.

2) A *positive matrix* is a (real) matrix $A = (a_{ij})_{i=\overline{1,n},\ j=\overline{1,n}}$ such that $a_{ij} \geq 0$ for all $i = \overline{1,n}$ and $j = \overline{1,n}$.

A *stochastic* (more precisely *row stochastic*) *matrix* is a positive matrix A, such that each row sum of A is 1, or equivalently, $Ae = e$, where $e = (1,1,...,1)$ is the unit element of $\mathbb{R}^n$.

A $(0,1)$*-matrix* is a matrix $A = (a_{ij})_{i=\overline{1,n},\ j=\overline{1,n}}$ such that for each pair (i, j) either $a_{ij} = 0$ or $a_{ij} = 1$.

A *permutation matrix* is a matrix $A = (a_{ij})_{i=\overline{1,n},\ j=\overline{1,n}}$ such that $Ae_i = e_k$, where i a k is a permutation of $\{1,...,n\}$ and $\{e_1, e_2, ..., e_n\}$ is the canonical basis of $\mathbb{R}^n$.

3) A *majorizing subspace* G of an ordered vector space E is a vector subspace $G \subseteq E$, such that for all $x \in E$, there exists $v \in G$ such that $x \leq v$ (or, equivalently, there exists $w \in G$ with $w \leq x$).

Now we recall something about the sublattice generated by a vector space or by an arbitrary set, respectively, as I mentioned in [3, 2.1].

Let E be a vector lattice and $G \subseteq E$ a vector subspace. Denote $\mathcal{S}(G)$ the vector sublattice generated by G. For every nonempty subset A of a vector lattice E, the symbol $A^{\wedge}$ will denote the collection of all vectors that can be written as *infima* of *finite* subsets of A (i.e., $a \in A^{\wedge} \Leftrightarrow \exists\, a_1, ..., a_n \in A : a = \bigwedge_{k=1}^{n} a_k$). Similarly, $A^{\vee}$ is the set consisting of all *suprema* of the *finite* subsets of A. Denote by $A^{\vee\wedge}$ the set $(A^{\vee})^{\wedge}$ and by $A^{\wedge\vee}$ the set $(A^{\wedge})^{\vee}$. It always turns out that $A^{\vee\wedge} = A^{\wedge\vee}$. If A is a nonempty subset of a vector lattice E, then the collection of all vector sublattices $H \subseteq E$ with $H \supseteq A$ is nonempty (since E is in this collection). The intersection of this collection of vector sublattices is the smallest vector sublattice that includes A. This vector sublattice is called the *vector sublattice* (or the *Riesz subspace*)

generated by A. We will denote it by $\mathcal{S}(A)$. It is known (see [3]) that if G is vector subspace of a vector lattice E, then the vector sublattice $\mathcal{S}(G)$ generated by G coincides with $G^{\wedge\vee}$ and also with $G^{\vee\wedge}$. We can look (see [3, Proposition 1]) that $\mathcal{S}(G) = M - M$ with $M = G^{\vee}$.

We mention the following result (see [4, Proposition 1]): "Let E be a vector lattice, $(G_\delta)_{\delta\in\Delta}$ a family of vector sublattices in E and $x_0 \in E \setminus span\left(\bigcup_{\delta\in\Delta} G_\delta\right)$. Denote $\mathcal{S}\left(\left(\bigcup_{\delta\in\Delta} G_\delta\right)\cup\{x_0\}\right)$ the vector sublattice of E, generated by $\left(\bigcup_{\delta\in\Delta} G_\delta\right)\cup\{x_0\}$. Then $\mathcal{S}\left(\left(\bigcup_{\delta\in\Delta} G_\delta\right)\cup\{x_0\}\right) = M - M$, with

$$M = \left\{ \bigvee_{i=\overline{1,n}} \left(\sum_{\delta\in\Delta} v_{\delta i} + \alpha_i x_0 \right) \middle| \, n\in\mathbb{N}^*,\ \forall i = \overline{1,n},\ (v_{\delta i})_{\delta\in\Delta} \in \Phi\left((G_\delta)_{\delta\in\Delta}\right) \text{ and } \alpha_i \in \mathbb{R}_+ \right\},$$

where $\Phi\left((G_\delta)_{\delta\in\Delta}\right)$ is the collection of all families $\{v_\delta \in G_\delta \,|\, \delta\in\Delta\}$ such that $v_\delta \neq 0$ for at most finitely $\delta\in\Delta$ or, equivalently, $v_\delta = 0$ for cofinitely many δ."

In [4] we proved the following results concerning the extension of a family of lattice operators (in the first result, the extension is made by using an additional set M).

Proposition 1. [4, Theorem 2] *Let E_0 and F be two vector lattices, $(G_\delta)_{\delta\in\Delta}$ a family of vector sublattices in E_0 and $M \subseteq E_0$ a wedge, closed under finite suprema, such that $M \supseteq G_\delta$, for all $\delta\in\Delta$. Consider $E = \mathcal{S}\left(\left(\bigcup_{\delta\in\Delta} G_\delta\right)\cup M\right)$ $\left(= M - M\right)$ the sublattice generated by $(G_\delta)_{\delta\in\Delta}$ and M. Let $T_\delta : G_\delta \to F$ $(\delta\in\Delta)$ be a lattice operator and $P : M \to F$ a mapping such that:*

1) $P(z_1 \vee z_2) = P(z_1) \vee P(z_2),\ \forall z_1,\ z_2 \in M$;

2) $P = T_\delta$ *on* G_δ, *for all* $\delta\in\Delta$;

3) P *is positively homogeneous*.

Then the following are equivalent.

i) *There exists a lattice operator* $L : E \to F$, *such that* $L = P$ *on* M (*and consequently* $L = T_\delta$ *on* G_δ, *for each* $\delta\in\Delta$);

ii) P *is additive on* M.

Proposition 2. [4, Theorem 3] *Let E be a vector lattice, F a Dedekind complete vector lattice and $(G_\delta)_{\delta\in\Delta}$ a family of vector sublattices in E. Let $T_\delta : G_\delta \to F$ $(\delta\in\Delta)$ be a lattice operator and $P : E \to F$ a mapping such that:*

1) $P(x_1 \vee x_2) = P(x_1) \vee P(x_2),\ \forall x_1,\ x_2 \in E$;

2) $P\left(\sum_{\delta\in\Delta} v_\delta + x\right) = \sum_{\delta\in\Delta} T_\delta(v_\delta) + P(x)$ *for all* $(v_\delta)_{\delta\in\Delta} \in \Phi\left((G_\delta)_{\delta\in\Delta}\right)$, *and* $x\in E$, *where* $\Phi\left((G_\delta)_{\delta\in\Delta}\right)$ *is the collection of all families* $\{v_\delta \in G_\delta \,|\, \delta\in\Delta\}$ *such that* $v_\delta \neq 0$, *for at most finitely many* $\delta\in\Delta$.

Then there exists a lattice operator $L : E \to F$, *such that* $L = T_\delta$ *on* G_δ, *for each* $\delta\in\Delta$.

I recalled these results only to keep in mind their hypothesis 1), a condition that was previously used by Z. Lipecki [8]. We will use a similar condition in our main result in this work – see hypothesis 2a) in Theorem 6 below.

In [4] we also started to study the connection between the common extension of a family of lattice operators and the notion of extreme points. As we said in [4], this idea was suggested by the following result concerning the characterization of a lattice operator on $£^n$ by using its matrix in the canonical basis of $£^n$.

Proposition 3. [10, Proposition 4.4] *A stochastic matrix A defines a lattice operator on $\mathbb{C}^n$ if and only if A is an extreme point in the set S_n of all stochastic matrices of order n.*

Remark. [4, Remark after Proposition 4] Notice that "*The matrix A is an extreme point in the set S_n if and only if A is a $(0,1)$-matrix with exactly one* 1 *in each row.*" [10, Proposition 4.3], and that "*A stochastic matrix A defines a lattice isomorphism* (that is, a bijective lattice operator) *if and only if A is a permutation matrix.*" [10, Corollary to the Proposition 4.4]. The method used in [10] to prove the last result serves to determine all lattice operators on $\mathbb{C}^n$. In fact if A defines a lattice operator, then $A \geq 0$ (since $|Ax| = Ax$, whenever $x \in \mathbb{C}^n$, $x \geq 0$) and each row of A contains at most one element $y > 0$. The converse is obvious. Similarly, A defines a lattice operator if $A \geq 0$ and the replacement of each non-zero entry by 1 transforms A in a permutation matrix.

In [4] we gave the following characterization of the extreme points of the set of all common positive extensions of a family of lattice operators.

Notice that, if $G \subset E$ is a vector subspace and $T : G \to F$ is a positive linear operator, we denote by $E_+(T)$ the set of all positive linear extensions of T to the whole E.

Proposition 4. [4, Theorem 5] *Let E be a vector lattice and F a Dedekind complete vector lattice. Let $(G_\delta)_{\delta\in\Delta}$ be a family of vector subspaces of E and for all $\delta \in \Delta$, consider $T_\delta : G_\delta \to F$ be a positive linear operator. Let also $L : E \to F$ be a common positive linear extension of the family $(T_\delta)_{\delta\in\Delta}$, that is, $L \in \bigcap_{\delta\in\Delta} E_+(T_\delta)$. Then the following are equivalent:*

i) $L \in extr\left(\bigcap_{\delta\in\Delta} E_+(T_\delta)\right)$;

ii) $\inf\left\{L\left(\left|x - \sum_{\delta\in\Delta} v_\delta\right|\right) \middle| (v_\delta)_{\delta\in\Delta} \in \Phi\left((G_\delta)_{\delta\in\Delta}\right)\right\} = 0$ *for all* $x \in E$, *where* $\Phi\left((G_\delta)_{\delta\in\Delta}\right)$

denotes the collection of all families $\{v_\delta \in G_\delta \,|\, \delta \in \Delta\}$ such that $v_\delta \neq 0$, for at most finitely $\delta \in \Delta$.

Recall – see [4] – that the above result generalizes [9, Theorem 3], that is, the following statement: "*Let E be a vector lattice, $G \subseteq E$ a vector subspace and F a Dedekind complete vector lattice. Let also $T : G \to F$ be a positive linear operator. Then $S \in extr E_+(T)$ if and only if $\inf_{v\in G} S(|x - v|) = 0$ for all $x \in E$.*".

3. Main result

In [5] we find the following result, where E is a vector lattice and F is a Dedekind complete vector lattice.

Proposition 5. [5, Theorem 2, p.287] *Let M be a vector sublattice of E and $T: M \to F$ a lattice operator. If we denote by $H(E,F)$ the set of all lattice operators of E into F, then:*

a) $extrE_+(T) \subset H(E,F)$;

b) *If* $\inf\{|y - T(z)| \mid z \in M\} = 0$, *for each* $y \in F$, *then* $E_+(T) \cap H(E,F) \subset extrE_+(T)$.

Now, by using Proposition 4, we are able to prove a generalization of Proposition 5, for a family of lattice operators $(T_\delta)_{\delta\in\Delta}$ instead of a single lattice operator.

Theorem 6. *Let E be a vector lattice, F a Dedekind complete vector lattice, $(G_\delta)_{\delta\in\Delta}$ a family of vector sublattices of E, at least one a majorizing subspace of E. Let $T_\delta: G_\delta \to F$ be $(\delta \in \Delta)$ a lattice operator. Suppose that:*

1) $\sum_{\delta\in\Delta} v_\delta \le 0$, *for* $(v_\delta)_{\delta\in\Delta} \in \Phi\left((G_\delta)_{\delta\in\Delta}\right) \Rightarrow \sum_{\delta\in\Delta} T_\delta(v_\delta) \le 0$ (*where* $\Phi\left((G_\delta)_{\delta\in\Delta}\right)$ *is the collection of all families* $\{v_\delta \in G_\delta \mid \delta \in \Delta\}$ *such that* $v_\delta \neq 0$ *for at most finitely many* $\delta \in \Delta$).

2) *The positive linear operator* (*well-defined according to* "1)") $T: span\left(\bigcup_{\delta\in\Delta} G_\delta\right) \to F$ *defined by* $T\left(\sum_{\delta\in\Delta} v_\delta\right) = \sum_{\delta\in\Delta} T_\delta(v_\delta)$, *for all* $(v_\delta)_{\delta\in\Delta} \in \Phi\left((G_\delta)_{\delta\in\Delta}\right)$ *is such that the canonical sublinear operator associated* $\overline{T}: E \to F$, *defined by* $\overline{T}(x) = \inf_{\sum_{\delta\in\Delta} v_\delta \ge x} T\left(\sum_{\delta\in\Delta} v_\delta\right)$ (*where the infimum is taken after all* $(v_\delta)_{\delta\in\Delta} \in \Phi\left((G_\delta)_{\delta\in\Delta}\right)$), *satisfies the conditions:*

2a) $\overline{T}\left(\bigvee_{\delta\in\Delta} v_\delta\right) = \bigvee_{\delta\in\Delta} \overline{T}(v_\delta)$, *for all* $(v_\delta)_{\delta\in\Delta} \in \Phi\left((G_\delta)_{\delta\in\Delta}\right)$;

2b) $-\overline{T}$ *is subadditive on the sublattice* $\mathcal{S}\left(\bigcup_{\delta\in\Delta} G_\delta\right)$ *generated by the family* $(G_\delta)_{\delta\in\Delta}$.

Then:

a) $L \in \bigcap_{\delta\in\Delta} extrE_+(T_\delta) \neq \varnothing \Rightarrow L$ *is a lattice operator* (*that is,* $L \in H(E,F)$);

b) *If* $\inf_{v_\delta \in G_\delta} |y - T_\delta(v_\delta)| = 0$, *for all* $y \in F$, $\forall \delta \in \Delta$, *then* $H(E,F) \cap \left(\bigcap_{\delta\in\Delta} E_+(T_\delta)\right) =$

$= \bigcap_{\delta\in\Delta} extrE_+(T_\delta)$, *if this last intersection set is nonempty.*

Remark. The following statements are useful for the proof of our Theorem 6:

- $span\left(\bigcup_{\delta\in\Delta} G_\delta\right)$ and hence $\mathcal{S}\left(\bigcup_{\delta\in\Delta} G_\delta\right)$ are majorizing subspaces of E;
- In the hypotheses of Theorem 6, it follows that $\bigcap_{\delta\in\Delta} extrE_+(T_\delta) \subseteq extr\left(\bigcap_{\delta\in\Delta} E_+(T_\delta)\right)$;
- $|L(x)| = L(|x|)$, for all $x \in E$.

(Obviously the inequality "$\leq$" in this equality is valid since L is a positive linear operator – see, for example [1, p.153].)

- $\overline{T}$ is sublinear;
- $\overline{T} = T$ on $span\left(\underset{\delta\in\Delta}{\cup} G_\delta\right)$;
- $\overline{T}\left(\underset{\delta\in\Delta}{\vee} v_\delta\right) = \underset{\delta\in\Delta}{\vee} \overline{T}\left(v_\delta\right)$, for all $\left(v_\delta\right)_{\delta\in\Delta} \in \Phi\left(\left(G_\delta\right)_{\delta\in\Delta}\right)$ (see, for example [8]);
- If $S \in \underset{\delta\in\Delta}{\bigcap} E_+\left(T_\delta\right)$, then $S = \overline{T}$ on $\mathcal{S}\left(\underset{\delta\in\Delta}{\cup} G_\delta\right)$.

References

[1] Cristescu, R.: *Ordered Vector Spaces and Linear Operators,* Ed. Academiei, Bucharest, Romania, Abacus Press, Tunbridge Wells, Kent, England, 1976.

[2] Dăneț, R.-M.: *Riesz Homomorphisms. Quasi-Riesz Homomorphisms*, in *Order Structures in Functional Analysis* (in Romanian) ed. R. Cristescu, Vol. **4**, 45-89, Publishing House of the Romanian Academy, Bucharest, 2001.

[3] Dăneț, R.-M., Popescu, M.-V., Popescu, N.: *On the simultaneous extensions of two lattice operators,* Proceedings of the 14th Workshop of Scientific Communications, Department of Mathematics and Computer Science, Dedicated to Professor Gavriil Păltineanu at 75th anniversary, Technical University of Civil Engineering Bucharest, May 27, 2017, 25-30.

[4] Dăneț, R.-M., Popescu, M.-V., Popescu, N.: *Common extension for a family of lattice operators,* Proceedings of the 15th Workshop of Scientific Communications, Department of Mathematics and Computer Science, Technical University of Civil Engineering Bucharest, June 9, 2018, 24-29.

[5] Lipecki, Z.: *Extension of positive operators and extreme points* II, Colloq. Math., Dédié à la mémoire d'Edward Marczewski, **XLII** (1979), 285-289.

[6] Lipecki, Z.: *Extension of vector lattice-homomorphisms*, Proc.Amer.Math.Soc., **79** (1980), 247-248.

[7] Lipecki, Z.: *Extensions of positive operators and extreme points* III, Colloq. Math. **XLVI** (1982), 263-268.

[8] Lipecki, Z.: *Extension of vector lattice-homomorphisms revisited*, Indag. Math. (Proceedings), A **88** (2) (1985), 229-233.

[9] Lipecki, Z., Plachky, D., Thomsen, W.: *Extension of positive operators and extreme points* I, Colloq. Math. **XLII** (1979), 279-284.

[10] Schaefer, H.H.: *Banach lattices and positive operators*, Springer Verlag, Berlin, Heidelberg, New York, 1974.

POLYNOMIAL APPROXIMATION OF VARIATIONAL PROBLEMS

LEONARD DĂUŞ AND GHIOCEL GROZA

Abstract. Solutions of variational problems are approximated by polynomials which yield simultaneous interpolation of a function and its derivatives.

Mathematics Subject Classification (2010): 41A10, 49M99
Key words: polynomial approximation, interpolation, generalized divided differences, variational problems

1. Introduction

Consider $C([a,b])$ the real Banach space of real continuous functions defined on the interval $[a,b]$ endows with supremum norm. By Weierstrass Theorem it follows that every $f \in C([a,b])$ may be approximated uniformly by polynomials. Combining the approximation with the interpolation at a finite number of points from $[a,b]$ it follows a problem of simultaneous interpolation and approximation. Such approximations may be very useful in different problems. If the approximated function is differentiable, that is $f \in C^m([a,b])$, it is desirable to obtain also simultaneous approximation of the function and its derivatives until of a fixed order, as in the case of Bernstein polynomials (see, for example [3]-[6]). There are many papers on numerical approximation of solutions of variational problems (see, for example, [2], [10], [12] and references therein). We approximate these solutions by interpolation polynomials.

2. On generalized divided differences

Let $\{\alpha_i\}_{i\geq 0}$ be a sequence of real numbers in the interval $[a,b]$ and $f \in C^m([a,b])$ a real function. If the terms of the sequence are distinct, then we can define the divided difference of the order n of f with respect to $\alpha_0, \alpha_1, ..., \alpha_n$, denoted by $[f(\alpha_0), f(\alpha_1), ..., f(\alpha_n)]$ (see, for example, [1]). Thus $[f(\alpha_0)] := f(\alpha_0)$,

$$[f(\alpha_0), f(\alpha_1)] := \frac{f(\alpha_1) - f(\alpha_0)}{\alpha_1 - \alpha_0},$$

and by recurrence, for $i \geq 1$,

$$[f(\alpha_0), ..., f(\alpha_i)] := \frac{[f(\alpha_1), ..., f(\alpha_i)] - [f(\alpha_0), ..., f(\alpha_{i-1})]}{\alpha_i - \alpha_0}. \tag{2.1}$$

Since, for distinct $\alpha_0, \alpha_1, ...\alpha_k$,

$$[f(\alpha_0), ..., f(\alpha_k)] = \sum_{i=0}^{k} \frac{f(\alpha_i)}{\prod\limits_{j=0, j\neq i}^{k} (\alpha_i - \alpha_j)},$$

it follows that the divided differences are symmetric functions of their arguments.

In the case of coincident points, the divided differences are defined in different ways. Thus it is know the following result:

Theorem 2.1. *([8], Ch. 6, Sec. 1) If $\alpha_0, \alpha_1, ...\alpha_m$ are distinct points in the interval $[a,b]$ and $f \in C^m([a,b])$, then*

$$[f(\alpha_0), ..., f(\alpha_m)] := \int_0^{t_0} dt_1 \int_0^{t_1} dt_2 ... \int_0^{t_{m-1}} f^{(m)}(t_0 + t_1(\alpha_1 - \alpha_0) + ... + t_m(\alpha_m - \alpha_{m-1}))dt_m, \tag{2.2}$$

where $t_0 = 1$ and $m \geq 1$.

Hence (2.2) is used to define the generalized divided differences for arbitrary points $\alpha_0, \alpha_1, ...\alpha_m$ from $[a,b]$.

There are several corollaries of Theorem 2.1 (see [8], Ch. 6, Sec. 1), two of them included in the following result:

Corollary 2.2. *If $f \in C^m([a,b])$ and $\alpha_0, \alpha_1, ...\alpha_m$ are arbitrary points in the interval $[a,b]$, then the following statements hold:*

(i) for every $k \leq m$, $[f(\alpha_0), ..., f(\alpha_k)]$, defined by (2.2), is a continuous function of its $k+1$ arguments in $[a,b]$ and coincides with that defined by (2.1), when the arguments are distinct;

(ii) for every $k \leq m$, there exists $\xi \in [\min\{\alpha_0, ..., \alpha_k\}, \max\{\alpha_0, ..., \alpha_k\}]$, such that

$$[f(\alpha_0), ..., f(\alpha_k)] := \frac{f^{(k)}(\xi)}{k!}.$$

Suppose that $\gamma_0, \gamma_1, ...\gamma_r \in [a,b]$ are distinct and k_i elements α_j are equal to γ_i, for $i = 0, 1, ..., r$, $j = 1, ..., k_i$, where $k_0 + k_1 + ... + k_r = m + 1$. Then we define

$$[f(\gamma_0)_{k_0}, f(\gamma_1)_{k_1}, ..., f(\gamma_r)_{k_r}] := [\underbrace{f(\gamma_0), f(\gamma_0), ..., f(\gamma_0)}_{k_0 \ times}, \underbrace{f(\gamma_1), ..., f(\gamma_1)}_{k_1 \ times}, ...,$$

$$\underbrace{f(\gamma_r), ..., f(\gamma_r)}_{k_r \ times}] = [f(\alpha_0), ..., f(\alpha_m)].$$

Corollary 2.3. *([8], Ch. 6, Sec. 1) If $f \in C^m([a,b])$ and $\alpha_0, \alpha_1, ...\alpha_r$ are distinct points in the interval $[a,b]$, then*

$$[f(\alpha_0)_{k_0}, f(\alpha_1)_{k_1}, ..., f(\alpha_r)_{k_r}]$$

$$= \frac{1}{(k_0 - 1)!(k_1 - 1)!...(k_r - 1)!} \frac{\partial^{k_0 + k_1 + ... + k_r - r - 1}[f(\alpha_0), ..., f(\alpha_r)]}{\partial \alpha_0^{k_0 - 1} \partial \alpha_1^{k_1 - 1} ... \partial \alpha_r^{k_r - 1}}, \tag{2.3}$$

where $k_i - 1 \leq m$, $i = 0, 1, ..., r$.

The equation (2.3) is taken as the definition of generalized divided differences in [9], p. 14.

Newton interpolating formula can be extended for arbitrary points of interpolation.

3. Simultaneous interpolation and approximation of functions and its derivatives

Let $f : [0,1] \to \mathbb{R}$. If n is a positive integer, then the nth Bernstein polynomial for $f(x)$ is given by

$$B_n(f;x) = \sum_{i=0}^{n} f\left(\frac{i}{n}\right) \left(\begin{array}{c} n \\ i \end{array} \right) x^i (1-x)^{n-i}.$$

Notice that

$$B_n(f;0) = f(0), \ B(f;1) = f(1).$$

The following result was proved by Bernstein (see [1]).

Theorem 3.1. *Let $f : [0,1] \to \mathbb{R}$ be bounded on $[0,1]$. Then*

$$\lim_{n\to\infty} B_n(f;x) = f(x)$$

at any point $x \in [0,1]$ at which f is continuous. If $f \in C([0,1])$, then the limit holds uniformly in $[0,1]$.

The results for the interval $[0,1]$ are easily transferred to $[a,b]$ by means of the one-to-one transformation

$$y = \frac{x-a}{b-a}$$

from $[a,b]$ onto $[0,1]$. If the function f is differentiable, not only do we have $B_n(f;x) \to f(x)$ but $B_n'(f;x) \to f'(x)$. A corresponding statement is true for higher derivatives. Hence the Bernstein polynomials therefore provide simultaneous approximation of the function and its derivatives. Thus [1]

Theorem 3.2. *If $f \in C^m([0,1])$, then*

$$\lim_{n\to\infty} B_n^{(m)}(f;x) = f^{(m)}(x)$$

uniformly on $[0,1]$.

In a forthcoming paper we'll give a more general theorem on simultaneous interpolation and approximation of functions and its derivatives

4. Applications

Let $(H, <\ ,\ >_H)$ be a real Hilbert space and let $B : H \times H \to \mathbb{R}$ be a continuous, symmetric bilinear form. B is called *H-coercive* if there exists a positive constant μ such that

$$B(u,u) \geq \mu \|u\|_H^2,\ \forall u \in H,$$

where $\|u\|_H = \sqrt{< u, u >_H}$. The following result is known (see, for example, [7] and [11]).

Theorem 4.1. *Let $(H, <\ ,\ >_H)$ be a real Hilbert space, $B : H \times H \to \mathbb{R}$ be a continuous, symmetric, H-coercive bilinear form and S be a convex and closed subset of H. Then for every continuous, linear functional $f : H \to \mathbb{R}$ there exist a unique element $u \in H$ such that*

$$f(w-u) \leq B(u, w-u),\ \forall w \in S,$$

and

$$L(u) = \inf_{w\in S}\{L(w)\},$$

where

$$L(w) = B(w,w)/2 - f(w). \tag{4.1}$$

For an interval $[a,b]$, we consider the Hilbert space $\left(W^{r,2}([a,b]), <\ ,\ >_r\right)$, where

$$W^{r,2}([a,b]) = \left\{u \in L^2([a,b]) : D^j u \in L^2([a,b]),\ 0 \leq j \leq r\right\}$$

and

$$< u, v >_r = \sum_{j=0}^{r} \int_a^b D^j u D^j v dx.$$

Let

$$\min I[y],\quad I[y] = \int_a^b F(x, y, y', ..., y^{(r)})dx, \tag{4.2}$$

be a variational problem, where $F \in C^1$, $x \in [a,b]$, $y \in C^r([a,b])$, with the boundary conditions

$$y(a) = y_1,\ y'(a) = y_1',\ ...\ , y^{(r-1)}(a) = y_1^{(r-1)},$$

$$y(b) = y_2,\ y'(b) = y_2',\ \dots, y^{(r-1)}(b) = y_2^{(r-1)}. \tag{4.3}$$

Consider $(H, <\ ,\ >_r)$, where $H = \{u \in W^{r,2}([a,b]) : u^{(j)}(a) = 0,\ u^{(j)}(b) = 0,\ j = 0, 1, ..., r-1\}$. Assume that, the problem (4.2), (4.3) is equivalent to a similar problem where, under the notations of Theorem 4.1, F has the form (4.1), with B a continuous, symmetric, H-coercive bilinear form. If n is a fixed positive integer, then, by considering $S = V_n$ the subspace of polynomial functions $P_n \in H$ of degree less than or equal to n, by Theorem 4.1, the variational problem (4.2), (4.3) has a unique solution $P_n \in S$. If y^* is the solution of the variational problem in H, it is known that

$$\lim_{n\to\infty} \|y^* - P_n\|_H = 0. \tag{4.4}$$

If the problem has a solution $y \in C^r([a,b])$, it can be proved that, for every $\varepsilon > 0$, there exists a polynomial P such that

$$\|y^{(k)} - P^{(k)}\|_{[a,b],\infty} < \varepsilon,\ k = 0, 1, ..., r, \tag{4.5}$$

and

$$y^{(j)}(\alpha_i) = P^{(j)}(\alpha_i),\ i = 0, 1,\ j = 0, 1, ..., r-1,\ \alpha_1 = a,\ \alpha_2 = b. \tag{4.6}$$

Hence it follows that in (4.4) the uniform convergence can be considered.

Example 4.2. Consider the variational problem [10]:

$$\min I[y],\ I[y] = \int_0^1 (y(x) + y'(x) - 4e^{3x})^2 dx; \tag{4.7}$$

subject to the boundary conditions

$$y(0) = 1,\ y(1) = e^3, \tag{4.8}$$

which has a unique solution in $C^1([0,1])$. By (4.4)-(4.6) it follows that the solution of the variational problem (4.7), (4.8) can be approximated by polynomials.

Table 1. Errors associated with Example 1

x	Exact u	DTM [10]	Present method
0.1	1.34985880	1.35035927	1.34985881
0.2	1.82211880	1.82312475	1.82211879
0.3	2.45960311	2.46112459	2.45960312
0.4	3.32011692	3.32216898	3.32011691
0.5	4.48168907	4.48429018	4.48168906
0.6	6.04964746	6.05280952	6.04964747
0.7	8.16616991	8.16985405	8.16616989
0.8	11.02317638	11.02713929	11.02317638
0.9	14.87973172	14.88307423	14.87973172
1.0	20.08553692	20.08553692	20.08553692

This can be written as

$$P_n(x) = y(0) + [y(0), y(1)]x + x(x-1)\sum_{k=2}^{n} a_k x^k.$$

The coefficients a_k, $k = 2, ..., n$, are determined as solutions of the system of equations

$$\frac{\partial I[P_n]}{\partial a_k} = 0. \tag{4.9}$$

Then, for $k = 2, ..., n$, we get

$$\int_0^1 2\left(\frac{\partial P_n(x)}{\partial a_k} + \frac{\partial P_n'(x)}{\partial a_k}\right)(P_n(x) + P_n'(x) - 4e^{3x})dx = 0.$$

Hence, for $i, k = 2, ..., n$, it follows that

$$\int_0^1 \left(x^{k+1}(x-1) + (2x-1)x^k + kx^k(x-1)\right)(P_n(x) + P_n'(x) - 4e^{3x})dx = 0$$

and

$$\sum_{i=2}^{n} c_{ik}a_i = d_k, \tag{4.10}$$

where

$$c_{ik} = \int_0^1 x^{k+i}(x^2 + (k+1)x - k - 1)(x^2 + (i+1)x - i - 1)dx,$$

$$d_k = \int_0^1 x^k(x^2 + (k+1)x - k - 1)(4e^{3x} - e^3 - (e^3 - 1)x)dx.$$

Then, by (4.10), we get $P_n(x)$ which approximates the exact solution. In Table 1 we compare the approximation of the solution of the variational problem (4.7), (4.8) obtained in this paper with the approximation by using differential transform method (DTM) in [10]. The exact solution of the problem is $y(x) = e^{3x}$.

Example 4.3. Consider the variational problem [2]:

$$\min I[y], \text{ if } I[y] = \int_0^{\pi/2} \left(y''^2(x) - y^2(x) + x^2\right)dx, \tag{4.11}$$

with the boundary conditions

$$y(0) = 1,\ y'(0) = 1,\ y\left(\frac{\pi}{2}\right) = 0,\ y'\left(\frac{\pi}{2}\right) = -1. \tag{4.12}$$

As in Example 4.2, the approximate solution has the form

$$P_n(x) = y(0) + [y(0), y(0)]x + [y(0), y(0), y(\pi/2)]x^2 + [y(0), y(0), y(\pi/2), y(\pi/2)]$$
$$\cdot x^2(x - \pi/2) + x^2(x - \pi/2)^2 \sum_{k=4}^{n} a_k x^k.$$

The coefficients a_k, $k = 4, ..., n$, are determined as solutions of the system of equations (4.9). In Table 2 we compare the approximation of the solution of the variational problem (4.11), (4.12) obtained for $n = 10$ and $n = 14$ with the exact solution of the problem $y(x) = \cos x$. Notice that for $n = 14$ the accuracy is higher than the approximation obtained in [2] by using Adomian decomposition.

Table 2. Errors associated with Example 2

x	Exact u	Approximate solution for n=10	Approximate solution for n=14
$0.1\pi/2$	0.98768834	0.98768834	0.98768834
$0.2\pi/2$	0.95105651	0.95105649	0.95105651
$0.3\pi/2$	0.89100652	0.89100636	0.89100652
$0.4\pi/2$	0.80901699	0.80901656	0.80901699
$0.5\pi/2$	0.70710678	0.70710617	0.70710678
$0.6\pi/2$	0.58778525	0.58778514	0.58778525
$0.7\pi/2$	0.45399049	0.45399183	0.45399049
$0.8\pi/2$	0.30901699	0.30901978	0.30901699
$0.9\pi/2$	0.15643446	0.15643662	0.15643446
$1.0\pi/2$	0.00000000	0.00000000	0.00000000

References

[1] P. J. Davis, *Interpolation and approximation*, Dover Publication Inc. New York, 1975.

[2] M. Dehghan and M. Tatari, *The use of Adomian decomposition method for solving problems in calculus of variations*, Mathematical Problems in Engineering, 2006 (2006) 1-12.

[3] G. Groza and M. Jianu, *Simultaneous interpolation and approximation for infinitely differentiable functions*, The 12th Workshop of Scientific Communications, Department of Mathematics and Computer Science, May 25, 2013, 50-53.

[4] G. Groza, M. Jianu and N. Pop, *Infinitely differentiable functions represented into Newton interpolating series*, Carpathian J. Math., **30**(2014), No. 3, 309-316.

[5] G. Groza and N. Pop, *Approximate solution of multipoint boundary value problems for linear differential equations by polynomial functions*, J. Difference Equ. Appl., **14** (2008), No. 12, 1289-1309.

[6] G. Groza and N. Pop, *A numerical method for solving of the boundary value problems for ordinary differential equations*, Result. Math., **53** (2009), No. 3-4, 295-302.

[7] C. Iacob, D. Homentcovski, N. Marcov and A. Nicolau, *Classic and modern mathematics*, vol. IV (in Romanian), Editura Tehnică, 1983, Bucureşti.

[8] E. Isaacson and H. B. Keller, *Analysis of numerical methods*, Dover, 1994, New York.

[9] L. M. Milne-Thompson, *The calculus of finite differences*, Macmillian Company, 1933, London.

[10] A. R. Nazemi, S. Hesam and A. Haghbin, *A fast numerical method for solving calculus of variation problems*, Adv. Model. Optim., **15** (2013), No. 2, 133-149.

[11] T. Petrila and C. I. Gheorghiu, *Finite-element methods* (in Romanian), Editura Academiei, 1987, Bucureşti.

[12] M. Razzaghi and M. Razzaghi, *Taylor Series Direct Method for Variational Problems*, J. Franklin Inst., **325** (1988), No. 1, 125-131.

Department of Mathematics and Computer Science, Technical University of Civil Engineering Bucharest, Bucharest, Romania

E-mail address: daus@utcb.ro

Department of Mathematics and Computer Science, Technical University of Civil Engineering Bucharest, Bucharest, Romania

E-mail address: grozagc@yahoo.com

CLIMATE CHANGE IMPACT ASSESSMENT ON SNOWMELT IN BUCEGI MOUNTAINS USING RCP SCENARIOS

Gabriela-Roxana Dobre
Department of Mathematics and Computer Science
Technical University of Civil Engineering Bucharest, Romania
E-mail: roxana.dobre@utcb.ro
Alina Elisabeta Sandu
Department of Mathematics and Computer Science
Technical University of Civil Engineering Bucharest, Romania
E-mail: *alina.sandu@utcb.ro*

Abstract: The study analyzes the changes in snow depth, snowmelt and mean snow water equivalent (SWE) in Bucegi Mountains under four possible climate futures scenarios, the Representative Concentration Pathways (RCPs), based on global annual greenhouse gases (GHGs) emissions. Using an energy balance model, we evaluate the snowmelt and SWE under the effect of the RCPs scenarios, defined by their total radiative forcing level, which span the range between $2.6 - 8.5\, W \cdot m^{-2}$. The effect of potential climate change scenario on the seasonal evolution of the SWE can be assessed by modifying the time series of adjustable parameters e.g. temperature and/or precipitation. If we do not apply strategies for reducing GHGs emissions, temperature will continue to rise. Snowmelt increases linearly with temperature, so a diminution of snow cover area and a decrease of the amount of snow in the cold season will reduce water availability for irrigation and agriculture.

Mathematics Subject Classification (2010): 97M50
Key words: Climate change; RCP scenario; Snowmelt

1. Introduction

In recent decades, changes in climate have caused impact on natural and human systems on all continents and across the oceans. Human influence on the climate system is clear and recent anthropogenic emissions of greenhouse gases (GHGs) are at peak levels. The atmosphere and the oceans have warmed, the amounts of snow and ice have diminished and sea level has risen. An increased intensity and frequency of rainfall, hurricanes, heat waves, wildfires, drought and more severe precipitation when it rains or snows have been observed. Under the highest emissions scenarios and assuming no change in current water resources management, annual trends toward earlier spring snowmelt and reduced snowpack are already affecting water resources in terms of quantity and quality [1, 5]. Limiting climate changes would require substantial and sustained reductions in GHGs emissions, else these trends are expected to continue, increasing the likelihood of severe, pervasive and irreversible impacts for people and ecosystems.

Emissions scenarios regarding plausible future emissions are based on socioeconomic, environmental, and technological trends while climate change scenarios are plausible representations of the future climate conditions (temperature, precipitation and other climatological phenomena). The Fifth Assessment Report of the Intergovernmental Panel on Climate Change from 2014 (IPCC-AR5) provides an overview of the state of knowledge concerning the science of climate change and gives a new set of scenarios, called Representative Concentration Pathways (RCPs). This new approach was motivated by the changing information needs of policy makers to achieve specific climate change targets: the

increase of global average temperature to a maximum of 2 °C above pre-industrial levels (year 1750); "overshoot" scenarios in which radiative forcing peaks and then declines to a target level; growing interest in a "risk management" approach that combines reductions in emissions and adaptation to reduce climate change damages.

The new RCPs scenarios represent GHGs concentration trajectories that describe four possible climate futures. The RCPs are named after a possible range of radiative forcing values (+2.6, +4.5, +6.0, and +8.5 $W \cdot m^{-2}$, respectively) in the year 2100 relative to pre-industrial values and they are depending on how much GHGs are emitted [5]. Regarding the snow cover, RCPs are consistent with a wide range of possible changes in future due to the GHGs emissions: permafrost warming and thawing in high-latitude regions and in high-elevation regions. In the Northern Hemisphere (NH) spring snow cover has continued to decrease in extent, while the decrease of winter precipitation and early snowmelt reduce water availability [1].

For Romania, significant trends were identified: the increase in the number of days with positive temperature, a slight decrease in winter precipitation explains the diminution of the snowfall days, also decreasing trends in the number of days with snow coverage and in the mean snow depth [2].

Using the meteorological observations a surface point energy balance model has been used to compute the energy balance components, snow water equivalent (SWE) and the surface melt rate. The model is built on Microsoft Excel and uses equations adapted from Dingman and Strasser et al. [3, 6]. We analyze the variability of SWE in Padina area from Bucegi Mountains, under the climate change scenarios RCP 8.5 and RCP2.6.

2. RCPs climate scenarios

Climate models are used to simulate global and regional climate variability and change over past periods, to project changes in the near future (decadal scale) and to predict changes over longer periods (century scale). They potentially provide valuable guidance to help policy makers and businesses to adapt and mitigate climate changes. Reliability of climate models has to be tested against what happened with climate in the past. If a model can correctly simulate trends from a particular starting point somewhere in the past, it can be used to predict with reasonable certainty what may happen in the future. However, different models include different entry elements and can therefore generate different predictions. Projections of climate change in the future are dependent on the sensitivity of the climate system to the GHGs.

Radiative forcing, expressed as Watts per square meter, can be defined as the difference in the balance of energy that enters the atmosphere and the amount that is returned to space compared to the pre-industrial era. The primary GHGs in Earth's atmosphere are water vapor, carbon dioxide, methane, nitrous oxide and ozone. Without GHGs, the average temperature of Earth's surface would be about −18 °C (0 °F), rather than the present average of ~14 °C. The dominant factor by far is the positive forcing from CO_2. As the radiative forcing increases, the global temperature rises. However, in the real atmosphere complex, water vapor, cloud and ice albedo, aerosols, ozone and other factors are influencing radiative forcing. For example, doubling CO_2 level results in forcing of $3.7\ W \cdot m^{-2}$ and will result in $\sim 1.2\ ^{\circ}C$ warming.
For a GHG, such as carbon dioxide, radiative transfer ΔF can be calculated as a function of changing concentration

$$\Delta F = 5.35 \cdot \ln\left(\frac{C}{C_0}\right)\ W \cdot m^{-2} \quad (1)$$

where C is CO_2 concentration in ppm and $C_0 = 278\ ppm$ is initial concentration (1750).
In order to analyze changes in snow depth, melted snow amount and SWE we are using the scenarios adopted by IPCC-AR5. Emissions scenarios are descriptions of potential future

discharges in the atmosphere of substances that affect the Earth's radiation balance, such as GHGs and aerosols. The scenarios are not forecasts or predictions, but reflect expert judgments represented in integrated assessment models. A GHG is a gas in an atmosphere that absorbs and emits radiation within the thermal infrared range. This process is the fundamental cause of the GHG effect.

IPCC-AR5 introduced a new set of scenarios, RCPs, to project future climate change with climate model simulations. The main RCPs are RCP 2.6, RCP 4.5, RCP 6.0, and RCP 8.5, named after the radiative forcing values that are projected for the year 2100.

- The RCP 2.6 scenario is characterized by very low GHGs concentrations, producing radiative forcing around $3.1\,W\cdot m^{-2}$ mid-century and dropping to $2.6\,W\cdot m^{-2}$ by 2100. Although theoretically possible, RCP 2.6 is a scenario difficult to attain, since in 2012 radiative forcing was already $2.9\,W\cdot m^{-2}$. To realize RCP 2.6, atmospheric CO_2 must be stabilized at $450\,ppm$ which requires a ~70% reduction of CO_2 emissions relative to the level in 2000.
- The RCP 4.5 (medium low) and RCP 6.0 (medium high) are stabilization scenarios on the assumption that technologies and strategies for reducing GHGs emissions are stable and radiative forcing does not further rise after 2100. Also RCP 2.6 and 4.5 scenarios include 'carbon dioxide removal' (CDR) programs to remain within the radiative forcing limit but these CDR programs are presently considered difficult to realize.
- The RCP 8.5 is characterized by high GHGs concentration levels, stabilizing emissions post-2100. Radiative forcing is set to reach $8.5\,W\cdot m^{-2}$ by 2100 and to continue to rise for some time after [1, 5].

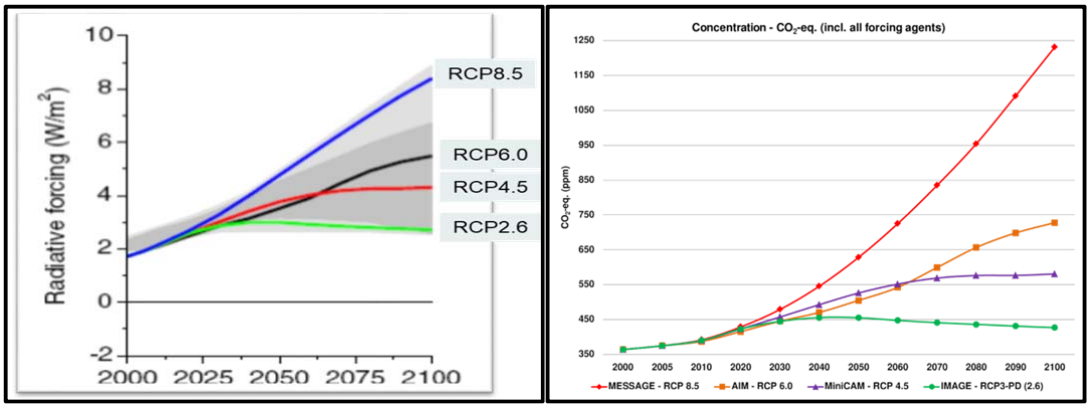

Fig. 1. a) Trends in radiative forcing for RCPs scenarios; b) GHGs concentrations, expressed as atmospheric CO2-equivalent concentrations (ppm), corresponding to each RCP scenario up to 2100

IPCC-AR5 also shows that increase of global mean surface temperatures for 2081–2100 relative to 1986–2005 is projected to 'likely be' in the range of $0.3 - 1.7°C$ (RCP 2.6 scenario), $1.1 - 2.6°C$ (RCP 4.5 scenario), $1.4 - 3.1°C$ (RCP 6.0 scenario), or $2.6 - 4.8°C$ (RCP 8.5 scenario). The temperature during the reference period 1986–2005, has already risen by $\sim 0.6\,°C$ relative to the pre-industrial temperature. Depending on the scenario considered, global average temperature on land surface is anticipated to rise with a maximum of 6 °C by 2100, relative to averaged 1986–2005 temperatures, with little difference between Winter and Summer. Sea surface temperature will rise as well with $\sim 2°C$. The sea surface tends to warm more than land surface, at least in Winter. Warm days will drastically increase in number, while cold days will decrease. In certain regions anomalies are to be expected, surface temperature for 2080-2099 is anticipated to rise up to a maximum of $10\,°C$, particularly in the Arctic, threatening massive melting of Greenland ice sheets. According to IPCC- AR5 arctic sea ice will virtually disappear ($< 1\,km^2$ in extent) by 2050. Antarctic sea

ice extent is also expected to decrease, but at a considerably slower rate. Decreased sea ice extent means less albedo and thus faster warming. In all RCP scenarios NH snow cover extent is anticipated to decrease, resulting in reduced albedo and further warming.

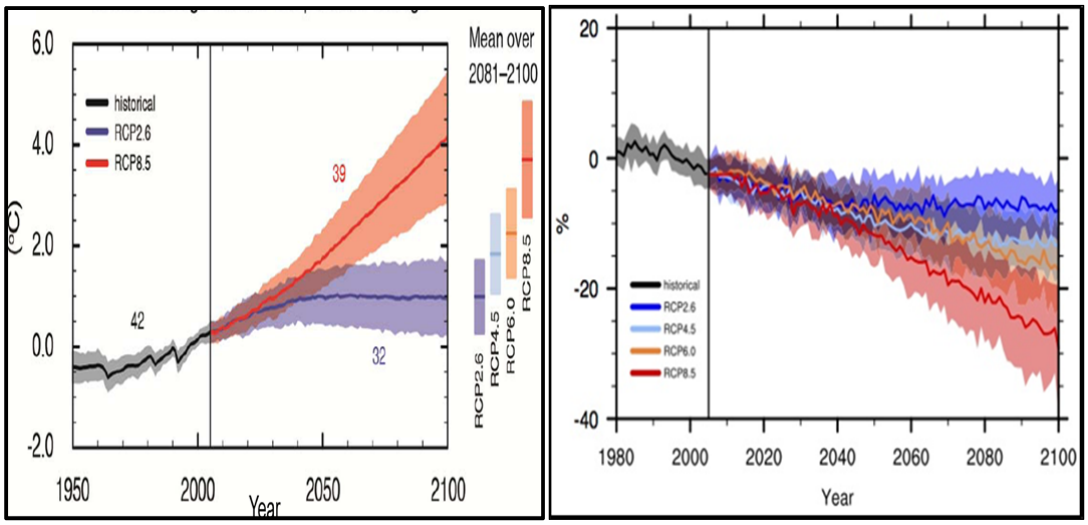

Fig. 2: a) Global average surface temperature change; b) Snow cover extent change

Table 1: Overview of the main characteristics of RCPs scenarios

RCPs	**Radiative forcing**	**Concentration (ppm)**	**Temperatures** (average increase relative to 1986-2005)	**Pathway**
RCP 2.6	Peak in radiative forcing at 3.1 $W \cdot m^{-2}$ before 2100 and then decline to 2.6 $W \cdot m^{-2}$	Peak ~490 ppm before 2100, then declines	$0.3 - 1.7$℃	Declining use of oil; Low energy intensity; A world population of 9 billion by year 2100; Use of croplands increase due to bio-energy production; More intensive animal husbandry; Methane emissions reduced by 40 per cent; CO2 emissions stay at today's level until 2020, then decline and become negative in 2100;
RCP 4.5	Stabilization without overshoot to 4.5 $W \cdot m^{-2}$after 2100	peak ~650 ppm at stabilization after 2100	$1.1 - 2.6$℃	Lower energy intensity; Strong reforestation programs; Decreasing use of croplands and grasslands due to yield increases and dietary changes; Stringent climate policies; Stable methane emissions; CO2
RCP 6.0	Stabilization without overshoot to 6 $W \cdot m^{-2}$ at stabilization after 2100	peak ~850 ppm at stabilization after 2100	$1.4 - 3.1$℃	Heavy reliance on fossil fuels; Intermediate energy intensity Increasing use of croplands and declining use of grasslands; Stable methane emissions; CO2 emissions peak in 2060 at 75 per cent above today's levels, then decline to 25 per cent above today
RCP 8.5	> 8.5 $W \cdot m^{-2}$in 2100	> 1370 ppm in 2100 (Three times today's CO_2 emissions by 2100)	$2.7 - 4.8$℃	Rapid increase in methane emissions; Increased use of croplands and grassland which is driven by an increase in population; A world population of 12 billion by 2100; Lower rate of technology development; Heavy reliance on fossil fuels; High energy intensity; No implementation of climate policies

3. The point energy balance model description

Basic approaches used for snowmelt and SWE are energy balance models (EBM) and Temperature index models (TIM) in which air temperature is used to index all of the energy fluxes or their combination as a hybrid method.

The physically based model [3, 4, 6] for the simulation of daily energy balance, SWE and melt rates of a snow cover using the energy balance for a snowpack:

$$\mathrm{E} = \mathrm{R_n} + \mathrm{H} + \mathrm{L} + \mathrm{A} + \mathrm{G} \quad (2)$$

where E is the energy available for snowmelt and the following fluxes are taken into account: the net radiation $\mathrm{R_n}$, the sensible heat flux H, the latent heat flux L, the advective energy supplied by solid or liquid precipitation A, and the soil heat flux G. All energy flux densities are expressed in $[\mathrm{Wm^{-2}}]$ for hourly step and in $[\mathrm{MJ \cdot m^{-2} \cdot day^{-1}}]$ for daily step.

Net radiation $\mathrm{R_n}$ is the difference between incoming $\mathrm{R_{in}}$ and outgoing radiation $\mathrm{R_{out}}$ of both short and long wavelengths. It is the sum between the net shortwave $\mathrm{R_{ns}}$ and the net outgoing longwave $\mathrm{R_{nl}}$ radiation.

$$\mathrm{R_n} = \mathrm{R_{in}} - \mathrm{R_{out}} = \mathrm{R_{ns}} + \mathrm{R_{nl}}. \quad (3)$$

Sensible heat is heat exchanged by a body that changes the temperature (from atmosphere into snowpack). It is expressed using wind speed $W\ [m \cdot s^{-1}]$ at 2 m, T_a, T_s [°C] are air temperature and snow surface temperature.

Daily sensible heat $H\ [\mathrm{MJ \cdot m^{-2} \cdot day^{-1}}]$

$$H = 0.372 \cdot W \cdot (T_a - T_s). \quad (4)$$

Latent heat of sublimation is the amount of heat exchanged; it occurs without change of temperature.

Daily latent heat $L\ [\mathrm{MJ \cdot m^{-2} \cdot day^{-1}}]$

$$L = 0.372 \cdot W \cdot (T_a - T_s). \quad (5)$$

The advective energy A supplied by precipitation P [mm] depends on its phase chosen in function of a threshold temperature $T_{wK}\ [K]$

In case of rainfall on snow for melting condition $T_{sK} \geq 273.16$

$$A = P \cdot c_{sw} \cdot (T_{aK} - 273.15) \quad (6)$$

where $c_{sw} = 4.18 \cdot 10^3\ Jkg^{-1}K^{-1}$ is the specific heat of water.

- If rain falls on cold snow $T_{aK} \geq 273.15$ refreezing is assumed so

$$A = P \cdot (c_{i+}c_{sw} \cdot (T_{aK} - 273.15)) \quad (7)$$

where $c_i = 3.375\ 10^5\ Jkg^{-1}$ is melting heat of ice.

- For snowfall

$$A = P \cdot c_{ss} \cdot (T_{wK} - T_{sK}) \quad (8)$$

where $c_{ss} = 2.1 \cdot 10^3 Jkg^{-1}K^{-1}$ is specific heat of snow.

The small mass changes δe in mm generated by (re)sublimation are simulated, for a time period Δt, with

$$\delta e = \frac{E \cdot \Delta t}{l_s} \quad (9)$$

where $l_s = 2.835 \cdot 10^6 Jkg^{-1}$ is the (re)sublimation heat of snow.

If the resulting energy balance is positive, melt can occur and the amount of melt water M in mm, for a time period Δt, is calculated with

$$M = \frac{E \cdot \Delta t}{c_i}. \quad (10)$$

Calculate SWE using SWE balance equation

$$SWE_i = \max(SWE_{i-1} + P_i + \delta e_i - M_i, 0). \quad (11)$$

The assumed scheme when melt can occur calculates melt rates if $T_{aK} \geq 273.16\,K$(air temperature) and snow temperature surface take a value of $T_{sK} = 273.16$ K. Also, the algorithm makes distinction between the snow and the rain phase using a threshold temperature of $275.16\,K$. The soil heat flux G, is small compared to R_n and it has not been taken into account.

4. Results and discussion

Study Area

The measurements were performed in the Bucegi Mountains located in the center of Romania (Fig.3). The study area is relevant for high altitude mountains in Romania, where snow cover can last, at altitudes of 1500 -1600 m above sea level, until April or May.

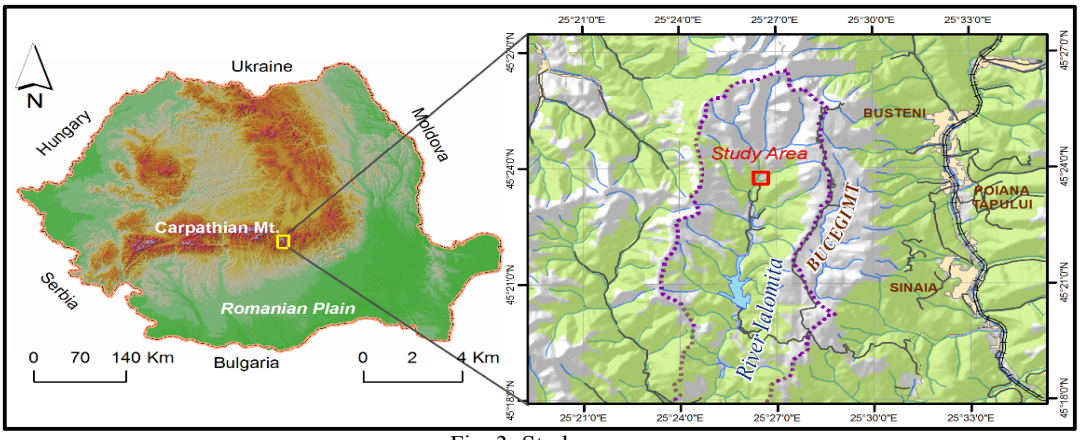

Fig. 3: Study area

Meteorological data

National Meteorological Administration provided data from Padina area for the same period, April, in order to evaluate mean SWE. We consider the year 2005 as historical year and compare evolution of SWE under RCP 2.6 and RCP 8.5 for years: 2015, 2020, 2030, 2040 and 2050. The daily data provided for that analysis is: snow depth $h_s\,[m]$, air temperature $T_{aK}\,[K]$, precipitation $P\,[mm]$, relative humidity RH [%], wind speed $W\,[m \cdot s^{-1}]$, cloud cover CC [%], net radiation $R_n\,[W \cdot m^{-2}]$.

Results Analysis

We analyzed the average air temperature and snow thicknesses for April in the Padina area, obtained from the simulations using the RCP 2.6 and RCP 8.5 scenarios and showed the following changes as compared to 2005 as the reference year.

Compared to the average temperature of April 2005 that was $3.6\,℃ = 276.7\,K$, for April 2050, for the RCP 2.6 scenario the average temperature dropped by 92% reaching a value of almost $0.8℃ = 274\,K$ and increased by 51.5% for the RCP 8.5 scenario reaching $5.4\,℃ = 278.6\,K$.

Compared to the average depth of the snow in April 2005, which was $36.1\,mm$, for April 2050, for the RCP 2.6 scenario the average snow depth increased by 18.4% to $42.6\,mm$ and decreased by 40% for the RCP 8.5 scenario reaching $21.6\,mm$.

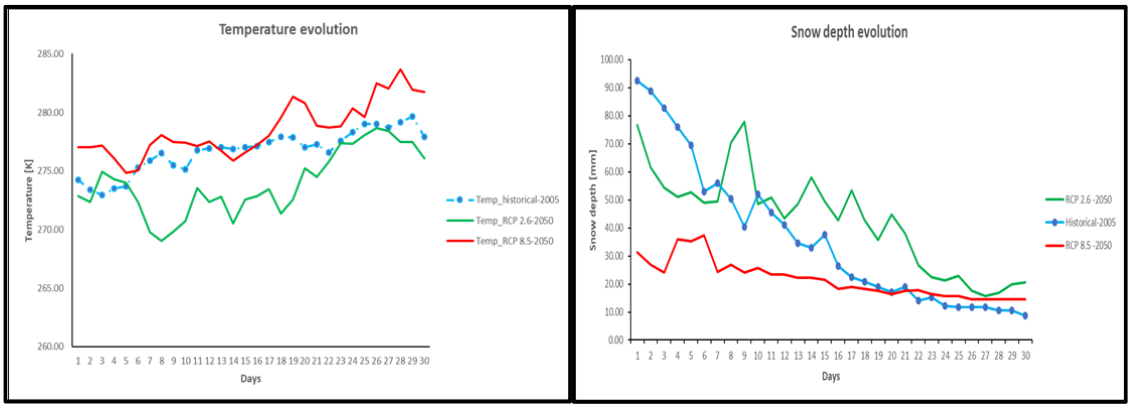

Fig. 4: a) Air temperature under RCP 2.6 and RCP 8.5 for 2050; b) Snow depth variation under RCP 2.6 and RCP 8.5 for 2050

The average SWE evolution for April compared to the reference period (2005), based on the RCP 2.6 scenario data showed an increase of 131.6% to its peak of 188.53 mm in 2015, followed by a decrease of 46.3% to a minimum value of 43.64 mm in 2040 is followed by a slow rise up to 59.35 mm until 2050, which represents a 27% decrease.

For April 2050, the RCP 2.6 scenario has highlighted the following (compared to the 2005 reference year): a fall in temperature by 2.7 ℃ to near the freezing limit 0.8 ℃ , the average thickness of the snow increased by 18.4%, the rate melting has decreased by 52% and average SWE has decreased by 27% and infiltration can be limited by the ice content in the soil, decreasing with the decrease of SWE.

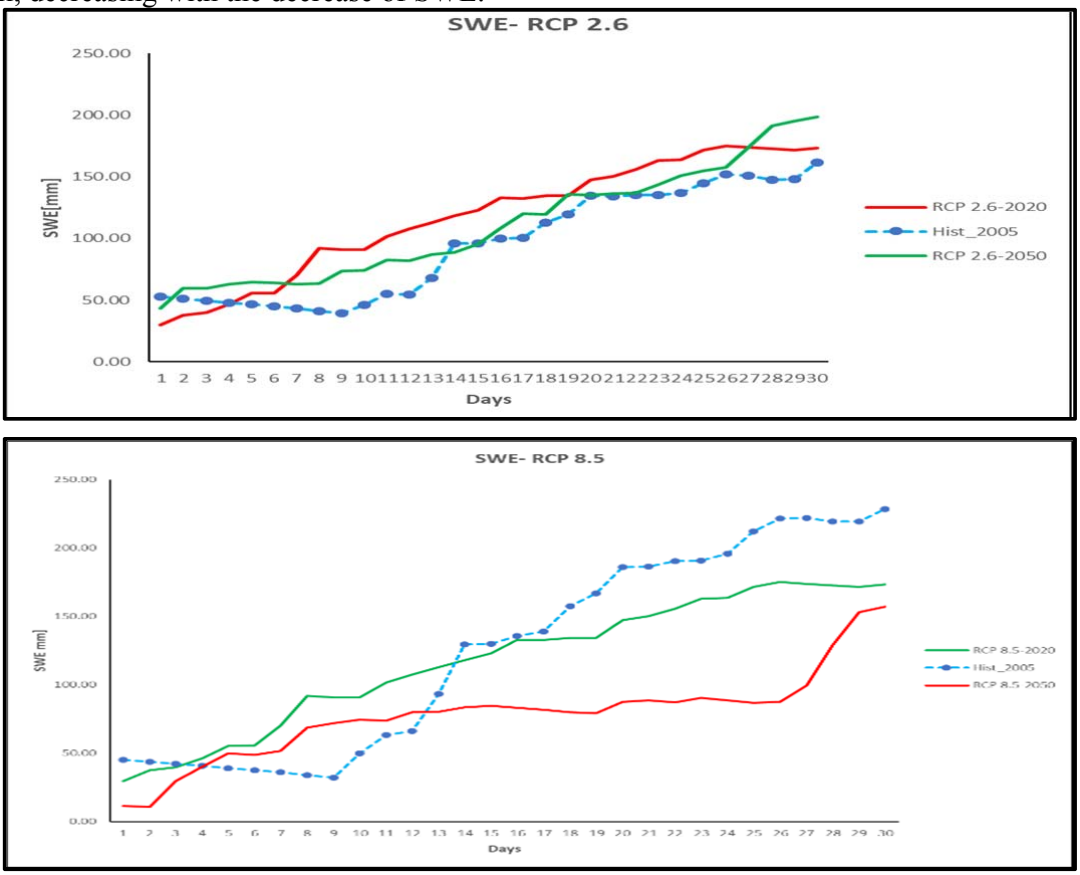

Fig. 5: SWE variation for 2015, 2020, 2030, 2040, 2050 based on: a) RCP 2.6; b) RCP 8.5

The average SWE evolution for April compared to the reference period (2005) based on the RCP 8.5 scenario data showed an increase of approximately 79% to the peak of 143.73 mm in 2015, followed by an increase of approximately 19% for 2030, 2040($\sim 97mm$) followed by a decrease of 11% to a value of 72,45 mm in 2050.

For the RCP 8.5 scenario for April 2050, the following (compared to the 2005 reference year) were highlighted: an increase in temperature by approximately 1.8℃, the average thickness of the snow decreased by 40%, the melting rate decreased by 45.5% and mean SWE was down 11%. Taking into account the net positive temperatures, if the soil is not saturated, the entire amount will infiltrate. If the soil is saturated, the amount of water resulting from the melting of the snow will flow down the slope as a surface runoff.

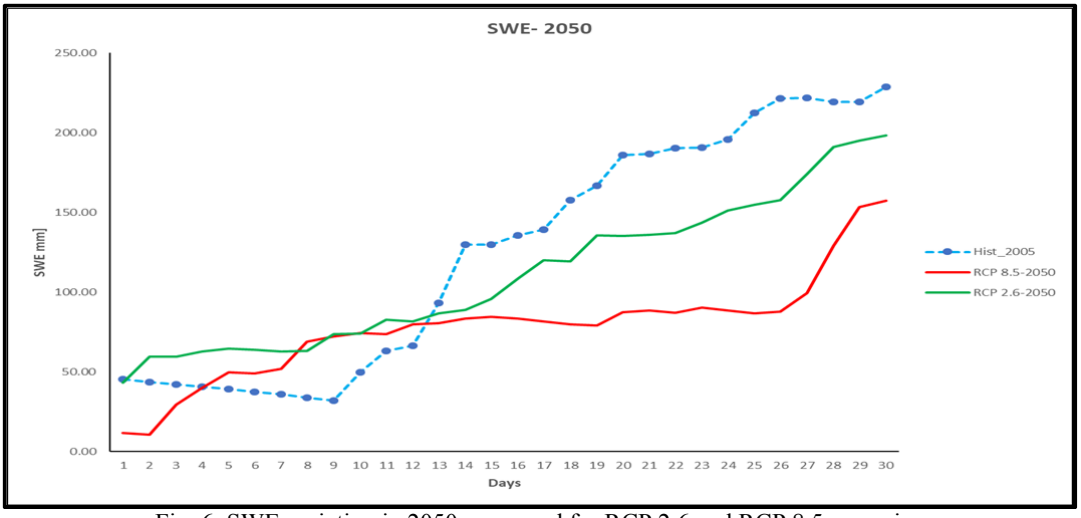

Fig. 6: SWE variation in 2050 compared for RCP 2.6 and RCP 8.5 scenarios

The April SWE variation in the Padina area, obtained from the RCP 2.6 and RCP 8.5 climate scenarios, is illustrated against the simulated results obtained in April 2005 when the SWE average is 81.38 mm.

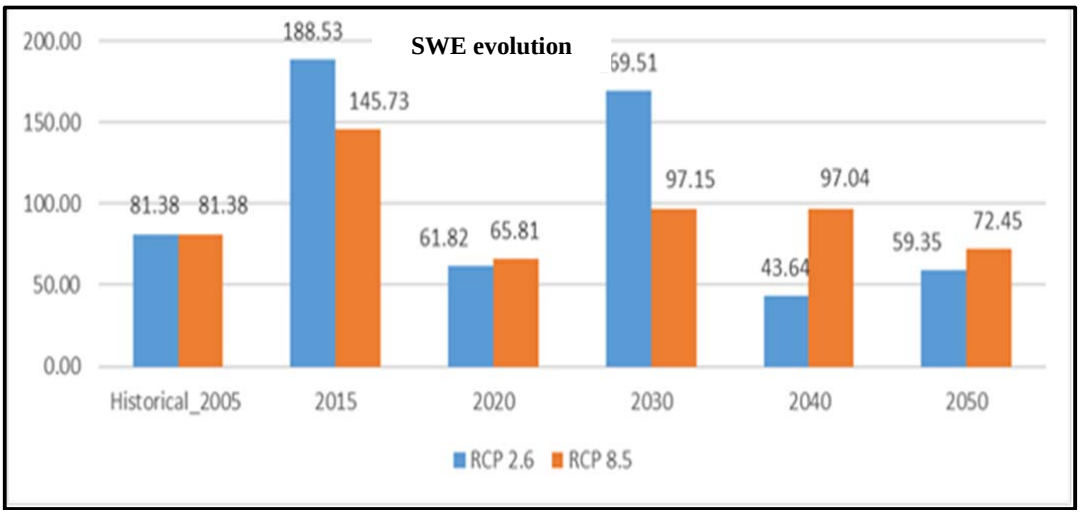

Fig. 7: Variation of the SWE for 2015, 2020, 2030, 2040, 2050 compared for RCP 2.6 and RCP 8.5 scenarios

6. Conclusions

The paper summarizes the main characteristics of the four RCPs developed for the climate modeling, depending on GHGs emissions. Daily model calculations are implemented in Excel so the portability of the spreadsheet version makes it suitable to be taken to the field. In addition, the model allows simulating the effect of potential future climate changes on the evolution of the snowpack, by modifying time series of input parameters.

Based on RCPs 2.6 and 8.5 we analyzed the climate changes impact on snow depth, snowmelt rates and SWE in Padina area from Bucegi Mountains. For April 2005, the reference year, the average temperature was 3.6 ℃, the average snow depth was 36.1 mm and SWE was $81.38\,mm$. The RCP 2.6 projected for April 2050 was that average temperature will decrease near the freezing limit of 0.8 □, the average thickness of the snow increased to $42.6\,mm$ and SWE decreases to $59.35\,mm$. For RCP 2.6 ambitious GHGs emissions reduction would be required over time in order to reach forcing levels. The RCP 8.5 is consistent with a future with no policy changes to reduce emissions. So, the projection of RCP 8.5 for April 2050 shows an increase of medium temperature up to 5.4 ℃, the snow depth decreases up to $21.6\,mm$ and also a slow decrease of SWE to $72{,}45\,mm$.

Acknowledgements

The authors are grateful to Scientific Researcher. Dr. Dragos-Stefan Gaitanaru and Prof. Dr. Constantin Radu from Groundwater Engineering Research Center, Technical University of Civil Engineering Bucharest (UTCB) for their support and comments during SnowBall project (EEA-JRP-RO-NO-2013-1-0285). We also would like to thank to the The National Meteorological Administration of Romania for sharing the hydrological and meteorological data.

References

[1] AR5-IPCC: *Climate Change*, Synthesis Report, 2014
https://www.ipcc.ch/pdf/assessment-report/ar5/syr/SYR_AR5_FINAL_full_wcover.pdf
[2] Birsan, M.-V., Dumitrescu, A.: *Snow variability in Romania in connection to large-scale atmospheric circulation*, Int. J. Climatol. 34, pp 134–144, 2014
doi: 10.1002/joc.3671
[3] Dingman, L.: *Physical Hydrology*, Prentice Hall. Chapter 5 – Snow and Snowmelt, 2002
[4] Gaitanaru, D.S, Dobre G.-R., Gogu, R.: Chapter 4-*Estimation of Snowmelt Infiltration*, Remote sensing, model and in-situ data fusion for snowpack parameters and related hazards in a climate change perspective, Printech, ISBN 978-606-23-0733-2, 2017
[5] Meinshausen, M. et al.: *The RCP greenhouse gas concentrations and their extensions from 1765 to 2300*, Climatic Change, 109 (1-2): 213–241, 2011
doi:10.1007/s10584-011-0156-z
[6] Strasser, U., Marke, T., *ESCIMO.spread – a spreadsheet-based point snow surface energy balance model to calculate hourly snow water equivalent and melt rates for historical and changing climate conditions*, Geosci. Model Dev., 3, pp 643-652,2010
doi: 10.5194/gmd-3-643-2010

GENERALIZED WINTGEN INEQUALITY FOR SUBMANIFOLDS IN QUATERNIONIC SPACE FORMS

VALENTIN GHIŞOIU AND GABRIEL MACSIM

Abstract. In this paper, we obtain the generalized Wintgen inequality, also known as the DDVV inequality, in the case of a Lagrangian submanifold in quaternionic space forms. We also give a proof for the DDVV inequality in the case of slant submanifolds of a quaternionic space form.

Mathematics Subject Classification (2010): 53C40, 53C25
Key words: Wintgen inequality, DDVV conjecture, Lagrangian submanifolds, slant submanifolds, quaternionic space forms

1. Preliminaries

Definition 1.1. If $\tilde{M}$ is a $4m$-dimensional manifold with the Riemannian metric g, then $\tilde{M}$ is called quaternion Kaehler manifold if there exist a 3-dimensional vector bundle σ of type (1,1) with local basis of almost Hermitian structures J_1, J_2, J_3 such that

$$J_\alpha \circ J_{\alpha+1} = -J_{\alpha+1} \circ J_\alpha = J_{\alpha+2},\ J_\alpha^2 = -\operatorname{Id},$$

where $\alpha, \alpha+1, \alpha+2$ are taken modulo 3.

In this case, σ is called the almost quaternionic structures on $\tilde{M}$, $\{J_1, J_2, J_3\}$ is the canonical local basis of σ. So, $(\tilde{M}, \sigma)$ is called an almost quaternionic manifold, with $\dim \tilde{M} = 4m,\ m \geq 1$.

Definition 1.2. A Riemannian metric $\tilde{g}$ on $\tilde{M}$ is said to be adapted to the almost quaternionic structure σ if it satisfies

$$\tilde{g}(J_\alpha X, J_\alpha Y) = \tilde{g}(X, Y),\ \forall \alpha = \overline{1,3}.$$

$(\tilde{M}, \sigma, \tilde{g})$ is called almost quaternionic Hermitian manifold.

Definition 1.3. If σ is parallel with respect to $\tilde{\nabla}$ of $\tilde{g}$, then $(\tilde{M}, \sigma, \tilde{g})$ is called quaternionic Kaehler manifold. Equivalently, locally defined 1-forms $\omega_1, \omega_2, \omega_3$ exist such that $\forall \alpha = \overline{1,3},\ \tilde{\nabla}_X J_\alpha = \omega_{\alpha+2}(X) J_{\alpha+1} - \omega_{\alpha+1} J_{\alpha+2}$, where $\alpha, \alpha+1, \alpha+2$ are taken modulo 3.

Remark 1.4. *Any quaternionic Kaehler manifold is an Einstein manifold (*$\dim \tilde{M} \geq 4$*).*

Definition 1.5. Let $(\tilde{M}, \sigma, \tilde{g})$ be a quaternionic Kaehler manifold and X be a non-null vector on $\tilde{M}$. Then the 4-plane spanned by $\{X, J_1X, J_2X, J_3X\}$ denoted by $Q(X)$ is called a quaternionic 4-plane. Any 2-plane in $Q(X)$ is called a quaternionic plane. The sectional curvature of a quaternionic plane is called a quaternionic sectional curvature.

Definition 1.6. A quaternionic Kaehler manifold is called a quaternionic space form if its quaternionic sectional curvature is constant, say c.

So, $(\tilde{M}, \sigma, \tilde{g})$ is a quaternionic space form if and only if

$$\tilde{R}(X,Y)Z = \frac{c}{4}\Big\{\tilde{g}(Y,Z)X - \tilde{g}(X,Z)Y + \sum_{\alpha=1}^{3}[\tilde{g}(Z, J_\alpha Y)J_\alpha X -$$

$$-\tilde{g}(Z, J_\alpha X)J_\alpha Y + 2\tilde{g}(X, J_\alpha Y)J_\alpha Z]\},$$

$\forall X, Y, Z \in \Gamma(T\tilde{M})$.

For a submanifold M of $\tilde{M}$, if $\{e_1, \ldots, e_n\}$ is an orthonormal basis of T_pM, $\{e_{n+1}, \ldots, e_{4m}\}$ an orthonormal basis of $T_p^\perp M$, $p \in M$, the mean curvature vector is given by

$$H(p) = \frac{1}{n}\sum_{i=1}^{n} h(e_i, e_i).$$

We denote by

$$h_{ij}^r = g(h(e_i, e_j), e_r),\ i, j = \overline{1, n},\ r = \overline{n+1, 4m}.$$

$$\|h\|^2(p) = \sum_{i,j=1}^{n} g(h(e_i, e_j), h(e_i, e_j)).$$

For a quaternionic Kaehler manifold, we have

$$\tilde{\nabla}_X J_\alpha = \sum_{\beta=1}^{3} Q_{\alpha\beta}(X)J_\beta,\ \alpha = \overline{1, 3},\ \forall X \in \Gamma(T\tilde{M}),$$

where $Q_{\alpha\beta}$ are certain 1-forms locally defined on $\tilde{M}$ such that $Q_{\alpha\beta} + Q_{\beta\alpha} = 0$.

Definition 1.7. A submanifold M of a quaternionic Kähler manifold $(\tilde{M}, \sigma, \tilde{g})$ is said to be a slant submanifold if for each non-zero vector X tangent to M at p, the angle $\theta(X)$ between $J_\alpha(X)$ and T_pM, $\alpha \in \{1, 2, 3\}$ is constant, i.e. it does not depend on the choice of $p \in M$ and $X \in T_pM$. In this case, the slant submanifolds with $\theta = 0$ are called quaternionic submanifolds and those with $\theta = \frac{\pi}{2}$ are called totally real submanifolds. A slant submanifold of a quaternionic Kähler manifold is said to be proper (or $\theta-$slant proper) if it is neither quaternionic nor totally real. An $n-$dimensional totally real submanifold of a quaternionic space form $\tilde{M}^{4m}(c)$ is said to be a Lagrangian submanifold if $n = m$.

2. Wintgen inequality

In 1979, P. Wintgen ([13]) proved that the Gauss curvature K, the squared mean curvature $\|H\|^2$ and the normal curvature $K^\perp$ of any surface M^2 in E^4 satisfy the inequality

$$K \leq \|H\|^2 - K^\perp.$$

The equality holds if and only if the ellipse of curvature of M^2 in E^4 is a circle.

An extension of the Wintgen inequality was given later by B. Rouxel ([11]) and by I.V.Guadalupe and L.Rodriguez ([5]) independently for surfaces M^2 of arbitrary codimension m in real space forms $\tilde{M}^{2+m}(c)$

$$K \leq \|H\|^2 - K^\perp + c.$$

In 2004, A.Mihai ([9]) found a corresponding inequality for totally real surfaces in $n-$dimensional complex space forms. Also, the equality case was studied and the author gived a non-trivial example of a totally real surface satisfying the equality case.

The conjecture of Wintgen inequality which is also known as the *DDVV conjecture* was formulated in 1999 by P.J.De Smet, F.Dillen, L.Verstraelen and L.Vrancken ([12]).

Conjecture. *Let $f : M^n \to \tilde{M}^{n+m}$ be an isometric immersion, where $\tilde{M}^{n+m}$ is a real space form of constant sectional curvature c. Then*

$$\rho \leq \|H\|^2 - \rho^\perp + c,$$

where ρ is the normalized scalar curvature and $\rho^\perp$ is the normalized normal scalar curvature.

Denoting by K and $R^\perp$ the sectional curvature function and the normal curvature tensor on M^n, respectively, the normalized scalar curvature and the normalized normal scalar curvature are given by

$$\rho = \frac{2\tau}{n(n-1)} = \frac{2}{n(n-1)} \sum_{1\le i<j\le n} K(e_i \wedge e_j),$$

$$\rho^\perp = \frac{2\tau^\perp}{n(n-1)} = \frac{2}{n(n-1)} \sqrt{\sum_{1\le i<j\le n} \sum_{1\le \alpha<\beta\le n} \left(R^\perp(e_i, e_j, \xi_\alpha, \xi_\beta)\right)^2},$$

where τ is the scalar curvature.

This conjecture was proven by the authors for submanifolds M^n of arbitrary dimension $n \ge 2$ and codimension 2 in real space forms $\tilde{M}^{n+2}(c)$ of constant sectional curvature c and a detailed characterization of the equality case in terms of the shape operators of M^n in $\tilde{M}^{n+2}(c)$ was given.

T.Choi and Z.Lu ([4]) proved that this conjecture is true for all 3−dimensional submanifolds M^3 of arbitrary codimension $m \ge 2$ in $\tilde{M}^{3+m}(c)$ and give also a characterization for the equality case.

Other extensions of the Wintgen inequality for invariant submanifolds in Kähler, nearly Kähler and Sasakian spaces have been studied by P.J.De Smet, F.Dillen, J.Fastenakels, A.Mihai, J.Van der Veken, L.Verstraelen and L.Vrancken.

Recently, Z.Lu and independently J.Ge and Z.Tang finally settled the general case of the DDVV-conjecture.

Theorem 2.1. *The Wintgen inequality*

$$\rho \le \|H\|^2 - \rho^\perp + c,$$

holds for every submanifold M^n in any real space form $\tilde{M}^{n+m}(c)$, $n \ge 2$, $m \ge 2$.

The equality case holds identically if and only if, with respect to suitable orthonormal frames $\{e_i\}$ and $\{\xi_\alpha\}$, the shape operators of M^n in $\tilde{M}^{n+m}(c)$ take the forms

$$A_{\xi_1} = \begin{pmatrix} \lambda_1 & \mu & 0 & \dots & 0 \\ \mu & \lambda_1 & 0 & \dots & 0 \\ 0 & 0 & \lambda_1 & \dots & 0 \\ \vdots & \vdots & \vdots & \ddots & \vdots \\ 0 & 0 & 0 & \dots & \lambda_1 \end{pmatrix}, \tag{2.1}$$

$$A_{\xi_2} = \begin{pmatrix} \lambda_2 + \mu & 0 & 0 & \dots & 0 \\ 0 & \lambda_2 - \mu & 0 & \dots & 0 \\ 0 & 0 & \lambda_2 & \dots & 0 \\ \vdots & \vdots & \vdots & \ddots & \vdots \\ 0 & 0 & 0 & \dots & \lambda_2 \end{pmatrix}, \tag{2.2}$$

$$A_{\xi_3} = \begin{pmatrix} \lambda_3 & 0 & 0 & \dots & 0 \\ 0 & \lambda_3 & 0 & \dots & 0 \\ 0 & 0 & \lambda_3 & \dots & 0 \\ \vdots & \vdots & \vdots & \ddots & \vdots \\ 0 & 0 & 0 & \dots & \lambda_3 \end{pmatrix}, \tag{2.3}$$

$A_{\xi_4} = \cdots = A_{\xi_m} = 0$, *where $\lambda_1, \lambda_2, \lambda_3$ and μ are real functions on M^n.*

Definition 2.2. Submanifolds satisfying the equality in the Wintgen inequality are called Wintgen ideal submanifolds ([6]).

3. An inequality for Lagrangian submanifolds in quaternionic space forms

I.Mihai proved the following generalized Wintgen inequality for Lagrangian submanifolds in complex space forms.

Theorem 3.1. *([10]) Let M^n a Lagrangian submanifold in a complex space form $\tilde{M}^m(4c)$. Then*

$$(\rho^\perp)^2 \leq (\|H\|^2 - \rho + c)^2 + \frac{4}{n(n-1)}(\rho - c)c + \frac{2c^2}{n(n-1)}.$$

We have proved a similar inequality for Lagrangian submanifolds of quaternionic space forms.

Let M^n be an $n-$dimensional totally real submanifold of an $4m-$dimensional quaternionic space form $\tilde{M}^{4m}(4c)$ and $\{e_1, \ldots, e_n\}$ an orthonormal frame on M^n and $\{\xi_{n+1}, \ldots, \xi_{4m}\}$ an orthonormal frame in the normal bundle $T^\perp M^n$, respectively.

The scalar normal curvature of M^n is defined by

$$K_N = \frac{1}{4}\sum_{r,s=n+1}^{4m} \text{Trace}[A_r, A_s]^2. \tag{3.1}$$

Then the normalized scalar normal curvature is given by

$$\rho_N = \frac{2\sqrt{K_N}}{n(n-1)}.$$

From (3.1) we get

$$K_N = \frac{1}{2}\sum_{1\leq r<s\leq 4m-n} \text{Trace}[A_r, A_s]^2 = \tag{3.2}$$

$$\sum_{1\leq r<s\leq 4m-n}\ \sum_{1\leq i<j\leq n} (g([A_r, A_s]e_i, e_j))^2$$

Denoting by $h^r_{ij} = g(h(e_i, e_j), \xi_r),\ i, j = \overline{1, n},\ r = \overline{1, 4m-n}$, we have

$$K_N = \sum_{1\leq r<s\leq 4m-n}\ \sum_{1\leq i<j\leq n} \left(\sum_{k=1}^{n}(h^r_{jk}h^s_{ik} - h^r_{ik}h^s_{jk})\right)^2. \tag{3.3}$$

We proved the following lemma

Lemma 3.2. *Let M^n be a totally real submanifold of an $4m-$dimensional quaternionic space form $\tilde{M}^{4m}(4c)$. Then we have*

$$\|H\|^2 - \rho_N \geq \rho - c. \tag{3.4}$$

The equality case holds identically if and only if, with respect to suitable orthonormal frames $\{e_i\}$ and $\{\xi_\alpha\}$, the shape operators of M^n in $\tilde{M}^{4m}(4c)$ take the same forms as in (2.1), (2.2), (2.3) and $A_{\xi_4} = \cdots = A_{\xi_{4m-n}} = 0$, where $\lambda_1, \lambda_2, \lambda_3$ and μ are real functions on M^n.

Using this lemma, we have proved the following main result

Theorem 3.3. *Let M^n be a Lagrangian submanifold of a quaternionic space form $\tilde{M}^{4n}(4c)$. Then*

$$\left(\rho^\perp\right)^2 \leq \left(\|H\|^2 - \rho + c\right)^2 + \frac{6}{n(n-1)}c^2 + \frac{4}{n(n-1)}c(\rho - c). \tag{3.5}$$

4. An inequality for slant submanifolds in quaternionic space forms

A similiar inequality to (3.4) can be proved in the case of a slant submanifold in a quaternionic space form.

We recall the definition of a slant submanifold in a quaternionic space form.

Definition 4.1. A submanifold M of a quaternionic Kähler manifold $(\tilde{M}, \sigma, \tilde{g})$ is said to be a slant submanifold if for each non-zero vector X tangent to M at p, the angle $\theta(X)$ between $J_\alpha(X)$ and T_pM, $\alpha \in \{1, 2, 3\}$ is constant, i.e. it does not depend on the choice of $p \in M$ and $X \in T_pM$.

Theorem 4.2. *Let M^n be an $n-$dimensional $\theta-$slant submanifold of an $4m-$dimensional quaternionic space form $\tilde{M}^{4m}(4c)$. Then, we have*

$$\|H\|^2 \geq \rho + \rho_N - c - \frac{9c}{n-1}\cos^2\theta. \tag{4.1}$$

Remark 4.3. *The result obtained in (4.2) taking M as a totally real submanifold is identic with (3.4) from lemma (3.2).*

5. Acknowledgement

The present paper is based on [8].

References

[1] S. Albeverio and W. Karwowski, *Diffusion on p-adic numbers*, in K. It and H. Hida (eds), Gaussian Random Fields, World Scientific, Singapore, 1991.
[2] A. Hohmann, and P. Deuflhard, *Numerical Analysis in Modern Scientific Computing. An introduction*, Springer, 2003.
[3] H. Kaneko, *On (r,p)-capacities for Markov processes*, Osaka J. Math. **23** (1986), 325-336.
[4] T. Choi and Z. Lu, *On the DDVV conjecture and the comass in calibrated geometry I*, Math. Z. **260** (2008), 409-429.
[5] I.V. Guadalupe and L. Rodriguez, *Normal curvature of surfaces in space forms*, Pacific J. Math. **106** (1983), 95-103.
[6] S. Haesen and L. Verstraelen, Natural intrinsic geometrical symmetries, *SIGMA Symmetry Integrability Geom. Methods Appl.* 5 (2009), 15, Paper 086.
[7] Z. Lu, *Normal scalar curvature conjecture and its applications*, J. Funct. Anal. **261** (2011), 1284-1308.
[8] G. Macsim and V. Ghişoiu, *Generalized Wintgen inequality for Lagrangian submanifolds in quaternionic space forms*, Math. Inequal. Appl., to appear.
[9] A. Mihai, *An inequality for totally real surfaces in complex space forms*, Kragujevac J. Math. **26** (2004), 83-88.
[10] I. Mihai, *On the generalized Wintgen inequality for Lagrangian submanifolds in complex space forms*, Nonlinear Anal. **95** (2014), 714-720.
[11] B. Rouxel, *Sur une famille des $A-$surfaces d'un espace Euclidien $\mathbb{E}^4$*, Őesterreischer Mathematiker Kongress, Insbruck, 1981, p.185.
[12] P.J. De Smet, F. Dillen, L. Verstraelen and L. Vrancken, *A pointwise inequality in submanifold theory*, Arch. Math. (Brno) **35** (1999), 115-128.
[13] P. Wintgen, *Sur l'inégalité de Chen-Willmore*, C.R.Acad.Sci., Paris Sér.A-B **288** (1979), A993-A995.

Department of Mathematics and Computer Science, Faculty of Mathematics and Computer Science, University of Bucharest, Bucharest, Romania
E-mail address: ghisoiu@fmi.unibuc.ro

Doctoral School of Mathematics, Faculty of Mathematics and Computer Science, University of Bucharest, Bucharest, Romania
E-mail address: gabi_macsim@yahoo.com

A GENERALIZATION OF THE BRIDGE AND TORCH PROBLEM. AN EXACT OPTIMIZATION ALGORITHM

Nicolaie-Marin Goşoniu
School No 39
Şoseaua Colentina 91, sector 3, 021167, Bucharest, Romania
E-mail: mgosoniu@yahoo.com
Marilena Jianu
Department of Mathematics and Computer Science
Technical University of Civil Engineering Bucharest
Bd. Lacul Tei 124, sector 2, 38RO-020396 Bucharest, Romania
E-mail: marilena_jianu@yahoo.com
Sever Angel Popescu
Department of Mathematics and Computer Science
Technical University of Civil Engineering Bucharest
Bd. Lacul Tei 124, sector 2, 38RO-020396 Bucharest, Romania
E-mail: angel.popescu@gmail.com

Abstract: In this note we give a combinatorial solution to the following interesting problem, called in the literature "bridge and torch problem"[3]: suppose that *k* people come to a river in the night. There is a narrow bridge, but it can only hold two people at a time. They have one torch and, because it's night, the torch has to be used when crossing the bridge. Each person can cross the bridge in his own time. When two people cross the bridge together, they must move at the slower person's pace. The question is, what is the minimum time they need to cross (all of them) to the other side. The particular case $k = 4$ is solved in [1] using functional programming languages. Graph theory was used in [2]. We use only elementary combinatorial optimization methods.
Mathematics Subject Classification (2010): 00A06, 00A08, 05A15
Key words: optimization problem, combinatorial optimization, bridge and torch problem

We denote by $P_1, P_2, \ldots, P_k$ the *k* persons, and by $m_1, m_2, ..., m_k$ each person's time needed for crossing the bridge. We can suppose without loss of the generality that $m_1 \le m_2 \le ... \le m_k$. When (P_i, P_j) cross together, the time they need is $\max\{m_i, m_j\}$. Let $f(m_1, m_2, ..., m_k)$ be the minimum time necessary for all the persons to cross to the other side. It is easy to see that $f(m_1, m_2) = m_2$ and $f(m_1, m_2, m_3) = m_1 + m_2 + m_3$.

It can also be easily proved the following lemma:

Lemma 1. *For a fixed* $k \ge 2$, *the function* $f(m_1, m_2, ..., m_k)$ *is "increasing", i.e. it has the following property: if* $(m_1, m_2, \ldots, m_k), (m'_1, m'_2, \ldots, m'_k) \in \mathbb{R}^k$ *such that* $m_i \ge m'_i, \forall i = \overline{1,k}$, *then:*

$$f(m_1, m_2, \ldots, m_k) \ge f(m'_1, m'_2, \ldots, m'_k).$$

Proof. Denote by $T = f(m_1, m_2, \ldots, m_k)$ the minimum time needed when each person P_i can cross the bridge in (at least) m_i minutes. Suppose now that we have other *k* persons, P'_i,

$i = \overline{1,k}$, each one crossing the bridge in m_i' minutes. If they perform exactly the same crossing as $P_1, P_2, \ldots, P_k$ do to obtain the minimum time, *T*, they will clearly obtain a shorter time, $T' \le T$ (since $m_i \ge m_i'$, $\forall i = \overline{1,k}$). But we also have $T' \ge f(m_1', m_2', \ldots, m_k')$ (because $f(m_1', m_2', \ldots, m_k')$ is the minimum value for $P_1', P_2', \ldots, P_k'$) and the lemma follows. □

Now, let us calculate $f(m_1, m_2, m_3, m_4)$. Taking into account that we should minimize the time "lost" when a person has to return with the torch, it is obvious that this person must be either P_1, or P_2. We have to choose between two alternatives:

- $(P_1, P_2), (P_1), (P_1, P_3), (P_1), (P_1, P_4) \rightarrow 2m_1 + m_2 + m_3 + m_4$
- $(P_1, P_2), (P_1), (P_3, P_4), (P_2), (P_1, P_2) \rightarrow m_1 + 3m_2 + m_4$.

The first alternative is optimal if and only if

$$2m_1 + m_2 + m_3 + m_4 \le m_1 + 3m_2 + m_4,$$

which is equivalent to

$$m_3 - m_2 \le m_2 - m_1.$$

Thus, for $k = 4$, we have:

$$f(m_1, m_2, m_3, m_4) = \begin{cases} 2m_1 + m_2 + m_3 + m_4, & \text{if } m_3 - m_2 \le m_2 - m_1 \\ m_1 + 3m_2 + m_4, & \text{if } m_3 - m_2 > m_2 - m_1. \end{cases}$$

Obviously, if $m_3 - m_2 = m_2 - m_1$, the minimum time is obtained for both alternatives.

Suppose, now, $k > 4$. As we saw above, in the optimal solution each person P_i, $i > 2$ crosses the bridge a single time, either in pair with P_1 who must cross back with the torch (and we denote by $\mu(m_i) = m_i + m_1$ the total time needed), or in pair with another person P_j, $j > 2$, but their crossing must be preceded by the pair (P_1, P_2) in order to have someone to take the torch back. In this case, we have the following sequence: $(P_1, P_2), (P_1), (P_i, P_j), (P_2)$, and the total time needed is denoted by $\tau(m_i, m_j) = \max\{m_i, m_j\} + 2m_2 + m_1$.

The alternative $(P_1, P_i), (P_1), (P_1, P_j), (P_1)$ is better than $(P_1, P_2), (P_1), (P_i, P_j), (P_2)$ iff

$$\mu(m_i) + \mu(m_j) \le \tau(m_i, m_j),$$

which is equivalent to

$$\min\{m_i, m_j\} - m_2 \le m_2 - m_1.$$

Since $\min\{m_i, m_j\} \le m_{k-1}, \forall\, i \ne j$, we have proved the following result:

Proposition 1. *If* $m_{k-1} - m_2 \le m_2 - m_1$, *then*

$$f(m_1, m_2, \ldots, m_k) = (k-2)m_1 + m_2 + m_3 + \ldots + m_k. \quad (1)$$

An optimal crossing is: $(P_1, P_2), (P_1), (P_1, P_3), (P_1), \ldots, (P_1, P_{k-1}), (P_1), (P_1, P_k)$ (the order may be changed).

Suppose, now, that $m_{k-1} - m_2 > m_2 - m_1$. Let us try to find the best alternative of crossing for the slowest person, P_k. As we saw above, P_k should cross in pair with another

person P_i such that $m_i - m_2 \le m_2 - m_1$. For any such person P_i, the time $\tau(m_i, m_k)$ is the same: $\tau(m_i, m_k) = m_k + 2m_2 + m_1$, so the total optimal time would be

$$m_k + 2m_2 + m_1 + f(m_1, m_2, \ldots, m_{i-1}, m_{i+1}, \ldots, m_{k-1}).$$

But, since $m_i \le m_{i+1}, \ldots, m_{k-2} \le m_{k-1}$, by Lemma 1 it follows that:

$$f(m_1, m_2, \ldots, m_{i-1}, m_i, \ldots, m_{k-2}) \le f(m_1, m_2, \ldots, m_{i-1}, m_{i+1}, \ldots, m_{k-1}),$$

so the best choice is the pair (P_k, P_{k-1}) and the next Proposition is proved.

Proposition 2. *If* $m_{k-1} - m_2 > m_2 - m_1$, *then*

$$f(m_1, m_2, \ldots, m_k) = m_k + 2m_2 + m_1 + f(m_1, m_2, \ldots, m_{k-2}). \tag{2}$$

In the same hypothesis, $m_{k-1} - m_2 > m_2 - m_1$, we denote by

$$d = \max\{j : m_2 - m_1 \ge m_j - m_2,\ 2 \le j \le k-1\} \text{ (see Fig. 1).}$$

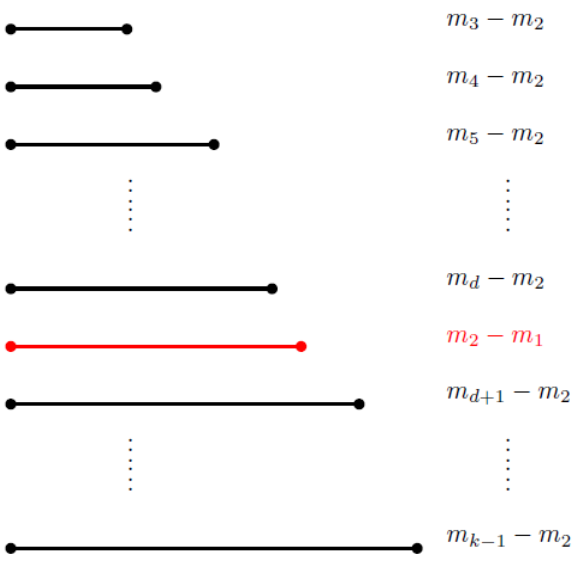

Fig. 1

Since $m_{k-1} - m_2 > m_2 - m_1$, it follows that $d \le k-2$. By Proposition 2, we can apply the recurrence formula (2) t times, where

$$t = \left[\frac{k-d}{2}\right], \tag{3}$$

and we obtain that

$$\begin{aligned} f(m_1, m_2, \ldots, m_k) = m_k + 2m_2 + m_1 + m_{k-2} + 2m_2 + m_1 + \ldots + \\ + m_{k-2t+2} + 2m_2 + m_1 + f(m_1, m_2, \ldots, m_{k-2t}). \end{aligned} \tag{4}$$

Now, by equation (3), it follows that $k - 2t - 1 \in \{d, d-1\}$, so $m_2 - m_1 > m_{k-2t-1} - m_2$. Thus, we can apply Proposition 1 and we have:

$$f(m_1, m_2, \ldots, m_{k-2t}) = (k - 2t - 2)m_1 + m_2 + m_3 + \ldots + m_{k-2t}.$$

After replacing in (4), the next theorem is proved:

Theorem 1. *If* $d = \max\{j : m_2 - m_1 \geq m_j - m_2,\ 2 \leq j \leq k-1\}$ *and* $t = \left\lfloor \frac{k-d}{2} \right\rfloor$, *then*:

$$f(m_1, m_2, \ldots, m_k) = (k-t-2)m_1 + (2t+1)m_2 + \sum_{i=3}^{k-2t} m_i + \sum_{j=0}^{t-1} m_{k-2j}\ . \qquad (5)$$

We can see that Theorem 1 is true even if $m_{k-1} - m_2 \leq m_2 - m_1$: in this case we have $d = k-1$, so $t = 0$ and we obtain the formula (1). If $m_2 - m_1 \leq m_3 - m_2$, which means that $d = 2$, then $t = n-1$ either if $k = 2n$ or $k = 2n+1$ and the formula (5) has the following forms (for *k* even or odd):

$$f(m_1, m_2, \ldots, m_{2n}) = (n-1)m_1 + (2n-1)m_2 + m_4 + m_6 + \ldots + m_{2n},$$
$$f(m_1, m_2, \ldots, m_{2n+1}) = nm_1 + (2n-1)m_2 + m_3 + m_5 + \ldots + m_{2n+1}.$$

References

[1] Martin, E.: Escape from Zurg, *Journal of Functional Programming*, **14** (2004) No. **3**, 253–261.

[2] Rote, G.: Crossing the bridge at night, *Bulletin of the European Association for Theoretical Computer Science,* **78** (2002), 241–246.

[3] https://en.wikipedia.org/wiki/Bridge_and_torch_problem

FULL HERMITE INTERPOLATION OF THE RELIABILITY OF HAMMOCK NETWORKS

Marilena Jianu
Department of Mathematics and Computer Science
Technical University of Civil Engineering Bucharest, Romania,
E-mail: marilena_jianu@yahoo.com
Leonard Dăuş
Department of Mathematics and Computer Science
Technical University of Civil Engineering Bucharest,, Romania
E-mail: daus@utcb.ro

Abstract: Although the hammock networks were introduced more than sixty years ago, there is no general formula of the associated reliability polynomials. Using the full Hermite interpolation polynomial, we propose an approximation for the reliability polynomial of a hammock network of arbitrary size.
Mathematics Subject Classification (2010): 05C31, 05A99, 94Cxx, 68Rxx
Key words: networks, reliability polynomial, lattice paths

1. Introduction

The concept of network reliability can be traced back to 1956, in the work of Moore and Shannon [8]. Their original purpose was to understand the reliability of electrical circuits/networks having unreliable individual components. In order to improve the reliability of such networks, they introduced a new type of circuit called brick-wall (or hammock) network. In the last few years, the interest regarding the work of Moore and Shannon has been growing, not only from theoretical point of view, but also because of its applicability in various fields ranging from biology/medicine to engineering and even social sciences.

The problem of finding the reliability polynomial of a network was proved to belong to the class of #P−complete problems ([2]). Although the brick-wall networks were proposed more than sixty years ago, for their reliability polynomials no general close form formula have been reported yet. Recently, in [3], the reliability polynomials have been calculated exactly for a few particular cases of small size, more precisely for the 29 hammock networks presented by Moore and Shannon in their original paper. Another important step was achieved in [5] where the first and second non-zero coefficients of the reliability polynomial have been computed, for any hammock network. Finally, a direct proof of duality properties for hammock networks was given in [6], reducing the requested calculus for finding reliability polynomials of all hammock networks.

The present paper aims to approximate the reliability of a hammock network by full Hermite interpolation polynomial. Introduced by Hermite in 1877 (see [7]), the full Hermite polynomial preserves not only the values of the function at certain nodes x_i, $i = 0,1,\ldots,n$ (as Lagrange polynomial does), but also the values of the derivatives of the function up to some arbitrary ranks k_i, $i = 0,1,\ldots,n$ (for all $k_i = 1$ the classical Hermite polynomial is obtained).

2. The reliability polynomial of a hammock network

A network is a probabilistic graph [2], $N=(V,E)$, where V is the set of nodes (vertices) and E is the set of (undirected) edges. The edges can be represented as independent identically distributed random variables: each edge operates (is closed) with probability p and fails (is open) with probability $q=1-p$. We assume that nodes do not fail; the fail of the network is always a consequence of edge failures. Let S and T be two special nodes (terminals). The two-terminal reliability of the network N is the probability that there exists a path (a sequence of adjacent edges) made of operational (closed) edges between S (source / input) and T (target / output). It is a polynomial function in p denoted by $h(p)$.

A *pathset* in the network N is a subset of E which contains a path between the nodes S and T. A minimal pathset (*minpath*) is a pathset P such that, if any edge e of P is removed, then $P-\{e\}$ is no longer a pathset (the nodes S and T are disconnected). We denote by $\mathcal{P}$ the set of all the pathsets of N. A *cutset* in the network N is a subset of edges, $C\subset E$, such that the complementary set, $E-C$, contains no path between S and T ($E-C$ is not a pathset). A minimal cutset (*mincut*) is a cutset C such that, if any edge e of C is removed, then $C-\{e\}$ is no longer a cutset ($E-C\cup\{e\}$ is a pathset). We denote by $\mathcal{C}$ the set of all the cutsets of N.

If $n=|E|$ is the size of the graph, N_i is the number of pathsets with exactly i edges and C_i, the number of cutsets with exactly i edges, then the reliability of the network can be expressed in the form (see [2]):

$$h(p)=\sum_{P\in\mathcal{P}}p^{|P|}q^{n-|P|}=\sum_{i=1}^{n}N_i p^i(1-p)^{n-i}, \tag{1}$$

or, in terms of cutsets, as

$$h(p)=1-\sum_{C\in\mathcal{C}}q^{|C|}p^{n-|C|}=1-\sum_{i=1}^{n}C_i(1-p)^i p^{n-i}. \tag{2}$$

A brick-wall network is formed by $w\times l$ identical devices disposed in w lines, each line consisting of l devices connected in series. Besides the horizontal connections, there exist also vertical connections. Out of all $(l-1)(w-1)$ possible vertical connections, half are present and the other half are absent, all the vertical connections being arranged regularly in an alternate way which gives rise to the "brick-wall" pattern. Brick-wall networks were also named by Moore and Shannon *hammock networks*, from their appearance when the nodes S and T are pulled apart and every vertical connection collapses into a node, as rectangular "bricks" deforms into rhombs. As can be seen, the "hammock" representation fits the above definition of the probabilistic graph, unlike the "brick-wall" representation, where the vertical edges have no probability assigned (it is assumed they are always closed).

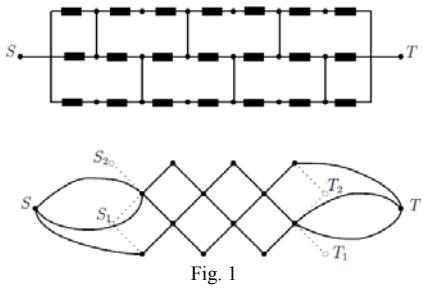

Fig. 1

In Fig. 1 a brick-wall network of dimensions $w=3$, $l=7$ and the corresponding hammock network are represented. Notice that, in order to preserve the regularity of the

network, the terminal nodes S and T can be replaced by some "fictive" terminal nodes, $S_1, S_2, \ldots, S_k$, respectively, $T_1, T_2, \ldots, T_h$, where $k, h \in \left\{\left[\frac{w}{2}\right], \left[\frac{w}{2}\right]+1\right\}$.

We introduced in [6] the concept of $\boldsymbol{X}$ – *path*: a lattice path that never passes twice through the same node and have steps in the set $S = \{(1,1), (-1,1), (1,-1), (-1,-1)\}$. Thus, from a lattice point (x, y) it is allowed to move in 4 directions and reach one of the 4 neighbor points: $(x+1, y+1)$, $(x-1, y+1)$, $(x+1, y-1)$, $(x-1, y-1)$. As one can notice, the sum of coordinates of any neighbor point has the same parity as $x+y$. We say that a lattice point (x, y) is even (odd) if $x+y$ is even (odd). An **X** – path is even (odd) if it contains even (respectively, odd) points.

Let $\mathcal{V}_{l,w} = \left\{A_{x,y} = (x, y) \in \mathbb{Z}^2 : 0 \le x \le l, 0 \le y \le w\right\}$ be the set of all lattice points in the rectangle $[0, l] \times [0, w]$ and $V_{l,w}^{(1)} = \left\{A_{x,y} \in \mathcal{V}_{l,w} : x+y = \text{even}\right\}$, $V_{l,w}^{(2)} = \left\{A_{x,y} \in \mathcal{V}_{l,w} : x+y = \text{odd}\right\}$ be the subsets of even (respectively, odd) points in $[0, l] \times [0, w]$. We denote by $\mathcal{E}_{l,w} = \left\{A_{x,y}A_{x',y'} : A_{x,y}, A_{x',y'} \in \mathcal{V}_{l,w}, \left|x-x'\right| = \left|y-y'\right| = 1\right\}$ the set of all the line segments of length $\sqrt{2}$ connecting points of $\mathcal{V}_{l,w}$. Let $E_{l,w}^{(1)} = \left\{A_{x,y}A_{x',y'} \in \mathcal{E}_{l,w} : x+y = \text{even}\right\}$ be the subset of even edges and $E_{l,w}^{(2)} = \left\{A_{x,y}A_{x',y'} \in \mathcal{E}_{l,w} : x+y = \text{odd}\right\}$, the subset of odd edges.

A *hammock network of the first kind* of dimensions (l, w) is the probabilistic graph $H_{l,w}^{(1)} = \left(V_{l,w}^{(1)}, E_{l,w}^{(1)}\right)$, while a *hammock network of the second kind* is $H_{l,w}^{(2)} = \left(V_{l,w}^{(2)}, E_{l,w}^{(2)}\right)$. We assume that each edge is closed with probability p and open with probability $1-p$. The input (source) nodes are $S_j = A_{0,y}$ (with y = even for the first kind and y = odd for the second kind), and the output (target) nodes are $T_k = A_{l,z}$ (with $l+z$ = even, respectively, odd).

A subset of even (respectively, odd) edges $P \subset E_{l,w}^{(i)}$ is a *pathset* in $H_{l,w}^{(i)}$ if it contains an **X** – path connecting a source node S_j with a target node T_k. Let $\mathcal{P}_{l,w}^{(i)}$ be the set of all pathsets in $H_{l,w}^{(i)}$. A subset $C \subset E_{l,w}^{(i)}$ is a *cutset* in $H_{l,w}^{(i)}$ if $E_{l,w}^{(i)} - C$ contains no **X** – path connecting a source node S_j with a target node T_k. Let $\mathcal{C}_{l,w}^{(i)}$ be the set of all cutsets in $H_{l,w}^{(i)}$. By using these notations in formulas (1) and (2), the reliability polynomials of hammock networks of the first and of the second kind, $h_{l,w}^{(1)}(p)$ and $h_{l,w}^{(2)}(p)$, are written:

$$h_{l,w}^{(i)}(p) = \sum_{P \in \mathcal{P}_{l,w}^{(i)}} p^{|P|}(1-p)^{lw-|P|} = 1 - \sum_{C \in \mathcal{C}_{l,w}^{(i)}} (1-p)^{|C|} p^{lw-|C|},\ i = 1, 2. \tag{3}$$

Remark 1 If l = odd or w = odd, then the hammock networks $H_{l,w}^{(1)}$ and $H_{l,w}^{(2)}$ are isomorphic and the reliability polynomials are identical: $h_{l,w}^{(1)} = h_{l,w}^{(2)}$.

Now, as in [6], we define the dual network. For every edge $e \in \mathcal{E}_{l,w}$, $e = A_{x,y}A_{x+1,y\pm1}$, we denote by $\overline{e} = A_{x+1,y}A_{x,y\pm1}$ its complementary edge (the edge that *cuts e*). It can be seen that the complementary edge of an even edge is odd and the complementary edge of an odd edge is even. Thus, if $e \in E_{l.w}^{(i)}$, then $\overline{e} \in \overline{E_{l,w}^{(i)}} = \mathcal{E}_{l,w} - E_{l,w}^{(i)} = E_{l,w}^{(2/i)}$. By using the notation $\overline{V_{l,w}^{(i)}} = \mathcal{V}_{l,w} - V_{l,w}^{(i)} = V_{l,w}^{(2/i)}$, the dual network of $H_{l,w}^{(i)} = \left(V_{l,w}^{(i)}, E_{l,w}^{(i)}\right)$ is $\overline{H_{l,w}^{(i)}} = \left(\overline{V_{l,w}^{(i)}}, \overline{E_{l,w}^{(i)}}\right)$ with the source nodes $S_j' = A_{x,0} \in \overline{V_{l,w}^{(i)}}$ and the target nodes $T_k' = A_{z,w} \in \overline{V_{l,w}^{(i)}}$. The probability of an edge $\overline{e} \in \overline{E_{l,w}^{(i)}}$ to be closed is the probability of the edge $e \in E_{l.w}^{(i)}$ to be open ("cut"): $q = 1-p$.

Remark 2 The networks $\overline{H_{l,w}^{(i)}}$ and $H_{w,l}^{(2/i)}$ are isomorphic (since they are symmetric with respect to the first bisectrix) and the reliability of the dual network can be written

$$\overline{h_{l,w}^{(i)}}(p) = h_{w,l}^{(2/i)}(1-p). \tag{4}$$

Theorem 1 [6] *Let* $\Sigma = \{e_1, e_2, \ldots, e_n\} \subset E_{l,w}^{(i)}$ *be a subset of edges of the network* $H_{l,w}^{(i)}$ *and let* $\overline{\Sigma} = \{\overline{e}_1, \overline{e}_2, \ldots, \overline{e}_n\} \subset \overline{E_{l,w}^{(i)}}$ *be the set of complementary edges. The following statements hold:*

i) If Σ *is a mincut in* $H_{l,w}^{(i)}$ *then* $\overline{\Sigma}$ *is a minpath in* $\overline{H_{l,w}^{(i)}}$.

ii) If Σ *is a minpath in* $H_{l,w}^{(i)}$ *then* $\overline{\Sigma}$ *is a mincut in* $\overline{H_{l,w}^{(i)}}$.

By Theorem 1 it follows that a set of edges $\Sigma = \{e_1, e_2, \ldots, e_n\} \subset E_{l,w}^{(i)}$ is a pathset in the network $H_{l,w}^{(i)}$ if and only if the set of complementary edges, $\overline{\Sigma} = \{\overline{e}_1, \overline{e}_2, \ldots, \overline{e}_n\} \subset \overline{E_{l,w}^{(i)}}$ is a mincut in the dual network, $\overline{H_{l,w}^{(i)}}$. As a consequence, by using the equation (3) and Remark 2, the next corollary follows.

Corollary 1 *For any* $l, w \geq 1$ *and* $i = 1, 2$ *the following relation is true for all* $p \in [0,1]$*:*

$$h_{l,w}^{(i)}(p) = 1 - h_{w,l}^{(2/i)}(1-p). \tag{5}$$

If at least one of the numbers l *and* w *is odd then* $h_{l,w}^{(1)} = h_{l,w}^{(2)} = h_{l,w}$ *and we have:*

$$h_{l,w}(p) = 1 - h_{w,l}(1-p). \tag{6}$$

Corollary 2 *Let* $h(p) = h_{l,w}^{(i)}(p)$ *be the reliability polynomial of a hammock network of dimensions* l, w*, either of kind 1 or 2. Then the following relations are true:*

$$h(0) = 0, \quad h(1) = 1 \tag{7}$$

$$h^{(k)}(0) = 0, \quad \forall k = 1, 2, \ldots, l-1 \tag{8}$$

$$h^{(k)}(1) = 0, \quad \forall k = 1, 2, \ldots, w-1. \tag{9}$$

Proof. Since any pathset of a hammock network has at least *l* edges, by equation (1), we have:

$$h(p) = \sum_{i=l}^{wl} N_i p^i (1-p)^{wl-i} = \sum_{i=l}^{wl} b_i p^i$$

and the relations (7) and (8) follows immediately.

Let $\overline{h}(p) = h_{w,l}^{(2/i)}(p)$ be the reliability polynomial of the dual network, Since *w* is the length of the dual network, it follows by (8) that $\overline{h}^{(k)}(0) = 0, \forall k = 1, 2, \ldots, w-1$. By Corollary 2 we have that $h(p) = 1 - \overline{h}(1-p)$, and it follows that $h^{(k)}(p) = (-1)^{k+1} \overline{h}^{(k)}(1-p)$. For $p = 1$ we obtain $h^{(k)}(1) = (-1)^{k+1} \overline{h}^{(k)}(0) = 0, \forall k = 1, 2, \ldots, w-1$.

3. Full Hermite interpolation

Given $x_0, x_1, \ldots, x_n$ distinct points in the interval $[a,b]$, $k_0, k_1, \ldots, k_n \geq 0$ nonnegative integers and $f : [a,b] \to \mathbb{R}$ a function of class $C^k[a,b]$, where $k = \max_{j=0,n} k_j$, the full Hermite interpolation problem is to find a polynomial $P(x)$ of degree at most $N = \sum_{j=0}^{n} k_j + n$ such that

$$P^{(i)}(x_j) = f^{(i)}(x_j), \forall i = 0, 1, \ldots, k_j, \forall j = 0, 1, \ldots, n. \tag{8}$$

Theorem 2 (see [7], [4], [9]) *Given the distinct points* $x_0, x_1, \ldots, x_n$, *the nonnegative integers* $k_0, k_1, \ldots, k_n \geq 0$ *and the arbitrary real numbers* $f_j^{(i)}$, $i = 0,1,\ldots,k_j$, $j = 0,1,\ldots,n$, *there exists a unique polynomial* $P(x)$ *of degree at most* $N = \sum_{j=0}^{n} k_j + n$ *such that*

$$P^{(i)}(x_j) = f_j^{(i)}, \forall i = 0,1,\ldots,k_j, \forall j = 0,1,\ldots,n. \tag{9}$$

The expression of this polynomial (called full Hermite interpolation polynomial) is

$$P(x) = \sum_{j=0}^{n} \sum_{i=0}^{k_j} f_j^{(i)} l_{i,j}(x), \tag{10}$$

where

$$l_{i,j}(x) = u_j(x) \frac{(x-x_j)^i}{i!} \sum_{r=0}^{k_j - i} \frac{1}{r!} v_j^{(r)}(x_j)(x-x_j)^r, \quad i = 0,1,\ldots,k_j,\ j = 0,1,\ldots,n, \tag{11}$$

$$u_j(x) = \prod_{\substack{t=0 \\ t \neq j}}^{n} (x-x_t)^{k_t+1}, \quad v_j(x) = \frac{1}{u_j(x)},\ j = 0,1,\ldots,n.$$

The full Hermite interpolation polynomial generalize both the Taylor polynomial (obtained for $n = 0$) and the Lagrange polynomial (when $k_j = 0, \forall j = 0,1,\ldots,n$). We can also notice that for $k_j = 1, \forall j = 0,1,\ldots,n$, the classical Hermite polynomial is obtained. This type of interpolation is also known as *osculating* interpolation. The Latin word *osculum*, literally *kiss*, when applied to a curve indicates that it just touches and has the same shape. Hermite interpolation polynomial has this osculating property: it matches a given curve and its derivative forces the interpolating curve to "kiss" the given curve ([1]).

We study now the particular case when $n = 1$. We have two distinct points, which may be the limits of the interval: $x_0 = a$, $x_1 = b$. We denote by $P_{k,m}(x)$ the full Hermite polynomial of order (k,m) interpolating the function $f \in C^{\max(k,m)}[a,b]$. Thus, $P_{k,m}(x)$ is the (unique) polynomial of degree at most $k+m+1$ such that

$$f^{(i)}(a) = P_{k,m}^{(i)}(a), \forall i = 0,1,\ldots,k, \tag{12}$$

$$f^{(i)}(b) = P_{k,m}^{(i)}(b), \forall i = 0,1,\ldots,m. \tag{13}$$

Corollary 3 *The full Hermite polynomial of order* (k,m) *interpolating* f *at the points* $x_0 = a$, $x_1 = b$ *can be written in the following form:*

$$P_{k,m}(x) = \sum_{i=0}^{k} f^{(i)}(a) A_i(x) + \sum_{i=0}^{m} f^{(i)}(b) B_i(x), \tag{14}$$

where

$$A_i(x) = \left(\frac{b-x}{b-a}\right)^{m+1} \frac{(x-a)^i}{i!} \sum_{r=0}^{k-i} \binom{m+r}{m} \left(\frac{x-a}{b-a}\right)^r, \quad i = 0,1,\ldots,k \tag{15}$$

$$B_i(x) = \left(\frac{x-a}{b-a}\right)^{k+1} \frac{(x-b)^i}{i!} \sum_{r=0}^{m-i} \binom{k+r}{k} \left(\frac{b-x}{b-a}\right)^r, \quad i = 0,1,\ldots,m. \tag{16}$$

Corollary 4 *The full Hermite polynomial of order* $(l-1, w-1)$, *interpolating the reliability polynomial of a hammock network of dimensions* (l,w), $h_{l,w}(p)$, *at* $p_0 = 0, p_1 = 1$ *can be written in the following form:*

$$P_{l-1,w-1}(p) = p^l \cdot \sum_{r=0}^{w-1} \binom{l+r-1}{l-1} (1-p)^r. \tag{17}$$

In Figure 2(a) the plots of the reliability polynomial of a hammock network of dimensions $l=3, w=4$, $h_{3,4}(p)$, and the full Hermite interpolation polynomial $P_{2,3}(p)$ are represented:

$$h_{3,4}(p)=12p^3-10p^4-10p^5-18p^6+64p^7-30p^8-38p^9+48p^{10}-20p^{11}+3p^{12}$$

$$P_{2,3}(p)=20p^3-45p^4+36p^5-10p^6.$$

As can be seen, when w and l are even numbers, the full Hermite interpolation polynomial of order $(l-1,w-1)$ is the same for both kinds of networks $h_{l,w}^{(1)}$ and $h_{l,w}^{(2)}$. In Figure 2(b) the plots of the reliability polynomials of the hammock networks of dimensions $l=w=4$ ($h_{4,4}^{(1)}(p)$ and $h_{4,4}^{(2)}(p)$) and the full Hermite interpolation polynomial $P_{3,3}(p)$ are represented:

$$h_{4,4}^{(1)}(p)=24p^4-24p^5-18p^6-40p^7+98p^8+40p^9-6p^{10}-472p^{11}+852p^{12}$$
$$-696p^{13}+308p^{14}-72p^{15}+7p^{16}$$

$$h_{4,4}^{(2)}(p)=18p^4-12p^5-14p^6-32p^7+10p^8+156p^9-126p^{10}-128p^{11}+188p^{12}$$
$$-24p^{13}-68p^{14}+40p^{15}-7p^{16}$$

$$P_{3,3}(p)=35p^4-84p^5+70p^6-20p^7.$$

It is worth to emphasize how accurate is the approximation of the polynomials of degree $w\cdot l$ by a polynomial of degree $w+l-1$.

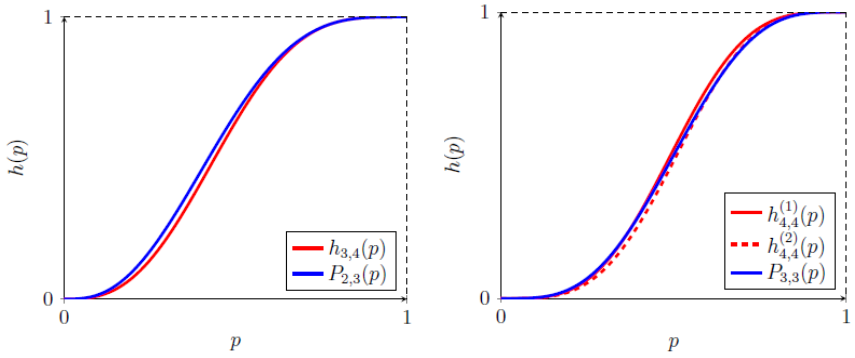

a) b)

Fig. 2

References

[1] Burden, R., Faires, D.: *Numerical Analysis*, Brooks/Cole, Cengage Learning (2011).

[2] Colbourn, C.J.: *The Combinatorics of Network Reliability*, Oxford University Press, Oxford, 1987.

[3] Cowell, S.R., Beiu, V., Dăuş, L., Poulin, P.: On the exact reliability enhancements of small hammock networks, *IEEE Access*, 6 (2018), pp. 25411 - 25426.

[4] Davis, P.: *Interpolation and Approximation*, Dover Publications, Inc., New York (1975).

[5] Dăuş, L., Beiu, V., Cowell, S.R., Poulin, P.: Brick-wall lattice paths and applications, *Tech. Rep. arXiv,* 17 Apr. 2018, http://arxiv.org/abs/222.7960

[6] Dăuş, L., Jianu, M.: The shape of the reliability polynomial of a hammock network, *Tech. Rep. arXiv,* 13 Jan. 2019, http://arxiv.org/abs/1901.04036

[7] Hermite, C.: Sur la formule d'interpolation de Lagrange, J. Reine Angew. Math., 84 (1878), pp. 70-79.

[8] Moore, E.F., Shannon, C.E.: Reliable circuits using less reliable relays Part I, J. Frankl. Inst. 262(3) (1956), pp. 191-208.

[9] Spitzbart, A.: A generalization of Hermite's interpolation formula, Amer. Math. Monthly, 67 (1960), pp. 42-46.

GLAD HELICES IN THREE DIMENSIONAL LIE GROUPS

FATMA KARAKUŞ, YUSUF YAYLI, AND MURAT AKSAR

Abstract. In this paper, we define the dot-Frenet frame, the alternative moving dot frame and the alternative moving frame. Then, we define τ-helix, ν-helix and glad helix (C-helix) in three dimensional Lie groups with a left invariant metric via the dot-Frenet frame, the alternative moving dot frame and the alternative moving frame, respectively. We obtain the axis of the τ-helix, ν-helix and glad helix (C-helix).

Mathematics Subject Classification (2010): Primary 05C38, 15A15; Secondary 05A15, 15A18
Key words: Helix, τ-helix, ν-helix, Glad helix, Lie Group

1. Introduction

Curves theory is important workframe in the differential geometry studies and we have a lot of curves such as geodesics, Salkowski, Bertrand and Mannheim curves, general helices or slant helices etc. Characterizations of these curves are extremely examined for a long time and are still studied by a lot of mathematician. In Euclidean 3-space, if the tangent vector field of any curve makes a constant angle with a fixed straight line then the curve is called as a *general helix* (a curve of constant slope). The well known results stated by Lancert and first proved by B. de Saint Venant in 1845 (see [3, 7, 8] for details). It is necessary and sufficient condition that any curve be a general helix is that the ratio of torsion to curvature be constant. The Lancert theorem was re-examined and solved by Barros [3] in 3-dimensional real space forms by using Killing vector fields along curves. The degenerate Semi-Riemannian geometry of Lie groups was studied by Çöken and Çiftçi [5] and a naturally reductive homogeneous semi-Riemannian space using the Lie group had been obtained by them. The general helices were defined in three dimensional Lie groups with a bi-invariant metric by Çiftçi [11] and a generalization of Lancert theorem was obtained by him. Also, a relation between the geodesics of the so-called cylinders and general helices was given in [11].

In Euclidean 3-space, a new kind of helix called *slant helix* was introduced by Izumiya and Takeuchi [1] and then studied by so many authors. A curve with curvature $\kappa > 0$ is called a *slant helix* if the principal normal lines of the curve make a constant angle with a fixed direction, [1]. A general helix is also a slant helix due to the principal normal lines of the general helix is perpendicular to a fixed direction. Moreover, Izumiya and Takeuchi proved that any space curve is a slant helix in $\mathbb{R}^3$ if and only if the geodesic curvature of the principal normal of a space curve is a constant function. Namely, the geodesic curvature function

$$\sigma = \frac{\kappa^2}{(\kappa^2+\tau^2)^{\frac{3}{2}}}\left(\frac{\tau}{\kappa}\right)' = constant.$$

In [2], the authors characterize slant helices by some differential equations in Euclidean 3-space. The relations between a general helix and a slant helix were investigated and then, the slant helix equations and its Frenet aparatus were given by Kula and etc. In [4], Kula and Yaylı have investigated spherical images of a slant helix and proved that the spherical images of a slant helix are spherical helices. The slant helices were defined in three dimensional Lie groups with a bi-invariant metric by Okuyucu and etc. [12] and some relations between slant helices and their involues, spherical images were given in [12].

C-slant helix which is a special case of k-slant helix by Ali (2012)[6] was defined by Uzunoğlu and etc. in [13]. The axis of the C-slant helix was obtained via the alternative moving frame and the Sabban frame, respectively. Furthermore, the authors have obtained some new characterizations of the C-slant helix and proved that a curve of C constant precession is a C-slant helix in [13].

In this paper, we define the dot-Frenet frame, the alternative moving dot frame and the alternative moving frame. Then, we define τ-helix, ν-helix and glad helix (C-helix) in three dimensional Lie groups with a left invariant metric via the dot-Frenet frame, the alternative moving dot frame and the alternative moving frame, respectively. We obtain the axis of the τ-helix, ν-helix and glad helix (C-helix).

2. Preliminaries

To meet the requirements in the next sections, here, the basic elements of the theory of three dimensional Lie groups with left-invariant metric are briefly presented.

Let G^3 be a three dimensional Lie group with left-invariant metric $\langle \cdot, \cdot \rangle$, g denotes the Lie algebra for G^3 which consists of the all smooth vector fields of G^3 invariant under left translation. There are two classes of three dimensional Lie groups: unimodular and non-unimodular.

In the case of unimodular group, there is an (positively oriented) orthonormal frame of left-invariant vector fields $\{e_1, e_2, e_3\}$ such that brackets satisfy [9, 10]:

$$[e_1, e_2] = \lambda_3 e_3, \qquad [e_3, e_1] = \lambda_2 e_2, \qquad [e_2, e_3] = \lambda_1 e_1.$$

The constant λ_i are called by the *structure constants*. The constants

$$\mu_i = \frac{1}{2}(\lambda_1 + \lambda_2 + \lambda_3) - \lambda_i,$$

are called by the *connection coefficients*.

In the case of non-unimodular group, there is an orthonormal frame $\{e_1, e_2, e_3\}$ such that [9, 10]

$$[e_1, e_2] = \alpha e_2 + \beta e_3, \qquad [e_1, e_3] = -\beta e_2 + \delta e_3, \qquad [e_2, e_3] = 0.$$

Denote by $\mu(X)$ an affine transformation given by

$$\mu(X) = \begin{cases} \mu_1 X^1 e_1 + \mu_2 X^2 e_2 + \mu_3 X^3 e_3 & \text{for unimodular group,} \\ \beta X^1 e_1 + \delta X^3 e_2 - \alpha X^2 e_3 & \text{for non-unimodular group.} \end{cases}$$

In three-dimensional case one can naturally define the *cross product* by

$$e_1 \wedge e_2 = e_3, \qquad e_2 \wedge e_3 = e_1, \qquad e_3 \wedge e_1 = e_2.$$

Then for both types of groups in terms of the cross product we have

$$\nabla_{e_i} e_k = \mu(e_i) \wedge e_k$$

and hence

$$\nabla_X e_k = \mu(X) \wedge e_k$$

Let $\gamma(s)$ be a parametrized curve on the group and $T = \dot{\gamma}$ be tangent vector field. For the arbitrary vector field X we have

$$\nabla_T X = \dot{X}^k e_k + \mu(T) \wedge X, \tag{2.1}$$

In what follows, we call the vector field

$$\dot{X} = \frac{dX^1}{ds} e_1 + \frac{dX^2}{ds} e_2 + \frac{dX^3}{ds} e_3$$

by *dot-derivative* of the vector field X along the curve γ.

Assuming $k_0 = \left|\dot{T}\right| \neq 0$, we can define a new frame $\{\tau, \nu, \beta\}$ along the curve γ by

$$\tau = T, \qquad \nu = \frac{1}{k_0}\dot{\tau}, \qquad \beta = \tau \wedge \nu. \tag{2.2}$$

We call (2.2) by *dot-Frenet frame* [9].

Proposition 2.1. *The dot-Frenet frame $\{\tau, \nu, \beta\}$ satisfies the dot-Frenet formulas, namely,*

$$\begin{aligned} \dot{\tau} &= k_0 \nu \\ \dot{\nu} &= -k_0 \tau + \varkappa_0 \beta, \\ \dot{\beta} &= -\varkappa_0 \nu \end{aligned} \tag{2.3}$$

where $k_0 = \left|\dot{T}\right| \neq 0$ and $\varkappa_0 = \left|\dot{\beta}\right|$ are called dot-curvature and dot-torsion, respectively [9].

Proposition 2.2. *The decomposition of $\mu(T)$ with respect to the dot-Frenet frame is of the form*

$$\mu(T) = \left(\varkappa + \dot{\alpha} - \varkappa_0\right)\tau + (k \sin\alpha)\,\nu - (k_0 - k\cos\alpha)\,\beta$$

[14].

Definition 2.3. *Let $\gamma(s)$ be a parametrized curve on the group. We can define by $\{\nu, C, W\}$ the alternative moving dot frame along the curve γ. Note that $\nu, C = \frac{\dot{\nu}}{\|\dot{\nu}\|}$ and $W = \frac{\varkappa_0 \tau + k_0 \beta}{\sqrt{\varkappa_0^2 + k_0^2}}$ are the dot-normal vector, the derivative of dot-normal vector and Darbux vector, respectively. The dot derivative of the alternative moving dot frame is given by*

$$\begin{aligned} \dot{\nu} &= f(s)\, C \\ \dot{C} &= -f(s)\,\nu + g(s)\, W, \\ \dot{W} &= -g(s)\, C. \end{aligned} \tag{2.4}$$

where $f(s) = \sqrt{\varkappa_0^2 + k_0^2}$, $\sigma = \frac{k_0^2}{\left(\varkappa_0^2 + k_0^2\right)^{\frac{3}{2}}} \left(\frac{\varkappa_0}{k_0}\right)'$, $g(s) = \sigma f(s)$ and $k_0, \varkappa_0$ are the dot-curvature and dot-torsion of the curve α in terms of dot Frenet frame, respectively.

Definition 2.4. *Let $\gamma(s)$ be a parametrized curve on the group and denote by $\{C, E, D\}$ the alternative moving frame along the curve. Note that $C, E = \frac{\dot{C}}{\left\|\dot{C}\right\|}$ and $D = C \wedge E$ are the derivative of dot-normal vector, the derivative of C and Darbux vector of the alternative moving dot frame, respectively. For the dot derivative of the alternative moving frame, we have*

$$\begin{aligned} \dot{C} &= \widetilde{f}(s)\, E \\ \dot{E} &= -\widetilde{f}(s)\, C + \widetilde{g}(s)\, D, \\ \dot{D} &= -\widetilde{g}(s)\, E. \end{aligned} \tag{2.5}$$

where $\widetilde{f}(s) = \sqrt{f^2(s) + g^2(s)}, \widetilde{H} = \frac{g(s)}{f(s)}, \widetilde{\sigma} = \frac{\left(\widetilde{H}\right)'}{f(s)\left(1+\widetilde{H}^2\right)^{\frac{3}{2}}}$, $\widetilde{g}(s) = \widetilde{\sigma}\widetilde{f}(s)$ and $f(s) = \sqrt{\varkappa_0^2 + k_0^2}$, $\sigma = \frac{k_0^2}{\left(\varkappa_0^2 + k_0^2\right)^{\frac{3}{2}}} \left(\frac{\varkappa_0}{k_0}\right)'$, $g(s) = \sigma f(s)$.

3. Helices on Lie Groups

In this section, we investigate τ-helix which is defined using the dot-Frenet frame $\{\tau, \nu, \beta\}$. We give the axis of $\tau-$helix in a three dimensional Lie group G with a left invariant metric. Moreover, we obtain its some new characterizations.

Definition 3.1. *Let $\alpha : I \subset \mathbb{R} \longrightarrow G$ be an arc length parametrized curve in terms of the dot-Frenet frame $\{\tau, \nu, \beta\}$ in a three dimensional Lie group G with a left invariant metric. A curve α is called τ-helix if the vector field τ makes a constant angle $\theta \neq \frac{\pi}{2}$ with a fixed direction u, that is,*

$$\langle \tau, u \rangle = \cos\theta \tag{3.1}$$

along the curve α.

Theorem 3.2. *Let $\alpha : I \subset \mathbb{R} \longrightarrow G$ be an arc length parametrized curve with the dot-Frenet frame $\{\tau, \nu, \beta\}$. Then the curve α is τ-helix if and only if*

$$\frac{\varkappa_0}{k_0} = \cot\theta = constant$$

where θ is a constant angle with the vector field τ, k_0 and $\varkappa_0$ are the dot-curvature and dot-torsion of the curve α in terms of dot-Frenet frame, respectively.

Proof. If $\alpha : I \subset \mathbb{R} \longrightarrow G$ is a parameterized τ-helix then there exist a unit left-invariant vector field u which is the axis of a τ-helix such that

$$\langle \tau, u \rangle = \cos\theta$$

where $\theta = constant$. Calculating the dot-derivative, we obtain

$$\left\langle \dot{\tau}, u \right\rangle + \left\langle \tau, \dot{u} \right\rangle = 0.$$

As $\dot{u} = 0$, by (2.3) we have

$$k_0 \langle \nu, u \rangle = 0.$$

Assume that $k_0 \neq 0$ we have

$$\langle \nu, u \rangle = 0. \tag{3.2}$$

This means that u lies in the $\tau\beta$-plane and hence,

$$u = \cos\theta\tau + \sin\theta\beta.$$

Calculating the dot-derivative and using (2.3), we obtain

$$\begin{aligned} \left\langle \dot{\nu}, u \right\rangle + \left\langle \nu, \dot{u} \right\rangle &= 0 \\ \langle -k_0\tau + \varkappa_0\beta, u \rangle &= 0 \\ -k_0\cos\theta + \varkappa_0\sin\theta &= 0 \end{aligned}$$

and hence,

$$\frac{\varkappa_0}{k_0} = \cot\theta = constant.$$

From $u = \cos\theta\tau + \sin\theta\beta$ and Eq. (2.3), the dot derivative of u becomes,

$$\begin{aligned} \dot{u} &= -\dot{\theta}\sin\theta\tau + \cos\theta\dot{\tau} + \dot{\theta}\cos\theta\beta + \sin\theta\dot{\beta} \\ &= (k_0\cos\theta)\,\nu - (\varkappa_0\sin\theta)\,\nu \\ &= (k_0\cos\theta - \varkappa_0\sin\theta)\,\nu \\ \dot{u} &= 0. \end{aligned}$$

And hence, u is left-invariant. □

Theorem 3.3. *Let $\alpha : I \subset \mathbb{R} \longrightarrow G$ be an arc length parametrized curve with the dot-Frenet frame $\{\tau, \nu, \beta\}$. If the axis of a τ-helix α is u, then is given by*

$$u = \frac{\varkappa_0}{\sqrt{\kappa_0^2 + k_0^2}}\tau + \frac{k_0}{\sqrt{\kappa_0^2 + k_0^2}}\beta$$

where θ is a constant.

Proof. If $\alpha : I \subset \mathbb{R} \longrightarrow G$ is a parameterized τ-helix then there exist a unit left-invariant vector field u which is the axis of a τ-helix such that we can write

$$u = \lambda_1\tau + \lambda_2\nu + \lambda_3\beta,$$

where $\lambda_1 = \langle \tau, u \rangle, \lambda_2 = \langle \nu, u \rangle$ and $\lambda_3 = \langle \beta, u \rangle$. By the definition of τ-helix, we can write

$$\langle \tau, u \rangle = \cos\theta.$$

Differentiating the last equality with respect to s and using the dot-Frenet formulas, we obtain

$$\langle \dot{\tau}, u \rangle + \langle \tau, \dot{u} \rangle = 0$$

$$\langle \nu, u \rangle = 0.$$

So that, we can easily see

$$\lambda_2 = \langle \nu, u \rangle = 0.$$

If we differentiate Eq. (3.2) with respect to s along the curve α and then use Eq. (2.3), we obtain

$$\langle \dot{\nu}, u \rangle = 0$$

$$\langle -k_0 \tau + \varkappa_0 \beta, u \rangle = 0$$

$$k_0 \langle \tau, u \rangle = \varkappa_0 \langle \beta, u \rangle$$

$$\langle \tau, u \rangle = \frac{\varkappa_0}{k_0} \langle \beta, u \rangle .$$

From $\langle \beta, u \rangle = \lambda_3$, we get

$$u = \frac{\varkappa_0}{k_0} \lambda_3 \tau + \lambda_3 \beta.$$

Since u is a unit left-invariant vector field i.e. $\|u\| = 1$, it follows that

$$\frac{\varkappa_0^2}{k_0^2} \lambda_3^2 + \lambda_3^2 = 1$$

$$\left(\frac{\varkappa_0^2}{k_0^2} + 1 \right) \lambda_3^2 = 1$$

$$\lambda_3 = \frac{k_0}{\sqrt{\varkappa_0^2 + k_0^2}}.$$

Therefore, the vector field u can be written

$$u = \frac{\varkappa_0}{\sqrt{\varkappa_0^2 + k_0^2}} \tau + \frac{k_0}{\sqrt{\varkappa_0^2 + k_0^2}} \beta,$$

which completes the proof. □

Definition 3.4. *Let $\alpha : I \subset \mathbb{R} \longrightarrow G$ be an arc length parametrized curve in terms of the alternative moving dot frame $\{\nu, C, W\}$ in a three dimensional Lie group G with a left invariant metric. A curve α is called ν-slant helix if the vector field υ makes a constant angle $\varphi \neq \frac{\pi}{2}$ with a fixed direction ξ, that is,*

$$\langle \nu, \xi \rangle = \cos \varphi \tag{3.3}$$

along the curve α.

Theorem 3.5. *Let $\alpha : I \subset \mathbb{R} \longrightarrow G$ be an arc length parametrized curve with the alternative moving dot frame $\{\nu, C, W\}$. Then the curve α is ν-slant helix if and only if*

$$\sigma = \frac{g(s)}{f(s)} = \cot \varphi = constant$$

where φ is a constant angle with the vector field ν, $f(s) = \sqrt{\varkappa_0^2 + k_0^2}$, $\sigma = \frac{k_0^2}{\left(\varkappa_0^2 + k_0^2\right)^{\frac{3}{2}}} \left(\frac{\varkappa_0}{k_0} \right)'$, $g(s) = \sigma f(s)$ and $k_0, \varkappa_0$ are the dot-curvature and dot-torsion of the curve α in terms of dot Frenet frame, respectively.

Proof. From the definition of ν-slant helix, we know the axis of the curve ξ is a fixed and unit direction. Then we have

$$\langle \nu, \xi \rangle = \cos \varphi$$

where $\varphi = constant$. Differentiating this equation and using Eq.(2.4) we obtain

$$\langle \dot{\nu}, \xi \rangle + \left\langle \nu, \dot{\xi} \right\rangle = 0.$$

As $\dot{\xi} = 0$, we have

$$f(s) \langle C, \xi \rangle = 0.$$

If we assume that $f(s) = \sqrt{\varkappa_0^2 + k_0^2} \neq 0$ we get

$$\langle C, \xi \rangle = 0. \tag{3.4}$$

This means that ξ lies in the νC-plane and hence,

$$\xi = \cos \varphi \nu + \sin \varphi W.$$

Calculating the dot-derivative and using Eq.(2.4), we obtain

$$\begin{aligned} \langle -f(s) \nu + g(s) W, \xi \rangle &= 0 \\ \langle -f(s) \nu, \xi \rangle + \langle g(s) W, \xi \rangle &= 0 \\ -f(s) \cos \varphi + g(s) \sin \varphi &= 0 \end{aligned}$$

and hence,

$$\sigma = \frac{g(s)}{f(s)} = \cot \varphi = constant.$$

From $\xi = \cos \varphi \nu + \sin \varphi W$ and Eq.(2.4), the dot derivative of ξ becomes,

$$\begin{aligned} \dot{\xi} &= f(s) \cos \varphi - g(s) \sin \varphi \\ &= (f(s) \cos \varphi - g(s) \sin \varphi) C \\ \dot{\xi} &= 0. \end{aligned}$$

And hence, ξ is left-invariant. □

Theorem 3.6. *Let $\alpha : I \subset \mathbb{R} \longrightarrow G$ be an arc length parametrized curve with the alternative moving dot frame $\{\nu, C, W\}$. If the axis of a ν-slant helix α is ξ, then is given by*

$$\xi = \frac{g(s)}{\sqrt{f^2(s) + g^2(s)}} \nu + \frac{f(s)}{\sqrt{f^2(s) + g^2(s)}} W$$

where θ is a constant.

Proof. If $\alpha : I \subset \mathbb{R} \longrightarrow G$ is a parameterized ν-slant helix then there exist a unit left-invariant vector field ξ which is the axis of a ν-slant helix such that we can write

$$\xi = \mu_1 \nu + \mu_2 C + \mu_3 W$$

where $\mu_1 = \langle \nu, \xi \rangle, \mu_2 = \langle C, \xi \rangle$ and $\mu_3 = \langle W, \xi \rangle$. By the definition of ν-slant helix, we can write

$$\langle \nu, \xi \rangle = \cos \varphi.$$

Differentiating the last equality with respect to s and using the alternative moving dot frame formulas, we obtain

$$\begin{aligned} \langle \dot{\nu}, \xi \rangle + \left\langle \nu, \dot{\xi} \right\rangle &= 0 \\ \langle C, \xi \rangle &= 0. \end{aligned}$$

So that, we can easily see

$$\mu_2 = \langle C, \xi \rangle = 0.$$

If we differentiate Eq. (3.4) with respect to s along the curve α and then use Eq.(2.4), we obtain

$$\left\langle \dot{C}, \xi \right\rangle = 0$$

$$\langle -f(s)\nu + g(s)W, \xi \rangle = 0$$

$$-f(s)\langle \nu, \xi \rangle = g(s)\langle W, \xi \rangle$$

$$\langle \nu, \xi \rangle = \frac{g(s)}{f(s)}\langle W, \xi \rangle .$$

From $\langle W, \xi \rangle = \mu_3$, we get

$$\xi = \frac{g(s)}{f(s)}\mu_3\nu + \mu_3 W.$$

Since ξ is a unit left-invariant vector field i.e. $\|\xi\| = 1$, it follows that

$$\frac{g^2(s)}{f^2(s)}\mu_3^2 + \mu_3^2 = 1$$

$$\left(\frac{g^2(s)}{f^2(s)} + 1\right)\mu_3^2 = 1$$

$$\mu_3 = \frac{f(s)}{\sqrt{f^2(s) + g^2(s)}}.$$

Therefore, the vector field ξ can be written

$$\xi = \frac{g(s)}{\sqrt{f^2(s) + g^2(s)}}\nu + \frac{f(s)}{\sqrt{f^2(s) + g^2(s)}}W,$$

which completes the proof. □

Definition 3.7. *Let $\alpha : I \subset \mathbb{R} \longrightarrow G$ be an arc length parametrized curve in terms of the alternative moving frame $\{C, E, D\}$ in a three dimensional Lie group G with a left invariant metric. A curve α is called glad helix (C-helix) if the vector field C makes a constant angle $\phi \neq \frac{\pi}{2}$ with a fixed direction ℓ, that is,*

$$\langle C, \ell \rangle = \cos\phi \tag{3.5}$$

along the curve α.

Theorem 3.8. *Let $\alpha : I \subset \mathbb{R} \longrightarrow G$ be an arc length parametrized curve with the alternative moving frame $\{C, E, D\}$. Then the curve α is glad helix (C-helix) if and only if*

$$\widetilde{\sigma} = \frac{\widetilde{g}(s)}{\widetilde{f}(s)} = \cot\phi = constant$$

and the axis of a glad helix (C-helix) is given by

$$\ell = \frac{\widetilde{g}(s)}{\sqrt{\widetilde{f}^2(s) + \widetilde{g}^2(s)}}C + \frac{\widetilde{f}(s)}{\sqrt{\widetilde{f}^2(s) + \widetilde{g}^2(s)}}D$$

where ϕ is a constant angle with the vector field C and $\widetilde{f}(s) = \sqrt{f^2(s) + g^2(s)}, \widetilde{H} = \frac{g(s)}{f(s)}, \widetilde{\sigma} = \frac{\left(\widetilde{H}\right)'}{f(s)\left(1+\widetilde{H}^2\right)^{\frac{3}{2}}}$, $\widetilde{g}(s) = \widetilde{\sigma}\widetilde{f}(s)$.

Proof. From the definition of glad helix (C-helix), we know the axis of the curve ℓ is a fixed and unit direction. Then we have

$$\langle C, \ell \rangle = \cos \phi$$

where $\phi = constant$. Differentiating this equation and using Eq.(2.5) we obtain

$$\left\langle \dot{C}, \ell \right\rangle + \left\langle C, \dot{\ell} \right\rangle = 0.$$

As $\dot{\ell} = 0$, we have

$$\widetilde{f}(s) \langle E, \ell \rangle = 0.$$

If we assume that $\widetilde{f}(s) = \sqrt{f^2(s) + g^2(s)} \neq 0$ we get

$$\langle E, \ell \rangle = 0. \tag{3.6}$$

This means that ℓ lies in the CE-plane and hence,

$$\ell = \cos \phi C + \sin \phi E.$$

Calculating the dot-derivative and using Eq.(2.5), we obtain

$$\begin{aligned} \left\langle -\widetilde{f}(s) C + \widetilde{g}(s) D, \ell \right\rangle &= 0 \\ \left\langle -\widetilde{f}(s) C, \ell \right\rangle + \langle \widetilde{g}(s) D, \ell \rangle &= 0 \\ -\widetilde{f}(s) \cos \phi + \widetilde{g}(s) \sin \phi &= 0 \end{aligned}$$

and hence,

$$\widetilde{\sigma} = \frac{\widetilde{g}(s)}{\widetilde{f}(s)} = \cot \phi = constant.$$

From $\ell = \cos \phi C + \sin \phi D$ and Eq.(2.5), the dot derivative of ℓ becomes,

$$\begin{aligned} \dot{\ell} &= \widetilde{f}(s) \cos \phi - \widetilde{g}(s) \sin \phi \\ &= \left(\widetilde{f}(s) \cos \phi - \widetilde{g}(s) \sin \phi \right) E \\ \dot{\ell} &= 0. \end{aligned}$$

And hence, ℓ is left-invariant.

However, if ℓ is the axis of a glad helix such that we can write

$$\ell = \eta_1 C + \eta_2 E + \eta_3 D$$

where $\eta_1 = \langle C, \ell \rangle, \eta_2 = \langle E, \ell \rangle$ and $\eta_3 = \langle D, \ell \rangle$. From Eq. (3.6)

$$\eta_2 = \langle E, \ell \rangle = 0.$$

Differentiating the last equality with respect to s and using the alternative moving frame formulas, we obtain

$$\begin{aligned} \left\langle -\widetilde{f}(s) C, \ell \right\rangle + \langle \widetilde{g}(s) D, \ell \rangle &= 0 \\ \langle C, \ell \rangle &= \frac{\widetilde{g}(s)}{\widetilde{f}(s)} \langle D, \ell \rangle. \end{aligned}$$

From $\langle D, \ell \rangle = \eta_3$, we get

$$\ell = \frac{\widetilde{g}(s)}{\widetilde{f}(s)} \eta_3 C + \eta_3 D.$$

Since ℓ is a unit left-invariant vector field i.e. $\|\ell\| = 1$, it follows that

$$\frac{\widetilde{g}^2(s)}{\widetilde{f}^2(s)} \eta_3^2 + \eta_3^2 = 1$$

$$\left(\frac{\widetilde{g}^2(s)}{\widetilde{f}^2(s)}+1\right)\eta_3^2=1$$

$$\eta_3=\frac{\widetilde{f}(s)}{\sqrt{\widetilde{f}^2(s)+\widetilde{g}^2(s)}}.$$

Therefore, the vector field ℓ can be written

$$\ell=\frac{\widetilde{g}(s)}{\sqrt{\widetilde{f}^2(s)+\widetilde{g}^2(s)}}C+\frac{\widetilde{f}(s)}{\sqrt{\widetilde{f}^2(s)+\widetilde{g}^2(s)}}D,$$

which completes the proof. □

References

[1] S. Izumiya and N. Takeuchi, New special curves and developable surfaces, *Turk. J. Math.* **28** (2004) 153-163.

[2] L. Kula, N. Ekmekci, Y. Yaylı and K. İlarslan, Characterizations of slant helices in Euclidean 3-space, *Turk. J. Math.* **34 (2)** (2010) 261-273.

[3] M. Barros, General Helices and a theorem of Lancert, *Proc. Am. Math. Soc.* **125 (5)** (1997) 1503-1509.

[4] L. Kula and Y. Yaylı, On slant helix and its spherical indicatrix, *Appl. Math. Comput.* **169 (1)** (2005) 600-607.

[5] A. C. Çöken and Ü. Çiftçi, A note on the geometry of Lie groups, *Nonlinear Anal. TMA* **68** (2008) 2013-2016.

[6] A. T. Ali, New special curves and their spherical indicatrix, *Glob. J. Adv. Res. Class. Mod. Geom.* **1 (2)** (2012) 28-38.

[7] D. J. Struik, Lectures on Classical Differential Geometry, Dover, New-York, 1988.

[8] M. A. Lancret, Mémoire sur les courbes á double courbure, Mémoires présentés à ĬInstitut **1** (1806) 416-454.

[9] A. Opariy and A. Yampolsky, Generalized helices in three dimensional Lie groups, *Turkish Journal of Math.* **43** (2019) 1447-1455.

[10] J. Milnor, Curvatures of Left Invariant Metrics on Lie Groups, *Advances in Math.* **21** (1976) 293-329.

[11] Ü. Çiftçi, A generalization of Lancret's theorem, *J. Geom. Phys.* **59** (2009) 1597-1603.

[12] O. Z. Okuyucu, İ. Gök, Y. Yaylı and N. Ekmekci, Slant helices in three dimensional Lie groups, *Appl. Math. Comput.* **221** (2013) 672-683.

[13] B. Uzunoğlu, İ. Gök and Y. Yaylı, A new approach on curves of constant precession, *Appl. Math. Comput.* **275** (2016) 317-323.

[14] F. Karakuş and Y. Yaylı, The Fermi-Walker derivative in three dimensional Lie groups with left-invariant metric (submitted).

(Fatma KARAKUŞ) Department of Mathematics, Faculty of Sciences and Arts, Sinop University, Sinop, 57000, Turkey

E-mail address: fkarakus@sinop.edu.tr

(Yusuf YAYLI) Department of Mathematics, Faculty of Sciences,Ankara University, Ankara, 06100, Turkey

E-mail address: Yusuf.Yayli@science.ankara.edu.tr

(Murat AKSAR) Department of Mathematics, Faculty of Sciences,Ankara University, Ankara, 06100, Turkey

E-mail address: maksar@ankara.edu.tr

TENSORIAL PRODUCT OF TWO PLANE CURVES

Elena Laura Macri
Student, Faculty of Railways, Roads and Bridges
Technical University of Civil Engineering Bucharest
Bd. Lacul Tei 124, sector 2, 38RO-020396 Bucharest, Romania
E-mail: macri_ela@yahoo.com
Adela Mihai
Assoc. Prof. Dr., Department of Mathematics and Computer Science
Technical University of Civil Engineering Bucharest
Bd. Lacul Tei 124, sector 2, 38RO-020396 Bucharest, Romania
E-mail: adela.mihai@utcb.ro

Abstract: The tensorial product of two plane curves represents a surface in the 4-dimensional Euclidean space $\boldsymbol{E}_4$. We study its properties by using the notion of surface of finite type.
Mathematical Subject Classification (2010): 53A04, 53A05
Key words: Tensorial product; surface of finite type

1. Introduction

One considers the curves:

$$C_1: [a_1, b_1] \to \boldsymbol{E}_2,$$
$$C_1(t) = r(t)(\cos t, \sin t)$$

and

$$C_2: [a_2, b_2] \to \boldsymbol{E}_2,$$

$$C_2(s) = \rho(s)(\cos s, \sin s).$$

The *tensorial product* of the C_1 and C_2 curves is written as:

$$C_1 \otimes C_2: [a_1, b_1] \times [a_2, b_2] \to \boldsymbol{E}_4,$$

$$(C_1 \otimes C_2)(t, s) = r(t)\rho(s)\,(\cos(t)\cos(s), \cos(t)\sin(s), \sin(t)\cos(s), \sin(t)\sin(s)).$$

The tensorial product of two plane curves (which do not pass through the origin) represents a surface in the 4-dimensional Euclidean space $\boldsymbol{E}_4$.

For simplicity, denote by $f = C_1 \otimes C_2$.

We will calculate the coefficients $g_{ij},\ i, j = 1,2$ of the first fundamental form (they are the elements of the matrix which we will denote by g) and also calculate the inverse of g, namely g^{-1}, with the elements $g^{ij},\ i, j = 1,2$.

More precisely, $g_{ij} = < \frac{\partial f}{\partial x^i}, \frac{\partial f}{\partial x^j} >$. In our case, $x^1 = t$ and $x^2 = s$ (for example, $g_{11} = < \frac{\partial f}{\partial t}, \frac{\partial f}{\partial t} >$, etc.); (g_{ij}) is a symmetric matrix in $M_2(\mathbb{R})$.

By denoting $\dot{\rho}(s) = \rho'(s)$ and $\dot{r}(t) = r'(t)$, we get:

$$g = (g_{ij}) = \begin{pmatrix} (r^2(t) + \dot{r}^2(t))\rho(s) & r(t)\dot{r}(t)\dot{\rho}(s)\rho(s) \\ r(t)\dot{r}(t)\dot{\rho}(s)\rho(s) & (\rho^2(s) + \dot{\rho}^2(s))r(t) \end{pmatrix}.$$

The $Laplacian\ \Delta f$ is given by

$$\Delta f(x^1, x^2) = -\frac{1}{\sqrt{\det g}} \sum_{i,j=1}^{2} \frac{\partial}{\partial x^i} (g^{ij} \sqrt{\det g} \frac{\partial f}{\partial x^j}),$$

with $x^1 = t$ and $x^2 = s$.

Also, the *second order Laplacian* is:

$\Delta^2 f(x^1, x^2) = \Delta h(x^1, x^2) = -\frac{1}{\sqrt{\det g}} \sum_{i,j=1}^{2} \frac{\partial}{\partial x^i} (g^{ij} \sqrt{\det g} \frac{\partial h}{\partial x^j})$, where $\Delta f = h$.

On the other hand, in [1] the following definitions are given:

- f is of *type* 1 if and only if there exists $\lambda \in (0, \infty)$ such that $\Delta f = \lambda f$;
- f is of *type* 2 if and only if there exist $\lambda_1, \lambda_2 \in (0, \infty)$, with $\lambda_1 \neq \lambda_2$ such that
$$\Delta^2 f = (\lambda_1 + \lambda_2)\Delta f - \lambda_1 \lambda_2 f.$$

The surfaces of finite type were introduced by Bang-Yen Chen in [1] and are particular cases of submanifolds. They represent a generalisation of the harmonic surfaces (surfaces with $\Delta f = 0$) and are connected to spectral geometry.

Characterizations of curves of finite type in the Euclidean space $\boldsymbol{E}_m$, in particular in $\boldsymbol{E}_3$, are known.

2. The main result

In this article, we study properties of some special surfaces in the 4-dimensional Euclidean space $\boldsymbol{E}_4$. More precisely, we will consider the tensorial product of the curves C_1 and C_2 and study under what conditions this product can be a finite type surface; we also determine its type.

If one takes the general case, the calculations are extremely long; consequently, we will firstly consider a particular case, when the *g* matrix is diagonal, which means that either $\dot{r}(t) = 0$ or $\dot{\rho}(s) = 0$.

For example, let $\dot{\rho}(s) = 0$. It follows that ρ is a constant value, and we can even consider $\rho(s) = 1$, so $C_2(s)$ is a circle of radius 1.

Therefore,
$f(t, s) = (C_1 \otimes C_2)(t, s) = r(t)(\cos(t)\cos(s), \cos(t)\sin(s), \sin(t)\cos(s), \sin(t)\sin(s))$.

This surface is called *the Vrănceanu rotation surface* (some properties of this surface have been studied in [2]).

Denote by

$A(t,s)$=$(\cos(t)\cos(s), \cos(t)\sin(s), \sin(t)\cos(s), \sin(t)\sin(s))$.

Therefore, $f(t,s) = r(t)A(t,s)$.

Consequently,

$$\frac{\partial f}{\partial t} = \dot{r}(t)A(t,s) + r(t)(J_0A)(t,s)$$

and

$$\frac{\partial f}{\partial s} = r(t)(J_1A)(t,s),$$

where $J_0(x,y,z,w) = (-z,-w,x,y)$ and $J_1(x,y,z,w) = (-y,x,-w,z)$ follow their usual notations from differential geometry.

From $g_{11} = r^2(t) + \dot{r}^2(t)$, $g_{12} = g_{21} = 0$ and $g_{22} = r^2(t)$ one obtains

$$\det g = r^2(t)[r^2(t) + \dot{r}^2(t)].$$

We will have:

$$g^{11} = \frac{1}{r^2(t)+\dot{r}^2(t)},\ g^{12} = g^{21} = 0 \text{ and } g^{22} = \frac{1}{r^2(t)}.$$

Then,

$$\Delta f(t,s) = E(t)A(t,s) + F(t)(J_0A)(t,s) = E(t)\frac{1}{r(t)}f(t,s) + F(t)(J_0A)(t,s),$$

which means that f is of type 1 is and only if $F(t) = 0$.

Taking into consideration the mathematical expression of $\Delta f(t,s)$, then $F(t)$, the coefficient of $(J_0A)(t,s)$, after calculations, is given by:

$$F(t) = \frac{\dot{r}(t)}{(\dot{r}^2(t)+r^2(t))^2}(r(t)\ddot{r}(t) - 3\dot{r}^2(t) - 2r^2(t)).$$

Then $F(t) = 0$ if and only if $\dot{r}(t) = 0$, which means that $r(t) = r$ is a constant, or $r(t)\ddot{r}(t) - 3\dot{r}^2(t) - 2r^2(t) = 0$.

From the above differential equation, it follows that the image of f is a minimal surface (see [2]). But this is not possible, because the image must be compact (being of finite type) and compact minimal submanifolds do not exist in the Euclidean space $\boldsymbol{E}_m$.

The coefficient of $A(t)$ is

$$-\frac{1}{r^2}(-r) - \frac{1}{r^2}(-r) = \frac{2}{r}.$$

So, it follows that, in the case under consideration, we showed that

$$\Delta f = \frac{2}{r}\cdot\frac{1}{r}\cdot f = \frac{2}{r^2}f.$$

3. Geometric interpretation and remarks

1) i) For $r = \rho = 1$ the image of $f = C_1 \otimes C_2$ is the Clifford torus.
   ii) For $r = constant, r \neq 1$ and $\rho = 1$ one obtains a generalised Clifford torus.
2) i) The Clifford torus is a minimal surface in $S^3(\sqrt{2})$, but it is not minimal in $\boldsymbol{E}_4$.

ii) The generalised Clifford torus is a minimal surface neither in $S^3(\sqrt{r^2+1})$ nor in $\boldsymbol{E}_4$.

3) For the generalised Clifford torus, one can use the *Beltrami formula* [1]:

$$\Delta f = -2H$$

to calculate the Laplacian, where H is the *mean curvature vector* of the surface.

4) The Takahashi Theorem [1] states that a 1-finite type submanifold (in particular surface) is spherical. Our result is in accordance with the Takahashi Theorem. Moreover, if $\rho \neq constant$, the Takahashi Theorem implies that the image of f is not of 1-finite type.

Finally, we propose to continue this study and to determine the tensorial product surface of two curves which are of type 2.

References

[1] Chen, B.Y.: *Total Mean Curvature and Submanifolds of Finite Type*, World Scientific, 1984.

[2] Mihai, I., Mihai, A., Ghișoiu, V.: *Problems in Differential Geometry* (in Romanian), Editura Universității București, 2012, 2014.

SPECIAL CURVES IN A MYLLER CONFIGURATION

GABRIEL FLORIN MACSIM, ADELA MIHAI AND ANDREEA OLTEANU

Abstract. We consider special curves (rectifying-type and Bertrand curves) in the simplest Myller configuration and study their properties, in order to compare these properties in both cases, Myller and Euclidean settings.

Mathematics Subject Classification (2010): 53A04
Key words: rectifying-type curves, Myller configuration, Bertrand curves

1. Introduction.

Academician Alexandru Myller studied in 1922 the notion of parallelism of $\left(\mathcal{C},\overline{\xi}\right)$ in the plane field $(\mathcal{C},\pi)$, obtaining an interesting generalization of the famous parallelism of Levi-Civita on the curved surfaces.

For a curve $\mathcal{C}$ drawn on a surface $\mathcal{S}$, let's consider a circumscribed developing surface Σ, which we can apply on a plane π. We obtain a curve $\mathcal{C}'$ into this plane, represented by all the points of the curve $\mathcal{C}$, connected to the respective tangent planes developed overlap each other on the plane π. In the same manner, a series (d) of tangent directions to the surface $\mathcal{S}$ at the points of the curve $\mathcal{C}$ becomes, by developing on the plane π, a series (d') of directions getting out from the points of the curve $\mathcal{C}'$. Thus, the directions (d) are parallel on the surface $\mathcal{S}$ if the directions (d') are parallel in the common sense.

This clasical definition of Levi-Civita parallelism was generalized to a more general concept by Alexandru Myller. In a natural way, for the surface Σ was considered the enveloping of the family of planes constructed from the points of the curve $\mathcal{C}$ together with the directions (d). Keeping unchanged the remainder of the definition we come to what Myller called *parallelism into a family of planes*. The curve $\mathcal{C}$ together with the family of planes on its points and the family of the given directions (d) (in an arbitrary way) in these planes constitutes what is named a *Myller configuration*.

To be more specifically, in the Differential Geometry of curves in the Euclidean space $\mathbb{E}_3$ one introduces, along a curve $\mathcal{C}$, standard vector fields, as tangent $\overrightarrow{t}$, principal normal $\overrightarrow{n}$ and binormal $\overrightarrow{b}$, as well as osculating, normal or rectifying planes, generated respectively by $\left(\overrightarrow{t},\overrightarrow{n}\right)$, $\left(\overrightarrow{n},\overrightarrow{b}\right)$ and $\left(\overrightarrow{t},\overrightarrow{b}\right)$.

More generally, one considers a *versor field* (i. e. a unit vector field) $\left(\mathcal{C},\overline{\xi}\right)$ and a plane field $(\mathcal{C},\pi)$. A pair $\left\{\left(\mathcal{C},\overline{\xi}\right),(\mathcal{C},\pi)\right\}$ such that $\overline{\xi}\in\pi$ is called a *Myller configuration* in $\mathbb{E}_3$ and is denoted by $\mathcal{M}(\mathcal{C},\overline{\xi},\pi)$. If, moreover, the planes π are tangent to $\mathcal{C}$, then we have a *tangent Myller configuration* $\mathcal{M}_t(\mathcal{C},\overline{\xi},\pi)$.

In [8] is given a systematic presentation of the geometry of Myller configurations $\mathcal{M}(\mathcal{C},\overline{\xi},\pi)$ and $\mathcal{M}_t(\mathcal{C},\overline{\xi},\pi)$.

If $\mathcal{C}$ is a curve on a surface $\mathcal{S}\subset\mathbb{E}_3$, with s the natural parameter of $\mathcal{C}$, $\overline{\xi}(s)$ the tangent versor fields to $\mathcal{S}$ along $\mathcal{C}$, $\pi(s)$ the tangent plane fields to $\mathcal{S}$ along $\mathcal{C}$, then $\mathcal{M}_t(\mathcal{C},\overline{\xi},\pi)$ is the tangent Myller configuration intrinsic associated to the geometric objects $\mathcal{S}$, $\mathcal{C}$, $\overline{\xi}$.

The geometry of the vector field $\left(\mathcal{C},\overline{\xi}\right)$ on a surface $\mathcal{S}$ is the geometry of the associated Myller configurations $\mathcal{M}_t(\mathcal{C},\overline{\xi},\pi)$. The geometric theory of $\mathcal{M}_t(\mathcal{C},\overline{\xi},\pi)$ represents a particular case of the general Myller configuration $\mathcal{M}(\mathcal{C},\overline{\xi},\pi)$. In the case when $\mathcal{M}_t(\mathcal{C},\overline{\xi},\pi)$ is the associated Myller configuration to a curve $\mathcal{C}$ on a surface $\mathcal{S}$ one obtains the classical theory of curves on surfaces.

This new introduced notion had a central role into the classical theory of surfaces and could be applied to the geometry of other spaces other than the Euclidean, giving the possibility to interpret and link among them many particular facts.

We cite from Miron's book [8] (Preface, written in 1966 by O. Mayer, and Introduction):

"Initiator of a modern education of Mathematics at the University of Iassy, founder of the Geometry School, which is still flourishing today, in the third generation, Alexandru Myller was also a hardworking researcher, well known inside the country and also abroad due his papers concerning Integral Equations and Differential Geometry. Some of Alexandru Myller's discoveries have penetrated fruitfully the impetuous torrent of ideas, which have changed the Science of Geometry during the first decades of the century. Among others, it is the case of "Myller configurations".

These investigations have been continued by Octav Mayer who introduced new fundamental invariants for $\mathcal{M}(\mathcal{C},\overline{\xi},\pi)$ and $\mathcal{M}_t(\mathcal{C},\overline{\xi},\pi)$. The importance of these studies was underlined by Levi-Civita in Addendum to his book *Lezioni di Calcolo Differentiale Assoluto,* 1925.

The notion of Myller configuration was extended to Riemannian geometry, symplectic geometry, in the geometry of versor fields in the Euclidean space with applications in hydromechanics, in Minkowski spaces, in Finsler, Lagrange and Hamilton spaces.

In this paper we consider special curves (rectifying-type and Bertrand curves) in the most simple Myller configuration and study their properties, in order to compare these properties in both cases, Myller and Euclidean settings.

2. Versor fields in $\mathbb{E}_3$. Frame of Frenet-type.

For a versor field $(\mathcal{C},\overline{\xi})$ in the Euclidean space $\mathbb{E}_3$, an invariant frame of Frenet-type is introduced, also the moving equations of this frame and the invariants $K_1(s)$, $K_2(s)$ are presented in [8].

In $\mathbb{E}_3$, a versor field $(\mathcal{C},\overline{\xi})$ can be analytical represented in an orthonormal frame $(\mathcal{R}=(O;\overrightarrow{i_1},\overrightarrow{i_2},\overrightarrow{i_3}))$ by

$$\overline{r}=\overline{r}(s),\ \overline{\xi}=\overline{\xi}(s),\ s\in I=(s_1,s_2),$$

where s is the arclenght on the curve $\mathcal{C}$,

$$\overline{r}(s)=x(s)\overrightarrow{i_1}+y(s)\overrightarrow{i_2}+z(s)\overrightarrow{i_3}=\overrightarrow{OP}(s),$$
$$\overline{\xi}(s)=\xi^1(s)\overrightarrow{i_1}+\xi^2(s)\overrightarrow{i_2}+\xi^3(s)\overrightarrow{i_3}=\overrightarrow{PQ}(s),$$
$$\|\overline{\xi}(s)\|^2=\langle\overline{\xi}(s),\overline{\xi}(s)\rangle=1.$$

The pair $(\mathcal{C},\overline{\xi})$ has a geometrical meaning. This implies that the pair $\left(\mathcal{C},\dfrac{d\overline{\xi}}{ds}\right)$ has a geometrical meaning. $K_1(s)=\left\|\dfrac{d\overline{\xi}}{ds}\right\|$ is an invariant of the field $(\mathcal{C},\overline{\xi})$.

Denote $\overline{\xi}_1(s)=\overline{\xi}(s)$ and by $\overline{\xi}_2(s)$ the versor of $\dfrac{d\overline{\xi}_1}{ds}$.

$$\frac{d\overline{\xi}_1(s)}{ds}=K_1(s)\overline{\xi}_2(s).$$

Obviously, $\overline{\xi}_2(s)$ is orthogonal to $\overline{\xi}_1(s)$.

One defines $\overline{\xi}_3(s)=\overline{\xi}_1(s)\times\overline{\xi}_2(s)$.

Then the frame $\mathcal{R}_{\mathcal{F}}(P(s);\overline{\xi}_1(s),\overline{\xi}_2(s),\overline{\xi}_3(s))$ is orthonormal, positively oriented. $\mathcal{R}_{\mathcal{F}}$ is called the *Frenet frame* of the versor field $(\mathcal{C},\overline{\xi})$ (invariant frame of Frenet-type).

The moving equations of $\mathcal{R}_{\mathcal{F}}$ are

$$\frac{d\overline{r}}{ds} = a_1(s)\overline{\xi}_1(s) + a_2(s)\overline{\xi}_2(s) + a_3(s)\overline{\xi}_3(s),$$

with $a_1^2(s) + a_2^2(s) + a_3^2(s) = 1$ and

$$\frac{d\overline{\xi}_1}{ds} = K_1(s)\overline{\xi}_2(s),$$

$$\frac{d\overline{\xi}_2}{ds} = -K_1(s)\overline{\xi}_1(s) + K_2(s)\overline{\xi}_3(s),$$

$$\frac{d\overline{\xi}_3}{ds} = -K_2(s)\overline{\xi}_2(s),$$

where $K_1(s) > 0$.

The functions $K_1(s),\ K_2(s),\ a_1(s),\ a_2(s),\ a_3(s),\ s \in I$, are invariants of the versor field $(\mathcal{C}, \overline{\xi})$.

$K_1(s)$ is called the *curvature* of $(\mathcal{C}, \overline{\xi})$ (called also K_1-*curvature*).

$K_2(s)$ is called the *torsion* of $(\mathcal{C}, \overline{\xi})$ (called also K_2-*torsion*).

$K_1(s),\ K_2(s)$ are invariants and have the same geometrical interpretation as the curvature and torsion of a curve in $\mathbb{E}_3$.

Obviously, if $a_1(s) = 1,\ a_2(s) = 0,\ a_3(s) = 0$, one obtains the Frenet equations of a curve in $\mathbb{E}_3$.

The fundamental theorem for the versor field $(\mathcal{C}, \overline{\xi})$ is stated below:

Theorem 2.1. [8] *If the functions $K_1(s) > 0,\ K_2(s),\ a_1(s),\ a_2(s),\ a_3(s),\ (a_1^2 + a_2^2 + a_3^2 = 1)$ of class $\mathcal{C}^\infty$ are a priori given, $s \in [a, b]$ there exists a curve $\mathcal{C} : [a, b] \to \mathbb{E}_3$ parametrized by arclenght s and a versor field $\overline{\xi}(s),\ s \in [a, b]$, whose the curvature, torsion and the functions $a_i(s)$ are $K_1(s),\ K_2(s)$ and $a_i(s)$. Any two such versor fields $(\mathcal{C}, \overline{\xi})$ differ by a proper Euclidean motion.*

We list the following geometric properties [8]:

1. The versor field $(\mathcal{C}, \overline{\xi})$ determines a ruled surface $S(\mathcal{C}, \overline{\xi})$.
2. The surface $S(\mathcal{C}, \overline{\xi})$ is with director plane if $K_2(s) = 0$.
3. The surface $S(\mathcal{C}, \overline{\xi})$ is developing if the invariant $a_3(s)$ vanishes.

If the surface $S(\mathcal{C}, \overline{\xi})$ is a cone, the versor field $(\mathcal{C}, \overline{\xi})$ is called *concurent*.

3. Rectifying and Bertrand curves.

Consider a unit-speed curve $x : I \to \mathbb{E}_3$ and the (common) Frenet frame $\{t, n, b\}$, where t is the *tangent vector field*, n is the *principal normal vector* field, b is the *binormal vector field*.

Question [8]: When does the position vector of a space curve $x : I \to \mathbb{E}_3$ always lie in its rectifying plane?

Such a curve is called a *rectifying curve* and its position vector x satisfies

$$x(s) = \lambda(s)t(s) + \mu(s)b(s),$$

for some functions λ and μ.

In [1], characterizations of rectifying curves are given and, moreover, classification of such curves is provided.

By applying a result from [1], one concludes that, up to rigid motion, rectyfing curves are characterized, in terms of mechanics, as those curves that are in equilibrium under a force field

$$F = ct - \tau n,$$

for a constant $c \neq 0$, when τ is the torsion of the curve x.

Other results were obtained in [2] and [3].

Furthermore, B.Y. Chen and F. Dillen established in [4] a simple link beetween rectifying curves and the notion of centrodes in mechanics. They also showed that rectifying curves are indeed the extremal curves which satisfy the equality case of a general inequality.

In [5] S. Deshmukh, B.Y. Chen and S.H. Al Shammari studied rectifying curves via the dilation of unit speed curves on the unit sphere S^2 in the Euclidean space $\mathbb{E}_3$. A main result of [4] is improved.

Other special curves in the Euclidean space $\mathbb{E}_3$ are the *Bertrand curves*.

Definition 3.1. *Two curves c and c^* are* Bertrand curves *if they have common principal normal lines.*

Their geometric properties are well-known:

1) The distance between corresponding points on two Betrand curves is constant.

2) The angle between corresponding tangent lines on two Bertrand curves is constant.

3) According to Lipschutz [6], if $\tau \neq 0$ along c, then c is a Bertrand curve (i.e. there exists a curve c^* such that c and c^* are Bertrand curves) if and only if there are constants γ and $\alpha,\ \alpha \neq 0$, such that

$$K + \gamma\tau = \frac{1}{\alpha}.$$

4) If $\tau \neq 0$ along c, then more than one curve c^* exists such that c and c^* are Bertrand curves if and only if c is a circular helix.

4. Rectifying curves in a Frenet-type frame.

We consider the curve $\overline{r}(s)$ and a frame of Frenet-type $\mathcal{R}_{\mathcal{F}} = \{P(s); \overline{\xi}_1(s); \overline{\xi}_2(s); \overline{\xi}_3(s)\}$.

Denote by

$$\frac{d\overline{r}}{ds} = \dot{\overline{r}}(s)$$

and

$$\frac{d\overline{\xi}_1(s)}{ds} = \dot{\overline{\xi}_1}(s),$$

$$\frac{d\overline{\xi}_2(s)}{ds} = \dot{\overline{\xi}_2}(s),$$

$$\frac{d\overline{\xi}_3(s)}{ds} = \dot{\overline{\xi}_3}(s).$$

We generalize the definition of the rectifying curve by:

Definition 4.1. [7] *$\overline{r}$ is a rectifying curve in the Frenet-type frame $\mathcal{R}_{\mathcal{F}}$ if:*

$$\overline{r}(s) = \lambda(s)\overline{\xi}_1(s) + \mu(s)\overline{\xi}_3(s), \tag{4.1}$$

where $\lambda,\ \mu$ are functions.

Remark 4.2. *From* (4.1) *we have, by using the moving equations of $\mathcal{R}_{\mathcal{F}}$:*

$$\begin{aligned}\dot{\overline{r}}(s) &= \dot{\lambda}(s)\overline{\xi}_1(s) + \lambda(s)\dot{\overline{\xi}}_1(s) + \dot{\mu}(s)\overline{\xi}_3(s) + \mu(s)\dot{\overline{\xi}}_3 = \\ &= \dot{\lambda}(s)\xi_1(s) + \lambda(s)K_1(s)\overline{\xi}_2(s) + \dot{\mu}(s)\xi_3(s) + \mu(s)\left(-K_2(s)\xi_2(s)\right) = \\ &= \dot{\lambda}(s)\xi_1(s) + \left[\lambda(s)K_1(s) - \mu(s)K_2(s)\right]\xi_2(s) + \dot{\mu}(s)\xi_3(s).\end{aligned} \tag{4.2}$$

From (4.2) and the expression of $\dot{\overline{r}}(s)$ in a Frenet-type frame, we obtain

$$\begin{cases} \dot{\lambda}(s) = a_1(s), \\ \lambda(s)K_1(s) - \mu(s)K_2(s) = a_2(s), \\ \dot{\mu}(s) = a_3(s), \end{cases} \tag{4.3}$$

with $a_1^2(s) + a_2^2(s) + a_3^2(s) = 1$.

Theorem 4.3. [7] *Let $\overline{r}(s) : I \to \mathbb{E}_3$ be a curve in $\mathbb{E}_3$ expressed in the Frenet-type frame $\mathcal{R}_{\mathcal{F}}$ by:*

$$\frac{d\overline{r}}{ds}(s) = a_1(s)\overline{\xi_1}(s) + a_2(s)\overline{\xi_2}(s) + a_3(s)\overline{\xi_3}(s),$$

with $K_1(s) > 0$, such that one of the following items holds:

$$i)\ \frac{d}{ds}\langle \overline{r}(s), \overline{\xi_1}(s)\rangle = a_1(s),$$
$$ii)\ \text{For } K_2(s) \neq 0,\ \frac{d}{ds}\langle \overline{r}(s), \overline{\xi_3}(s)\rangle = a_3(s).$$

Then $\overline{r}(s)$ is a rectifying curve.
Conversely, if $\overline{r}(s)$ is a rectifying curve, then i) and ii) hold.

By straightforward calculation, we also proved the following

Theorem 4.4. [7] *A rectifying curve $\overline{r}(s)$ in a Frenet-type frame $\mathcal{R}_{\mathcal{F}}$ with $a_2(s) = 0,\ a_1(s) = a_1,\ a_3(s) = a_3,\ a_1, a_3 =$constants, is given, up to a parametrization, by*

$$\overline{r}(s) = (d \cdot \sec t)y(t),$$

where d is a positive number and $y = y(t)$ is a constant speed curve in $\mathcal{S}^2$.

Remark 4.5. [7] *The converse statement holds if $a_2 = a_3 = 0$; then $a_1 = 1$ and the Frenet-type frame $\mathcal{R}_{\mathcal{F}}$ coincides with classical Frenet frame.*

In the last part of this section, we recall a characterization of rectifying curves, via its K_1-curvature and K_2-torsion.

Theorem 4.6. [7] *Let $\overline{r} : I \to \mathbb{E}_3$ be a curve in the Frenet-type frame $\mathcal{R}_{\mathcal{F}}$, $\dot{\overline{r}}(s) = a_1(s)\overline{\xi}_1(s) + a_2(s)\overline{\xi}_2(s) + a_3(s)\overline{\xi}_3(s)$. Then $\overline{r}$ is congruent to a rectifying curve $\overline{r}(s) = \lambda(s)\overline{\xi}_1(s) + \mu(s)\overline{\xi}_3(s)$ if and only if the K_1-curvature and the K_2-torsion satisfy the relation $\lambda(s)K_1(s) - \mu(s)K_2(s) = a_2(s),\ \forall s \in I$.*

A curve in $\mathbb{E}_3$ is a *generalized helix* if and only if the ratio $\dfrac{\tau}{K}$ ($\tau =$ torsion, $K =$ curvature) is a nonzero constant on the curve.

Remark 4.7. [7] *Theorem* 4.6 *gives a very simple characterization of rectifying curves if $a_2(s) = 0$ and $K_2(s) \neq 0$, in terms of the ratio $\dfrac{K_2(s)}{K_1(s)}$.*

We conclude that the properties of rectifying-type curves in a Myller configuration differ from those of the rectifying curves in the Euclidean space.

5. Bertrand curves in a Frenet-type frame.

Let

$$\dot{\overline{r}}(s) = a_1(s)\overline{\xi_1}(s) + a_2(s)\overline{\xi_2}(s) + a_3(s)\overline{\xi_3}(s)$$

and

$$\dot{\overline{r^*}}(s) = a_1^*(s)\overline{\xi_1^*}(s) + a_2^*(s)\overline{\xi_2^*}(s) + a_3^*(s)\overline{\xi_3^*}(s)$$

be 2 curves in a Frenet-type frame $\mathcal{R}_{\mathcal{F}}$.

Similar to the classical definition, we say that

Definition 5.1. *$\overline{r}$ and $\overline{r^*}$ are* Bertrand curves *if they have common $\overline{\xi}_2$ lines, i.e. $\overline{\xi_2}(s) = \pm\overline{\xi_2^*}(s)$ and the distance between the corresponding points is constant, α.*

Next, we give the justification for the definition.

Denoting by $\alpha(s)$ the distance between the corresponding points $\overline{r}(s)$ and $\overline{r^*}(s)$ measured on $\overline{\xi_2}(s) = \pm\overline{\xi_2^*}(s)$, we have

$$\overline{r^*}(s) = \overline{r}(s) + \alpha(s)\cdot\overline{\xi_2}(s).$$

It follows that

$$\dot{\overline{r^*}}(s) = \dot{\overline{r}}(s) + \dot{\alpha}(s)\cdot\overline{\xi_2}(s) + \alpha(s)\cdot\dot{\overline{\xi_2}}(s),$$

which implies that

$$a_1^*(s)\overline{\xi_1^*}(s) + a_2^*(s)\overline{\xi_2^*}(s) + a_3^*(s)\overline{\xi_3^*}(s) =$$
$$a_1(s)\overline{\xi_1}(s) + a_2(s)\overline{\xi_2}(s) + a_3(s)\overline{\xi_3}(s) + \dot{\alpha}(s)\overline{\xi_2}(s) + \alpha(s)\left[-K_1(s)\overline{\xi_1}(s) + K_2(s)\overline{\xi_3}(s)\right].$$

By making the scalar product with $\overline{\xi_2}(s)$ we obtain $\pm a_2^*(s) = a_2(s) + \dot{\alpha}(s)$. Then $\dot{\alpha}(s) = 0$ is equivalent with $\pm a_2^*(s) = a_2(s)$.

We can consider $a_2^*(s) = a_2(s)$ by changing the orientation of $\overline{\xi_2^*}(s)$.

It follows that $\alpha(s) = ct = \alpha$, which means that distance between corresponding points is constant.

Then we can write $\overline{r}(s)$ and $\overline{r^*}(s)$ Bertrand curves as

$$\overline{r^*}(s) = \overline{r}(s) + \alpha\overline{\xi_2}(s),\ \alpha\in\mathbb{R}.$$

It follows that

$$\dot{\overline{r^*}}(s) = \dot{\overline{r}}(s) + \alpha\dot{\overline{\xi_2}}(s) = a_1(s)\overline{\xi_1}(s) + a_2(s)\overline{\xi_2}(s) + a_3(s)\overline{\xi_3}(s) + \alpha(s)\left[-K_1(s)\overline{\xi_1}(s) + K_2(s)\overline{\xi_3}(s)\right].$$

So, we get

$$\dot{\overline{r^*}}(s) = \left[a_1(s) - \alpha K_1(s)\right]\overline{\xi_1}(s) + a_2(s)\overline{\xi_2}(s) + \left[a_3(s) + \alpha K_2(s)\right]\overline{\xi_3}(s). \tag{5.1}$$

On the other hand, for two Bertrand curves, we have

$$\frac{d}{ds}\langle\overline{\xi_1}(s), \overline{\xi_1^*}(s)\rangle = \langle\dot{\overline{\xi_1}}(s), \overline{\xi_1^*}(s)\rangle + \langle\overline{\xi_1}(s), \dot{\overline{\xi_1^*}}(s)\rangle =$$
$$= \langle K_1(s)\overline{\xi_2}(s), \overline{\xi_1^*}(s)\rangle + \langle\overline{\xi_1}(s), K_1^*(s)\overline{\xi_2^*}(s)\rangle =$$
$$= \langle\pm K_1(s)\overline{\xi_2^*}(s), \overline{\xi_1^*}(s)\rangle + \langle\overline{\xi_1}(s), \pm K_1^*(s)\overline{\xi_2}(s)\rangle.$$

This implies that

$$\frac{d}{ds}\langle\overline{\xi_1}(s), \overline{\xi_1^*}(s)\rangle = \tag{5.2}$$
$$\pm K_1(s)\langle\overline{\xi_2^*}(s), \overline{\xi_1^*}(s)\rangle \pm K_1^*(s)\langle\overline{\xi_1}(s), \overline{\xi_2}(s)\rangle = 0.$$

From (5.2) it follows that $\langle\overline{\xi_1}(s), \overline{\xi_1^*}(s)\rangle$ = constant, i.e. the angle between $\overline{\xi_1}(s)$ and $\overline{\xi_1^*}(s)$, in corresponding points, is constant, say

$$\langle\overline{\xi_1}(s), \overline{\xi_1^*}(s)\rangle = \cos\beta. \tag{5.3}$$

The relation (5.3) is similar with a classical property of Bertrand curves in a Frenet frame.

Based on the these remarks, we consider that the definitions and studies of Bertrand curves and some other special curves in Myller configurations would be of real interest in Differential Geometry.

References

[1] B.Y. Chen, *When does the position vector of a space curve always lie in its rectifying plane?*, The Amer. Math. Monthly **110(2)** (2003), 147–152.

[2] B.Y. Chen, *Differential geometry of rectifying submanifolds*, Int. Electron. J. Geom. **9** (2016), 1–8.

[3] B.Y. Chen, *Rectifying curves and geodesics on a cone in the Euclidian* 3*-space*, Tamkang J. Math. **48(2)** (2017), 209–214.

[4] B.Y. Chen and F. Dillen, *Rectifying curves as centrodes and extremal curves*, Bull. Inst. Math. Acad. Sinica **33(2)** (2005), 77–90.

[5] S. Deshmukh, B.Y. Chen and S.H. Al Shammari, *On rectifying curves in Euclidian* 3*-space*, Turkish J. Math. **42(2)** (2018), 609–620.

[6] M. Lipschutz, *Theory and Problems of Differential Geometry*, Schaum's Outline Series, McGraw-Hill Inc., 1969.

[7] G. Macsim, A. Mihai and A. Olteanu, *On rectifying-type curves in a Myller configuration*, Bull. Korean Math. Soc. **56(2)**, 2019, 383-390.

[8] R. Miron, *The Geometry of Myller Configurations. Applications to Theory of Surfaces and Nonholonomic Manifolds*, Ed. Acad. Române, 2010.

Doctoral School of Mathematics, Faculty of Mathematics and Computer Science, University of Bucharest, Bucharest, Romania

E-mail address: gabi_macsim@yahoo.com

Department of Mathematics and Computer Science, Technical University of Civil Engineering Bucharest, Bucharest, Romania

E-mail address: adela.mihai@utcb.ro

Department of Mathematics, Physics and Terrestrial Measurements, Faculty of Land Reclamation and Environmental Engineering, University of Agronomic Sciences and Veterinary Medicine of Bucharest, Romania

E-mail address: andreea.olteanu@fifim.ro

TEACHING AND LEARNING BASED ON COMPETENCIES – RULES_MATH PROJECT

Ion Mierluş-Mazilu
Department of Mathematics and Computer Science
Technical University of Civil Engineering Bucharest, Romania,
E-mail: ion.mierlusmazilu@utcb.ro

Abstract: As we all know, Mathematics is an essential part of any engineering degrees and it is a tool that engineers still use throughout his or her life. It is therefore important that this knowledge and competencies are properly seated. Thinking about this, we proposed the 'New Rules for assessing Mathematical Competencies' project to change the educational paradigm and to get a common European teaching and learning system based on competencies rather than contents. In this paper I will present the Rules_Math project ideas.
Mathematics Subject Classification (2010): 97D40, 97M10
Key words: teaching, learning, competences

1. Introduction

The main objective of the RULES_MATH project is to develop assessment standards for a competencies-based teaching-learning system for mathematics in engineering education.
The aims of the project can be summarize as follows:

(1) To develop a collaborative, comprehensive and accessible competencies-based assessment model for mathematics in engineering context.

(2) To elaborate and collect the resources and materials needed to devise competencies-based assessment courses.

(3) To disseminate the model to European HEIs through the partner networks and also promote the dissemination all over Europe.

The institutions involved in RULES_MATH project have long experience in innovation and they have adapted their degrees to the Bologna Accord. Concerning the target groups to be addressed:

(1) The primary target group of the RULES_MATH project is the pool of mathematical university teachers, trainers, lecturers, and researchers from engineering undergraduate degrees, master degrees, or PhD level (including staff from project partners) who are interested in changing their teaching system in the mathematical teaching/learning field. Including who would like to enhance their mathematical competencies using the most advanced e-learning tools, digital assessment, study materials, and courses.

(2) Secondary target group is that of students from engineering undergraduate degrees, master degrees or PhD programmes. They will have access to the assessment materials (new competencies-based resources) that will improve their learning method making themselves the responsible of the acquisition of competencies and knowledge.

As the results of the RULES_MATH project will be available as OER, this can ensure the exchange of experiences and ideas, possibilities and resources for work development, research work, etc. Targeted sectors are research training organizations, university enterprise training partners, research centers and scientific institutes. Training organizations, schools and university training organizations could also be beneficiaries. Potential final users are also

private individuals as home self-learners, interested in self education who, for personal reasons, may not normally engage with formal education, including disabled people and people perceiving discrimination due to social and gender stereotypes.
The RULES_MATH project will focus on mathematical competencies and not just on the mathematical contents which was the case in earlier times in other educational projects. Since mathematics lecturers are much more familiar with the content view (the mathematical structure) it is a major challenge for them to deal with competencies-oriented assessment goals. This project may provide material for supporting them in this respect. Furthermore, the development of a new mathematical approach is being demanded by engineering and science trainers to motivate students, and also for students to be motivated with mathematics learning.

2. Mathematical Analysis and Calculus; Integral Calculus; Methods and applications of Integration.

Mathematical Analysis is composed of two main parts: the Differential Calculus (for functions of several variables) and Integral Calculus. This chapter, entitled “Methods of Integration” is the key that opens the wide door of the Integral Calculus, the branch of Mathematical Analysis that can be associated with the top of the tree, where most people finally find the answer about Mathematics applicability in the real world. This means that almost all of the Mathematical notions (theorems etc.) studied in high-school or further have contributed to the base on which Integral Calculus will be modeled.
It would be better if we thought about the road between two destinations which people go through by train. Integral Calculus is exactly the final destination
Naturally, we question ourselves: “Why is Integral Calculus so important for our lives?”.
The answer for this question is simple, but very suggestive, given by a famous mathematician R. Penrose: “The better we understand the laws of Physics and we approach deeper in the laws of nature, the more we will be led in the world of Mathematical concepts.” Actually, Integral Calculus finds a Mathematical model for almost all phenomenon’s in the nature and this is reason for which an engineer must be familiarized with these concepts.
Their concrete applicability will presented in the next chapter, but now, let’s concentrate on the introductive part of Integral Calculus, the first and most important condition which must be accomplished that we work with Integrals.

3. Competencies

After completing this chapter “Methods of Integration”, the competencies that students must acquire are:

C1. Thinking Mathematically

The achievement of this competence will be assured by the followings:

a) Obtain definite and indefinite integrals of rational functions in partial fraction form.
b) Apply the method of integration by parts to indefinite and definite integrals.
c) Use the method of substitution on indefinite and definite integrals.
d) Solve practical problems which require the evaluation of an integral.
e) Recognize simple examples of improper integrals.
f) Use the formula for the maximum error in a trapezoidal rule estimate.
g) Use the formula for the maximum error in a .Simpson's rule estimate.

C2. Reasoning Mathematically

The achievement of this competence will be assured by the followings:

a) Solve practical problems which require the evaluation of an integral.
b) Recognize simple examples of improper integrals.

C3. Posing and Solving Mathematical Problems

The achievement of this competence will be assured by the followings:

a) Solve practical problems which require the evaluation of an integral.
b) Use the formula for the maximum error in a trapezoidal rule estimate.
c) Use the formula for the maximum error in a Simpson's rule estimate.

C4. Modelling Mathematically

The achievement of this competence will be assured by the followings:

a) Solve practical problems which require the evaluation of an integral.

C5. Representing Mathematical Entities

The achievement of this competence will be assured by the followings:

a) Obtain definite and indefinite integrals of rational functions in partial fraction form
b) Use the method of substitution on indefinite and definite integrals

C6. Handling Mathematical Symbols and Formalism

The achievement of this competence will be assured by the followings:

a) Obtain definite and indefinite integrals of rational functions in partial fraction form.
b) Apply the method of integration by parts to indefinite and definite integrals.
c) Use the method of substitution on indefinite and definite integrals.
d) Solve practical problems which require the evaluation of an integral.
e) Recognize simple examples of improper integrals.
f) Use the formula for the maximum error in a trapezoidal rule estimate.
g) Use the formula for the maximum error in a .Simpson's rule estimate.

C7. Communicating In, With, And About Mathematics

The achievement of this competence will be assured by the followings:

a) Solve practical problems which require the evaluation of an integral.

C8. Making Use of Aids and Tools

The achievement of this competence will be assured by the followings:

a) Solve practical problems which require the evaluation of an integral.
b) Use the formula for the maximum error in a trapezoidal rule estimate.
c) Use the formula for the maximum error in a Simpson's rule estimate.

The Table shows the list of the competencies that we measure with the global test model that is proposed, where

■ = very important
■ = medium important
■ = less important

Table: Competencies that we measure with the global test model that is proposed.

Analysis and Calculus		C1	C2	C3	C4	C5	C6	C7	C8
	Methods of integration								
	Obtain definite and indefinite integrals of rational functions in partial fraction form	■	■	■	■	■	■	■	■
	Apply the method of integration by parts to indefinite and definite integrals	■	■	■	■	■	■	■	■
	Use the method of substitution on indefinite and definite integrals	■	■	■	■	■	■	■	■
	Solve practical problems which require the evaluation of an integral	■	■	■	■	■	■	■	■
	Recognize simple examples of improper integrals	■	■	■	■	■	■	■	■
	Use the formula for the maximum error in a trapezoidal rule estimate	■	■	■	■	■	■	■	■
	Use the formula for the maximum error in a Simpson's rule estimate	■	■	■	■	■	■	■	■

	Applications of integration	
	Find the length of part of a plane curve	
	Find the curved surface area of a solid of revolution	

4. Learning Outcomes

The learning outcomes to be achieved with this procedure are detailed in Table 2.

Table: Learning outcomes(LO) involved in this assessment activity.

Analysis and Calculus	
	Methods of integration
	Obtain definite and indefinite integrals of rational functions in partial fraction form
	Apply the method of integration by parts to indefinite and definite integrals
	Use the method of substitution on indefinite and definite integrals
	Solve practical problems which require the evaluation of an integral
	Recognize simple examples of improper integrals
	Use the formula for the maximum error in a trapezoidal rule estimate
	Use the formula for the maximum error in a Simpson's rule estimate
	Applications of integration
	Find the length of part of a plane curve
	Find the curved surface area of a solid of revolution

5. Example

You can see some catenaries (Figure) in the following representation for different values of parameter a

Figure: Catenaries graphs.

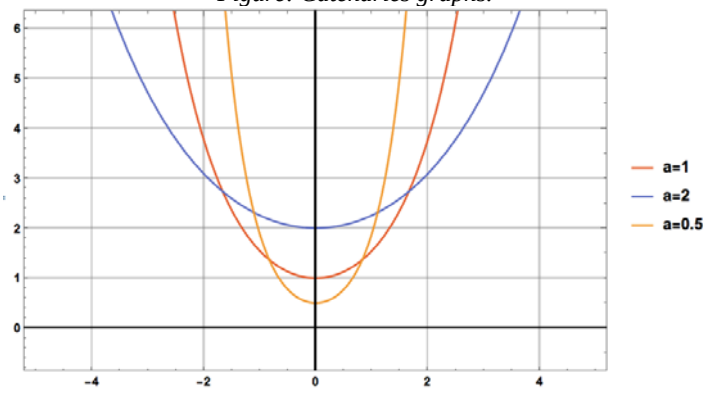

Calculate the area bounded by the curve and the *OX* axis in the interval [*0, 1*] for $a = 1$. Also calculate the arc length of the catenary between *0* and *a*, knowing that the length of a curve is calculated through the formula $L = \int_A^B \sqrt{1+(f'(x))^2}\,dx$ for the parameter values that appear in the previous graphs. Finally, calculate the lateral surface obtained by rotating around the axis *OX* of the previous catenary, knowing that said area is given by $A_L = 2\pi\int_A^B |f(x)|\sqrt{1+(f'(x))^2}\,dx$.

References

[1] https://rules-math.com/

[2] Mierlus-Mazilu, I., Carabaneanu, L., Trandafir, R.: *Trends in E-Learning*, Ser. A, Research Reports 5, Tampere Polytechnic, ISBN 952-5264-46-7 3, 2006, 106-111.

STEREOGRAPHIC PROJECTION REVISITED

Adela Mihai
Department of Mathematics and Computer Science
Technical University of Civil Engineering Bucharest, Romania
E-mail: adela.mihai@utcb.ro
Daniel Tudor
Department of Mathematics and Computer Science
Technical University of Civil Engineering Bucharest, Romania
E-mail: danieltudor@gmail.com

Abstract: We recall the definition of the stereographic projection from both points of view, coming from Geometry and Complex Analysis. In the last section we present some generalization.
Mathematics Subject Classification (2010): 30C35, 40E99
Key words: Stereographic projection

1. Introduction. Basics on Stereographic Projection

Stereographic projection (originally called the *planisphere projection*) is one of the most known maps, with many applications in cartography, planetary science, crystallography, geology, photography, etc.

We will start with the definition from [3].

Let $\mathbb{C}$ denote the set of complex numbers and consider $\mathbb{C} \cup \{\infty\}$. In order to think of $\mathbb{C} \cup \{\infty\}$ as a sphere, one introduces a metric, so that the result is homeomorphic to a sphere; this metric allows us to speak of continuous maps from $\mathbb{C} \cup \{\infty\}$ to itself.

One considers a map from $S^2(1) \subset \boldsymbol{E}^3$ (the unit sphere in the Euclidean space $\boldsymbol{E}^3$) to $\mathbb{C} \cup \{\infty\}$, being a homeomorphism from $\mathbb{C}$ to $S^2(1) - \{\text{North Pole}\}$ (in fact minus a simple point, for example the North Pole $(0,0,1)$).

More precisely, we will use the stereographic projection from $S^2(1)$ to $\mathbb{C} \cup \{\infty\}$.

By identifying $\mathbb{C}$ with the horizontal plane $\mathbb{R}^2 \times \{0\}$ in $\boldsymbol{E}^3$, the following Figure 1 illustrates geometrically the stereographic projection (in *1*-dimension).

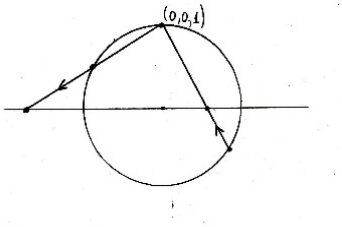

Figure 1

Half of the $S^2(1)$ lies above the plane and half below. One maps $(0,0,1)$ to ∞. Given any point $\in S^2(1)$, one defines $\Phi(p) \in \mathbb{C}$, such that $(0,0,1), p$ and $\Phi(p)$ are collinear.

Then Φ is given by

(1) $\Phi(x,y,z) = \left(\frac{x}{1-z}\right) + \left(\frac{y}{1-z}\right) i,$

and its inverse

(2) $\Phi^{-1}(x+iy) = \left(\frac{2x}{1+x^2+y^2}, \frac{2y}{1+x^2+y^2}, 1 - \frac{2}{1+x^2+y^2}\right).$

A nice exposition on the extended complex plane and stereographic projection is given in [1]; the transformation $w = \frac{1}{z}$ maps the complex plane onto itself, with two exceptions: $z = 0$ has no image and $w = 0$ has no preimage. This is the reason for which one considers the *extended complex plane* $\mathbb{C} \cup \{\infty\}$, also called the *inversive plane.*

For $\forall r > 0$ the set $\{z/|z| > r\}$ is considered to be a neighborhood of ∞; it is mapped onto a neighborhood of the origin $|w| < \frac{1}{r}$ by $w = \frac{1}{z}$.

To visualize $\mathbb{C} \cup \{\infty\}$ one uses a sphere. Consider the sphere tangent to $\mathbb{C}$ at the origin and radius $\frac{1}{2}$. The line joining any point *P* in the plane to $N(0,0,1)$ intersects the sphere in $Q(\alpha,\beta,\gamma)$ and, conversely, the line joining *N* to any point *Q* on the sphere meets the plane in a point *P* (Figure 2).

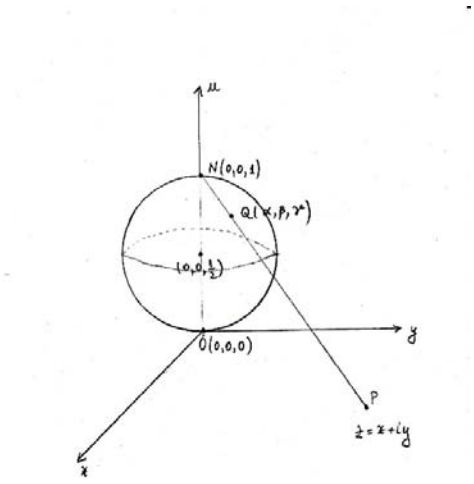

Figure 2

Then, the points of the extended complex plane $\mathbb{C} \cup \{\infty\}$ may be identified with the points of the sphere, the ideal point ∞ corresponding to *N*. This is the reason for which the extended complex plane is sometimes referred as the *complex sphere* or as the *Riemann sphere*. This mapping of $\mathbb{C} \cup \{\infty\}$ to the sphere and, generally, the inverse mapping of the sphere onto $\mathbb{C} \cup \{\infty\}$ are both referred as *stereographic projection*.

The coordinate expressions for the stereographic projection are:

(3) $x = \frac{\alpha}{1-\gamma}, y = \frac{\beta}{1-\gamma}, z = \frac{\gamma}{1-\gamma}$

and, conversely,

(4) $\alpha = \frac{x}{1+r^2}, \beta = \frac{y}{1+r^2}, \gamma = \frac{r^2}{1+r^2},$

where $z = x + i \cdot y$ represents *P*, *Q* has the coordinates (α,β,γ) and $r = |z| = \sqrt{x^2+y^2}$.

It immediately follows that the relations (1) and (2) are equivalent with (3) and (4), i.e. (1) and (2) match the geometrical description.

At the end of this section, we recall few definitions which we need in sections 3 and 4.

A (complex) *linear fractional transformation* has the form $T_A(z) = \frac{a \cdot z + b}{c \cdot z + d}$, with $det \begin{pmatrix} a & b \\ c & d \end{pmatrix} = 1, a, b, c, d \in \mathbb{C}$.

Such maps are also called *Mobius transformation*. Remark that the denominator of $T_A(z)$ is nonzero for $z \neq -\frac{d}{c}$. Then one introduces an extra point ∞ and defines $T_A(-\frac{d}{c}) = \infty$.

A *generalized circle* in $\mathbb{C} \cup \{\infty\}$ is either a circle in $\mathbb{C}$ or a set of the form $L \cup \{\infty\}$, where L is a straight line in $\mathbb{C}$. From topological point of view, the generalized circles are all homeomorphic to circles.

It is known that $T(C)$ is also a generalized circle and T a linear fractional transformation [3]. Also, it is easy to prove that there exists a linear fractional transformation T such that $T(\mathbb{R} \cup \{\infty\}) = \mathbb{C}$ (see [3]).

On the other hand, considering $f : U \to \mathbb{C}$ (U an open subset of $\mathbb{C}$) a continuous map, one says that f has a *complex derivative* at $z \in U$ if the quotient $f'(z) = \lim_{h \to 0} \frac{f(z+h) - f(z)}{h}$ exists and is finite (h is allowed to be a complex number). f is said to be *complex analytic* in U if $f'(z)$ exists for all $z \in U$ and the function $z \to f'(z)$ varies continuously in U.

Complex analytic functions are sometimes called *holomorphic functions*.

Besides the property of having complex derivative at each point, a complex analytic function satisfies the Cauchy Integral Formula and agrees with its Taylor series in a neighborhood of each point.

A linear fractional transformation is an example of a complex analytic function.

2. Properties of the Stereographic Projection

Proposition 2.1. [3] *The map Φ gives a homeomorphism from $S^2 - \{(0,0,1)\}$ to $\mathbb{C}$.*

Also, if $C \subset S^2$ is a circle, then $\Phi(C)$ is either a circle in $\mathbb{C}$ or else a straight line (union ∞). When the circle C contains $N(0,0,1)$ the proof is obvious from the geometric description. The idea is that any circle $C \subset S^2$ has the form $\Pi_C \cap S^2$, for some plane Π_C. If $N(0,0,1) \in \Pi_C, \Phi(\Pi_C) = (\mathbb{C} \cup \Pi_C) \cup \{\infty\}$.

A general geometric proof based on conic sections is given in [2]. Also, in [1], the following result is geometrically proved.

Theorem 2.2. [1] *Stereographic projection maps lines and circles in the plane to circles on the sphere, and, conversely, circles on the sphere map stereographically to lines and circles in the plane.*

Proposition 2.3. [1] *The angle between two lines is equal to the angle between their image circles under the stereographic projection.*

Recall that a transformation T mapping a subset of the plane into the plane is said to be *conformal at P* if it preserves the angle between any two curves at P; T is *conformal* if it is conformal at each point of its domain.

Theorem 2.4. [1] *Stereographic projection is a conformal map.*

3. Stereographic Projection Revisited

Let $\Phi : S^2 \to \mathbb{C} \cup \{\infty\}$ be the stereographic projection.

In [3] the following result is proved by using geometrical tools:

Proposition 3.1. [3] *The differential $d\Phi$ is a similarity on the tangent plane T_x at $x \in S^2 - \{(0,0,1)\}$.*

This Proposition can be also proved by using formula (1).

Another interesting result is the following:

Proposition 3.2. [3] *If I is an isometry of S^2, then $I^* = \Phi \circ I \circ \Phi^{-1}$ is a linear fractal transformation.*

Proof. [3] One can find a linear fractal transformation *T* such that $J = T \circ T^*$ fixes ∞. It suffices to show that *J* is a linear fractional transformation.

The map *J* is smooth except at perhaps a finite list of points. Moreover, by Proposition 3.1., it follows that the differential *dJ* is a similarity at all but finitely many points. Hence *J* is a homeomorphism of $\mathbb{C}$ that is holomorphic except at finitely many points.

One recalls the following Lemma from [3]:

Lemma 3.3. [3] *Suppose f is a homeomorphism of $\mathbb{C}$ that is complex analytic except at finitely many points. Then $f(z) = Az + B$, for some constants A and B.*

By applying Lemma 3.3, the map *J* is linear, and hence a linear fractional transformation. Then I^* is a linear fractional transformation.

The next Proposition has a direct geometric proof, but we recall how can get the result from Complex Analysis.

Proposition 3.4. [3] *Stereographic projection maps circles on S^2 to generalized circles in $\mathbb{C} \cup \{\infty\}$.*

Sketch of the Proof. [3] Consider a circle *C* on S^2 and *I* an isometry on S^2 such that *I*(*C*) contains the North Pole (0,0,1). Then can be shown that $L = \Phi(I(C))$ is a straight line (union ∞), i.e. $\Phi(I(C))$ is a generalized circle. But $\Phi(L) = I^*(\Phi(C))$, with $I^* = \Phi \circ I \circ \Phi^{-1}$. From Lemma 3.3. it follows that I^* is a linear fractal transformation. Therefore, so is $J = (I^*)^{-1}$.

But $\Phi(C) = J(L)$, with *J* a linear fractional transformation and *L* a generalized circle. One can prove that the linear fractional transformations map generalized circles to generalized circles; then *J*(*L*) is also a generalized circle.

4. Generalization

The definition of stereographic projection from the above sections can be generalized, so that it works in all dimensions.

For example, let us consider $S^n(1) \subset \boldsymbol{E^{n+1}}$, the *n*-dimensional sphere of radius *1* in the (*n+1*)-dimensional Euclidean space, and take the stereographic projection from the South Pole $S(0,0,-1)$ as it is illustrated in Figure 3:

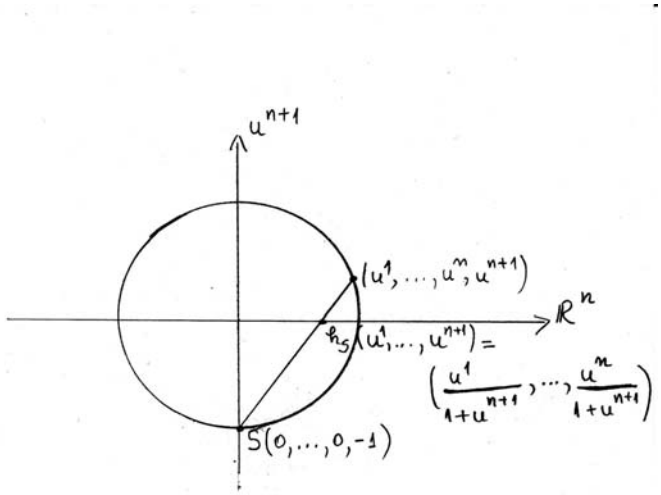

Figure 3

Main Result: *The generalized stereographic projection maps spheres of any dimension in* $\boldsymbol{E^n}$ *to spheres of the same dimension, when the spheres are not passing by the South Pole S.*

The *proof* can be deduced from the 2-dimensional case and symmetry, as well as by using Complex Analysis tools.

We recall the *geometrical proof* given in [1], which is interesting, based on the property of stereographic projection to be an inversion (which can be easily shown by similar triangles)!

More precisely, the *inversion* in $S_r(x_0)$ (where x_0 is the center, r is the radius) is the mapping $g: \mathbb{R}^n - \{x_0\} \to \mathbb{R}^n$, $g(x) = x_0 + r^2 \frac{x - x_0}{|x - x_0|^2}$.

The inversion maps hyperplanes and spheres in $\boldsymbol{E^n}$ to hyperplanes and spheres:

$$H: \ \sum_{i=1}^n A_i x^i = D, A_i, D \in \mathbb{R}$$

is an (*n - 1*)-dimensional linear subspaces of $\boldsymbol{E^n}$;

$$S_r(x_0): \ \sum_{i=1}^n (x^i - x_0^i)^2 = r^2 \ \text{ or } \ A\sum_{i=1}^n (x^i)^2 + \sum_{i=1}^n B_i x^i + C = 0, A \neq 0$$

is the sphere in $\boldsymbol{E^n}$.

If *D=0*, then *H* is a hyperplane through the origin and considering inversion in the unit sphere about the origin, every ray from the origin in the hyperplane remains in the hyperplane.

If $y = g(x) = \frac{x}{|x|^2}$, then $|x|^2 = \frac{1}{|y|^2}$. So, if $D \neq 0$, g maps $\sum_{i=1} A_i x^i = D$ into

$$D|y|^2 - \sum_{i=1}^n A_i y^i = 0,$$

which is a sphere passing through the origin.

Similarly, a sphere passing through the origin (*C=0*) is mapped to

$$\sum_{i=1}^n B_i y^i = -A,$$

which is a plane.

Finally, the sphere $A\sum_{i=1}^n (x^i)^2 + \sum_{i=1}^n B_i x^i + C = 0$ is mapped to the sphere

$$C|y|^2 + \sum_{i=1}^{n} B_i y^i + A = 0.$$

The following result holds [1]:

Proposition 3.1. [1]

i) The inverse of a hyperplane through the center of inversion is the hyperplane itself.

ii) The inverse of a hyperplane not passing through the center of inversion is a sphere passing through the center of inversion.

iii) The inverse of a sphere through the center of inversion is a hyperplane not passing through the center of inversion.

iv) The inverse of a sphere not passing through the center of inversion is a sphere not passing through the center of inversion.

To complete *the proof of the Main Result*, one remarks that iv) of the above Proposition 3.1. gives the geometrical proof for spheres of maximum dimension. By applying both i) and iv) we get the result for spheres of any dimension in $\boldsymbol{E}^{\mathrm{n}}$.

References

[1] Blair, D.E.: *Inversion Theory and Conformal Mapping*, Student Math. Library 9, AMS, 2000.

[2] Hilbert, D., Cohn-Vossen, A.: *Geometry and the Imagination*, Chelsea Publishing Company, New York, 1952.

[3] Schwartz, R.E.: *Mostly Surfaces*, Student Math. Library 60, AMS, 2011.

ABOUT SOME PROPERTIES OF λ-MEASURES

Lucian Niță
Department of Mathematics and Computer Science
Technical University of Civil Engineering of Bucharest, Romania
E-mail: *luci6691@yahoo.com*
Ştefania Constantinescu
Department of Mathematics and Computer Science
Technical University of Civil Engineering of Bucharest, Romania
E-mail: c_*aurora32@yahoo.com*

Abstract: In this paper we define the concept of λ-measure as a monotone set function, which satisfies a particular formula (different from the classical measures) for computing its values for the union of two disjoined sets. We give a theorem (see [1]) which connect the λ -measures to the classical measures. By using this theorem, we deduce some properties of λ-measures, regarding regularity, absolute continuity and -measurable functions. Then, we introduce a concept of integral with respect to a λ-measure. Some properties of this integral are given (monotony, non-linearity, Beppo-Levi and Lebesgue type theorems). Finally, we prove a Radon-Nicodim type theorem.
Mathematics Subject Classification (2010): 28A05, 28A10, 28A25, 28C15
Key words: λ-measure, regularity, integral, Radon-Nicodim theorem

1. Preliminaries

Let T be non-empty set and $\Re$ a ring of parts of T.

Definition 1.1. The set function g_λ, positive, monotone, satisfies *the* λ *rule* if

$$g_\lambda(A\cup B)=g_\lambda(A)+g_\lambda(B)+\lambda g_\lambda(A)g_\lambda(B),\forall A,B\in\Re, \text{ with } A\cap B=\varnothing.$$

Observation 1.2. Because g_λ is monotone, it results that $g_\lambda(A\cup B)\geq g_\lambda(A)$, hence

$$g_\lambda(A)+g_\lambda(B)+\lambda g_\lambda(A)g_\lambda(B)\geq g_\lambda(A);$$

if $g_\lambda(A)<\infty$, we obtain $g_\lambda(B)\left(1+\lambda g_\lambda(A)\right)\geq 0$, i.e. $\lambda>-\dfrac{1}{g_\lambda(A)}$.

Hence, if $\exists A\in\Re$ with $g_\lambda(A)<\infty$ we will impose the condition $\lambda>-\dfrac{1}{\sup g_\lambda}$.

Definition 1.3. a) Let $g_\lambda:\Re\to[0,\infty]$ monotone.

a) We say that g_λ satisfies *the* λ *finite rule* if $\forall(E_i)_{1\leq i\leq n}\subset\Re$, with $E_i\cap E_j=\varnothing$ for $i\neq j$, we have:

$$g_\lambda\left(\bigcup_{i=1}^{n}E_i\right)=\begin{cases}\dfrac{1}{\lambda}\left\{\prod_{i=1}^{n}\left[1+\lambda g_\lambda(E_i)\right]-1\right\},\lambda\neq 0\\ \sum_{i=1}^{n}g_\lambda(E_i),\lambda=0\end{cases}.$$

b) We say that g_λ satisfies *the* λ *countable rule* if $\forall (E_n)_{n\geq 1} \subset \Re$ disjunctive two by two, with $\bigcup_{n\geq 1} E_n \in \Re$, we have:

$$g_\lambda\left(\bigcup_{n\geq 1} E_n\right) = \begin{cases} \frac{1}{\lambda}\left\{\prod_{n\geq 1}\left[1+\lambda g_\lambda(E_i)\right]-1\right\}, \lambda \neq 0 \\ \sum_{n\geq 1} g_\lambda(E_n), \lambda = 0 \end{cases}.$$

Proposition 1.4. If g_λ satisfies the λ rule, then it satisfies the λ finite rule.

Proof.

By induction: for $n=2$, it results directly from definition. We suppose as true the relation from the λ finite rule for $n=k-1$ and we prove it for $n=k$. We will consider the case $\lambda \neq 0$ (for $\lambda = 0$, it is obvious). We have:

$$g_\lambda\left(\bigcup_{i=1}^{k} E_i\right) = g_\lambda\left(\bigcup_{i=1}^{k-1} E_i \cup E_k\right) = g_\lambda\left(\bigcup_{i=1}^{k-1} E_i\right)\left[1+\lambda g_\lambda(E_k)\right] + g_\lambda(E_k) =$$

$$= \frac{1}{\lambda}\left\{\prod_{i=1}^{k-1}\left[1+\lambda g_\lambda(E_i)\right]-1\right\}\left[1+\lambda g_\lambda(E_k)\right] + g_\lambda(E_k) =$$

$$= \frac{1}{\lambda}\left\{\prod_{i=1}^{k}\left[1+\lambda g_\lambda(E_i)\right]-\left[1+\lambda g_\lambda(E_k)\right]\right\} + g_\lambda(E_k) = \frac{1}{\lambda}\left\{\prod_{i=1}^{k}\left[1+\lambda g_\lambda(E_i)\right]-1\right\}.$$

Definition 1.5. g_λ is called λ*-measure on* $\Re$ if it satisfies the λ countable rule and $(\exists) E \in \Re$ with $g_\lambda(E) < \infty$.

Proposition 1.6. If g_λ is a λ-measure on $\Re$, then $g_\lambda(\varnothing) = 0$ and g_λ satisfy the λ finite rule.

Proof.

We will suppose that $\lambda \neq 0$; the proof for $\lambda = 0$ is obvious. According to 1.5. there exists $E \in \Re$, with $g_\lambda(E) < \infty$.

Let $(E_n)_{n\geq 1}$ be a sequence of sets with $E_1 = E,\ E_k \neq \varnothing, \forall k \geq 2.$ Then

$$g_\lambda(E) = g_\lambda\left(\bigcup_{n\geq 1} E_n\right) = \frac{1}{\lambda}\left\{\prod_{n=1}^{\infty}\left[1+\lambda g_\lambda(E_n)\right]-1\right\} \Rightarrow$$

$$\Rightarrow 1+\lambda g_\lambda(E) = \left[1+\lambda g_\lambda(E)\right]\prod_{n=2}^{\infty}\left[1+\lambda g_\lambda(E_n)\right].$$

Because $\lambda \in \left(-\frac{1}{\sup g_\lambda}, \infty\right)$ and $g_\lambda(E) < \infty$, we have $0 < 1+\lambda g_\lambda(E) < \infty$.

We deduce that $\prod_{n=2}^{\infty}\left[1+\lambda g_\lambda(E_n)\right] = 1$, hence $1+\lambda g_\lambda(\varnothing) = 1$, i.e. $g_\lambda(\varnothing) = 0$.

The other assertion of the proposition is now obvious, by taking the sequence $(E_j)_{j\geq 1}, E_j = \varnothing$ for $j > n$.

Proposition 1.7. Let g_λ be a λ-measure, $E, F \in \Re$. We have:

a) $g_\lambda(E\setminus F)=\dfrac{g_\lambda(E)-g_\lambda(E\cap F)}{1+\lambda g_\lambda(E\cap F)}$

b) $g_\lambda(E\cup F)=\dfrac{g_\lambda(E)+g_\lambda(F)-g_\lambda(E\cap F)+\lambda g_\lambda(E)g_\lambda(F)}{1+\lambda g_\lambda(E\cap F)}$.

Theorem 1.8. Let $\lambda\neq 0$.

a) Let $g_\lambda:\Re\to[0,\infty]$ be a λ-measure. The set function

$\mu:\Re\to[0,\infty],\mu(A)\overset{def}{=}\dfrac{\ln(1+\lambda g_\lambda(A))}{\lambda}$ is a positive measure.

b) Let $\mu:\Re\to[0,\infty]$ be a positive measure. Then, the set function

$g_\lambda:\Re\to[0,\infty],g_\lambda\overset{def}{=}\dfrac{e^{\lambda\mu(A)}-1}{\lambda}$ is a λ-measure.

Proof.

a) Let $(E_n)_{n\geq 1}\subset\Re$ disjunctive two by two, with $\bigcup_{n\geq 1}E_n\in\Re$. We have successively:

$$\mu\left(\bigcup_{n\geq 1}E_n\right)=\frac{\ln\left[1+\lambda g_\lambda\left(\bigcup_{n\geq 1}E_n\right)\right]}{\lambda}=\frac{\ln\left\{1+\prod_{n\geq 1}\left[1+\lambda g_\lambda(E_n)\right]-1\right\}}{\lambda}=$$

$$=\frac{1}{\lambda}\sum_{n\geq 1}\ln\left[1+\lambda g_\lambda(E_n)\right]=\sum_{n\geq 1}\mu(E_n).$$

b) $g_\lambda\left(\bigcup_{n\geq 1}E_n\right)=\dfrac{e^{\lambda\mu\left(\bigcup_{n\geq 1}E_n\right)}-1}{\lambda}=\dfrac{1}{\lambda}\left[e^{\lambda\sum_{n\geq 1}\mu(E_n)}-1\right]=$

$$=\frac{1}{\lambda}\left[\prod_{n\geq 1}e^{\lambda\mu(E_n)}-1\right]=\frac{1}{\lambda}\left\{\prod_{n\geq 1}\left[1+\lambda g_\lambda(E_n)\right]-1\right\}.$$

Now, let (T,τ) be a topological space and $\Re$ $\sigma-$algebra of the borelian sets on T.

Definition 1.9. The positive measure $\mu:\Re\to[0,\infty]$ is called *regulate* if:

i) $\mu(A)=\sup_{\substack{K\subset A\\ K-compact}}\mu(K),\forall A\in\Re$

ii) $\mu(A)=\inf_{\substack{G\supset A\\ G\in\tau}}\mu(G)$.

(The same definition can be extended for $\lambda-$measures.)

2. The obtained results

Theorem 2.1. Let $g_\lambda:\Re\to[0,\infty]$ ($\Re$- the borelians of the topological space (T,τ)) and μ the positive measure associated (according to 1.8). Then g_λ is regulate if and only if μ is regulate.

Proof.

"$\Rightarrow$" i) $\mu(A)=\inf_{\substack{G\supset A\\ G\in\tau}}\mu(G)$. For $\forall\varepsilon>0,\exists G\in\tau,G\supset A,$ with $\mu(G)\leq\mu(A)+\varepsilon$.

By taking $\varepsilon = \frac{1}{n}$, $\exists G_n \in \tau, G_n \supset A,$ with $\mu(A) \le \mu(G_n) \le \mu(G_n) + \frac{1}{n}$, hence

$$\lim_{n\to\infty} \mu(G_n) = \mu(A).$$

(The sequence $(G_n)_{n\ge 1}$ can be supposed decreasing, otherwise we can take $D_n = \bigcap_{k=1}^{n} G_k$).

We have: $g_\lambda(G_n) = \frac{e^{\lambda\mu(G_n)} - 1}{\lambda} \underset{n\to\infty}{\to} \frac{e^{\lambda\mu(A)} - 1}{\lambda} = g_\lambda(A)$, hence

$$g_\lambda(A) \le \inf\{g_\lambda(G) \mid G \in \tau, G \supset A\} \le \inf\{g_\lambda(G_n) \mid n \ge 1\} = g_\lambda(A).$$

ii) We suppose that $\mu(A) = \sup_{\substack{K\subset A \\ K\in\mathcal{K}}} \mu(K)$ ($\mathcal{K}$ being the class of the compacts included in T).

For $\forall n \in \mathbb{N}^*$, we will find $K_n \in \mathcal{K}, K_n \subset A,$ such that $\mu(A) \ge \mu(K_n) \ge \mu(A) - \frac{1}{n}$.

(We can suppose $(K_n)_{n\ge 1}$ increasing, otherwise we take $K_n^{'} = \bigcup_{j=1}^{n} K_j$.)

Hence, $\sup_n \mu(K_n) = \lim_{n\to\infty} \mu(K_n) = \mu(A)$.

We have: $g_\lambda(A) \ge sup\{g_\lambda(K) | K \subset A, K \in \mathcal{K}\} \ge \sup_n g_\lambda(K_n) = g_\lambda(A)$.

"$\Leftarrow$" By reducing to absurdity: we suppose that g_λ is regulate, but μ is not regulate.

1°) $\exists A \in \Re$ such that $\mu(A) < \inf\{\mu(G) \mid G \in \tau, G \supset A\} \Rightarrow \exists \varepsilon > 0$ such that $\forall G \in \tau$ with $G \supset A$, $\mu(G) > \mu(A) + \varepsilon$. We can write: $\frac{e^{\lambda\mu(G)} - 1}{\lambda} > \frac{e^{\lambda[\mu(A)+\varepsilon]} - 1}{\lambda}$, hence

$$\inf \frac{e^{\lambda\mu(G)} - 1}{\lambda} = \frac{e^{\lambda \inf \mu(G)} - 1}{\lambda} \ge \frac{e^{\lambda[\mu(A)+\varepsilon]} - 1}{\lambda} > \frac{e^{\lambda\mu(A)} - 1}{\lambda}.$$

Hence, $\inf\{g_\lambda(G) \mid G \in \tau, G \supset A\} > g_\lambda(A)$, false!

2°) Similar, if we suppose that $\mu(A) > sup\{\mu(K) | K \in \mathcal{K}, K \subset A\}$, we obtain a contradiction.

Theorem 2.2. Let $g_\lambda^{(1)}$ and $g_\lambda^{(2)}$ be $\lambda-$measures on $\sigma-$algebra $\Re$ of T and μ_1, μ_2 the classical associated measures. Then $(\mu_1 << \mu_2) \Leftrightarrow (g_\lambda^{(1)} << g_\lambda^{(2)})$.

Proof.

"$\Rightarrow$" Let $g_\lambda^{(2)}(A) = 0 \Rightarrow \frac{\ln[1 + \lambda g_\lambda^{(2)}(A)]}{\lambda} = 0 \Rightarrow \mu_2(A) = 0 \Rightarrow \mu_1(A) = 0 \Rightarrow$

$$\Rightarrow \frac{e^{\lambda\mu_1(A)} - 1}{\lambda} = 0 \Rightarrow g_\lambda^{(1)}(A) = 0 \Rightarrow g_\lambda^{(1)} << g_\lambda^{(2)}.$$

"$\Leftarrow$" If $\mu_2(A) = 0 \Rightarrow \frac{e^{\lambda\mu_2(A)} - 1}{\lambda} = 0 \Rightarrow g_\lambda^{(2)}(A) = 0 \Rightarrow g_\lambda^{(1)}(A) = 0 \Rightarrow$

$$\Rightarrow \frac{\ln[1 + \lambda g_\lambda^{(1)}(A)]}{\lambda} = 0 \Rightarrow \mu_1(A) = 0.$$

The integral with respect to a λ-measure

Let $\Re$ a $\sigma-$algebra of parts of the non-empty set T, g_λ a λ-*measure,* $\mu=\dfrac{\ln\left(1+\lambda g_\lambda\right)}{\lambda}$ the associated measure.

Let $f:T\to\mathbb{R}$ be a measurable function (where, on $\mathbb{R}$ we consider the $\sigma-$algebra of the borelian sets).

Definition 2.3.

a) We call *the integral of* f *with respect to* g_λ, the number $\int f\,d\,g_\lambda \overset{def}{=} \dfrac{e^{\lambda\int f\,d\,\mu}-1}{\lambda}$.

b) We say that *f is integrable with respect to* g_λ if and only if f is integrable with respect to μ.

Proposition 2.4. (properties of the integral with respect to a λ-measure)

a) If $f_1\le f_2$, then $\int f_1\,d\,g_\lambda\le\int f_2\,d\,g_\lambda$.

b) If $f\equiv 1$, $\int f\,d\,g_\lambda=g_\lambda(T)$ and $\forall A\in\Re$, $\int 1_A\,d\,g_\lambda=g_\lambda(A)$.

c) If $f\ge 0$, $\left(\int f\,d\,g_\lambda=0\right)\Rightarrow(f=0$ a.p.t with respect to $g_\lambda)$.

Proof.

a) Obvious.

b) $\int f\,d\,g_\lambda=\dfrac{e^{\lambda\int f\,d\,\mu}-1}{\lambda}=\dfrac{e^{\lambda\mu(T)}-1}{\lambda}=g_\lambda(T)$.

Similar, $\int 1_A\,d\,g_\lambda=\dfrac{e^{\lambda\int 1_A\,d\,\mu}-1}{\lambda}=\dfrac{e^{\lambda\mu(A)}-1}{\lambda}=g_\lambda(A)$.

c) $\int f\,d\,g_\lambda=0\Leftrightarrow e^{\lambda\int f\,d\,\mu}=1\Leftrightarrow\int f\,d\,\mu=0\overset{f\ge 0}{\Leftrightarrow}f=0\ \ \mu-$a.p.t $\Leftrightarrow f=0\ \ g_\lambda$-a.p.t.

Proposition 2.5. (non-liniarity of the integral with respect to a λ-measure)

a) For $\alpha\in\mathbb{R}$, constant, $\int\alpha f\,d\,g_\lambda=\dfrac{\left(1+\lambda\int f\,d\,g_\lambda\right)^\alpha-1}{\lambda}$.

b) $\int(f_1+f_2)\,d\,g_\lambda=\dfrac{\left(1+\lambda\int f_1\,d\,g_\lambda\right)\left(1+\lambda\int f_2\,d\,g_\lambda\right)-1}{\lambda}$.

c) $\int\left(\sum_{k=1}^{n}f_k\right)d\,g_\lambda=\dfrac{1}{\lambda}\left\{\prod_{k=1}^{n}\left[1+\lambda\int f_k\,d\,g_\lambda\right]-1\right\}$.

Proof.

a) $\int\alpha f\,d\,g_\lambda=\dfrac{e^{\alpha\left(\lambda\int f\,d\,\mu\right)}-1}{\lambda}=\dfrac{\left(e^{\lambda\int f\,d\,\mu}\right)^\alpha-1}{\lambda}=\dfrac{\left(1+\lambda\int f\,d\,g_\lambda\right)^\alpha-1}{\lambda}$.

b) $\int(f_1+f_2)\,d\,g_\lambda=\dfrac{e^{\lambda\int(f_1+f_2)\,d\,\mu}-1}{\lambda}=\dfrac{e^{\lambda\int f_1\,d\,\mu}e^{\lambda\int f_2\,d\,\mu}-1}{\lambda}=\dfrac{\left(1+\lambda\int f_1\,d\,g_\lambda\right)\left(1+\lambda\int f_2\,d\,g_\lambda\right)-1}{\lambda}$.

c) By induction: the proof (for $n=2$) was done at b). We suppose the relation true for $n-1$ and we verify it for n.

$$\int\left(\sum_{k=1}^{n} f_k\right) d\, g_\lambda = \int\left(\sum_{k=1}^{n-1} f_k + f_n\right) d\, g_\lambda \underset{(\textit{the}\ \text{induction hypothesis})}{\overset{b)}{=}}$$

$$= \frac{\left\{1+\lambda\cdot\frac{1}{\lambda}\left[\prod_{k=1}^{n-1}\left(1+\lambda\int f_k\, d\, g_\lambda\right)-1\right]\left(1+\lambda\int f_n\, d\, g_\lambda\right)\right\}-1}{\lambda} = \frac{\prod_{k=1}^{n}\left(1+\int f_k\, d\, g_\lambda\right)-1}{\lambda}.$$

Example 2.6. Let $T=\mathbb{R}^2$, μ- the Lebesgue measure on T. Let us compute $I=\int e^{-\left(x^2+y^2\right)} d\, g_\lambda$ (where g_λ is the $\lambda-$measure associated to the Lebesgue measure for a fixed λ). We have:

$$I=\frac{e^{\lambda\int e^{-\left(x^2+y^2\right)} d\mu}-1}{\lambda}.$$

Using the polar coordinates, it results that $\int e^{-\left(x^2+y^2\right)} d\mu=\pi$, hence $I=\frac{e^{\lambda\pi}-1}{\lambda}$.

Theorem 2.7. (Beppo-Levi type theorem)

Let $\left(f_n\right)_{n\geq 1}\subset\mathcal{M}$ (the class of functions $f:T\to\mathbb{R}_+$, measurable) be an increasing sequence. We suppose that $\exists f:T\to\mathbb{R}$ such that $f_n\longrightarrow f$ (the convergence being punctual).

Then $f\in\mathcal{M}$ and $\int f\, d\, g_\lambda=\lim_{n\to\infty}\int f_n\, d\, g_\lambda$.

Proof.

Obviously, $f\geq 0$ and f is measurable as the punctual limit of a sequence of measurable functions. Applying the Beppo-Levi theorem for μ, it results: $\int f\, d\mu=\lim_{n\to\infty}\int f_n\, d\mu$, hence:

$$\int f\, d\, g_\lambda=\frac{e^{\int f\, d\mu}-1}{\lambda}=\frac{e^{\lim_{n\to\infty}\int f_n\, d\mu}-1}{\lambda}=\lim_{n\to\infty}\frac{e^{\int f_n\, d\mu}-1}{\lambda}=\lim_{n\to\infty}\int f_n\, d\, g_\lambda.$$

Corollary 2.8. If $\left(f_n\right)_{n\geq 1}\subset\mathcal{M}$ and the function series $\sum_{n=1}^{\infty} f_n$ converges punctually to f. Then:

$$\int f\, d\, g_\lambda=\frac{1}{\lambda}\left[\prod_{n=1}^{\infty}\left(1+\lambda\int f_n\, d\, g_\lambda\right)-1\right].$$

Proof.

$\sum_{k=1}^{n} f_k\longrightarrow f$, punctual and the sequence $\left(\sum_{k=1}^{n} f_k\right)_{n\geq 1}$ is increasing;

According 2.7.:

$$\int f\, d\, g_\lambda=\lim_{n\to\infty}\int\left(\sum_{k=1}^{n} f_k\right) d\, g_\lambda=\lim_{n\to\infty}\frac{1}{\lambda}\left[\prod_{k=1}^{n}\left(1+\lambda\int f_k\, d\, g_\lambda\right)-1\right]=\frac{1}{\lambda}\left[\prod_{k=1}^{\infty}\left(1+\lambda\int f_n\, d\, g_\lambda\right)-1\right].$$

Theorem 2.9. (Lebesgue type theorem, of dominant convergence)

Let $\left(f_n\right)_{n\geq 1}$ be a sequence of μ-measurable functions. We suppose that there exists $g\in\mathcal{M}$, integrable with respect to g_λ, such that: $\left|f_n\right|\leq g$, $g_\lambda-$a.p.t. If $f_n\to f$, $g_\lambda-$a.p.t., then f is integrable and we have: $\int f\, d\, g_\lambda=\lim_{n\to\infty}\int f_n\, d\, g_\lambda$.

Proof.

From the dominant convergence theorem for μ, it results:

$$\int f\, d\mu = \lim_{n\to\infty} \int f_n\, d\mu \in \mathbb{R}$$

because ($\mu-$ a.p.t.) $\Leftrightarrow$ ($g_\lambda-$a.p.t.).

It results: $\int f\, d\, g_\lambda = \dfrac{e^{\int f\, d\mu} - 1}{\lambda} = \lim_{n\to\infty} \dfrac{e^{\int f_n\, d\mu} - 1}{\lambda} = \lim_{n\to\infty} \int f_n\, d\, g_\lambda \in \mathbb{R}.$

Theorem 2.10. (Radon-Nicodim type theorem)

If $g_\lambda^{(1)} << g_\lambda^{(2)}$, then $\exists f \in \mathcal{M}$ such that, $\forall A \in \Re$, $g_\lambda^{(1)}(A) = \int_A f\, d\, g_\lambda^{(2)}$.

Proof.

Let μ_1, μ_2 be the classical measure associated to $g_\lambda^{(1)}$ and $g_\lambda^{(2)}$. From 2.2, as $g_\lambda^{(1)} << g_\lambda^{(2)}$, we have $\mu_1 << \mu_2$, hence (theorem Radon-Nicodim for μ_1, μ_2) $\exists f \in \mathcal{M}$ such that

$$\mu_1(A) = \int_A f\, d\, \mu_2, \forall A \in \Re,$$

hence $\dfrac{e^{\lambda \mu_1(A)} - 1}{\lambda} = \dfrac{e^{\lambda \int_A f\, d\, \mu_2} - 1}{\lambda}$, i.e. $g_\lambda^{(1)}(A) = \int_A f\, d\, g_\lambda^{(2)}$.

References

[1] Wang, Z., Klir, G.: *Generalized Measure Theory*, International Series on Systems Science and Engineering 25, 2009.

[2] Chitescu, I., Secelean, N.A.: *Elemente de Teoria Măsurii şi a Integralei*, Ed. Fundaţiei "România de Mâine", Bucureşti, 1999.

[3] Boboc, N., Bucur, G.: *Măsură şi Capacitate*, Ed. Ştiinţifică şi Enciclopedică, Bucureşti, 1985.

ANALYSIS OF SOFTWARE PACKAGES FOR MODELING WATER QUALITY IN A WATER DISTRIBUTION NETWORK

Alina Elisabeta Sandu
Department of Mathematics and Computer Science
Technical University of Civil Engineering Bucharest, Romania
E-mail: alina.sandu@utcb.ro
Gabriela-Roxana Dobre
Department of Mathematics and Computer Science
Technical University of Civil Engineering Bucharest, Romania
E-mail: roxana.dobre@utcb.ro

Abstract: For the safety of drinking water, a permanent concern is water quality monitoring in distribution network. For an effective monitoring, many of the hydraulic modeling software packages for water distribution networks contain water quality modeling modules.
One important aspect for studying and monitoring the quality of water in distribution networks is based on developing computer programs for modeling parameters and water quality. Development and improvement of public water supply systems represent an objective necessity worldwide. An analysis of the main existing programs used in water distribution network for monitoring the quality of the water can be very usefully for developing new models in this area of engineering. The main components of the calculus program Epanet and Qualnet are analyzed and described.
In the last chapter of this paper it is presented a study case, the monitoring of the chlorine concentrations in the water distribution network from the Prundu district in Pitesti municipality. This network is formed by 439 joints, 459 trunks and is gravitationally supplied from the Războieni storage complex. 18649 consumers are fastened at this distribution network, the pressure varies between 45-49 mCA and the building height regime is placed between (P+4) and (P+10).

Mathematics Subject Classification (2010): 68U20
Key words: water quality modeling

1. Introduction

Developing and improving public water supply systems represents a must all around the world. The purpose of the potable water distribution system is to furnish the water necessary to the solicited quantity and, from a qualitative point of view, without any risks over the human's health. The water quality can be ensured when leaving the chemical treatment station, but as the water flows, the distribution system can suffer some changes.

The storage conduits and equipment from the distribution network are a complex system of uncontrolled chemical and biological reacting substances, which may produce significant variations in the water quality. The main factors that lead to deterioration of the water quality within the distribution network are:

- connecting and disconnecting the power supplies (alternate supply);
- contamination through the leakage connections, non-insulated conduit junctions or failures within the network;
- metallic conduit corrosion and protection coating disintegration;
- losses of the residual disinfectant in the storage installations with long term retaining;

- disinfectant reactions with organic and non-organic complexes causing taste and smell problems;
- bacterium regeneration and possibility of new pathogen agent development;
- turbidity augmentation caused by the entrainment of the particles previously deposited;
- formation of some sub-products of the disinfection.

For an efficient monitoring of water quality there are many software, which studies the hydraulic behaviour of the network and have modules that simulate the variation of water quality. Any of these software programs have in background a strong mathematical model for calculus and for solving the problems that can appear in the distribution water networks.
One important aspect of optimization of water distribution network operation is based on developing computer programs for controlling hydraulic parameters and water quality. For that, a mathematical model is essential. To model a fluid flow thru a water distribution network one of the most used equations is the transport and diffusion equation. With this equation we can model the variation of residual chlorine.
The components of the transport and diffusion equation are: the concentration of residual chlorine, time, time distance, fluid velocity, length section, the diffusion constant and the transport constant.

The transformation of the substances from the potable water, as they circulate through a distribution system is a difficult and complex problem. The distribution networks can expand on thousands of conduit kilometres, which make the proper observing process impossible. The water course and flow time through the distribution system vary due to the loop disposing of the networks and due to the continuous changes of the water use in time and space.

The mathematical modulation of the water qualitative changes within the distribution system is an observing process component. These models are efficient, form the cost point of view, in studying the spatial and temporal variation of the number of water quality constituents, among which the following are included:

- The water volume from a specific source;
- The water age in the system;
- The concentration of a non-reactive tracing component, either added or eliminated from the system (for example, Fluorine or Natrium);
- The concentration and the loss rate of a secondary disinfectant (for example, Chlorine);
- The concentration and the augmentation rate of the disinfection sub-products, such as Trihalomethane
- The number and quantity of bacteria attached to the system or freely running.

Managers can use these models in order to help them run various studies regarding the water quality. The following examples can be taken into consideration:

- System hydraulic model calibration and testing using the chemical tracer agents;
- Storage installation localization and dimensioning and system operation modification in order to diminish the water age;
- Modification of the architecture and operating method of a system in order to furnish a desired water combination from various sources;
- Finding the best combination between the conduit replacement, conduit relining, conduit cleaning, reducing the water storage timeframe and the location and the injection rate at the re-pumping stations to maintain the desired disinfectant level across the system;
- Estimating and minimizing the risk of the consumer's exposure to disinfection sub-products;
- Estimating the system vulnerability to external contamination incidents.

The water quality modulation establishes the manner in which a dissolved substance concentration varies in time across the network, under a known set of hydraulic conditions and characteristics of source alimentation. The fundamental equations are based on the mass conservation principles combined with reaction Kinetics.

2. The Epanet program

The Epanet program was designed to ensure the quality of the water furnished to the consumers through the distribution network. The Epanet program contains an integrated environment for network data entry editing, water hydraulic and quality change simulation and also for result viewing in different forms. These include network maps, data tables and variation curves.

The Epanet program ensures a complex hydraulic analysis, which includes:

- The analyzed network has no seize limit
- It calculates the burden loss, at the user's choice, using the Hazen – Williams, Darcy – Weisbach or Chezy – Manning relations
- It sets the functioning of constant or variable revolution pumps.
- It calculates the pumping necessary energy and its costs.
- It sets different types of fillets, such as closure fillets or those of debit control pressure or run-back regulation.
- It allows any shape of the storage tanks.
- It can take into consideration the demands of the multiple consumer categories, each with his/her own in time parameter variation model.
- It sets the debit dependence according to the pressure.
- It allows the introduction of some simple or complex conditions in the operating system.

The Epanet program provides the following elements in the water quality modulation:

- It sets the movement of a non-reactive material within the network in the clock unit.
- It sets the movement and the evolution of a reactive material.
- It sets the water quality within a network from the point of view of its age.
- It follows the percentage from a joint debit which goes, in time, to the other joints.
- It sets the proper flow in the tube section and the flow tube wall environment.
- It allows the deduction or the extension of the reactions up to an imposed concentration limit.
- It uses global reaction coefficients, which can be modified.
- It allows the concentration variation in time in any point of the network.
- It sets the storage in the tank.

The Epanet program can follow the concentration variation of a substance on the score of the reactions during the distribution system transit. In order to accomplish this variation it is necessary to be aware of the substance reaction rate and of how it depends on the concentration.

The variation of a free surface in the tank nodes it is consider to respect the relation:

$$\Delta y = (q / A)\Delta t$$

where: Δy - the variation of the water level;

q - the flow entering or leaving the tank node (+ or -);

A - the surface of the horizontal section of the tank;

Δt - the time interval for the dynamic analysis.

For each section between nodes i and j and for each node k there are resolved the following equations set:

$$h_i - h_j = f(q_{ij})$$
$$\sum_i q_{ik} - \sum_j q_{kj} - Q_k = 0$$

where: q_{ij} = the flow between nodes i and j ,(m^3/s) ;

h_i = absolute piezometric elevation in node i (piezometric elevation plus land elevation), (m) ;

Q_k = the consumed flow in node k (m^3/s) ;

f = functional relationship between load losses and the flow in the network.

The simulation of the water quality it is realized by Epanet program by using the flows from the hydraulic simulation for chasing the propagation of the contaminant thru the network. A conservation equation of the mass it is resolved for each pipe between node i and j :

$$\frac{\partial c_{ij}}{\partial t} = \frac{q_{ij}}{A_{ij}}\left(\frac{\partial c_{ij}}{\partial x_{ij}}\right) + \theta(c_{ij}), \tag{1}$$

where : c_{ij} = the concentration of the substance in pipe i,j as function of distance and time

C_{ij} = $C_{ij}[X_{ij}, t]$ ($mass\ units/m^3$) ;

x_{ij} = the distance thru the pipe i,j (m) ;

q_{ij} = the flow in pipe i,j (m^3/s) ;

A_{ij} = the area of the axial section in the pipe i,j (m^2);

$\theta(c_{ij})$ = the reaction rate of the substance within the pipe i,j ($mass\ units\ /\ m^3/d$).

The equation (1) is resolved considering the initial conditions known at the initial time $t = 0$ and it will be apply the next boundary condition at the enter of the pipe in node i ,where $x_{ij} = 0$:

$$c_{ij}(0,t) = \frac{\sum_k q_{ki} c_{ki}(L_{ki}, t)}{\sum_k q_{ki}} \tag{2}$$

The sum it will be made for all pipes k,i for witch the flow enter in node i, the starting node of the pipe i,j . ($L_{k,i}$ = the length of the pipe k,i). So, the boundary conditions for the pipe k,i depend of concentrations of every starting nodes of pipes k,i that enter in pipe i,j .

The equations (1) and (2) form a set of differential equations witch described all the network pipes. Epanet program solves these equations by using the finite volume method.

The general expression for decrease of the chlorine can be described by the following equation:

$$\frac{dC}{dt} = K_b \cdot C - \frac{K_f}{R}(C - C_w) \tag{3}$$

where : $\frac{dC}{dt}$ = the rate of decrease of residual chlorine concentration ($mg/l/s$);

C = the concentration of the chlorine inside the pipe (mg/l);

t = the time (s);

K_f = the speed of mass transfer (m/s);

R = hydraulic radius (m);

Cw = the concentration of the chlorine at the pipe wall (mg/l);

Kb = chlorine depletion coefficient (s).

The first term of equation (3) describes the reaction inside the pipe, the second term contains

Cw and represents the rate of reaction of the transported substance with the pipe wall. It is presumed that this reaction is of the first order and can be written:

$$K_f(C - C_w) = K_w - C_w \tag{4}$$

where *Kw* = a react kinetic constant at the pipe wall (m/s).

By resolving after *Cw* and replacing in (3), we obtain:

$$\frac{dC}{dt} = -K_b \cdot C - \frac{K_w \cdot K_f \cdot C}{R(K_w + K_f)} \tag{5}$$

and

$$K_t = K_b + \frac{K_w \cdot K_f}{R(K_w + K_f)} \tag{6}$$

After replacing (6) in equation (5) results :

$$\frac{dC}{dt} = -K_t \cdot C \tag{7}$$

So it will be obtain the model of first order for decreasing the chlorine concentration in a pipe:

$$C_t = C_0 \cdot e^{-K_t \cdot t} \tag{8}$$

where: *Ct* = the concentration of the chlorine at the time *t* (mg/l);
Co = the initial concentration of the chlorine (mg/l).

3. The Qualnet program

The Qualnet is a software program for model the variation of water quality in a water distribution network and it was developed at LA Washington State University. This software program can model the residual chlorine variation in a water distribution network, spatial and temporal, at a moderate speed conditions. The Qualnet can model both transport and chlorine dispersion in a pipeline. This software program first analyzes the initial conditions of the water distribution network. The "slow" variation conditions are then integrated into the equations that govern this process.

A dispersion equation of first order it is used to calculate the chlorine concentration in time. There are used numerical methods to resolve these equations that described the processes of dispersion, diffusion and decreasing of the chlorine concentrations in a pipeline.

To describe a slow flow variation in the pipe it will be used a dynamic equation of the following form:

$$\frac{L}{g \cdot A} \cdot \frac{dQ}{dt} = H_1 - H_2 - \frac{kQ}{Q^m} \tag{9}$$

where : *L* = the length of the pipe (m) ;
g = the gravitational acceleration (m/s) ;
A = area of the pipe section (m^2) ;
Q = the flow (m^3/s) ;
t = time (s) ;
H1,H2 = piezometric elevation upstream and downstream of the pipeline (m)
k , m = constants witch enter in exponential type formulas for the calculus of load losses (in Darcy – Weisbach formula or Hazen – Williams).

4. Study case

The Chlorine concentration variation calculus using the Epanet program, was done in the joints of the water distribution network from the Prundu district from Pitesti municipality. This network is formed by 439 joints, 459 pipelines and is gravitationally supplied from the Războieni storage complex. 18649 consumers are fastened at this distribution network, the pressure varies between 45-49 mCA and the building height regime is placed between (P+4) and (P+10). This distribution network is over 40 years old and within this timeframe no major intervention has been done regarding the conduit rehabilitation, most of them being made from steel tubs. The summed up length of the network conduit is bigger than 13000 m and the diameters vary from 80 mm to 600 mm.

The hydraulic model is the main component in the residual Chlorine concentration variation within the distribution network. During the entire simulation period, the Chlorine concentration in the network injection joint was considered to be constant, this value maintain itself at 0,5 mg/l.

In table 1 are represented some of the obtained results from the Epanet modelling program from the hydraulic point of view. These results are calculated for the pipelines at a maximum consume hour, at 7 p.m.

Table 1. The hydraulic analysis results for some pipelines at 7 p.m.

Nr. Crt.	Pipeline	Lenght (m)	Diameter (mm)	Flow (dm^3/s)	Speed (m/s)	Load losses (m/km)	Chlorine concentration (mg/l)
1	1	118	400	282.75	2.25	34.28	0.5
2	30	9	150	0.08	0	0	0.44
3	40	11	100	1.1	0.14	1.05	0.37
4	60	10	250	1.6	0.03	0.01	0.47
5	70	45	250	21.7	0.44	2.59	0.46
6	80	36	100	8	1.02	53.93	0.43
7	90	180	300	85.45	1.21	14.87	0.45
8	150	24	250	35.82	0.73	7.05	0.44
9	200	10	100	0.66	0.08	0.37	0.34
10	300	19	150	15.74	0.89	22.24	0.32
11	330	19	100	0.52	0.07	0.23	0.3
12	360	8	200	4.33	0.14	0.35	0.36
13	425	7	150	-4.06	0.23	1.5	0.29
14	459	10	150	-25.11	1.42	309.76	0.49

In the next maps are represented some of the obtained results from the Epanet modelling program from the quality of the water point of view. These results are calculated for the nodes of the network at different consume hours.

The initial conditions are null concentrations in all network joints, excepting the injection joint 1 where the value 0,5 mg/l was initialized. The Chlorine concentration variation simulation in the network joints started at the time moment zero and the transformation taking place every hour in a 24 hour timeframe was observed. This way, some representative maps were created at the minimum consume hour, 3:00 am (figure 1), at a medium consume hour, 8:00 am (figure 2) and at a maximum consume hour, 7:00 pm (figure 3). All these maps are made by Epanet software program. It is one of the most important results that can be done with the Epanet software program, not many programs have these possibilities.

On this maps, it can be observed that in certain areas the points with a concentration under 0,10 mg/l are better delimited; under this value the safety limit regarding the water quality cannot be conserved.
On the 3:00am map (figure 1) the areas where the Chlorine concentration is under 0,1 mg/l in order to ensure the quality according to the delivered water within the network are reduced. At 8:00 am (figure 2) some areas are highlighted and the Chlorine concentration remains under 0,1 mg/l.
At 7:00 pm (figure 3) we can observe that the results obtained with the program and the "risk" areas with concentrations under 0,10 mg/l are not found on the map.

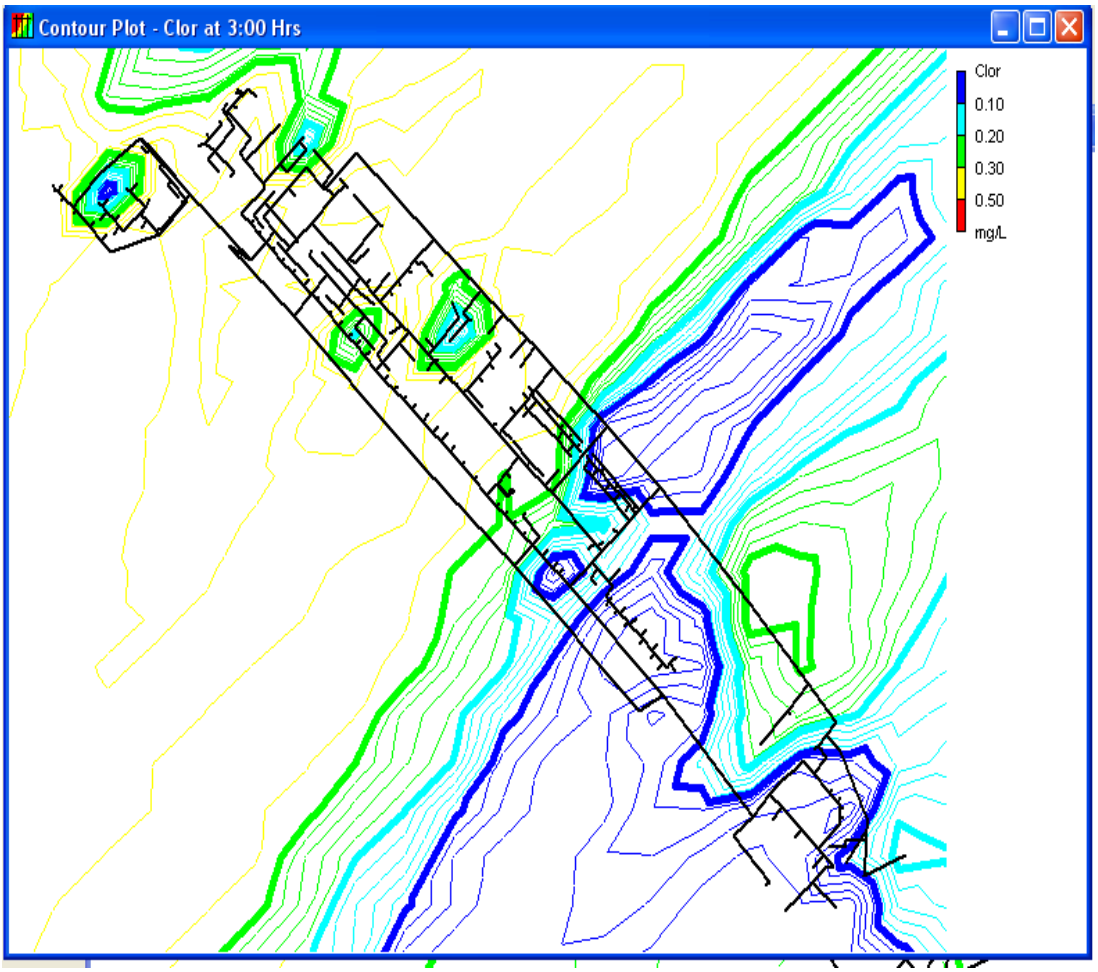

Figure 1. Network map at 3:00 am with Chlorine concentration areas

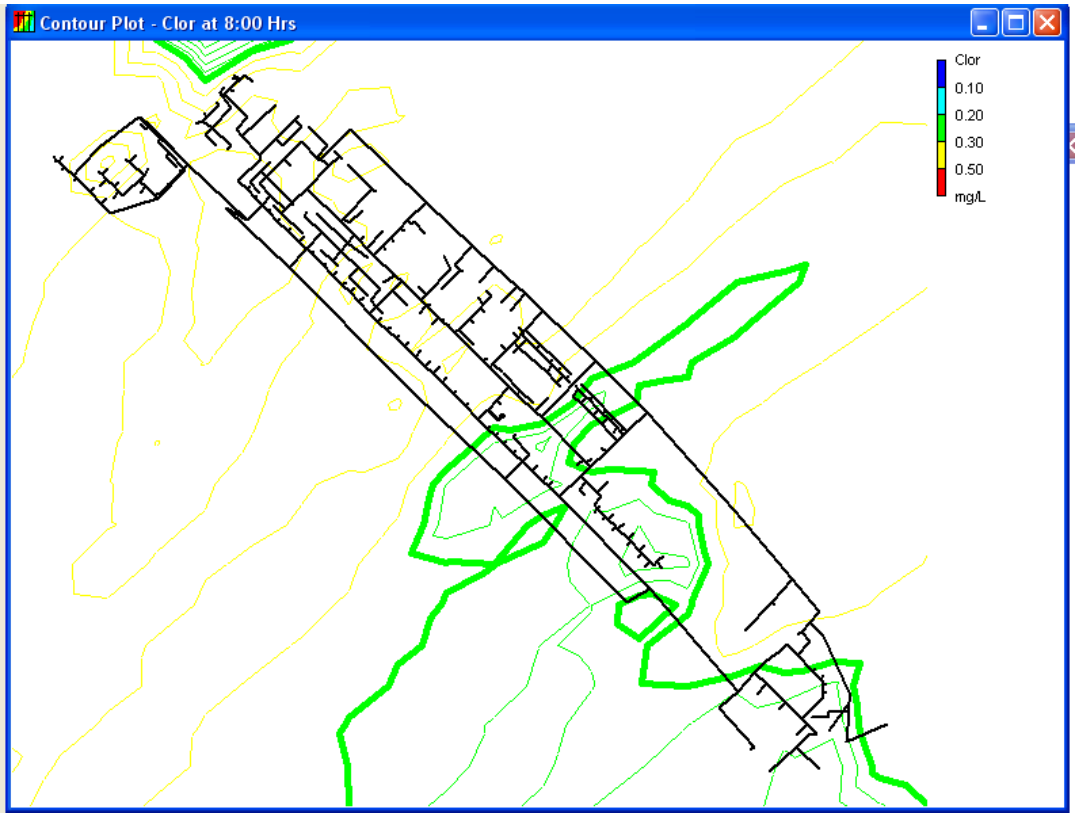

Figure 2. Network map at 8:00 am with Chlorine concentration areas

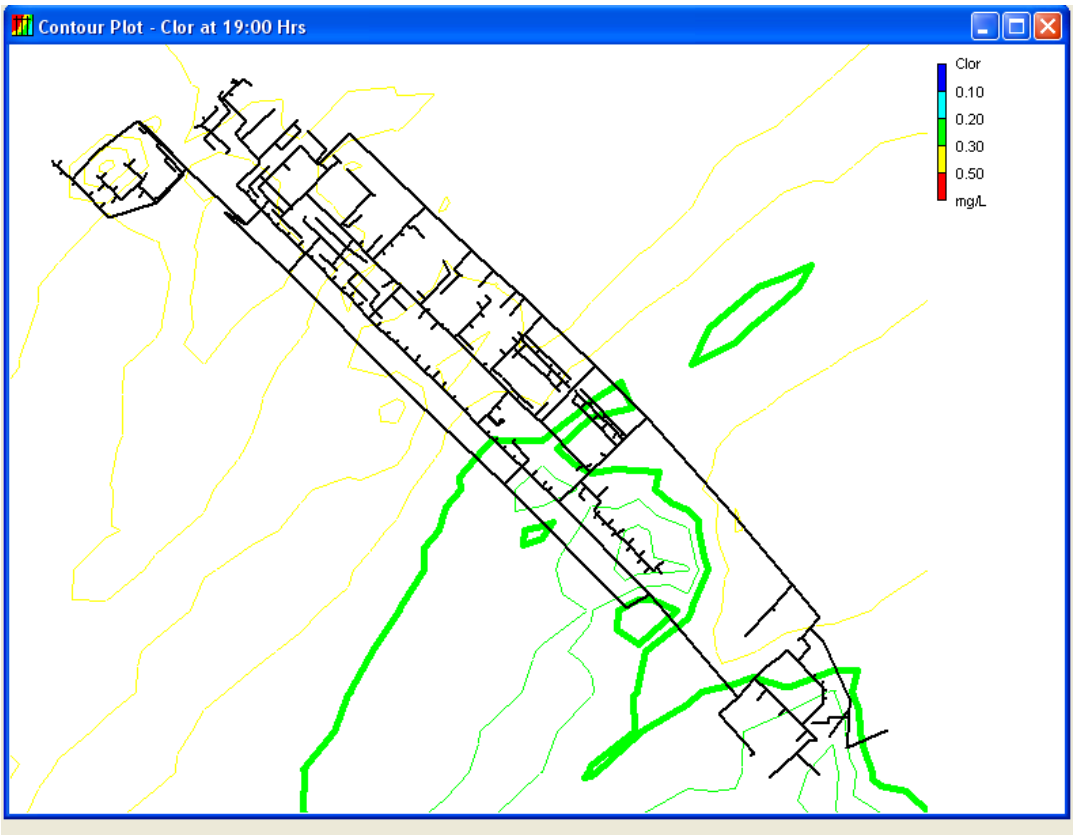

Figure 3. Network map at 7:00 pm with Chlorine concentration areas

Table 2. The chlorine concentrations values calculated with Epanet program for some centred network nodes at a medium consume hour, 8am

The chlorine concentrations values for some centred network nodes									
Node	93	154	174	187	230	237	300	321	367
Chlorine concentartion (mg/l)	0,44	0,43	0,42	0,38	0,32	0,37	0,34	0,28	0,27

Table 3. The chlorine concentrations values calculated with Epanet program for some marginal network nodes at a medium consume hour, 8am

The chlorine concentrations values for some marginal network nodes								
Node	47	121	230	378	383	385	370	430
Chlorine concentartion (mg/l)	0,35	0,45	0,32	0,22	0,24	0,25	0,24	0,37

We can notice from these two tables that the concentration values are adjacent both for the network central joints and the network marginal joints, the values of the second ones being adjacent to the minimum admissible value of 0.10 mg/l for ensuring the conform water quality within the network.

We noticed that for a more accurate program keying, more field data and more measurements for residual Chlorine decay rate determining were necessary. As in the modeled network there are different material conduits and different age pipelines, the Chlorine decay rate can vary for every pipeline and, therefore, a medium decay rate value was chosen for this modulation.

In the speciality literature there are at this moment many models for determinate the kinetic decrease of the chlorine in the report with pipe wall reactions, but this can be also made with experimental models in the lab.

The rate reaction of the chlorine at the pipe wall is it invers proportional with pipe diameter and can be limited by the rate transfer mass from the wall and chlorine.

Labs studies prove that wall rate reaction for ferrous pipes makes that the rate reaction of the chlorine at the pipe wall to be bigger and much significant from the one created by biofilm.

References

[1] Sandu, A.E.: *Dimensioning of a water distribution network, made with RET and Epanet*, The proceedings of the 1st Workshop of Mathematics and Educational Symposium of Department of Mathematics and Computer Science, ISSN 2392-6317, TUCEB, 2014.

[2] Sandu, A.E.: *Analysis of the software packages for hydraulic calculation of a water distribution network*, The proceedings of Mathematics and Educational Symposium of Department of Mathematics and Computer Science, the 2nd edition, ISSN 2067-3132, TUCEB, 2016.

[3] Rossman, L.: EPANET 2 Users Manual, U.S. Environmental Protection Agency, 2000, 600/R-00/057, Cincinnati, OH.

[4] Tuțuianu, A.E.: *Program de calcul pentru monitorizarea calităţii apei în reţelele de distribuţie a apei*, Teza de doctorat, UTCB, 2013.

[5] Perju, S., Stănescu, I.: *Numeric Modelling of the Residual Chlorine Concentration Evolution in a Water Distribution Network*, Revista de chimie, vol. 66, issue 6, 2015.
[6] Clark, R.M., Grayman, W.M.: *Modeling Water Quality in Drinking Water Distribution Systems*, American Water Works Association, Denver, CO, 1998.

META-ANALYSIS, A STATISTICAL MATHOD FOR SUMMARISING RESULTS

Narcisa Teodorescu
Department of Mathematics and Computer Science
Technical University of Civil Engineering Bucharest, Romania
E-mail: narcisa.teodorescu@gmail.com

Abstract: A major task in all areas of science is the development of theory. In many cases, the researches have available the results of a number of previous studies on the subject of interest. Meta-analysis can discover new knowledge not inferable from any individual study and can sometimes answer questions that were never addressed in any of the individual studies contained in the meta-analysis. This paper's aim is to present the fundamental principles of meta-analysis, as a statistical method for summarising results of correlational studies.
Mathematics Subject Classification (2010): 62-02
Key words: meta-analysis, correlations, statistical methods

1. Introduction

A meta-analysis is a statistical analysis that combines the results of multiple scientific studies. Meta-analysis can be performed when there are multiple scientific studies addressing the same question, with each individual study reporting measurements that are expected to have some degree of error. The aim then is to use approaches from statistics to derive a pooled estimate closest to the unknown common truth based on how this error is perceived. Existing methods for meta-analysis yield a weighted average from the results of the individual studies, and what differs is the manner in which these weights are allocated and also the manner in which the uncertainty is computed around the point estimate thus generated. In addition to providing an estimate of the unknown common truth, meta-analysis has the capacity to contrast results from different studies and identify patterns among study results, sources of disagreement among those results, or other interesting relationships that may come to light in the context of multiple studies [5].

A key benefit of this approach is the aggregation of information leading to a higher statistical power and more robust point estimate than is possible from the measure derived from any individual study. However, in performing a meta-analysis, an investigator must make choices which can affect the results, including deciding how to search for studies, selecting studies based on a set of objective criteria, dealing with incomplete data, analyzing the data, and accounting for or choosing not to account for publication bias. Judgment calls made in completing a meta-analysis may affect the results. For example, Wanous and colleagues examined four pairs of meta-analyses on the four topics of (a) job performance and satisfaction relationship, (b) realistic job previews, (c) correlates of role conflict and ambiguity, and (d) the job satisfaction and absenteeism relationship, and illustrated how various judgement calls made by the researchers produced different results [23].

The historical roots of meta-analysis can be traced back to 17th century studies of astronomy [18], while a paper published in 1904 by the statistician Karl Pearson in the *British Medical Journal* [17] which collated data from several studies of typhoid inoculation is seen as the first time a meta-analytic approach was used to aggregate the outcomes of multiple clinical studies [15], [16]. The first meta-analysis of all conceptually identical experiments concerning a particular research issue, and conducted by independent researchers, has been identified as

the 1940 book-length publication *Extrasensory Perception After Sixty Years*, authored by Duke University psychologists J. G. Pratt, J. B. Rhine, and associates [19]. This encompassed a review of 145 reports on ESP experiments published from 1882 to 1939, and included an estimate of the influence of unpublished papers on the overall effect (the *file-drawer problem*). Although meta-analysis is widely used in epidemiology and evidence-based medicine today, a meta-analysis of a medical treatment was not published until 1955. In the 1970s, more sophisticated analytical techniques were introduced in educational research, starting with the work of Gene V. Glass, Frank L. Schmidt and John E. Hunter.

The term "meta-analysis" was coined in 1976 by the statistician Gene V. Glass [4], who stated *"my major interest currently is in what we have come to call ...the meta-analysis of research. The term is a bit grand, but it is precise and apt ... Meta-analysis refers to the analysis of analyses"*. Although this led to him being widely recognized as the modern founder of the method, the methodology behind what he termed "meta-analysis" predates his work by several decades. The statistical theory surrounding meta-analysis was greatly advanced by the work of Nambury S. Raju, Larry V. Hedges, Harris Cooper, Ingram Olkin, John E. Hunter, Jacob Cohen, Thomas C. Chalmers, Robert Rosenthal, Frank L. Schmidt, and Douglas G. Bonett.

2. Study artifacts and their impact on study outcomes

The goal of a meta-analysis of correlations is a description of the distribution of actual correlations between a given independent and a given dependent variable. If all studies were conducted perfectly, then the distribution of study correlations could be used directly to estimate the distribution of actual correlations. However, studies are never perfect. As a result, the relationship between study correlations and actual correlations is more complicated. There are many dimensions along which studies fail to be perfect. Thus, there are many forms of error in study results. Each form of error has some impact on the results of a meta-analysis. Some errors can be corrected and some cannot. We refer to study imperfections as “artifacts” to remind ourselves that errors in study results produced by study imperfections are artifactual or man-made errors and not properties of nature. Correction of artifacts requires auxiliary information such as study sample sizes, study means and standard deviations, estimates of reliability, and so on.

The complexity of formulas depends on two things: (1) the extent of variation in artifacts and (2) the extent of variation in actual correlations. Formulas for meta-analysis would be simplest if artifacts were homogeneous across studies, that is, if all studies had the same sample size, all had the same reliability for the independent and dependent variables, all had the same standard deviations, and so forth. If artifacts were homogeneous, then the primary calculations would all be simple averages and simple variances. In actuality, artifacts vary from study to study; hence, more complicated weighted averages are necessary.

The complexity of formulas depends on two things: (1) the extent of variation in artifacts and (2) the extent of variation in actual correlations. Formulas for meta-analysis would be simplest if artifacts were homogeneous across studies, that is, if all studies had the same sample size, all had the same reliability for the independent and dependent variables, all had the same standard deviations, and so forth. If artifacts were homogeneous, then the primary calculations would all be simple averages and simple variances. In actuality, artifacts vary from study to study; hence, more complicated weighted averages are necessary.

We have identified 11 artifacts that alter the size of the study correlation in comparison to the actual correlation. The most damaging artifact in narrative reviews has been sampling error. Sampling error has been falsely interpreted as conflicting findings in almost every area of research in the social sciences. However, some of the other artifacts induce quantitative errors so large as to create qualitatively false conclusions [8], [9] or to greatly alter the practical

implications of findings [21]. This is especially important to consider when several artifacts work in conjunction.

1. Sampling error:

Study validity will vary randomly from the population value because of sampling error.

2. Error of measurement in the dependent variable:

Study validity will be systematically lower than true validity to the extent that job performance is measured with random error.

3. Error of measurement in the independent variable:

Study validity for a test will systematically understate the validity of the ability measured because the test is not perfectly reliable.

4. Dichotomization of a continuous dependent variable:

Turnover, the length of time that a worker stays with the organization, is often dichotomized into "more than…" or "less than…" where…is some arbitrarily chosen interval such as one year or six months.

5. Dichotomization of a continuous independent variable:

Interviewers are often told to dichotomize their perceptions into "acceptable" versus "reject."

6. Range variation in the independent variable:

Study validity will be systematically lower than true validity to the extent that hiring policy causes incumbents to have a lower variation in the predictor than is true of applicants.

7. Attrition artifacts: Range variation in the dependent variable:

Study validity will be systematically lower than true validity to the extent that there is systematic attrition in workers on performance, as when good workers are promoted out of the population or when poor workers are fired for poor performance.

8. Deviation from perfect construct validity in the independent variable:

Study validity will vary if the factor structure of the test differs from the usual structure of tests for the same trait.

9. Deviation from perfect construct validity in the dependent variable:

Study validity will differ from true validity if the criterion is deficient or contaminated.

10. Reporting or transcriptional error:

Reported study validities differ from actual study validities due to a variety of reporting problems: inaccuracy in coding data, computational errors, errors in reading computer output, typographical errors by secretaries or by printers. Note: These errors can be very large in magnitude.

11. Variance due to extraneous factors that affect the relationship:

Study validity will be systematically lower than true validity if incumbents differ in job experience at the time their performance is measured (because job experience affects job performance).

3. Planning meta-analysis

The stages of meta - analysis are very similar to the stages of a poll. First, both in polls both opinion and meta-analysis should be delimited and formulated the problem that it wants to be investigated. Once this stage has been exceeded, a strategy of sampling for identification of subjects (or research reports) relevant for study. In other words, you must delimited the population we want to share study.

Once we know how we get to the subjects or research reports, must be collected relevant data for the issue to which we try to find an answer. Like the ones which organizes and conducts polls opinion use questionnaires, researchers who make meta-analyses will use standardization sheets of the results. In close relationship with this at the moment, a database should be organized allowing storage, processing and drafting reports.

Last but not least, both the social investigation and the meta-analysis should end with a research report.

Like any scientific approach, meta-analysis starts from the formulation of some hypotheses research. Discussing the hypothesis issue in meta-analysis, Mullen (1989) [14] argues that this stage is crucial for the smooth running of of the whole approach, involving decisions of researchers in four major aspects: (1) the dependent variable, (2) the variable independent, (3) sampling and procedure and (4) statistical tests used.

In selecting studies for meta-analysis, the researcher must take into account the fact that the operational definitions may vary from one tool to another, even if in construction started from conceptual definitions similar or even identical. Difference to level operational definitions can make the link of that construct and another construct be more intense or less intense. May much, different variants of the same tools lead to differences in definitions operational. In other words, inclusion in the same meta-analysis of studies that measure the same construct with different tools can leads to erroneous results and for this reason the researcher must take into account the tool used by article authors for measuring variables of interest.

Variation of the operational definition may leads to heterogeneous results (which varies more than we expected), but this is not mandatory. Our recommendation for those who are propose to achieve meta-analysis is to include studies using tools different, but to keep a strict record of methods of data collection used by the authors of those studies. In case the reported results of studies are not homogeneous, the authors of the meta-analysis have several options that will be mentioned later in this paper.

To locate relevant studies, Mullen [14] proposes the call to two search strategies:

· Ancestry strategy - recommends searching for new articles based on the bibliography of those we already have. The search result will be a set of older articles than we already have, articles that in turn may be the basis for a new search to identify older items;

Descendancy approach - the researcher can start from a very referenced article or reference, focusing on searching for new manuscripts that have the reference in the bibliography. Such a strategy is very effective when it starts from references where established psychological tests are presented for the first time because it ensures both the stability of evaluation tools and the possibility of identifying articles that do not have the main objective to study the variables that are of interest to us for meta-analysis. For example, if we perform a search after the article in which [1] describe the counterproductive behaviors assessment questionnaire, we will only get those articles that used this questionnaire and not articles that appealed to parallel samples ([22], for example). Such an approach can increase the rigor of meta-analysis by keeping constant the operational definition of the dependent variable constant.

The collection of relevant information for the meta-analysis is done according to the research objectives and depending on the design experimental studies that are being analyzed (correlation studies, experimental studies, etc.). At this stage, it is important that the issue to be studied is best delineated from the four points discussed previously.

Each study contains several types of information, each with its usefulness in the meta-analytical approach:

- Study identification information;
- Information on potential moderating variables of effect size;
- Information for calculating the magnitude of the effect.

Collecting all of these data does not guarantee that all will be useful because the studied relationship may be homogeneous, which excludes the analysis of the moderating variables. Even in situations of heterogeneity of results, it is unlikely that all of this data will be useful in explaining it. However, omission of information at the time of data collection may oblige the researcher to resume all articles to enter that information.

4. Runnind the meta-analysis

Meta-analysis aims to identify an average effect and establish a confidence interval for this effect. The main difference between the statistical calculations we are accustomed to and the calculations required to run a meta-analysis is that they are weighted statistics.

In the meta-analysis we will identify studies that are more important and studies that are less important. Classical authors in the field of meta-analysis (Hedges, Rosenthal, Hunter and Schmidt) recommend that the importance of studies in weighted average calculation be given by the inverse of the variance of the reported study effect size ($1/var_{studiu}$). The argument for this weighting criterion is relatively simple: more importantly, those studies reporting effects whose confidence interval is lower (less variation) compared to studies reporting effects with a high confidence interval.

Depending on the magnitude of the effect considered in the meta-analysis, this variance is calculated differently (for more details, see [3], [11]). For the correlation coefficient r (Pearson), the variance of effect size is 1/(*N*-3), where *N* is the number of subjects tested.

Testing heterogeneity of studies

Testing heterogeneity of studies is a form of meta-analysis that aims to identify the impact of sampling error on the effects of different studies. The methodology for testing the heterogeneity of studies is presented extensively in [13] and [6].

Testing heterogeneity of studies is based on the χ^2 test, which tests the existence of differences between the observed values and the expected values. In a meta-analytical study, χ^2 is used to test the differences between the values obtained from different studies and the weighted average of these studies.

Calculating the mean effect size is the first step of any meta-analysis. This average is called the "average observed" and is obtained taking into account the number of subjects in each study, so studies with a large number of subjects (ie with a lower sampling error) have a higher weight in this study average (1). It is also important to mention that, for calculating the mean effect size, the z (Fisher) transformation of the correlation coefficients can be used.

$$z_{mediu\_observat} = \frac{\sum[z_{studiu} \times (N_{studiu} - 3)]}{\sum(N_{studiu} - 3)} \quad (1)$$

Once the weighted average of the effect size is calculated, the value of the χ^2 test can be calculated to see if the differences between the observed study (observed values) and the calculated mean (expected value) are significant. In the literature, the test used for assessing heterogeneity is marked with Q (Rosenthal et al 2006 [20]). The calculation formula is as follows:

$$Q = \sum\left[(N_{studiu} - 3) \times \left(z_{studiu} - z_{mediu\_observat}\right)^2\right]. \quad (2)$$

Finding the significance level of the homogeneity test is done using the tables of χ^2, at a degree of freedom equal to the number of samples (usually denoted by *k*) minus 1.

Meta-analysis of "bare bones"

The name of the meta-analysis of naked bone meta-analysis ([10]) comes from attempting to assess and evaluate the influence of erroneous sampling. The result of such an analysis is an estimate of variation in effect size from one study to another in the absence of any influence from erroneous sampling.

The theory behind this type of meta-analysis is simple: the dispersion of the reported results of studies (S^2_{total}) is the sum of the influence of the research artefacts described above. The

differences due to the sampling error (S_1^2), the differences due to variations of internal consistency (S_2^2) and the differences due to the amplitude restrictions (S_3^2) contribute cumulatively to the differences that we get to observe when we want to run a meta-analysis (see (3)).

$$S_{total}^2 = S_1^2 + S_2^2 + S_3^2 + S_{necunoscut}^2 \quad (3)$$

The approach proposed by Hunter and Schmidt [2] consists in calculating the explanatory power of each artifact. For example, if we get to know S_{total}^2 and S_1^2 (dispersion due to sampling error), we can calculate to what extent the sampling error plays a more or less important role in explaining the observed differences between studies (S_1^2 / S_{total}^2).

The first step of any meta-analytical approach is to calculate the effect magnitude indicator for correlation coefficients. Then its variance can be calculated in the sample of studies (S_{total}^2). This indicator shows the degree to which the results of the different studies are similar or different from the mean calculated by formula (1).

$$S_{total}^2 = \frac{\sum\left[\left(r_{studiu} - r_{mediu\_observat}\right)^2 \times \left(N_{studiu} - 3\right)\right]}{\sum\left(N_{studiu} - 3\right)} \quad (4)$$

The calculation formula of S_1^2 is presented below (5).

$$S_1^2 = \frac{\left(1 - r_{mediu\_observat}\right)^2}{N_{mediu} - 1} \quad (5)$$

As can be seen, this formula uses N_{mediu}, which represents the average of the number of subjects in the meta-analysis studies.

The difference between the observed variance (S_{total}^2) and the variance due to the sampling error (S_1^2) reflects the "real variance" of the effect size at the population level [10]. If the actual variation in effect size is high, we can talk about a heterogeneity of the results of different studies, and we should try to explain this variability based on the characteristics of the studies. In order to identify the heterogeneity of the results of the meta-analysis studies, Hunter and Schmidt [10] recommend the reporting of the sampling variance to the observed variance of the effect size.

If the ratio S_1^2 / S_{total}^2 is less than .75 we can speak of heterogeneous results because such a result indicates that over 25% of the variance of the study results is due to variables that were not taken into account. The heterogeneity of the results of the meta-analysis studies obliges the researcher to try to explain this result.

Huffcut [7] describes several ways to reduce unexplained variance as follows:

- Isolate studies based on a researcher-defined criterion or cluster analysis;
- Eliminating the influence of research artifacts;
- Introducing the results in a statistical analysis (regression analysis or variance analysis) in an attempt to explain their variations based on the characteristics of the studies.

6. Reporting the results

As any scientific approach, the results obtained following a meta-analysis should be reported in a standardized form [3], [7]:

- how to search for meta-analysis;
- the main decisions taken during the selection of studies;
- the main results obtained.

Regarding the search method for the meta-analysis studies, the international search databases and the keywords used in this search are usually reported. Where other strategies have been used, they should be reported. Decisions taken during the selection of studies refer to the inclusion of selection criteria, criteria that may refer to:

- selection of studies using only one instrument
- selecting studies that have only referred to a particular theory
- selecting studies that have only addressed a certain type of subject

In reporting the results obtained, information such as: the number of analyzed samples (k), the total number of subjects tested in these samples (N), the observed mean effect size, the standard deviation of the effect size average, the confidence interval of this value averages and statistical indices on the homogeneity of the results reported by the studies included in the analysis (Q or variance explained by the sampling error, depending on the method used in the meta-analysis).

A frequent question that occurs when we propose to begin a meta-analysis is how to make a meta-analysis of the relationship we are interested in. The answer to this question depends on several factors, as follows: the degree of standardization of the methodology used in the studies that analyze the relationship we want to investigate, the quality of these studies and the number of available studies (k).

First, a review of the methodology used in the literature should provide the answer to questions such as: what are the methods of data collection? are these equivalent methods so that they can be combined? A high degree of standardization of the methodology used ensures the reproducibility of the obtained results, which is a prerequisite for the meta-analytical approach. The use of various data collection methods may represent an artifact that influences the heterogeneity of the reported results of different studies, resulting in an inconclusive outcome [10].

The quality of the studies included in the meta-analysis is still an issue discussed in the literature because there is no formal definition of it. The quality of studies is mainly related to their internal validity or the use of statistical methods appropriate to the experimental design. These issues need to be evaluated, and on the basis of this assessment the decision is made to include the study in the meta-analysis. Some authors [10] recommend the use of experts who, based on a grid, assess the quality of studies. The resulting quality indices will be used in the weighting of the results of the studies, the average result being double weighted: based on the variance of the effect size and on the basis of these quality indices.

The number of articles needed to run a quality meta-analysis is an uncertain issue in the literature. On the one hand, it should be as large as possible to ensure a higher level of generalization of the result. On the other hand, published meta-analyzes are frequently performed on a relatively small number of studies: for example, [20] present a synthetic table with studies that turned to meta-analysis by testing heterogeneity and the parameter k (the number of independent samples taken into account) varies between 5 and 76 samples. Currently, specialist journals publish meta-analyzes that report average results by aggregating 4-7 studies.

The relationship between the number of samples included in the meta-analysis (k) and its quality depends primarily on the two parameters that we discussed: studies must be of a quality and have similar methodologies (desirable would be that the methods used are

identical, but this is not always possible). Secondly, the result of the meta-analysis must be homogeneous. If the researcher reaches a heterogeneous outcome based on a relatively small number of studies (4-7 studies) he will no longer have the opportunity to study the source of this heterogeneity, which implies the lack of an important objective of meta-analytical research.

6. Conclusions

In conclusion, a quality meta-analysis is an approach that synthesizes quality research (garbage in-garbage out is best suited in this context) with similar or identical methodologies and results in a homogeneous outcome. As we can see, we excluded the criterion of the number of studies precisely due to the fact that there is no relationship between it and the homogeneity of the result of the meta-analysis.

References

[1] Bennett, R.J., Robinson, S.L.: Development of a measure of workplace deviance. *Journal of Applied Psychology*, **85(3)**, 2000, 349-360.

[2] Borenstein, M., Hedges, L., Higgins, J., Rothstein, H.: *Introduction to meta-analysis*. Chichester, UK: Wiley, 2009.

[3] Durlak, J.A.: *Basic Principles of Metaanalysis*. In Roberts, M.C. & Ilardi, S.S. (coord.): *Handbook of research methods in Clinical Psychology*, Blackwell Publishing House, 2005.

[4] Glass, G.V.: *Primary, secondary, and meta-analysis of research,* Educational Researcher, **5(10)**, 3–8, 1976.

[5] Greenland, S., O'Rourke, K.: *Meta-Analysis*. *in Modern Epidemiology*, 3rd ed. Edited by Rothman KJ, Greenland S, Lash T. Lippincott Williams and Wilkins; 2008.

[6] Hohn, M., Vârgă, D., Măruster, L.: *Curs de statistică aplicată în stiinte sociale. Volumul II*, Timisoara: Tipografia Universitătii de Vest, 1999.

[7] Huffcutt, A.I.: *Research Perspectives on Meta-analyis*. In Rogelberg, S.G. (coord.). *Handbook of Research Methods in Industrial and Organizational Psychology*. Blackwell Publishing House, 2007.

[8] Hunter, J.E., Schmidt, F.L.: *Error in the meta-analysis of correlations: The mean correlation.* Unpublished manuscript, Department of Psychology, Michigan State University, 1987.

[9] Hunter, J.E., Schmidt, F.L.: *Error in the meta-analysis of correlations: The standard deviation.* Unpublished manuscript, Department of Psychology, Michigan State University, 1987.

[10] Hunter, J.E., Schmidt, F.L.: *Methods of Meta-Analysis. Correcting Error and Bias in Research Findings*, Thousand Oaks: Sage Publishers, 2004.

[11] Kirk, R.E.: *The Importance of Effect Magnitude*. In Davis, S.F. (coord.) *Handbook of Research Methods in Experimental Psychology*. Blackwell Publishing House, 2005.

[12] Maricutoiu, L.: Introducere în metaanaliza: Metaanaliza corelaţiilor, *Psihologia Resurselor umane*, **6(2)** (2008), 112-127.

[13] Miclea, M.: „*Meta-analiza*". în Radu, I. (coord.). *Metodologia cercetării si analiza datelor*, Cluj Napoca, p.309-334, 1994.

[14] Mullen, B.: *Basic Advanced Meta-analysis*, New Jersey: Lawrence Erlbaum, 1989.

[20] Nordmann, A.J., Kasenda, B., Briel, M.*: Meta-analyses: what they can and cannot do*, Swiss Medical Weekly, **142**, 2012.

[15] O'Rourke, K.: *An historical perspective on meta-analysis: dealing quantitatively with varying study results*, J R Soc Med.,**100(12**), 579–582, 2007.

[16] Pearson, K.: *Report on certain enteric fever inoculation statistics*, BMJ. **2(2288)**, 1243–1246, 1904.

[17] Plackett, R.L.: *Studies in the history of probability and statistics: VII. The Principle of the Arithmetic Mean*, Biometrika, **45(1–2)**, 1958, 133. Retrieved 29 May 2016.
[18] Pratt, J.G., Rhine, J.B., Smith, B.M., Stuart, C.E., Greenwood, J.A.: *Extra-Sensory Perception after Sixty Years: A Critical Appraisal of the Research in Extra-Sensory Perception*, New York, Henry Holt, 1940.
[19] Rosenthal, R., DiMatteo, M.R.: Metaanalysis: *Recent Developments in QuantitativeMethods for Literature Reviews*. Annual Review of Psychology, **52**,p 59-82, 2001.
[20] Schmidt, F.L., Hunter, J.E.: *Development of a general solution to the problem of validity generalization*,Journal of Applied Psychology, **62**, p. 529–540, 1977.
[21] Spector, P.E., Fox, S., Penney, L.M., Bruusema, K., Goh, A., Kessler, S.: Thedimensionality of counterproductivity: Are all counterproductive behaviors created equal? *Journal of Vocational Behavior*, **68**, 2006, 446-460.
[22] Walker, E., Hernandez, A.V., Kattan, M.W.: *Meta-analysis: Its strengths and limitations,* Cleve Clin J Med., **75(6)**, 2008, 431–9.

APPLICATIONS OF SCALAR PRODUCT IN EUCLIDEAN GEOMETRY

Daniel Tudor
Department of Mathematics and Computer Science
Technical University of Civil Engineering Bucharest, Romania
E-mail: danieltudor@gmail.com
Dan Caragheorgheopol
Department of Mathematics and Computer Science
Technical University of Civil Engineering Bucharest, Romania
and
"Ilie Murgulescu" Institute of Physical Chemistry of the Romanian Academy
Splaiul Independentei 202, RO-060021 Bucharest, Romania
E-mail: dancaraghe@gmail.com
Lucian Niţă
Department of Mathematics and Computer Science
Technical University of Civil Engineering Bucharest, Romania
E-mail: lucian.s.nita@gmail.com

Abstract: In this paper, we propose to solve, using scalar product of two vectors, some problems of Euclidean geometry, with synthetic hypothesis (apparently, no connections in hypothesis with vector geometry). This type of problems is a good starting point for preparing for Traian Lalescu Student Contest.
Mathematics Subject Classification (2010): 97G70
Key words: Vector geometry, scalar product

1. Introduction

It is well known that the scalar product of two vectors $\vec{a}$ and $\vec{b}$ is defined as the real number $|\vec{a}|\cdot|\vec{b}|\cdot\cos(\sphericalangle(\vec{a},\vec{b}))$ if both vectors $\vec{a}$ and $\vec{b}$ are nonzero, or 0 if one of the vectors $\vec{a}$ and $\vec{b}$ is null ($|\vec{a}|$ denotes the length of vector $\vec{a}$, $\sphericalangle(\vec{a},\vec{b})$ the angle between the vectors $\vec{a}$ and $\vec{b}$). The algebraic properties of the scalar product are the commutativity and the distributivity over addition: $\vec{a}\cdot\vec{b}=\vec{b}\cdot\vec{a}$, $\vec{a}\cdot(\vec{b}+\vec{c})=\vec{a}\cdot\vec{b}+\vec{a}\cdot\vec{c}$. The most used property of scalar product comes from the definition and it is an expression for the cosine of the angle between two vectors $\vec{a}$ and $\vec{b}$: $\cos(\sphericalangle(\vec{a},\vec{b}))=\dfrac{\vec{a}\cdot\vec{b}}{|\vec{a}|\cdot|\vec{b}|}$. From this expression, one deduces that two vectors are perpendicular if their scalar product is null. Moreover, two lines are perpendicular if the scalar product of their direction vectors is null.

In the first year, the first classes at Algebra and Geometry courses are about vector geometry and the algebraic and geometric properties of scalar, vector and mixed products. In the following section, we present some problems with synthetic hypothesis of Euclidean geometry which will be solved using the properties of scalar product of two vectors. This kind of problems is a way to find a transition between classic Euclidean geometry and vector geometry. But considering the difficulty of these problems, they can be used as the first lessons for the students who want to train themselves for Traian Lalescu Student Contest.

We will often use in these problems the following known vectors relation, given by the situation of Figure 1: $\overrightarrow{OM} = \frac{MB}{AB} \cdot \overrightarrow{OA} + \frac{MA}{AB} \cdot \overrightarrow{OB}$ (*).

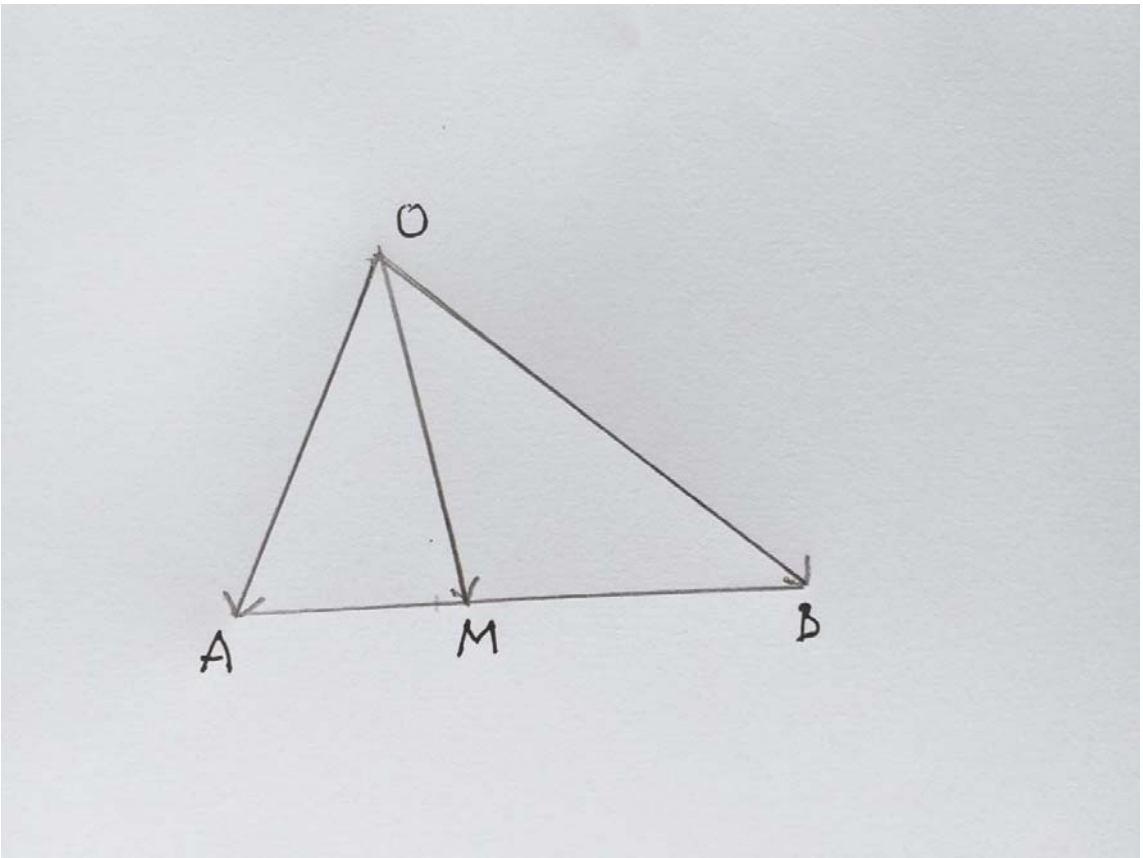

Figure 1

2. Proposed problems

Problem 2.1 Let $AP \perp BC$, $P \in (BC)$ and $E \in (AB)$, $F \in (AC)$ such that the circle of diameter [*EF*] cuts (*BC*) in *P* (Figure 2). Prove that $BE \cdot CF \cdot AP^2 = AE \cdot AF \cdot BP \cdot CP$.

Solution

Since the lines *PE* and *PF* are perpendicular, it results $\overrightarrow{PE} \cdot \overrightarrow{PF} = 0$.

But $\overrightarrow{PE} = \frac{BE}{AB} \cdot \overrightarrow{PA} + \frac{AE}{AB} \cdot \overrightarrow{PB} = \frac{BE \cdot AP}{AB} \cdot \frac{\overrightarrow{PA}}{AP} + \frac{AE \cdot BP}{AB} \cdot \frac{\overrightarrow{PB}}{BP} = \frac{BE \cdot AP}{AB} \cdot \vec{u} + \frac{AE \cdot BP}{AB} \cdot \vec{v}$, and $\overrightarrow{PF} = \frac{CF}{AC} \cdot \overrightarrow{PA} + \frac{AF}{AC} \cdot \overrightarrow{PB} = \frac{CF \cdot AP}{AC} \cdot \frac{\overrightarrow{PA}}{AP} + \frac{AF \cdot CP}{AC} \cdot \frac{\overrightarrow{PB}}{BP} = \frac{CF \cdot AP}{AC} \cdot \vec{u} - \frac{AF \cdot CP}{AC} \cdot \vec{v}$, where $\vec{u}$ and $\vec{v}$ are two perpendicular, norm one vectors (it follows from $AP \perp BC$).

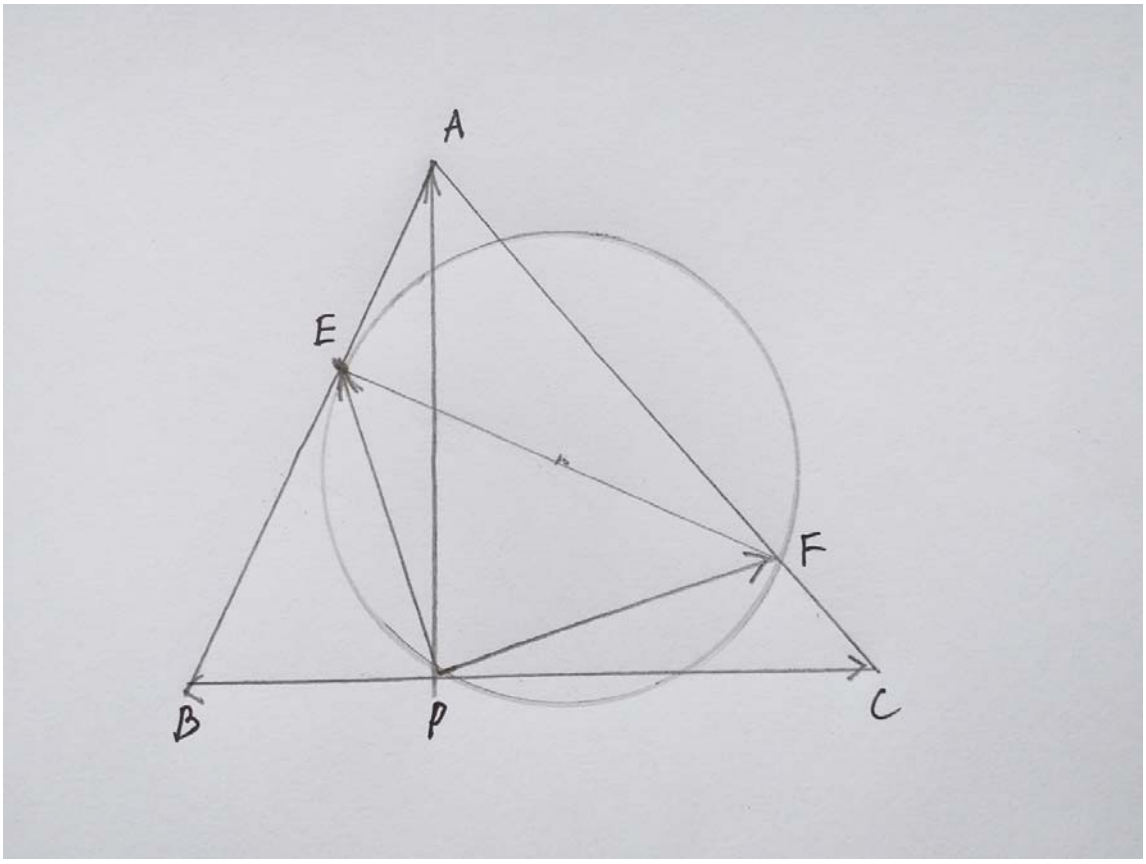

Figure 2

It results $\overrightarrow{PE}\cdot\overrightarrow{PF}=0=\frac{BE\cdot AP}{AB}\cdot\frac{CF\cdot AP}{AC}-\frac{AE\cdot BP}{AB}\cdot\frac{AF\cdot CP}{AC}$ which is equivalent to $BE\cdot CF\cdot AP^2=AE\cdot AF\cdot BP\cdot CP.$

Problem 2.2 Let $ABCD$ be a quadrilateral inscribed in a circle of diameter (AC). It is known that there exists points $E\in(CD)$, $F\in(BC)$ such that $AE\perp DF$; $AF\perp BE$ (Figure 3). Prove that $AB=AD$.

Solution

Since $\overrightarrow{AF}\cdot\overrightarrow{BE}=0\Leftrightarrow\overrightarrow{AF}\cdot(\overrightarrow{AE}-\overrightarrow{AB})=0$ and $\overrightarrow{AE}\cdot\overrightarrow{DF}=0\Leftrightarrow\overrightarrow{AE}\cdot(\overrightarrow{AF}-\overrightarrow{AD})=0$ we easily obtain

$$\overrightarrow{AE}\cdot\overrightarrow{AF}=\overrightarrow{AE}\cdot\overrightarrow{AD}\text{ and }\overrightarrow{AE}\cdot\overrightarrow{AF}=\overrightarrow{AF}\cdot\overrightarrow{AB}\Leftrightarrow\overrightarrow{AE}\cdot\overrightarrow{AD}=\overrightarrow{AF}\cdot\overrightarrow{AB}.$$

This is equivalent to:

$$(\overrightarrow{AD}+\overrightarrow{DE})\cdot\overrightarrow{AD}=(\overrightarrow{AB}+\overrightarrow{BF})\cdot\overrightarrow{AB}\Leftrightarrow AD^2+\overrightarrow{DE}\cdot\overrightarrow{AD}=AB^2+\overrightarrow{BF}\cdot\overrightarrow{AB}.$$

But $\measuredangle ADE=\measuredangle ABF=90^0\Leftrightarrow\overrightarrow{DE}\cdot\overrightarrow{AD}=\overrightarrow{BF}\cdot\overrightarrow{AB}=0$, which implies that $AB=AD.$

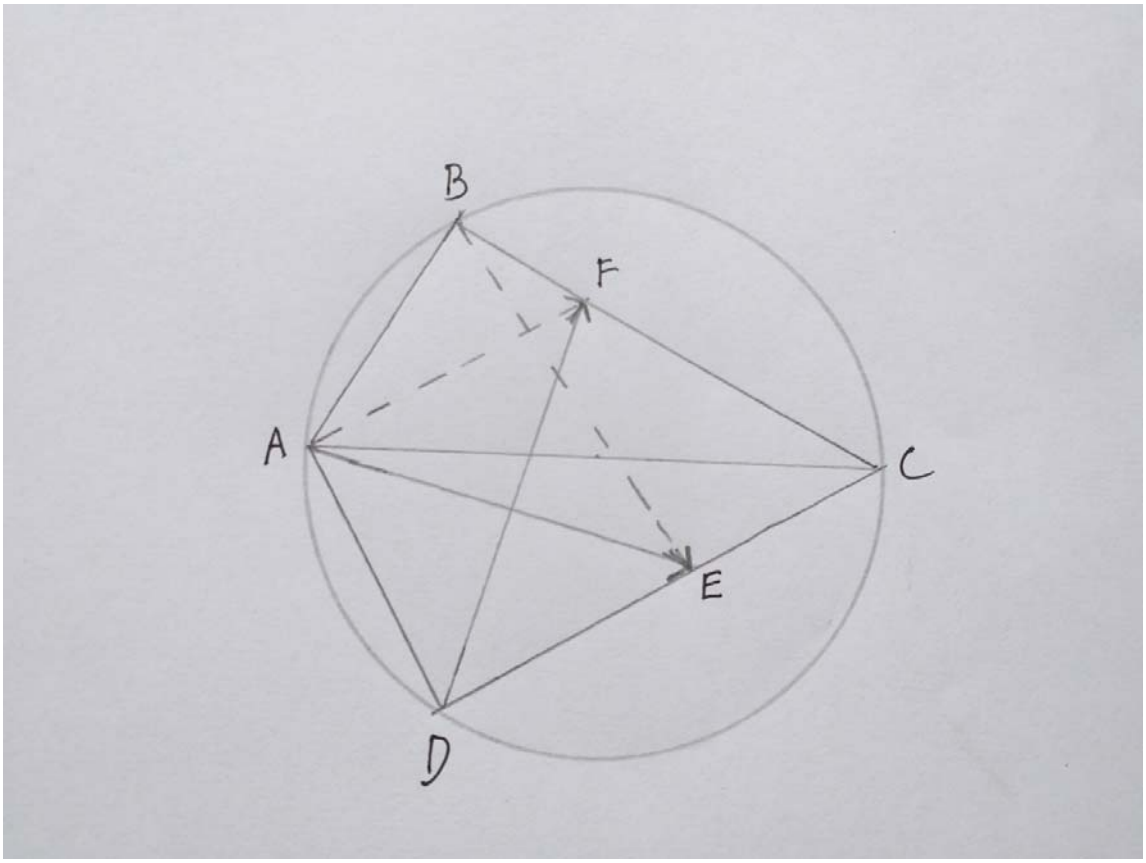

Figure 3

Problem 2.3. Let $ABCD$ be a convex quadrilateral and let $A' \in (AB)$, $B' \in (BC)$, $C' \in (CD)$, $D' \in (DA)$ such that $AA' = CC'$; $BB' = DD'$. Prove that if the line that passes through the midpoints of (AC') and ($A'C$) is perpendicular on the line that passes through the midpoints of (BD') and ($B'D$), then $ABCD$ is inscribed in a circle (Figure 4).

Solution

Let M, M', N, N' be the midpoints of $[AC'], [A'C], [B'D], [BD']$, respectively. Then $\overrightarrow{MM'} = \overrightarrow{AA'} + \overrightarrow{C'C}$ (this is a known consequence of (*)) and $\overrightarrow{NN'} = \overrightarrow{B'B} + \overrightarrow{DD'}$.

Given $\overrightarrow{MM'} \cdot \overrightarrow{NN'} = 0$, we obtain:

$$AA' \cdot DD' \cdot \cos A + AA' \cdot BB' \cos B + CC' \cdot BB' \cos C + CC' \cdot DD' \cos D = 0.$$

$\Leftrightarrow B + D = \pi$

But $CC' = AA'$ and $BB' = DD'$, implying that: $4 \cos \frac{B+D}{2} \sin \frac{C+D}{2} \sin \frac{A+D}{2} = 0.$

Since $\sin x = 0 \Rightarrow x = k\pi,\ k \in \mathbb{Z}$, it would imply that either $C + D = 2\pi$ or $A + D = 2\pi$, contradiction because the quadrilateral is convex.

This implies that $\cos \frac{B+D}{2} = 0 \Leftrightarrow B + D = \pi$, meaning that the quadrilateral is inscribed in a circle.

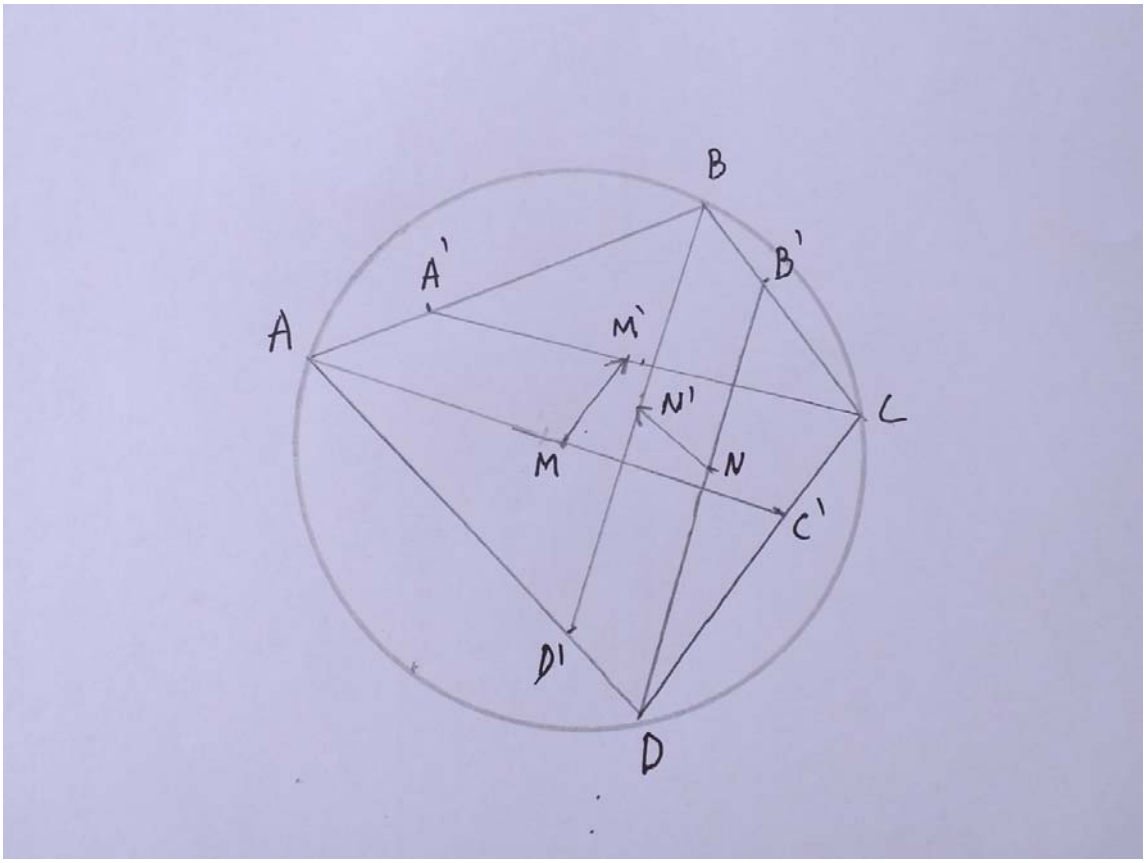

Figure 4

Problem 2.4 Let ABC be a triangle, M the midpoint of $[BC]$ and D on $[BC]$ such that (AD is the bisector of $\measuredangle BAC$. Using the known notations for half perimeter and the length of a side, prove that: $\cos(\measuredangle MAD) = \dfrac{p(p-a)}{AM \cdot AD}$

Solution

Using Bisector Theorem, one deduces that $\overrightarrow{AD} = \dfrac{b\overrightarrow{AB} + c\overrightarrow{AC}}{b+c}$. M is the midpoint of $[BC]$ implies $\overrightarrow{AM} = \dfrac{\overrightarrow{AB} + \overrightarrow{AC}}{2}$. These both relations are the consequences of (*).

It suffices to prove that $\overrightarrow{AM} \cdot \overrightarrow{AD} = p(p-a)$. We have:

$$\overrightarrow{AM} \cdot \overrightarrow{AD} = \frac{\overrightarrow{AB} + \overrightarrow{AC}}{2} \cdot \frac{b\overrightarrow{AB} + c\overrightarrow{AC}}{b+c} = \frac{1}{2(b+c)}(b\overrightarrow{AB}^2 + c\overrightarrow{AC}^2 + (b+c)\overrightarrow{AB} \cdot \overrightarrow{AC}) =$$

$$= \frac{1}{2(b+c)}(bc^2 + cb^2 + (b+c)\frac{b^2+c^2-a^2}{2}) = \frac{1}{2(b+c)}(bc(b+c) + (b+c)\frac{b^2+c^2-a^2}{2}) =$$

$$= \frac{bc}{2} + \frac{b^2+c^2-a^2}{4} = \frac{(b+c)^2-a^2}{4} = \frac{(a+b+c)(b+c-a)}{4} = p(p-a).$$

References

[1] Păltineanu, G., Donescu, Șt., Zamfir, M.: *Geometrie analitică și diferenţială*, Editura Conspress, Bucureşti, 2011.
[2] *Short List for National Mathematics Olympiad* 2002-2014
[3] *Gazeta Matematică, Seria B*, 2019.

A NOTE ABOUT BASIC PROPERTIES OF STRONGLY AND WEAKLY DECOMPOSABLE OPERATORS

Mariana Zamfir
Department of Mathematics and Computer Science
Technical University of Civil Engineering of Bucharest, Romania
E-mail: zamfirvmariana@yahoo.com

Abstract: In this work we present several basic properties which characterize the strongly and the weakly decomposable operators on Banach spaces. We extend the results obtained by Colojoară and Foiaş in [6], respectively by Apostol in [3] for decomposable operators to strongly and weakly decomposable operators.
Mathematics Subject Classification (2010): 47B47, 47B40
Key words: spectral maximal space; strongly decomposable; weakly decomposable; direct sum

1. Introduction

This present paper centres around certain characterizations of strongly and weakly decomposable operators on an arbitrary complex Banach space.
The purpose of Section 1 is to present briefly the necessary background material for the present work. We assume that the reader is familiar with the elementary spectral theory of bounded linear operators on Banach spaces.
Throughout this paper $\mathbf{B}(X)$ will be assumed to be the Banach algebra of all linear bounded operators on a given complex Banach space X, and $\mathbf{C}$ denotes the complex plane.
If $T \in \mathbf{B}(X)$ and Y is a linear closed subspace of X, invariant to T, let us denote by $T|Y$ the restriction operator of T to Y.
Note that the *spectrum* of an operator $T \in \mathbf{B}(X)$ is defined as the set $\sigma(T) = \mathbf{C} \setminus \rho(T)$, where the *resolvent set* $\rho(T)$ consists of all complex numbers $\lambda \in \mathbf{C}$ for which the operator $\lambda I - T$ is inversable in $\mathbf{B}(X)$.

Definition 1.1. ([6], [7]) An operator $T \in \mathbf{B}(X)$ is said to have the *single-valued extension property* if for any analytic function $f : D \to X$ (where $D \subset \mathbf{C}$ is open) with the property $(\lambda I - T) f(\lambda) \equiv 0$, it results that $f(\lambda) \equiv 0$.

For the operator $T \in \mathbf{B}(X)$ having the single-valued extension property and for any $x \in X$, we consider the open set $\rho_T(x)$ of all elements $\xi \in \mathbf{C}$ such that there is an X-valued analytic function $\lambda \to x_T(\lambda)$ defined on a neighborhood of ξ which verifies the relation

$$(\lambda I - T) x_T(\lambda) \equiv x .$$

The set $\rho_T(x)$ is called the *local resolvent set of x with respect to T* and the closed set $\sigma_T(x) = \mathbf{C} \setminus \rho_T(x)$ is the *local spectrum of x with respect to T*.
We also have $\rho(T) \subset \rho_T(x)$, $\sigma_T(x) \subset \sigma(T)$ and we denote by

$$X_T(F)=\{x\in X;\ \sigma_T(x)\subset F,\ F\subset \mathbf{C}\}$$ ([6], [7]).

Definition 1.2. ([8]) A subspace $Y\subseteq X$ is called *spectral maximal space* of $T\in \mathbf{B}(X)$ if it is invariant to T (i.e. $TY\subseteq Y$) and for any other subspace $Z\subseteq X$, also invariant to T, the inclusion $\sigma(T\mid Z)\subseteq\sigma(T\mid Y)$ implies the inclusion $Z\subseteq Y$.

Definition 1.3. ([3], [8]) An operator $T\in \mathbf{B}(X)$ is called *strongly decomposable* if for any finite open covering $\{G_i\}_{i=1}^n$ of the spectrum $\sigma(T)$, there is a system $\{Y_i\}_{i=1}^n$ of spectral maximal spaces of T such that the following two conditions are verified:

(i) $\sigma(T\mid Y_i)\subseteq G_i$, for all $i=1,2,...,n$

(ii) $Y=Y_1\cap Y+Y_2\cap Y+...+Y_n\cap Y$, for any spectral maximal space Y of T.

If the condition (ii) is replaced by the condition $X=Y_1+Y_2+...+Y_n$, then the operator T is called *decomposable*.

Every strongly decomposable operator is obviously decomposable ([3]).

Definition 1.4. ([6]) An operator $T\in \mathbf{B}(X)$ is called *weakly decomposable* if the following conditions are hold:

(i) T has the single-valued extension property and $X_T(F)$ is closed, for any $F\subset\mathbf{C}$ closed;

(ii) for any finite open covering $\{G_i\}_{i=1}^n$ of $\sigma(T)$, there is a system $\{Y_i\}_{i=1}^n$ of spectral maximal spaces of T such that:

1) $\sigma(T\mid Y_i)\subset G_i$, $i=1,2,...,n$

2) $X=\overline{Y_1+Y_2+...+Y_n}$.

In Section 2, we present several basic results which characterize the strongly and weakly decomposable operators; these results were obtained by Colojoară and Foiaş in [6] and [8], by Bacalu in [4] and [5], and by Zamfir in [12].

In the remaining sections, we will discuss about the restrictions and direct sums of strongly and weakly decomposable operators; several results were obtained by Apostol in [1], [2] and [3], by Bacalu in [4] and [5], and by Zamfir in [12].

2. Basic properties of strongly and weakly decomposable operators

Remark 2.1. ([8], [12]) If $T\in \mathbf{B}(X)$ is a strongly (weakly) decomposable operator, it results that:

1) T has the single-valued extension property.

2) $X_T(F)$ is a spectral maximal space of T, for any $F\subset\mathbf{C}$ closed and

$$\sigma(T\mid X_T(F))\subset F\cap\sigma(T).$$

3) any spectral maximal space Y of T can be defined by the relation

$$Y = X_T\left(\sigma\left(T \mid Y\right)\right).$$

Lemma 2.1. ([8]) Let $T \in \mathbf{B}\left(X\right)$ be a strongly decomposable operator. If there is no spectral maximal space $Y \neq \left\{0\right\}$ of T such that $\sigma\left(T \mid Y\right) \subset G$, where $G \subset \mathbf{C}$ is an open fixed set, then

$$G \bigcap \sigma\left(T\right) = \varnothing.$$

Lemma 2.2. ([4], [5]) An operator $T \in \mathbf{B}\left(X\right)$ is strongly decomposable if and only if the following assertions are established:

(i) $X_T\left(F\right)$ is closed, for any $F \subset \mathbf{C}$ closed;

(ii) for any finite open covering $\left\{G_i\right\}_{i=1}^{n}$ of the spectrum $\sigma\left(T\right)$, for any spectral maximal space Y of T and for all elements $x \in X$, we have $x = y_1 + y_2 + \ldots + y_n$, where $y_i \in Y_i$, $\sigma_{T|Y}\left(y_i\right) \subset G_i \bigcap \sigma\left(T \mid Y\right)$, $i = 1, 2, ..., n$.

Lemma 2.3. ([12]) Let $T \in \mathbf{B}\left(X\right)$ be a weakly decomposable operator. If there is no spectral maximal space $Y \neq \left\{0\right\}$ of T such that $\sigma\left(T \mid Y\right) \subset G$, where $G \subset \mathbf{C}$ is an open fixed set, then

$$G \bigcap \sigma\left(T\right) = \varnothing.$$

Lemma 2.4. ([12]) An operator $T \in \mathbf{B}\left(X\right)$ is weakly decomposable if and only if the following conditions are verified:

(i) T has the single-valued extension property and $X_T\left(F\right)$ is closed, for any $F \subset \mathbf{C}$ closed;

(ii) for any finite open covering $\left\{G_i\right\}_{i=1}^{n}$ of $\sigma\left(T\right)$, the set of all elements $x \in X$, with $x = x_1 + x_2 + \ldots + x_n$, $\sigma_T\left(x_i\right) \subset G_i$, $i = 1, 2, ..., n$, is dense in X.

3. Restrictions of strongly and weakly decomposable operators

Proposition 3.1. ([1], [2], [3]]) Let $T \in \mathbf{B}\left(X\right)$ be a strongly decomposable operator and let Y be a spectral maximal space of T. Then the restriction operator $T \mid Y \in \mathbf{B}\left(Y\right)$ is a strongly decomposable operator.

Theorem 3.1. ([1], [2], [3]) The necessary and sufficient condition for an operator $T \in \mathbf{B}\left(X\right)$ to be strongly decomposable is that the restriction $T \mid Y$ to be decomposable operator, for any spectral maximal space Y of T.

Proposition 3.2. ([1]) Let $T, P \in \mathbf{B}\left(X\right)$ be two operators such that T is strongly decomposable and P has the properties: $P^2 = P$ and $TP = PT$. Then $T \mid PX$ is strongly decomposable.

Proposition 3.3. ([12]) Let $T \in \mathbf{B}(X)$ be a weakly decomposable operator and let Y be a spectral maximal space of T. Then the restriction operator $T|Y \in \mathbf{B}(Y)$ is a weakly decomposable operator.

Proposition 3.4. ([12]) Let $T \in \mathbf{B}(X)$ be a weakly decomposable operator and $P \in \mathbf{B}(X)$ such that $P^2 = P$ and $TP = PT$. Then $T|PX$ is weakly decomposable operator.

4. Direct sums of strongly and weakly decomposable operators

Lemma 4.1. ([5], [6]) Let $T_1 \in \mathbf{B}(X_1)$, $T_2 \in \mathbf{B}(X_2)$, and $T_1 \oplus T_2 \in \mathbf{B}(X_1 \oplus X_2)$. Then:

(i) $\sigma\big((T_1 \oplus T_2)|(Y_1 \oplus Y_2)\big) = \sigma(T_1|Y_1) \cup \sigma(T_2|Y_2)$, for $Y_i \subseteq X_i$ linear closed subspace invariant to T_i, $i = 1, 2$.

(ii) If $Y \subseteq X_1 \oplus X_2$ is a spectral maximal space of $T_1 \oplus T_2$, then $Y = Y_1 \oplus Y_2$, where Y_1 is a spectral maximal space of T_1 and Y_2 is a spectral maximal space of T_2.

Theorem 4.1. ([4], [5]) Let $T_1 \in \mathbf{B}(X_1)$ and $T_2 \in \mathbf{B}(X_2)$ be two strongly decomposable operators. Then $T_1 \oplus T_2 \in \mathbf{B}(X_1 \oplus X_2)$ is a strongly decomposable operator.
Conversely, if $T_1 \oplus T_2 \in \mathbf{B}(X_1 \oplus X_2)$ is strongly decomposable, then both T_1 and T_2 are strongly decomposable.

Proposition 4.1. ([12]) If $T_1 \in \mathbf{B}(X_1)$ and $T_2 \in \mathbf{B}(X_2)$ are two weakly decomposable operators, then the operator $T_1 \oplus T_2 \in \mathbf{B}(X_1 \oplus X_2)$ is weakly decomposable.

Proposition 4.2. ([12) Let $T_1 \in \mathbf{B}(X_1)$, $T_2 \in \mathbf{B}(X_2)$. If the operator $T_1 \oplus T_2 \in \mathbf{B}(X_1 \oplus X_2)$ is weakly decomposable, then both T_1 and T_2 are weakly decomposable.

References

[1] Apostol, C.: *Spectral decompositions and functional calculus*, Rev. Roum. Math. Pures et Appl., 13, 1481-1528, 1968.
[2] Apostol, C.: *Teorie spectrală şi calcul funcţional*, Stud. Cerc. Mat., 20, 635-668, 1968.
[3] Apostol, C.: *Restrictions and quotients of decomposable operators in a Banach Space*, Rev. Roum. Math. Pures et Appl., 13, 147-150, 1968.
[4] Bacalu, I.: *Descompuneri spectrale reziduale* (*Residually spectral decompositions*), Stud. Cerc. Mat., I (1980), II (1980).
[5] Bacalu, I.: *S -Spectral Decompositions*, Ed. Politehnica Press, Bucharest, 2008.
[6] Colojoară, I., Foiaş, C.: *Theory of generalized spectral operators*, Gordon Breach, Science Publ., New York-London-Paris, 1968.
[7] Dunford, N., Schwartz, J.T.: *Linear Operators*, Interscience Publishers, New-York, Part I: General Theory, 1958; Part II: Spectral Theory, Self Adjoint Operators in Hilbert Space, 1963; Part III: Spectral Operators, 1971.
[8] Foiaş, C.: *Spectral maximal spaces and decomposable operators in Banach spaces*, Archiv der Math., 14, 341-349, 1963.
[9] Lange, R., Wang, S.: *New approaches in spectral decomposition*, Amer. Math. Soc, 1992.

[10] Laursen, K.B., Neumann, M.M.: *An introduction to local spectral theory*, London Math. Soc. Monographs New Series, Oxford Univ. Press., New-York, 2000.
[11] Vasilescu, F.H.: *Analytic Functional Calculus and Spectral Decompositions*, D. Reidel Publishing Company, Dordrecht; Ed. Academiei, Bucharest, 1982.
[12] Zamfir, M.: *Some properties of weakly decomposable operators*, Proc. of 1-st Workshop, Technical University of Civil Engineering, Bucharest, Romania, MatrixRom, ISSN 2392-6317, 152-157, 2014.
[13] Zamfir, M.: *About direct sums of decomposable operators and decomposable systems*, Proc. of 15-th Workshop of Scientific Communications, Technical University of Civil Engineering, Bucharest, Romania, MatrixRom, ISSN 2601-9299, 82-87, 2018.

AN EXAMPLE OF A TRANSCENDENTAL P-ADIC ELEMENT WITH A NON-ZERO DISCRIMINANT-LIKE INVARIANT

SEVER ACHIMESCU AND CORNELIU STELIAN ANDRONESCU

Abstract. In [2] it is defined an invariant $l(T) \in [0, +\infty]$ for each transcendental element T over $\mathbf{Q_p}$. Also, in [2], using an argument from [3], it is constructed an example of $T \in \mathbf{C_2} - \mathbf{Q_2}$ with $l(T) = 2$. In this paper we construct another example of $T \in \mathbf{C_p} - \mathbf{Q_p}$ with $l(T) < +\infty$. Such examples are useful for studying how the discriminant-like $\Delta_{\mathbf{Q_p}}(T)$ defined in [1] and $l(T)$ are related to each other.

Mathematics Subject Classification (2010): 11S99
Key words: discriminant

References

[1] S. Achimescu, C.S. Andronescu, V.Alexandru, *A notion analogous to the discriminant for transcendental elements in certain extensions of local fields*, Rend. Sem. Mat. Univ. Padova. accepted
[2] V. Alexandru, N. Popescu, *On the closed subfields of Cp*, J. of Number Theory 68, **2** (1998), 131-150.
[3] N. Popescu, A. Zaharescu *On a structure of irreducible polynomials over local fields*, J. of Number Theory 52, **2** (1995), 98-118.

Department of Mathematics and Computer Science, Technical University of Civil Engineering Bucharest, Bucharest, Romania
E-mail address: sachimescu@yahoo.com

Department of Mathematics and Computer Science, University of Pitesti, Pitesti, Romania
E-mail address: corneliuandronescu@yahoo.com

OPTIMAL INEQUALITIES FOR THE CASORATI CURVATURE OF STATISTICAL SUBMANIFOLDS

SIMONA DECU

Abstract. A fundamental problem in the general theory of Riemannian submanifolds is to establish simple relationships between the main *intrinsic invariants* and the main *extrinsic invariants* of the submanifolds [2]. On the other hand, in 1985 Amari defined the notion of *statistical manifold* in the basic study on information geometry [1]. In this paper, we investigate curvature properties for statistical submanifolds of Kenmotsu statistical manifolds of constant ϕ-sectional curvature. We establish some inequalities involving the normalized δ-Casorati curvatures (extrinsic invariants) and the scalar curvature (intrinsic invariant). Moreover, we study the equality cases of these inequalities. This talk is based on joint works with S. Haesen, L. Verstraelen and G.-E. Vîlcu.

Mathematics Subject Classification (2010): 53B20; 53C40; 53B15
Key words: Casorati curvature, statistical submanifold, Kenmotsu statistical manifold, dual connections

References

[1] S. Amari, *Differential-Geometrical Methods in Statistics*; in J. Berger, S. Fienberg, J. Gani, K. Krickeberg, I. Olkin and B. Singer (eds), Lecture Notes in Statistics, Springer-Verlag, 1985.
[2] B.-Y. Chen, *Pseudo-Riemannian Geometry, δ-Invariants and Applications*, World Scientific, Singapore, 2011.
[3] S. Decu, S. Haesen, L. Verstraelen, and G.-E. Vîlcu, *Curvature invariants of statistical submanifolds in Kenmotsu statistical manifolds of constant ϕ-sectional curvature*, Entropy **20** (2018).

Department of Applied Mathematics, Bucharest University of Economic Studies, Bucharest, Romania; *Costin C. Kiriţescu* National Institute of Economic Researches - Mountain Economy Centre (CE-MONT), Romanian Academy, Bucharest, Romania
E-mail address: simona.decu@gmail.com, simona.marinescu@csie.ase.ro

LEARNING HAZARD AND RELIABILITY THEORY THROUGH SERIOUS GAMES

Corina Grosu
Politehnica University of Bucharest,
Bucharest, Romania
E-mail: cgr90@yahoo.co
Marta Grosu
Politehnica University of Bucharest,
Bucharest, Romania
E-mail: marta_grosu@yahoo.com

Abstract: Probability distribution laws form an important part of the mathematical models with which students become acquainted through various university courses. Among them, a role apart is played by the Weibull distribution , due to its versatility and extremely large palette of real-life applications. In order to stress the importance of this law, we have built an e-learning game on Android tablets, featuring the catastrophic possibility of a bridge collapse, thus asking for adequate solutions based on a huge amount of previously collected data from different situations and regions. Notions like Q-Q plot and choosing between exponential, log-normal or Weibull distribution are part of our scenario and make the mathematical levels of the game a real test of students' abilities to adapt and eventually improve theoretical models for in hand problems.

Since visual elements and fight to win tactics are more likely to attract students' attention over contextual applications of mathematical models, we have built on the template from [5] and contributed, like in our previous e-learning games [2], [3], [4] with animated images and special effects created in Poser [6], Autodesk 3ds Max [1].

References

[1] 3ds Max tutorials: http://www.cgtutorials.com, http://cg.tutsplus.com, http://www.lynda.com/3ds-Max-tutorials/Getting-Started-CAT-Rigging-Tools-3ds-Max

[2] Grosu, C., Grosu, M., 2016: *Real Complex Travel,* The 12th International Scientific Conference "eLearning and Software for Education", *eLearning Vision 2020,* Bucharest, vol.1, 511 – 518.

[3] Grosu, C., Grosu, M., 2017: *Environmental Modeling with Math Game,* The 13th International Scientific Conference "eLearning and Software for Education", *Could technology support learning efficiency,* Bucharest, vol.1, 304 – 309.

[4] Grosu, C., Grosu, M., 2018: *Fake Warning: Playing with Imprecise Predictions,* The 14th International Scientific Conference "eLearning and Software for Education", *Could technology support learning efficiency,* Bucharest, vol.1, 304 – 309.

[5] Horton, J., 2015: Android Game Programming by Example, PACKT Publishing, Birmingham – Mumbai

[6] http://my.smithmicro.com/poser-3d-animation-software.html

BIG DATA ANALYSIS TECHNIQUES

Esa Kujansuu
ICT Engineering Department,
Tampere University of Applied Sciences
Kuntokatu 3, FI-33520 Tampere, Finland
E-mail: esa.kujansuu@tamk.fi

Abstract: In this paper we will present Big Data analysis techniques. Big Data analysis techniques use Machine Learning to build predictive models based on more data points and features than traditional statistical modelling. These characteristics allow us to use the great variety of data sources available. These models can be trained and evaluated using historical data to assure that their prediction is accurate and beneficial.
These Big Data analysis techniques are widely used, for example in business, industry and health care (detection of fraud, prediction of creditworthiness, early detection of production variability, detecting at-risk patients, among others), with successful results.
Mathematics Subject Classification (2010): 997R50, 62-07
Key words: Data bases, information systems, Data analysis

FRACTIONAL-ORDER HYBRID OF BLOCK-PULSE FUNCTIONS AND BERNOULLI POLYNOMIALS FOR SOLVING FRACTIONAL DIFFERENTIAL EQUATIONS AND SYSTEMS OF FRACTIONAL DIFFERENTIAL

O. POSTAVARU[1], M. RAZZAGHI[2] AND I. MIHAI[1]

Abstract. In this work we aim to find a method for solving fractional differential equations in the Caputo sense. We derive an exact Riemann-Liouville fractional integral operator for the fractional-order hybrid of block-pulse functions and Bernoulli polynomials. This procedure, allows as to remodel the fractional differential equations into a system of algebraic equations which can be solved using the Newton's iterative method. The accuracy and the efficiency of the present method is discussed on some illustrative examples. The conclusion is that our method gives better results than other results presented in literature.

Mathematics Subject Classification (2010): 34A38, 11B68, 35R11
Key words: Hybrid systems; Bernoulli polynomials; Fractional partial differential equations.

[1] Faculty of Mathematics and Computer Science, University of Bucharest, Bucharest, 010014, Romania
E-mail address: opostavaru@linuxmail.org

[2] Department of Mathematics and Statistics, Mississippi State University, Mississippi State, MS 39762, USA
E-mail address: razzaghi@math.msstate.edu